DISS. ETH NO. 17750

The Role of Intermediate Degradation Products for the Assessment of Persistent Organic Pollutants in a Global Multi-Media Model

A dissertation submitted to

ETH ZURICH

for the degree of
Doctor of Sciences

presented by
Urs Walter Schenker
ing. gén. rur. dipl. EPF Lausanne
born on December 7th, 1977
citizen of Schönenwerd, Däniken, and Olten (SO)

accepted on the recommendation of
Prof. Dr. Konrad Hungerbühler
PD Dr. Martin Scheringer
Dr. Kathrin Fenner

Zurich, 2008

La dernière démarche de la raison est de reconnaître
qu'il y a une infinité de choses qui la surpasse.

Blaise Pascal

Danksagung

Viele Menschen haben mich im Laufe dieser Doktorarbeit unterstützt, inspiriert, und motiviert – ich bin ihnen allen zu grossem Dank verpflichtet. Ohne sie wäre diese Arbeit nicht möglich gewesen.

Zuallererst möchte ich Konrad Hungerbühler und Martin Scheringer, meinen beiden Betreuern danken. Konrad hat mir die Möglichkeit gegeben, in der Gruppe S&U zu arbeiten, und mit kritischen Fragen meine Ideen und Thesen geprüft. Martin hat mitgeholfen, meine Gedankengänge zu präzisieren, hat meine Gedanken kritisch hinterfragt, und neue Ideen in meine Arbeit eingebracht. Insbesondere danke ich ihm für das Korrekturlesen der Artikel. Kathrin Fenner danke ich für die Übernahme des Korreferats.

Im Laufe dieser Doktorarbeit hatte ich viele interessante wissenschaftliche Diskussionen über Umweltmodellierung, insbesondere mit Fabio, Matt und Christian. Die intensiven Diskussionen über die Weiterentwicklung von CliMoChem, welche ich mit Fabio geführt habe, werden mir in guter Erinnerung bleiben. Bei Fabian möchte ich mich für die gute Zeit während seiner Diplomarbeit bedanken. Meinem Bruder Rolf danke ich für die guten Ideen wenn Excel mal wieder nicht so wollte wie ich...

I would also like to thank Tom McKone and Randy Maddalena for hosting me in their group in Berkeley. I had a great experience in California! Thanks also to Seb for introducing me to the social life in crazy California.

Mit den Mitgliedern der Gruppe S&U habe ich in den letzten drei Jahren auch privat viel Zeit verbracht. Vielen Dank für die schönen Momente als: Kletterer, Töggele-Partner, Mountain-biker, Kinobesucher, Biertrinker, Theaterzuschauer, Inlineskater, Töggele-Gegner und so weiter: Matze, Fabio, Gilles, David, Christiane, Andrej, Gregor, Fabian, Stefano, Capello.

Freunden und Kollegen gebührt spezieller Dank für ihre Unterstützung im Laufe dieser Diss: Jösu, Pädu, Jürgen, Séb, Nat, David, Monica, Rainer, Kai, Phil, Henner, Simu, Manu, Vivä, Oksana und Luc.

Schlussendlich gebührt meiner Familie der grösste Dank für ihre Unterstützung während der letzten 30 Jahre: Annina, Walter und Rolf haben mir immer ihr Vertrauen geschenkt, und mir einen Rückzug aus der Hektik des Alltages erlaubt.

Table of Contents

Summary

Humans and the environment are exposed to an ever increasing amount of chemicals. Some of these substances are emitted purposely into the environment as agro-chemicals, others as undesired emissions during the production, in the waste-management process, or in the case of an accident. An important indicator for the hazard of a chemical is its persistence in the environment: substances that are readily degraded by biotic or abiotic processes are believed to be a less substantial concern than substances that will persist for a long time in the environment. Therefore, some of the most persistent chemicals have been phased out in many countries already, and the phase-out of new chemicals that persist in the environment is discussed.

Models are frequently used to predict the behavior of chemicals in the environment. The assessment of degradation processes of chemicals is one of the key tasks performed with model simulations. If a chemical is degraded in these models, it usually disappears from the modeled system. In reality however, the degradation of a chemical will result in a number of intermediate degradation products, often only slightly different from the original substance. The characteristics of the degradation products might be similar to the characteristics of the original product and therefore degradation products should be taken into account in the assessment of chemicals. Whereas some models have been developed that take into account the formation of degradation products on a local scale, these processes have not been included in global models, yet. To assess the long-range transport processes of chemicals, global models are required. Only such models can be used to elucidate the processes that transport chemicals from the regions where they are emitted to remote places like the Arctic.

In the present thesis, intermediate degradation products are included in the global environmental fate model “Climatic Zone Model for Chemicals”, CliMoChem. In a first step, the basics to calculate intermediate degradation products in a global model are established. A method is presented that allows optimizing the amount of information that can be gained from measurements of substance properties, and that allows to identify inconsistencies between the measurements of different properties of the same substance. This is particularly valuably for intermediate degradation products, because measurements of their substance properties are scarce, and it is crucial to extract as much information as possible from existing measurements. A new version of the CliMoChem model is then presented that is capable of

simulating parent compounds and intermediate degradation products simultaneously. Existing indicators to classify chemicals according to their ability to undergo long-range transport and their potential for accumulation in the Arctic are extended to take into account intermediate degradation products. With the example of a series of pesticides, the value of these indicators is demonstrated.

In a series of case studies, the model framework is applied to substances with persistent intermediate degradation products that are globally distributed. First, the precursor substances of perfluorooctanoate (PFO) are modeled in the environment. The fate of fluorotelomer alcohols (FTOHs) and perfluorooctylsulfonamido ethanols (FOSEs), and their degradation into PFO is simulated. Levels of FOSEs in Arctic atmosphere suggest that emissions cannot have decreased recently, despite the main manufacturer claiming to have phased out FOSEs. Atmospheric degradation of FTOHs and FOSEs result in similar amounts of PFO in Arctic oceans, but direct emissions of PFOs are about two orders of magnitude more important. On the other hand, FTOHs and FOSEs result in a significant amount of PFOs that is deposited to Arctic ice surfaces, similar in magnitude to predictions from ice core measurements.

In a second case study, the fate of polybrominated diphenyl ethers (PBDEs) is assessed. This substance class is used as a flame retardant in textiles and polymers, has been shown to accumulate in the environment, and is believed to have endocrine effects. While lower brominated PBDEs have been phased-out in the European Union, the highly brominated congeners may still be used. Heavy PBDEs have been shown to degrade into lighter congeners under laboratory conditions. If these processes turn out to be relevant in the environment, heavy PBDEs should be phased-out, too. We have calculated the fate of various PBDEs congeners, and taken into account the ability of heavy congeners to debrominate. Results show that debromination is a considerably less important source for lighter congeners in the environment than direct emissions of these congeners. However, the phase-out of the lighter congeners will not result in a complete disappearance of these compounds in the environment, because they are constantly regenerated from the degradation of the heavier PBDEs.

In a third case study, the behavior of DDT and its degradation products DDE and DDD is modeled. Model results for the present are compared to measurements in the environment, and future concentrations are predicted under the assumption that DDT will be used for malaria combat purposes in the future. It is shown that CliMoChem reproduces

measurements in the environment fairly well. Future concentrations of DDT are expected to decrease strongly in the Arctic, independent on whether DDT continues to be used in the tropical regions for malaria combat purposes or not. In the tropical countries, however, DDT concentrations will remain fairly high if emissions continue, whereas an emission stop of DDT would reduce concentrations drastically.

Finally, in a last chapter, the uncertainties associated to model calculations are assessed. Monte Carlo simulations are performed for the DDT case study. The uncertainties of the model output are relatively high, and the main contributors to these uncertainties are substance properties and emission rates of DDT. A Bayesian updating method is introduced that allows field data to be used to improve model predictions. Updated model results are closer to measurements, and an alternative set of model inputs is suggested. Differences between the initial and updated set of model inputs are assessed, and implications for future modeling discussed.

In the concluding section, the findings from this thesis are summarized, and limitations of the methods and used tools discussed. A decision guideline is presented that helps guiding researchers when assessing chemicals and their degradation products in a global context. In the outlook, possible future applications for global fate models with intermediate degradation products and uncertainty calculations are discussed.

Zusammenfassung

Die Zahl der Chemikalien, welcher Menschen und ihre Umwelt ausgesetzt sind, steigt stetig an. Einige dieser Chemikalien werden absichtlich freigesetzt, wie im Fall von Pflanzenschutzmitteln, andere gelangen durch unbeabsichtigte Emissionen während der Produktion, im Abfallmanagement oder im Störfall in die Umwelt. Ein wichtiger Faktor bei der Risikoabschätzung von Chemikalien ist ihre Persistenz in der Umwelt: Substanzen welche durch biotische oder abiotische Prozesse rasch abgebaut werden können sind weniger bedenklich als Substanzen welche lange Zeit in der Umwelt verbleiben werden. Aus diesem Grund dürfen eine Reihe besonders persistenter Substanzen in vielen Ländern bereits nicht mehr verwendet werden, und die Regulierung von neuen Substanzen wird diskutiert.

Zur Beschreibung des Verhaltens von Chemikalien in der Umwelt werden Modelle verwendet. Die Beschreibung der Abbauprozesse von Chemikalien nimmt in diesen Modellstudien eine Schlüsselrolle ein: wird eine Substanz in einem Umweltmodell abgebaut verschwindet sie üblicherweise aus den Systemgrenzen des Modells. In der Realität jedoch entsteht beim Abbau meist ein Zwischenprodukt welches sich oft nur unwesentlich von der Originalsubstanz unterscheidet. Weil die Eigenschaften solcher Zwischenprodukte sehr ähnlich wie jene der Originalsubstanz sein können, empfiehlt es sich auch, Zwischenprodukte in einer Risikoabschätzung zu berücksichtigen. Es existieren heute einige lokale Umweltmodelle, welche Zwischenprodukte berücksichtigen, allerdings sind diese bis anhin in keinem globalen Modell eingebaut worden. Globale Modelle wurden entwickelt, um die Ferntransportprozesse von Chemikalien zu studieren, insbesondere jene Prozesse, die Chemikalien von ihren Emissionsorten in abgelegene Regionen wie die Arktis verfrachten.

Im Rahmen dieser Doktorarbeit werden Zwischenprodukte in das globale Umweltverteilungsmodell „Climatic Zone Model for Chemicals“, CliMoChem, eingebaut. In einem ersten Schritt werden Grundlagen erarbeitet um Zwischenprodukte in einem globalen Modell zu berücksichtigen. Eine Methode um aus gemessenen Daten bestmögliche Substanzeigenschaften zu extrahieren wird vorgestellt. Diese Methode erlaubt es auch, Unstimmigkeiten zwischen Messungen verschiedener Eigenschaften einer gleichen Substanz zu erkennen. Dies ist besonders wichtig für Zwischenprodukte, weil deren Substanzeigenschaften nur sehr selten gemessen wurden. Eine neue Version des CliMoChem Modells wird vorgestellt, welche das Umweltverhalten von Ausgangs- und Zwischen-

produkten gleichzeitig berechnen kann. Bestehende Indikatoren zur Klassifizierung von Chemikalien nach ihrer Fähigkeit für Ferntransport und arktischem Verschmutzungspotential werden erweitert, so dass diese auch die Bildung von Zwischenprodukten berücksichtigten. Am Beispiel von Pestiziden wird die Bedeutung dieser Indikatoren aufgezeigt.

In einer Reihe von Fallstudien wird das Umweltverhalten von global verteilten Chemikalien mit persistenten Zwischenprodukten studiert. In einer ersten Fallstudie werden Vorläufersubstanzen von Perfluorooktanoat (PFO) modelliert: Das Verhalten von Fluorotelomeralkoholen (FTOHs) und Perfluorooktylsulfonamido Ethanol (FOSE) wird studiert, insbesondere die Bildung von PFO durch den Abbau von FTOHs und FOSE. Messungen der Luftkonzentration von FOSE in der Arktis legen nahe, dass Emissionen dieser Substanzen noch nicht zurückgegangen sind, obwohl diese vom ehemaligen Hauptproduzenten angeblich nicht mehr hergestellt werden. FTOHs und FOSE generieren ähnliche Mengen an PFO in der Arktis, direkte PFO-Emissionen sind jedoch etwa um den Faktor 100 höher. FTOHs und FOSE führen zu relevanten Mengen atmosphärischer Deposition von PFO auf arktischen Eisflächen, welche mit Messungen in Eiskernen übereinstimmen.

In einer zweiten Fallstudie wird das Verhalten von Polybromierten Diphenylethern (PBDEs) untersucht. Diese werden als Flammenhemmer in Textilien und Polymeren eingesetzt. Hohe Konzentrationen dieser Substanzen wurden in der Umwelt gefunden, und es wird vermutet, dass PBDEs endokrine Effekte haben. Niederbromierte PBDEs wurden in der Europäischen Union verboten, aber höherbromierte PBDEs sind noch immer zugelassen. Höherbromierte PBDEs werden unter Laborbedingungen in niederbromierte PBDEs abgebaut, und falls diese Prozesse auch in der Umwelt stattfänden, sollten auch höherbromierte PBDEs nicht mehr zugelassen werden. Wir haben das Verhalten von verschiedenen PBDEs berechnet, und dabei berücksichtigt, dass höherbromierte PBDEs debromiert werden können. Gemäss unseren Resultaten sind höherbromierte PBDEs nur eine Nebenquelle für niederbromierte PBDEs, deren Konzentrationen in der Umwelt hauptsächlich durch direkte Emissionen bestimmt werden. Trotzdem werden die Konzentrationen von niederbromierten PBDEs nicht auf Null zurückgehen, sollten höherbromierte PBDEs weiterhin verwendet werden, da sie eine kontinuierliche Quelle für niederbromierte PBDEs darstellen.

In einer dritten Fallstudie wird das Verhalten von DDT und den Abbauprodukten DDE und DDD beschrieben. Modellresultate werden mit Umweltmessungen verglichen, und zukünftige Konzentrationen vorhergesagt, unter der Annahme dass DDT weiterhin zur

Bekämpfung von Malaria verwendet wird. Berechnete Umweltkonzentrationen stimmen gut mit Messwerten überein. Die zukünftige DDT Konzentration wird in der Arktis stark zurückgehen, unabhängig davon ob DDT weiterhin verwendet wird. In den Tropen wird die zukünftige DDT Konzentration stark davon abhängen, wieviel DDT für die Bekämpfung von Malaria weiterhin verwendet wird.

Schlussendlich werden im letzten Kapitel mittels Monte Carlo Simulationen am Beispiel von DDT die Unsicherheiten von Modellresultaten untersucht. Die Unsicherheiten sind relativ hoch, und Substanzeigenschaften und Emissionswerte tragen am meisten zu den Unsicherheiten bei. Umweltmessungen werden verwendet um mittels eines bayesschen Lernmechanismus Modellrechnungen zu verbessern. Die neuen Modellvorhersagen liegen näher bei gemessenen Werten aus der Umwelt, und ein neuer Satz von Eingabeparametern für das Modell wird vorgeschlagen. Unterschiede zwischen den ursprünglichen und den verbesserten Eingabeparametern werden diskutiert, und die Bedeutung für zukünftige Modellrechnungen erwägt.

Im Abschlusskapitel werden die wichtigsten Befunde dieser Doktorarbeit zusammengefasst, und die Grenzen der Methodik und der verwendeten Werkzeuge diskutiert. Als Hilfe für zukünftige Modellierungsprojekte von Chemikalien und ihren Abbauprodukten in einem globalen Kontext wird ein Entscheidungsschema präsentiert. Im Ausblick werden mögliche zukünftige Anwendungsgebiete für globale Verteilungsmodelle mit Abbauprodukten diskutiert.

Chapter 1:

Introduction

1.1 Environmental Significance

1.1.1 Chemicals in the Environment

Humans are exposed to an increasing amount of chemicals in the air they breathe or the food they eat. These chemicals enter the environment in different ways, purposely emitted as in the case of agrochemicals, or as undesired emissions during the production process, in the use phase, in case of an accident, or along the waste management process. Up to a Hundred thousand different chemicals are known and used today, and the identification of potentially hazardous substances is a very challenging task. A small group of chemicals known as "persistent organic pollutants" (POPs) has hitherto attracted much of the attention from the scientific community because they are believed to be toxic to humans and biota, bioaccumulate in the food-chain, and degrade very slowly in the environment.

In high concentrations, POPs can have a wide range of impacts, such as reduced fertility, malformations, higher risks for cancer developments, decreased life expectancy, and so on. The famous insecticide dichloro-diphenyl-triochloroethane (DDT) for example (more precisely its degradation product DDE) has been identified as being responsible for eggshell thinning among falcons (Enderson, 1970, Switzer et al., 1972, Wiemeyer and Porter, 1972), resulting in decreased reproductive success. It has also been linked to developmental abnormalities of alligators (Guillette et al., 1994, Semenza et al., 1997), and has been responsible for high death tolls among fish in rivers and creeks (Miramichi Salmon Conservation Center, 2008).

The Arctic ecosystem is particularly vulnerable to environmental contaminants: Given the cold climate in the Arctic, POPs have a tendency to precipitate into surface media (due to their lower vapor pressure) where they are more easily accessible to biota, and degrade very slowly. POPs have therefore been detected in very high concentrations in Arctic ecosystems, and specific monitoring programs have been launched. The Arctic Monitoring and Assessment Program has released several reports that demonstrate toxic effects of POPs in the Arctic regions: In the 3rd and 6th chapter of their 2002 report (Arctic Monitoring and Assessment Program, 2004), reduced immunological response in polar bear and northern fur seals in the Arctic due to exposure to PCBs are mentioned. Immunological, behavioral, and reproductive effects, as well as reduced adult survival have been found among glaucous gulls due to high exposure to DDT, mirex and PCBs. Furthermore, the report states that levels of

various POPs detected in the Arctic are sufficiently high to cause subtle health effects among rhesus monkeys or humans.

Even without the knowledge of specific health effects, the persistence and accumulation of chemicals in the environment is a problem in itself. If a persistent chemical is emitted in large quantities, its concentrations will increase to high levels. If the chemical is shown to have adverse health effects later on, and its future use is prohibited, high concentrations from past use will persist for a very long time, even after the phase-out of the chemical. Half-lives of several years, even decades, area not uncommon for chemicals. Therefore, a high persistence of a chemical is today considered a problem, even if no toxic effect of that chemical is yet known.

1.1.2 The Use of Models

Models are a useful tool to evaluate the risk of chemicals in the environment. Environmental contaminant fate models mimic the behavior of chemicals in the environment. They are designed to take into account the affinity of chemicals for different environmental compartments like water, atmosphere, soils, and vegetation. They take into account the ability of chemicals to travel in atmosphere and oceans, and calculate the amount of chemicals that are degraded in different environmental compartments. Temporally resolved models (also called level 4 models, according to the classification in Mackay (1979)) may be used to simulate concentrations of chemicals as a function of time.

Early attempts of modeling POPs on a global scale can be found at the beginning of the 1970s, when consciousness arose about the persistence of pesticides such as DDT. Two early models in the 1970s (Woodwell et al., 1971, Cramer, 1973) calculated the fate of DDT on a global scale, using approximated half-lives for different media to account for the unknown transportation processes between media.

The first models which used physical-chemical laws to calculate the distribution of chemical species have been suggested by Baughman and Lassiter (1978), and later been applied by Mackay (1979). Models like the one developed by Mackay (1979) typically contain one box with 3 or more different compartments (one or several atmospheric compartments, soil, oceanic surface water, freshwater and sediment compartments) and are used to establish the mass balance for chemicals in a region, for instance the Province of Ontario (Mackay and Paterson, 1991).

As it became obvious that many POPs are transported not only on a local, but a global scale, these models were adapted. As temperature and other environmental parameters are strongly variable on the global scale, it became necessary to construct models with several boxes, each of which contained several compartments. Different geometrical forms were established, for instance the ring model ChemRange (Scheringer, 1996), the Bergen Model (Strand and Hov, 1993, Strand and Hov, 1996), zonally averaged models like GloboPOP (Wania and Mackay, 1995) and CliMoChem (Scheringer et al., 2000, Wegmann, 2004), and other two dimensional models like BETR (Toose et al., 2004).

Parallel to the use of multi-media box models for the calculation of POPs' fate, global circulation models (GCMs) used to predict complex meteorological phenomena have been adapted to model persistent organic pollutants. Typical characteristics of GCMs include very high spatial resolutions (100km grid cells), a high temporal resolution (time steps of some minutes or hours), and a very complex representation of wind and ocean current regimes. They model atmospheric transport and chemical reactions of well known substances very accurately; however, they require huge computational efforts, and have little advantage if substance properties are poorly known. Examples of global circulation models that were adapted to POPs are presented in Koziol and Pudykiewicz (2001), Cohen et al. (2002), and Semeena and Lammel (2003).

1.1.3 The Importance of Degradation Products

When assessing the fate of chemicals in a global environmental fate model, the degradation of a substance is the key loss process for a chemical. In reality, however, a substance that degrades will not completely disappear, but will be transformed into other chemical products (incomplete degradation). In many cases, the first degradation products are complex molecules, only slightly different from the original products. Therefore, the characteristics (toxicity, persistence) of the degradation products might be similar to the characteristics of the original products and it is therefore not appropriate to ignore degradation products in the assessment of chemical products (Boxall et al., 2004). The knowledge of the dynamics of degradation products is of great importance in environmental fate studies of chemicals. Until now, these studies have possibly underestimated the impact of chemicals, because persistent intermediate degradation products could not be taken into account. Knowing the concentration of degradation products in the environment would allow their contribution to be included in exposure and human health assessments.

1.1.4 Legal Framework

The first efforts to phase-out some of the most dangerous chemicals have started after the publication of Rachel Carson's book "Silent Spring" (1962). The book describes a possible future scenario in which chemicals are used ubiquitously and without consideration of their side effects on ecosystems and human health. The perspective of a complete disappearance of songbirds, depicted in this scenario, raised serious concerns in the United States and Europe. It triggered the adoption of the first clean air act in the US in 1963 and later the banning of the worst environmental contaminants in the US and many other industrialized countries.

Since then, the legal framework on man-made chemicals has changed considerably. In the European Union, for instance, the recently adopted legislation "REACH" (Registration, Evaluation, Authorisation and Restriction of Chemicals), (European Commission, 2008) sets out guidelines for the protection of human health and the environment with increasing requirements based on the tonnage of production or import for about 30'000 chemicals. It lays responsibility on industry for assessing and characterizing the risks posed by chemicals.

On the global scale, a more strict legislation of chemicals took longer to be adopted: the Stockholm Convention on Persistent Organic Pollutants (United Nations Environmental Program, 2004) is a framework that entered into force in 2004. It aims at protecting humans and the environment from persistent organic pollutants (POPs). POPs are defined by the Stockholm Convention as "chemicals that remain in the environment for long periods, become widely distributed geographically, accumulate in the fatty tissue of living organisms and are toxic to humans and wildlife" (United Nations Environmental Program, 2008). In a first step, 12 chemicals (often called "the dirty dozen") have been suggested for strict regulation by the convention. More chemicals are expected to be included in the convention, and criteria for their inclusion are currently discussed.

These legal frameworks have also recognized the importance of degradation products, and give specific recommendations as how to treat degradation products when performing chemicals risk assessments:

- In the Stockholm Convention on Persistent Organic Pollutants (United Nations Environmental Program, 2004) a substance is defined as "the parent compound and all its transformation products with POP characteristics".

- The EU Technical Guidance Document on the risk assessment of notified new substances (European Chemicals Bureau, 2005) states that "if stable degradation products are formed, the risk assessment should include these" (Part II, page 48).
- The new European Chemicals Regulation REACH (European Union, 2006) requires transformation and degradation products of chemicals to be identified, and their fate in the environment (Annex I, §5.2.4), toxicological data (Annex VIII, §9.3.1), and substance properties (Annex IX, §7.15) be assessed.

In most current modeling studies, intermediate degradation products are not taken into account. One reason might be that models capable of calculating degradation products are still scarce, and a framework that guides researchers when taking into account degradation products in their calculations exists only on a local scale.

1.2 Objectives

The objective of this thesis is to develop methods and tools that allow intermediate degradation products of persistent chemicals to be taken into account in global multi-media contaminant fate models. Building on previous work in our group on the local scale (Fenner, 2001), the importance of intermediate degradation products for the risks of environmental contaminants at a global scale shall be evaluated. This evaluation should result in criteria that characterize situations (that is, a combination of substance properties, emission patterns, degradation pathways, and degradation yields) in which intermediate degradation products play an important role in the risk of persistent environmental contaminants on a global scale. Furthermore, the methods and tools should be applied to a number of case studies for which intermediate degradation products are believed to be important.

The influence of intermediate degradation products of persistent chemicals is studied at a global scale using the environmental contaminant fate model "Climatic Zone Model for Chemicals", CliMoChem {Scheringer, 2002 #315; Wegmann, 2004 #399}. The model is modified to take into account the formation, distribution, and degradation of intermediate degradation products. A method is developed to optimize partitioning information from measurements. This is particularly valuable for intermediate degradation products for which property measurements are scarce. Three substance groups have been identified for which intermediate degradation products play important roles:

- The first example are fluorotelomer alcohols (FTOHs) and perfluorooctylsulfonamido ethanols (FOSEs), which have been shown to degrade into perfluorooctanoate (PFO). PFO has been measured in high concentrations in the Arctic, and its high persistence has resulted in the phase-out of PFO from production. However, if FTOHs and FOSEs were important sources of PFO, they would have to be phased-out equally.
- The second example are polybrominated diphenyl ether (PBDEs) which are used as flame retardants. Lower brominated PBDEs have been banned in the European Union because of concerns over their long-range transport and bioaccumulation potential, whereas highly brominated PBDEs are still in use. We assess if highly brominated congeners degrade into lower brominated congeners in a relevant amount in the environment.
- Finally, the environmental fate of DDT and its degradation products DDE and DDD are assessed. Concentrations of the three substances are compared to measurements in the environment, and predictions on future levels of DDT are made.

Uncertainties in model calculations can be high, in particular if poorly known substances are involved. Given that the properties of intermediate degradation products are generally poorly known, uncertainties in model calculations involving intermediate degradation products are generally high. Therefore, a method to quantify and propagate uncertainties in a global environmental contaminant fate model is presented. A Bayesian Monte Carlo method to reduce uncertainties of model results by using field data is applied to the DDT case study.

1.3 Scientific Background

The degradation of a chemical can yield a number of degradation products, which often are structurally related. If these are believed to be of environmental significance, their behavior in the environment should be evaluated. Although it is feasible to model first the parent compound and then the degradation products in a separate modeling stage, this requires very complex emission terms to be considered. Therefore, it is desirable to model the degradation products at the same time as the parent chemical itself, which requires current models to be adapted.

In the last years, several models have been developed that are capable of including transformation products. Fenner et al. (2000, 2001), have developed a 1-box, 3-compartments model capable of assessing the fate of a parent compound and several degradation products.

They have introduced the concept of "fractions of formation" to account for variable amounts of degradation products formed from one single parent compound. In their case studies, they have assessed the fate of nonylphenol ethoxylate (Fenner, 2001, Fenner et al., 2002), perchloroethylene, atrazine (Fenner et al., 2000, Fenner, 2001), and methyl *tert*-butyl ether (Fenner et al., 2000).

The concept of persistence (Scheringer, 1996) was broadened to take into account degradation products' persistence, leading to what is called joint persistence. It has been shown that significant contribution to the joint persistence can come from the transformation products (Fenner, 2001, Fenner et al., 2003). In the above mentioned case studies, a maximal factor of 10 was found to exist between the persistence of the parent compound only and the joint persistence.

A similar model was developed by Cahill et al. (2003). This model is based on the EQC model (Mackay et al., 1996) and was applied to chlorpyriphos, pentachlorophenol and perfluorooctane sulfate. Quartier and Müller-Herold (2000) suggested an analytical method to include transformation products in the concept of spatial range.

When assessing the behavior of chemicals in a global environment, uniform models with only one box for each environmental medium are insufficient: they do not allow assessing how chemicals migrate away from their source regions, and cannot take into account the impact of varying environmental parameters (for instance temperature) at different locations on the globe. Therefore, spatially resolved models were developed (Wania and Mackay, 1995, Scheringer et al., 2000, MacLeod et al., 2001, Toose et al., 2004). These models feature a variable number of regions with variable properties (temperature, land cover, vegetation type). Simpler models are only one-dimensional, and assume that properties of the environment and pollutant concentrations are homogeneous in the East-West direction (Wania and Mackay, 1995, Scheringer et al., 2000).

1.4 Structure of this Thesis

This thesis is built up by six main sections (chapters 2 – 7), and a last section (chapter 8) that summarizes the overall significance of degradation products for the assessment of POPs in a global perspective, displays some of the limitations, and gives an outlook for the future. The structure of the six main sections which have previously been published or submitted to peer

reviewed journals, is graphically displayed in Table 1.1 and described in more detail in the following paragraphs.

Table 1.1: Structure of this thesis.

topic of the chapter	title of the publication - journal
optimization of input data (chapter 2)	*Improving Data Quality for Environmental Fate Models: A Least-Squares Adjustment Procedure for Harmonizing Physicochemical Properties of Organic Compounds* **Environ. Sci. Technol. 2005, 39, 8434−8441**
method development (chapter 3)	*Including Degradation Products of Persistent Organic Pollutants in a Global Multi-Media Box Model* **Env. Sci. Pollut. Res. 2007, 14 (3), 145−152**
1. case study (chapter 4)	*Contribution of Volatile Precursor Substances to the Flux of Perfluorooctanoate to the Arctic* **Environ. Sci. Technol. 2008, 42, 3710-3716**
2. case study (chapter 5)	*Modeling the Environmental Fate of Polybrominated Diphenyl Ethers (PBDEs): the Importance of Photolysis for the Formation of Lighter PBDEs* **submitted for publication in Environ. Sci. Technol.**
3. case study (chapter 6)	*Investigating the Global Fate of DDT: Model Evaluation and Estimation of Future Trends* **Environ. Sci. Technol. 2008, 42, 1178−1184**
uncertainty of results (chapter 7)	*Using Information on Uncertainty to Improve Environmental Fate Modeling: A case Study on DDT* **submitted for publication in Environ. Sci. Technol.**

Substance properties are essential inputs for model calculations. They are, however, particularly challenging to obtain in the case of poorly known intermediate degradation products. Therefore, in the second chapter (*Improving Data Quality for Environmental Fate Models: A Least-Squares Adjustment Procedure for Harmonizing Physicochemical Properties of Organic Compounds*), a method is presented that allows combining information on partitioning properties, vapor pressure, and solubilities in water and octanol to improve overall confidence in measured partitioning properties. The least-squares adjustment procedure also allows one to detect biased substance property measurements.

In the third chapter (*Including Degradation Products of Persistent Organic Pollutants in a Global Multi-Media Box Model*), the basic modeling framework to integrate intermediate degradation products into global environmental fate models is presented: additional requirements for model input data, and methods for their determination are presented. An updated version of the CliMoChem model is introduced, and results with generic peak

emissions of pesticides are displayed. A framework of hazard indicators that include degradation products is discussed. Special attention is given to hazard indicators that can only be calculated in spatially explicit models.

In the forth chapter (*Contribution of Volatile Precursor Substances to the Flux of Perfluorooctanoate to the Arctic*), a first case study where intermediate degradation products play an important role is introduced: fluorotelomer alcohols (FTOHs) and perfluorinated sulfonamido ethanols (FOSEs) are known precursor substances of perfluorooctanoic acid (PFO) in the Arctic. This chapter compares the relative importance of direct emissions of PFO with emissions and degradation of FTOHs and FOSEs.

In the fifth chapter (*Modeling the Environmental Fate of Polybrominated Diphenyl Ethers (PBDEs): the Importance of Photolysis for the Formation of Lighter PBDEs*), a case study on polybrominated diphenyl ethers (PBDEs) is presented. PBDEs are flame retardants, incorporated into textiles and polymer products to reduce their fire hazard. Whereas highly brominated PBDEs are currently not regulated, lowly brominated PBDEs have been phased-out in the European Union and Japan. This chapter discusses the importance of the environmental degradation of heavily brominated PBDEs into lower brominated PBDEs. If this process would be relevant in the environment, highly brominated PBDEs might have to be phased-out, too.

In the sixth chapter (*Investigating the Global Fate of DDT: Model Evaluation and Estimation of Future Trends*), a case study on DDT discusses the ability of the CliMoChem model to reproduce measurements in the environment, and the possibility of using the CliMoChem model to predict future concentrations of DDT. Differences between the evolution of DDT concentrations in the tropics (where the substance will in the future still be used for malaria combat purposes) and the Arctic (where DDT has accumulated as a result of previous DDT usage in temperate regions) are assessed.

In the seventh chapter (*Using Information on Uncertainty to Improve Environmental Fate Modeling: A Case Study on DDT*), the uncertainties of the model results on present and future DDT concentrations are analyzed. Therefore, Monte Carlo simulations are performed on the model inputs, and probabilistic distributions of the model results are given. Using Bayesian updating techniques, input data for the model is re-assessed, and updated model results that better fit measurements in the environment are presented.

Chapter 2:

Improving Data Quality for Environmental Fate Models: A Least-Squares Adjustment Procedure for Harmonizing Physicochemical Properties of Organic Compounds

Urs Schenker, Matthew MacLeod, Martin Scheringer, Konrad Hungerbühler

Institute for Chemical and Bioengineering, ETH Zurich, CH-8093 Zurich, Switzerland

Keywords: partition coefficients, energies of phase transfer, internal consistency, polychlorinated biphenyls

Reproduced with permission from:
Environmental Science and Technology, 2005
Volume 39, Issue 21, pages 8434-8441
DOI: http://dx.doi.org/10.1021/es0502526

Abstract

Physicochemical properties (vapor pressure, aqueous solubility, octanol solubility, Henry's law constant, and octanol−air and octanol−water partition coefficients) and their temperature dependencies are required for fate modeling of environmental pollutants. To be internally consistent, measured values for these properties often must be adjusted. The goal of adjusting the property values for consistency is to more accurately estimate the true values. However, consistency and accuracy are not synonymous. If there are systematic errors in one property, then adjustment for consistency may reduce the accuracy of other property data. Here, we provide methods for achieving consistency and improving accuracy in the selection of partitioning properties from literature sources. First, we show that a widely used procedure does not always minimize the adjustments of property values derived from the literature when harmonizing them according to thermodynamic constraints. In such cases, the final adjusted values (FAVs) are unnecessarily different from the literature-derived values (LDVs) selected from measurements. We present an improved procedure based on the theory of least squares that minimizes the adjustment of LDVs and allows quantitative propagation of uncertainty from LDVs to FAVs. When this procedure is applied to partitioning properties for 30 organic chemicals, FAVs obtained differ by up to 30% from those calculated with the current adjustment procedure. Second, we point out that the adjustment procedure is only appropriate for correcting random errors in measurement data. Biased LDVs must be identified and corrected prior to harmonization. Using a set of 16 PCB congeners as a case study, we provide methods to identify biased data and discuss possible sources of bias. We present a new interpretation of property data for the PCBs and a new set of internally consistent properties and quantitative structure-property relationships that we recommend as the best currently available.

2.1 Introduction

The distribution of organic chemicals between environmental media is a key factor in determining their risk and hazard profiles. For a system consisting of air, water, and soil, the partitioning can be quantitatively described by a set of three solubilities: solubility in air (S_A), which can be derived from the vapor pressure (P) as $S_A = P/(R \times T)$, solubility in water (S_W), and solubility in octanol (S_O), assuming partitioning into soil is dominated by organic matter that can be represented by octanol. (R is the gas constant and T the absolute temperature.) If ideal solute−solvent interactions are assumed, then the ratios of these solubilities are a set of equilibrium partition coefficients: the air−water partition coefficient (K_{AW}; the dimensionless form of the Henry's law constant), the octanol−water partition coefficient (K_{OW}), and the octanol−air partition coefficient (K_{OA}).

Accurate measurement of solubilities and partition coefficients is a challenge, particularly for semivolatile organic chemicals that have properties near the extreme limits of analytical techniques. Pontolillo and Eganhouse (2001) reviewed data on aqueous solubility and octanol−water partition coefficients for DDT and DDE. They found high variability in reported values and reporting errors that raise questions about the quality of the available data. They recommended improvement of measurement and reporting techniques to increase the reliability of reported physicochemical properties of hydrophobic organic compounds.

A contribution to improving data quality has been made by Cole and Mackay (2000) who pointed out that partitioning data could be evaluated for consistency by using relationships linking the solubilities in air, water, and octanol and the three partition coefficients. Their "three-solubility" approach allows missing property data to be estimated and can identify inconsistencies in reported values. Energies of phase transition (ΔU) that describe the temperature dependence of partition coefficients and solubilities must conform to similar constraints as the partition coefficients.

The equations given by Cole and Mackay provide information about the relationships between partitioning properties of ideal substances. That information is used when adjusting a data set for consistency. However, there is an infinite number of consistent data sets. Our approach is based on the premise that the most accurate set of data is the internally consistent values that are minimally adjusted from measured values while taking into account the relative uncertainties in measurements of each property. The more accurately known

properties are given a higher weight in the adjustment procedure than those known with less accuracy. Beyer et al. (2002) have developed an adjustment procedure that aims at finding this optimal data set by assigning each property value an uncertainty factor and adjusting the values iteratively. They illustrated their procedure using partitioning data for 52 organic compounds.

The adjustment procedure developed by Beyer et al. requires a single literature-derived value (LDV) and an uncertainty factor for each property as inputs. The LDV is then adjusted into consistency with other measurements to derive a final adjusted value (FAV). Li et al. (2003) provide guidelines for estimating LDVs and corresponding uncertainty factors from measurement data in the literature in their case study of 16 PCBs. Their method has been applied to hexachlorocyclohexane isomers by Xiao et al. (2004) and organochlorine pesticides by Shen and Wania (2005). As described by Li et al., when a given property of a specific chemical has been measured by several laboratories with different techniques, the selection of LDVs from available data is a somewhat subjective process. Therefore, LDVs derived by different analysts from the same source data are likely to differ to some extent.

The goal of adjusting partitioning properties for internal consistency is to improve the accuracy of the data used in environmental fate modeling and in hazard and risk assessments. However, property data that have been adjusted for consistency are not necessarily more accurate than the initial measurements: If there are systematic errors in data for one property, then adjustment to achieve consistency will reduce the accuracy of other property data. We therefore propose that consistency and accuracy of physicochemical properties be addressed in parallel.

With respect to consistency, we provide a least-squares-based method that harmonizes property data by introducing smaller adjustments than those of the Beyer procedure. Although Beyer et al. (2002) state that their procedure aims to minimize the adjustment of LDVs, it does not include a mechanism to actually minimize the adjustments. Concerning accuracy, the theory of least-squares minimization dictates that the adjustment procedure can only be applied if errors in the LDVs are random. This condition has not been previously recognized, and it can be employed to select suitable LDVs from values reported in the literature. We propose criteria for the selection of LDVs that help to identify biased measurements and illustrate how biased data can, in some cases, be corrected prior to adjustment for consistency. In addition to systematic measurement error, we identify two

possible sources of bias in LDVs: (a) correction of vapor pressure and solubility measurements to the subcooled liquid state and (b) estimation of the influence of water dissolved in octanol on measurements of octanol−water and octanol−air partition coefficients.

In addition, the least-squares procedure presented here provides quantitative information about how uncertainty in LDVs propagates to uncertainties in the FAVs, which will improve communication of uncertainties associated with models using these data as inputs.

Using our improved methodology, we provide a new set of internally consistent partitioning data and energies of phase transition for 16 PCB congeners that in some cases differ significantly from previously reported values. We also provide a spreadsheet tool for applying the least-squares adjustment procedure to new data sets.

2.2 Least-Squares Adjustment Procedure

2.2.1 Theory

The three-solubility approach (Cole and Mackay, 2000) relies on harmonizing data describing solubilities in air, water, and octanol with equilibrium partition coefficients between these three solvents. It assumes ideal behavior of the solutions up to the solubility limit. The approach assumes that intermolecular interactions in the subcooled liquid are identical to those experienced by a dispersed molecule in solution in air, water, or octanol.

Intermolecular interactions within the solid phase influence the solubility of chemicals in a way that is not relevant to their partitioning when dispersed as individual molecules in a solvent. Therefore solubility data for solids must be corrected to the subcooled liquid state. The fugacity ratio (F) is the ratio of solubilities of the solid (S_S) and subcooled liquid state (S_L) (Schwarzenbach et al., 2003):

$$S_{AL} = S_{AS} / F \quad \text{(eq. 2.1)}$$

$$S_{WL} = S_{WS} / F \quad \text{(eq. 2.2)}$$

$$S_{OL} = S_{OS} / F \quad \text{(eq. 2.3)}$$

where the subscripts A, W, and O refer to air, water, and octanol as solvents, respectively. We discuss methods to estimate F below. For reasons of simplicity, the index L, referring to the subcooled liquid state, is henceforth omitted. Unless otherwise stated, solubilities refer to the subcooled liquid state.

A complication arises in the case of K_{OW} since it is measured as the partition coefficient between water saturated with octanol and octanol saturated with water. Whereas the solubility properties of octanol-saturated water are not markedly different from those of pure water, water-saturated octanol (wet octanol) has solubility properties significantly different from those of dry octanol (Pinsuwan et al., 1995). This introduces an inconsistency with measurements of the octanol−air partition coefficient based on dry octanol. Dry octanol has thus far been adopted as the reference solvent for adjusting partitioning properties for internal consistency (Cole and Mackay, 2000, Beyer et al., 2002). K_{OW} values based on wet octanol must therefore be converted into K_{OW}* values, where the asterisk indicates dry octanol. Beyer et al. (Beyer et al., 2002) derived an empirical relationship that is based on the ratio of solubilities in pure ocatanol and water that can be used to convert K_{OW} into K_{OW}*

$$\log(K_{OW}^*) = 1.35 \cdot \log(K_{OW}) - 1.58 \qquad \text{(eq. 2.4)}$$

This approach was also followed by Li et al., who derived values of 1.16 and 0.64 instead of 1.35 and 1.58 for a relationship based on PCB data.

2.2.2 Method

We present a procedure to calculate a set of consistent partitioning properties that are minimally adjusted from the selected LDVs according to their relative uncertainties. This procedure is based on the normal distribution theory and the theory of least squares. The method is used in the field of geodesy and was described in detail in 1872 by Helmert (1872) as an application of the least-squares theory of Gauss. Details can be found in Helmert (1872) or in modern geodesy textbooks (Mikhail and Ackermann, 1976, Hoepcke, 1980, Niemeier, 2001). Below we provide theory and mathematical development of the method as applied to the problem of harmonizing partitioning data.

In the simplest case where only partition coefficients have been measured, one equation relates the three LDVs

$$\log(K_{AW}) - \log(K_{OW}^*) + \log(K_{OA}) = w \qquad \text{(eq. 2.5)}$$

where w (denoted by ε in Beyer et al. (2002)) is the misclosure error. If the LDVs for the partition coefficients are internally consistent, then w is zero, but in general this is not the case. The aim of the adjustment procedure is to calculate a set of consistent parameters (the FAVs, denoted by a bar). By definition, the misclosure error w is 0 in a consistent data set

$$\overline{\log(K_{AW})} - \overline{\log(K_{OW}^*)} + \overline{\log(K_{OA})} = 0 \qquad \text{(eq. 2.6)}$$

The LDVs and FAVs are linked by the adjustments v_i

$$\overline{\log(K_{\mathrm{AW}})} = \log(K_{\mathrm{AW}}) - v_1 \qquad \text{(eq. 2.7)}$$

$$\overline{\log(K_{\mathrm{OW}}^*)} = \log(K_{\mathrm{OW}}^*) - v_2 \qquad \text{(eq. 2.8)}$$

$$\overline{\log(K_{\mathrm{OA}})} = \log(K_{\mathrm{OA}}) - v_3 \qquad \text{(eq. 2.9)}$$

In the special case when relative uncertainties in the measured partition coefficients are equal, one obtains from eq. 2.5 to eq. 2.9

$$v_1 - v_2 + v_3 = w \ . \qquad \text{(eq. 2.10)}$$

The set of FAVs deviating minimally from the LDVs is found by minimizing the sum of squares of v_1, v_2, and v_3 under the condition of eq. 2.10. For this purpose, the Lagrange theorem for minimizing an equation under a constraint is applied. (The function Ω is called the Lagrangian and $2k$ the Lagrange multiplier.)

$$\Omega = {v_1}^2 + {v_2}^2 + {v_3}^2 - 2 \cdot k\left(v_1 - v_2 + v_3 - w\right) \qquad \text{(eq. 2.11)}$$

The minimizing condition is that the partial derivatives of Ω with respect to all v_i are equal to 0. This condition is fulfilled by

$$v_1 = -v_2 = v_3 = k = \frac{w}{3} \qquad \text{(eq. 2.12)}$$

Combined with eq. 2.7 to eq. 2.9, these v_i allow the FAVs to be calculated. The procedure can be extended to account for different relative uncertainties in the LDVs. In that case, the sum of squares weighted with the inverses of the LDVs different variances is minimized.

The procedure can further be applied to a system of coupled equations. If LDVs for all three solubilities and all three partition coefficients are available, then the thermodynamic constraints can be written as

$$\log(S_{\mathrm{A}}) - \log(S_{\mathrm{W}}) - \log(K_{\mathrm{AW}}) = w_1 \qquad \text{(eq. 2.13)}$$

$$\log(S_{\mathrm{A}}) - \log(S_{\mathrm{O}}) + \log(K_{\mathrm{OA}}) = w_2 \qquad \text{(eq. 2.14)}$$

$$\log(S_{\mathrm{W}}) - \log(S_{\mathrm{O}}) + \log(K_{\mathrm{OW}}^*) = w_3 \qquad \text{(eq. 2.15)}$$

If one or more LDV is missing, then these three equations can be combined with each other to express suitable constraints. For instance, if data on S_{O} are missing, then eq. 2.14 can be subtracted from eq. 2.15 to obtain two equations relating the five available LDVs. In the first

part of the Supporting Information, we provide mathematical details to treat the problem when data for all properties are known.

2.2.3 Comparison of the Least-Squares Method to the Beyer Method

Beyer et al. (2002) describe an analytical and an iterative adjustment procedure. Only the iterative procedure has been used by other authors (Li et al., 2003, Xiao et al., 2004). Similarities and differences between the adjustment procedures are analyzed in the Supporting Information. All three adjustment procedures are equivalent if there are only data to specify one equation linking the chemical properties. This is the case for 22 of the 52 chemicals assessed by Beyer et al.

When the new least-squares procedure is applied to the data presented by Beyer et al. for the remaining 30 chemicals for which sufficient data are available so that two or three equations relate the property values, the sum of squares of the adjustments is always smaller with the least-squares method than that with the Beyer iterative method (Figure 2.1). The adjustments of each LDV in the cases of 1,2,3,4-tetrachlorodibenzodioxin (1,2,3,4-TCDD) and PCB-52 (in nonlog units) are also compared in Figure 2.1. Both methods adjust the properties of the two chemicals in the same direction; however the extent of the adjustments is different.

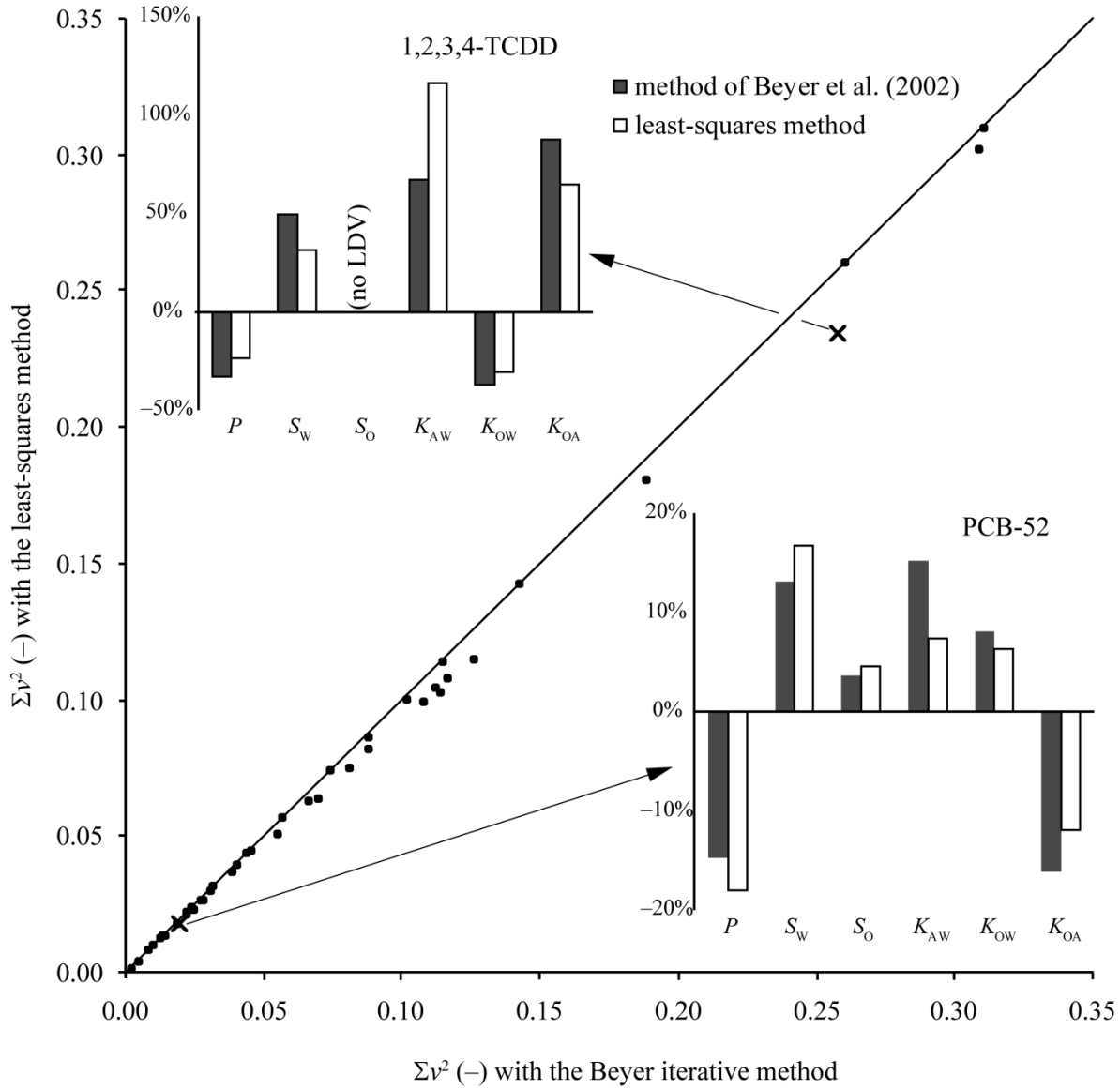

Figure 2.1: Sum of squares of the adjustments applied to LDVs to achieve internal consistency (Σv^2), calculated with the method of Beyer et al. and the least-squares method. For all chemicals, the sum of squares of adjustments from the least-squares method is smaller than that from the Beyer method. The small figures show the percentage adjustments of the LDVs of the physicochemical properties of 1,2,3,4-TCDD and PCB-52.

As illustrated in the Supporting Information, the least-squares method allows variance in the FAVs to be propagated to variance in the LDVs. Because of the additional information gained from the relationships between the properties, variance in the FAV always decreases relative to the corresponding LDV, typically by 30-50%. If the LDV of one property has a high variance compared to the other properties, then the FAV of that property also has a higher variance than FAVs of other properties.

2.3 Application of the Least-Squares Adjustment Procedure to PCBs

Li et al. (2003) have compiled PCB property data based on a review of 80 publications. They have estimated LDVs for partitioning data and energies of phase transition for 16 PCB congeners and applied the Beyer iterative adjustment procedure to derive FAVs. We rely on their summaries of reported data for properties of the PCBs and reinterpret the data using the least-squares adjustment procedure and new quality criteria for LDVs.

Li et al. have attributed uncertainty factors to all chemical properties according to quantitative and qualitative criteria. Those include the number of reported values, the correlation coefficients of the regressions of properties against temperature, knowledge about the measurement methodology, and an assessment of the general reliability of the data. We interpret their uncertainty factors as relative variances for the least-squares adjustment procedure. Thus, if the LDVs of two properties are assigned uncertainty factors of 1 and 4 respectively, by Li et al., then we assume the variance of the second property to be 4 times greater than that of the first property. This approach assumes the measurement errors to be normally distributed in log units.

Because the new adjustment procedure is based on the theory of least squares, the FAVs are the best approximation of the true values only if the differences between LDVs and the true values are due to random errors. The adjustment procedure cannot be used to compensate for systematic errors in the LDVs (Helmert (1872) page 76 or Mikhail and Ackermann (1976) page 68). If biased measurements are included in the adjustment procedure, then they will reduce the accuracy of values of other properties that are unbiased. We therefore examine the misclosure errors to assess if errors in the LDVs are randomly distributed. Because measurement errors of unbiased data have an expectation value of zero, the misclosure errors for unbiased data, which are the sum of the measurement errors, also have an expectation value of zero.

In the harmonization of energies of phase transitions presented by Li et al., LDVs, especially for ΔU_W and ΔU_{AW}, are uniformly adjusted across the homologous series either positively or negatively. This observation prompted us to examine the misclosure errors for the ΔU values in more detail.

Analogues to eq. 2.13 to eq. 2.15, which express the thermodynamic constraints for partitioning data, can be written for the internal energies of phase transition. However, for all but one congener, there is no LDV for the energy of phase change for dissolution in octanol (ΔU_O). Therefore, misclosure errors based on these equations can only be calculated for one congener. Taking the sum of the ΔU analogues to eq. 2.13 to eq. 2.15 yields a new equation (eq. 2.17) where ΔU_O does not appear. Thus, the following two independent equations are selected to calculate the misclosure errors for energies of phase transition of the PCBs

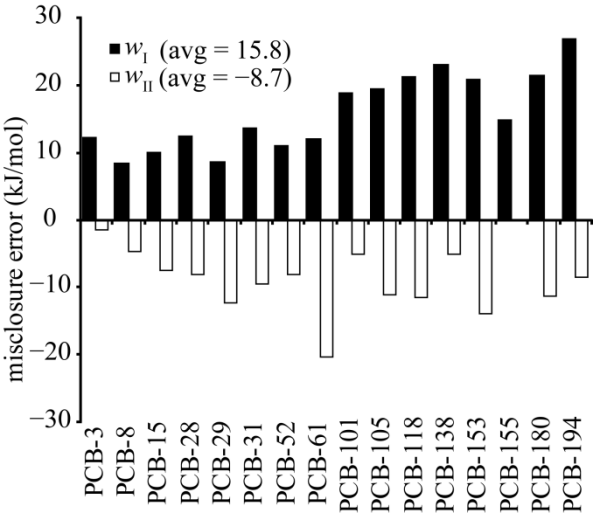

Figure 2.2: Misclosure errors w_I and w_{II} in the energies of phase transition for the PCBs as reported by Li et al. (2003). Neither of the two misclosure errors has an average value of zero.

$$\Delta U_A - \Delta U_W - \Delta U_{AW} = w_I \qquad \text{(eq. 2.16)}$$

$$\Delta U_{AW} - \Delta U_{OW} + \Delta U_{OA} = w_{II} \qquad \text{(eq. 2.17)}$$

Figure 2.2 displays the misclosure errors in the energies of phase transition for the 16 PCB congeners obtained with the LDVs suggested by Li et al. Neither of the two misclosure errors w_I and w_{II} has an average near zero, and values are consistently positive or negative across the series of PCBs. This is evidence of a bias in values of one or more of these properties. In our view, it is inappropriate to apply the adjustment procedure to this set of LDVs, and the LDVs should be reviewed. We present an alternative selection of LDVs based on the literature data summarized by Li et al.; in particular, we suggest alternative values for ΔU_{AW} and ΔU_W.

Li et al. (2003) reviewed ΔU_{AW} values from three studies (Burkhard et al., 1985a, Burkhard et al., 1985b, ten Hulscher et al., 1992). The LDVs for 14 of the 16 congeners were taken from the data reported by Burkhard et al. (1985b) (ref. 13 in Li et al. (2003)) but adjusted with a calibration factor of 0.846. This factor is the ratio of the ΔU_{AW} values for PCB-28 and PCB-52 in Burkhard et al. (1985a) (ref. 79 in Li et al., 2003) and in ten Hulscher et al. (1992) (ref. 11 in Li et al., 2003). Li et al. used the calibration factor to bring the larger set of ΔU_{AW} values estimated by Burkhard et al. (1985b) into agreement with the more recent

measurements reported in ten Hulscher et al. (1992). For PCB-28 and PCB-52, Li et al. selected the measured ΔU_{AW} values from ten Hulscher et al. (1992) as LDVs.

However, Burkhard et al. (1985b) do not report actual measurements of the energies of phase change of the air−water partition coefficient, ΔU_{AW}. Instead, they report estimates of ΔU_{AW} inferred from information about the temperature dependence of vapor pressure and water solubility. Thus, the values of ΔU_{AW} reported by Burkhard et al. (1985b) and used by Li et al. (2003) are in fact values of $(\Delta U_A - \Delta U_W)$. For the adjustment procedure, these data should be split up and included in the calculation of LDVs for ΔU_A and ΔU_W. However, Burkhard et al. (1985b) do not provide their individual ΔU_A and ΔU_W values.

Therefore, we treat the $(\Delta U_A - \Delta U_W)$ values reported by Burkhard et al. (1985b) as representative of ΔU_{AW} for congeners without agreed upon measurement data; we denote these values by ΔU_{AW}*. This approach is appropriate if (a) the estimated variance of ΔU_{AW}* has been correctly derived from the variances of ΔU_A and ΔU_W and (b) the estimates of ΔU_A and ΔU_W used by Li et al. and Burkhard et al. are not taken from the same sources, in which case these data would be given too much weight by appearing in two forms in the three-solubility equations. None of the references for ΔU_W used by Li et al. was also used by Burkhard et al. There are 14 congeners without agreed upon measurements of ΔU_{AW}. In the compilation of ΔU_A values for three of these congeners, one out of the four references used by Li et al. was also used by Burkhard et al. For the other 11 congeners, Li et al. and Burkhard et al. used entirely different sources. We therefore judge that the ΔU_{AW}* data presented by Burkhard et al. provide independent information that can be included in the adjustment procedure.

As stated above, the ΔU_{AW}* values reported by Burkhard et al. were calibrated with a factor of 0.846 by Li et al. to derive their LDVs. If the uncalibrated values are inserted in the misclosure equations, then the averages of w_I and w_{II} across the homologous series shift considerably toward zero (to values of 5.67 and 0.25, from 15.8 and –8.7, respectively). Therefore, the values originally reported by Burkhard et al. (1985b) better fulfill the thermodynamic constraints. The calibration factor used by Li et al. appears to introduce a bias relative to reported values of ΔU_A, ΔU_W, ΔU_{OW} and ΔU_{OA}.

The w_I misclosure error can be further reduced by re-evaluating the fugacity ratios used by Li et al. Vapor pressure and solubility in water and octanol of the PCBs have often been measured for the solid state, whereas the properties of the subcooled liquid are required for the adjustment procedure (van Noort, 2004). Li et al. estimate the fugacity ratio of the PCBs from the estimated entropy of fusion at the melting point (Schwarzenbach et al., 2003, page 123). Van Noort (2004) shows that this procedure assumes that both enthalpy and entropy of the solid-liquid transition are constant with temperature, and demonstrates that significant errors are possible due to this assumption. On the basis of measurements, van Noort provides empirical equations to calculate temperature-dependent entropies of fusion and fugacity ratios for chlorobenzenes, PAHs, and other chlorinated compounds. He suggests that these equations can also be used to calculate fugacity ratios of PCBs.

We have calculated temperature-dependent fugacity ratios using the method of van Noort (2004) for the PCBs and recalculated subcooled liquid-state water and octanol solubilities and vapor pressures for the measurements that were based on the solid state. In the Supporting Information, Table 9.23 compares fugacity ratios according to Li et al. (2003) and van Noort and shows our new values for water and octanol solubility and vapor pressure. Because the fugacity ratio calculated with the van Noort method is temperature-dependent, the ΔU_A and ΔU_W values calculated from the original measurement data are particularly affected by this correction.

Concerning ΔU_W, the energy of the phase transition for dissolution of the subcooled liquid in water, Li et al. have reported only six measured values. For the other congeners, they estimated LDVs as the average of the six measured values. Following Cole and Mackay (2000), we did not attempt to estimate LDVs for congeners for which no measurements or independently calculated data were available. Instead, we deduced FAVs for ΔU_W from the FAVs for the other energies of phase transition derived from the adjustment procedure.

Finally, the LDVs for ΔU_{OW} reported by Li et al. are estimated from measurements for three PCB congeners (Lei et al., 2000) and data for other chlorinated organic chemicals. We treat these LDVs as calculated values of ΔU_{OW} and include them in the adjustment procedure with a high estimate of relative variance since they have been extrapolated from very limited data.

When we insert our new LDVs for ΔU_A, ΔU_W, and ΔU_{AW} in eq. 2.16 and eq. 2.17, then misclosure errors illustrated in Figure 2.3 are obtained. Averages of w_I and w_{II} across the series of PCBs are much smaller in absolute value than those derived from the LDVs selected by Li et al., and positive and negative values are found for both misclosure errors. The evidence of bias in the misclosure errors illustrated in Figure 2.2 has been eliminated, and therefore this set of LDVs is more appropriate as a starting point for the adjustment procedure. Our selected LDVs for all quantities are given in Table 9.7 and Table 9.8 in the Supporting Information.

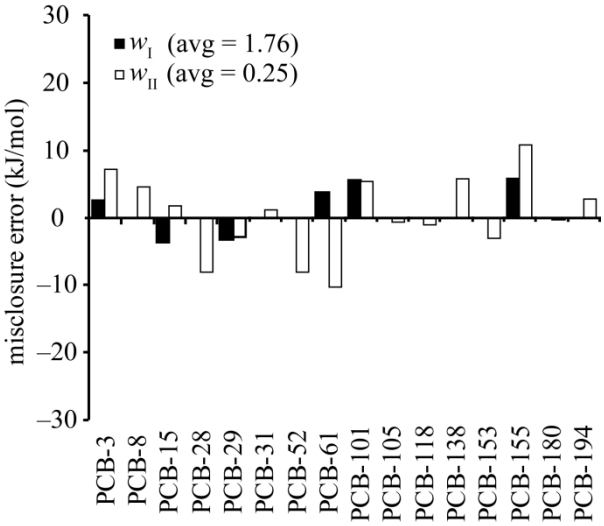

Figure 2.3: Misclosure errors w_I and w_{II} obtained with new LDVs. Where no w_I (black bars) is shown, there is no ΔU_W data available to calculate w_I. The misclosure errors have an average closer to zero and no obvious bias.

Table 2.1 and Table 2.2 present the FAVs of partitioning properties and energies of phase change for the PCB data set. The new values differ from those presented by Li et al. by more than 15% in 17% of the cases for the partitioning properties (in non-log scales) and in 25% of the cases for the energies of phase transition. This is also illustrated by the plots of quantitative structure-property relationships (QSPR) presented in Figure 2.4 and Figure 2.5. Such plots, relating chemical partitioning properties to molar mass, have also been presented by Li et al., and we have therefore included the relationships that they derived: The solid lines represent the linear regressions of our new FAVs versus molar mass, and the dashed lines represent the linear regressions for the FAVs of Li et al. Differences are small for the partition coefficients and solubilities (within the confidence interval given by Li et al.) but are in some cases large for the energies of phase transition. The values for ΔU_{AW} have been shifted up because the calibration factor applied by Li et al. has been removed and the slope of the ΔU_W relationship is steeper.

Table 2.1: FAVs of the PCB partitioning properties calculated with LDVs from Table 9.7 in the Supporting Information.

	$\log S_A$ (mol/m³)	$\log S_W$ (mol/m³)	$\log S_O$ (mol/m³)	$\log K_{AW}$ (–)	$\log K_{OW}$* (–)	$\log K_{OA}$ (–)	P (Pa)	$\log K_{OW}$ (–)
PCB-3	–3.75	–1.70	3.01	–2.06	4.71	6.77	4.38×10^{-1}	4.61
PCB-8	–4.25	–2.19	3.10	–2.06	5.29	7.35	1.39×10^{-1}	5.11
PCB-15	–4.70	–2.53	3.04	–2.17	5.57	7.74	4.95×10^{-2}	5.35
PCB-28	–4.98	–3.05	2.87	–1.93	5.92	7.86	2.58×10^{-2}	5.66
PCB-29	–4.74	–2.86	3.06	–1.88	5.92	7.80	4.49×10^{-2}	5.65
PCB-31	–4.99	–3.12	2.95	–1.87	6.07	7.94	2.54×10^{-2}	5.78
PCB-52	–5.33	–3.37	2.89	–1.96	6.26	8.22	1.15×10^{-2}	5.95
PCB-61	–5.59	–3.51	2.97	–2.08	6.48	8.56	6.41×10^{-3}	6.14
PCB-101	–6.06	–3.99	2.77	–2.08	6.76	8.83	2.15×10^{-3}	6.38
PCB-105	–6.44	–4.05	3.18	–2.39	7.22	9.62	8.98×10^{-4}	6.78
PCB-118	–6.45	–4.09	2.99	–2.36	7.08	9.44	8.88×10^{-4}	6.65
PCB-138	–6.67	–4.70	3.00	–1.97	7.70	9.67	5.33×10^{-4}	7.19
PCB-153	–6.65	–4.52	2.79	–2.13	7.31	9.45	5.51×10^{-4}	6.86
PCB-155	–5.89	–4.50	3.22	–1.39	7.72	9.11	3.20×10^{-3}	7.21
PCB-180	–7.27	–4.77	2.89	–2.51	7.66	10.17	1.32×10^{-4}	7.15
PCB-194	–8.07	–5.29	3.07	–2.77	8.36	11.13	2.12×10^{-5}	7.76

Table 2.2: FAVs of the energies of phase transition calculated with LDVs from Table 9.8 in the Supporting Information.

	ΔU_A (kJ/mol)	ΔU_W (kJ/mol)	ΔU_O (kJ/mol)	ΔU_{AW} (kJ/mol)	ΔU_{OW} (kJ/mol)	ΔU_{OA} (kJ/mol)
PCB-3	69.8	16.9	1.52	52.9	–15.3	–68.3
PCB-8	70.6	15.7	–3.31	54.9	–19.0	–73.9
PCB-15	75.0	19.5	–3.26	55.5	–22.8	–78.3
PCB-28	77.1	25.3	–1.28	51.8	–26.6	–78.4
PCB-29	75.3	16.5	–7.25	58.7	–23.8	–82.5
PCB-31	77.0	18.0	–3.42	59.0	–21.5	–80.4
PCB-52	77.7	23.9	–3.60	53.8	–27.5	–81.3
PCB-61	85.0	19.5	–8.06	65.5	–27.5	–93.1
PCB-101	84.1	18.9	–0.329	65.2	–19.3	–84.4
PCB-105	88.6	23.5	–0.921	65.1	–24.4	–89.5
PCB-118	90.4	25.2	0.609	65.2	–24.5	–89.8
PCB-138	93.9	29.2	7.03	64.7	–22.2	–86.9
PCB-153	91.8	23.6	–2.99	68.2	–26.6	–94.8
PCB-155	92.4	24.8	5.48	67.6	–19.4	–86.9
PCB-180	94.1	25.1	–1.08	69.0	–26.1	–95.2
PCB-194	101	30.9	4.90	70.1	–26.0	–96.1

In Figure 2.4 and Figure 2.5, we have correlated physicochemical properties with molar mass. In addition, the number of orthochlorines in a PCB molecule influences some of the properties of PCBs (Falconer and Bidleman, 1994, Huang and Hong, 2002, Li et al., 2003). We therefore present two-parameter regressions for all of the physicochemical properties in the Supporting Information (Table 9.12). Including the number of orthochlorines improves the correlation coefficients (R^2) for vapor pressure, K_{AW}, K_{OA}, and ΔU_{OA}. If those four properties need to be estimated for compounds that are not included in the present data set, then we recommend that two-parameter regressions as presented in the Supporting Information be used.

The K_{AW} and ΔU_{AW} data presented here are in some cases not consistent with the measurements reported by Bamford et al. (2000). The Bamford et al. data have generated considerable controversy (Baker et al., 2004, Goss et al., 2004) and were not relied upon by Li et al. in their selection of LDVs for the PCBs. Because of the possibility of experimental error (Goss et al., 2004), our recommended LDVs also do not rely upon these data. However, Bamford et al. have presented the only direct measurements of ΔU_{AW} for many PCB congeners, and if their data can be corroborated by additional measurements using different techniques or by consistent measurements of ΔU_W and/or ΔU_{OW}, then this would significantly alter the LDVs and FAVs presented here.

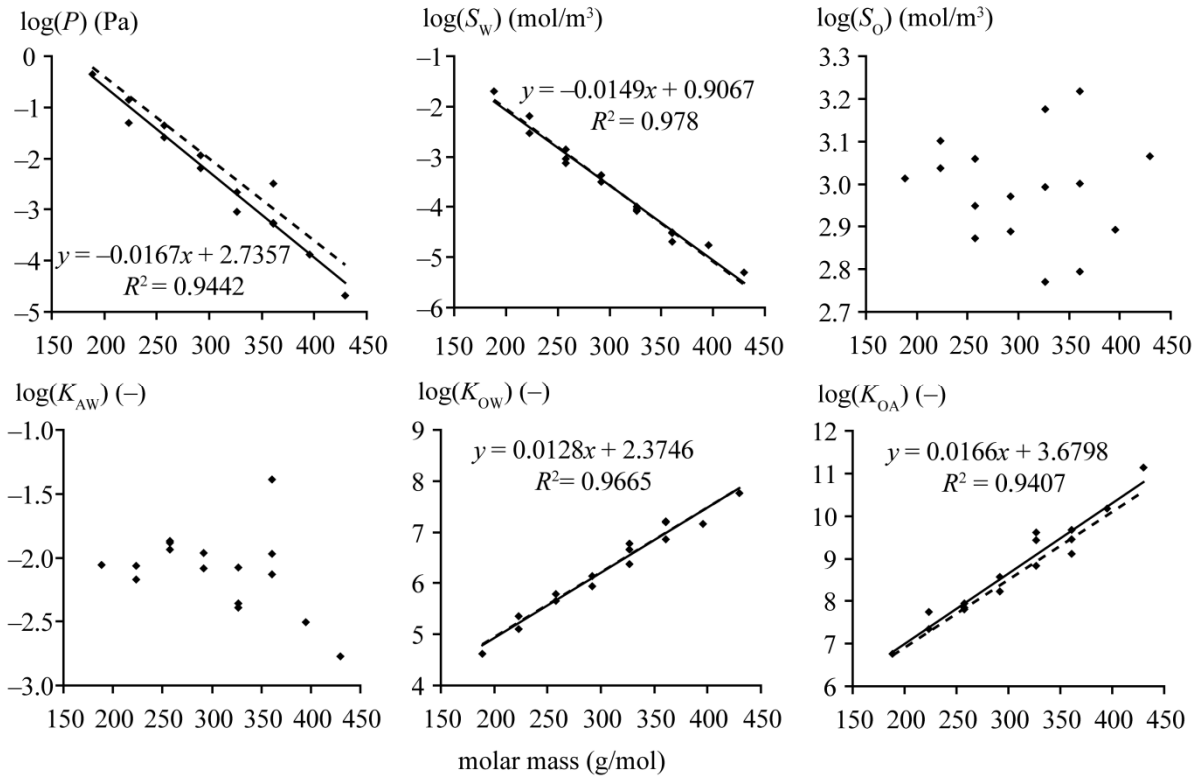

Figure 2.4: QSPR plots of the chemical properties of the PCB data set: solid lines, linear regressions of our new FAVs versus molar mass; dotted lines, regressions found by Li et al. (2003) with their FAVs.

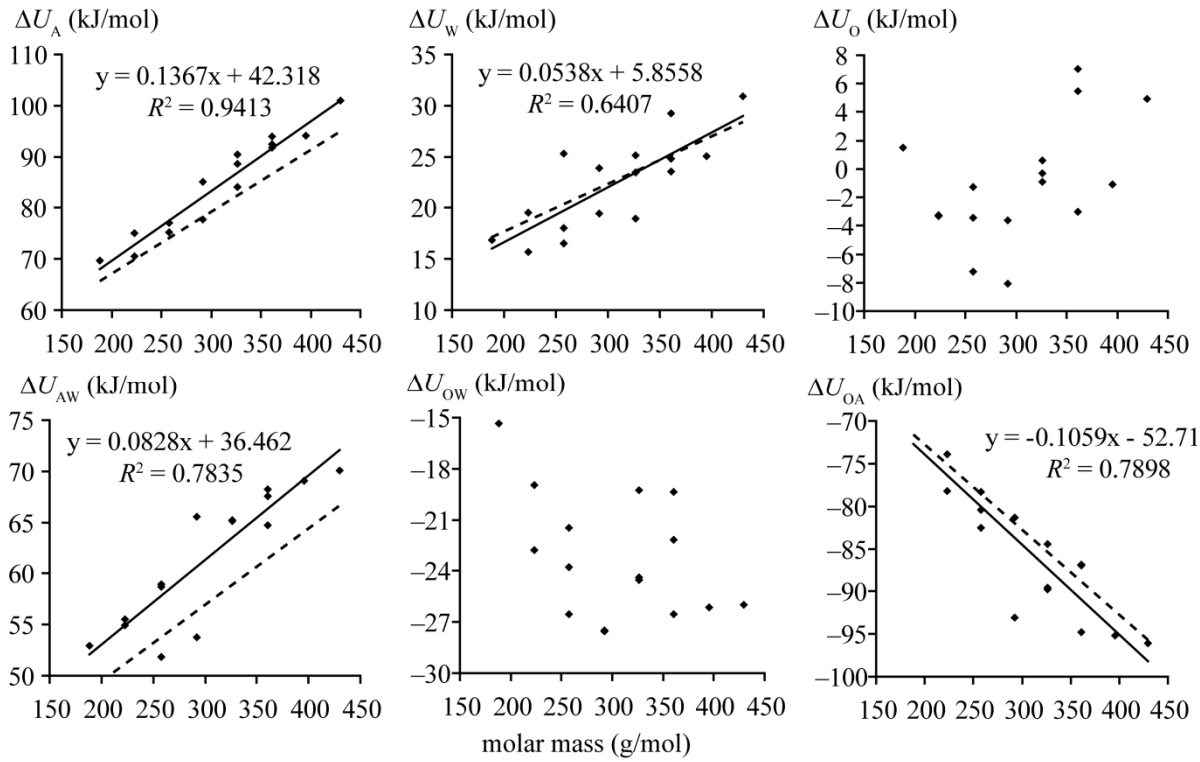

Figure 2.5: QSPR plots of the energies of phase transition of the PCB data set: solid lines, linear regressions of our new FAVs versus molar mass; dotted lines, regressions found by Li et al. (2003) with their FAVs.

The QSPR regression plots of our FAVs show increasing ΔU_W with increasing molar mass for the PCB congeners. The 95% confidence interval for the slope of this relationship lies between 0.04 and 0.08, indicating that the trend is statistically significant. However, the 95% confidence interval of the slope for the corresponding six LDVs (Table 9.8 in the Supporting Information) is between –0.12 and +0.17, implying no significant relationship between the LDVs for ΔU_W and molar mass. Thus the adjustment procedure introduces a relationship that is not evident in the available measurement data. As discussed by Baker et al. (2004), specific interactions between highly chlorinated PCBs and water may take place for which there is no evidence in the limited data on ΔU_W and ΔU_{OW} currently available. Measurements of ΔU_W and/or ΔU_{OW} for additional PCB congeners will help to resolve the current controversy over K_{AW} and ΔU_{AW} and reduce uncertainty in these values.

2.4 Discussion

Comparison with the least-squares method has shown that the Beyer adjustment procedure does not generally minimize the deviations of FAVs from LDVs when partitioning properties are adjusted for consistency. Minimal, uncertainty-weighted adjustments are obtained with the least-squares method presented in this paper; we provide an Excel spreadsheet on our homepage (Schenker et al., 2005b) to facilitate future calculations using this method. In this spreadsheet and in the Supporting Information, we also provide FAVs for the LDVs reported by Xiao et al. (2004) for hexachlorocyclohexane isomers and by Shen and Wania (2005) for organochlorine pesticides. We suggest that those values be used for modeling purposes, because they are optimally adjusted from their LDVs.

As shown in Figure 2.1, the least-squares adjustment procedure yields adjusted values that can be markedly different from the values calculated with the method by Beyer et al. The impact of the differences on results from multimedia models is difficult to predict in a general way. For PCB-52 the differences between adjustment methods are small, and we expect uncertainties in other modeling input parameters to be more influential. However, results for 1,2,3,4-TCDD demonstrate that the two methods can result in differences in individual property values on the order of a factor of 2, which could significantly alter model results.

There are some obvious advantages of the least-squares adjustment procedure. First, measurements of partitioning properties require considerable effort. If results from these

measurements are adjusted to achieve consistency, then no unnecessary changes should be introduced. Second, in the least-squares method variances can be quantitatively propagated from LDVs to FAVs. The ability to calculate variances of the FAVs allows one to perform more systematic uncertainty analyses of fate and exposure models. However, to take full advantage of the potential of the least-squares method, relative variances of the LDVs must be replaced by absolute values. We recommend that in the future, when physicochemical properties are measured, variances of these measurements also be determined and reported.

Another important and useful advantage of the least-squares method is that it provides criteria for selecting and evaluating LDVs for groups of chemicals. The goal of adjusting property values for consistency is to obtain values that are as accurate as possible by incorporating all available information. The theory of least-squares states that adjustment is only appropriate for correcting random measurement errors. If biased values for individual properties are included in the procedure, then other values could be made less accurate by forcing the values to be consistent. As illustrated here for the PCBs, LDVs that are not systematically biased can be obtained by interpreting measurement data with reference to the average value and distribution of the misclosure errors. Bias in selected LDVs is likely most easily recognized in a homologous series of chemical compounds where relationships between chemical properties and structural descriptors can be analyzed. However, it may also be possible to identify bias in data sets for unrelated chemical compounds if measurements using the same analytical technique can be collected.

Three possible sources of bias in LDVs are (a) systematic errors that might be inherent to certain measurement techniques and become discernible if data obtained with different techniques are compared, (b) bias introduced by the method selected to estimate properties for the subcooled liquid state from data for solid substances, and (c) bias caused by the method selected to account for the different properties of wet octanol compared to dry octanol. We discuss each of these possible sources of bias below and make recommendations for dealing with them.

It will sometimes be necessary to correct data sets for systematic differences between analytical techniques. However, whenever measurement data are calibrated care should be taken not to introduce a bias relative to other property data. This can be achieved by analyzing the impact of the calibration on the misclosure errors, as we have illustrated for the PCB data set above.

With respect to the correction of property data to the subcooled liquid state, continued theoretical and laboratory research will allow more accurate incorporation of the extensive number of property measurements that have been made for solids into three-solubility analyses. In this paper, the PCB data have been corrected with the temperature-dependent fugacity ratio as suggested by van Noort (2004), which reduced the averages of the misclosure errors especially for the energies of phase change. Ideally, the data reported by Beyer et al. should also be reanalyzed using temperature-dependent fugacity ratios. However, these data have additional important weaknesses, i.e., the uncertainty factors of the chemical properties are all assumed to be 1, and the LDVs are usually based only on one literature value. For these chemicals, we therefore have only recalculated FAVs with the least-squares method using the LDVs suggested by Beyer et al. These data are presented in the Supporting Information,Table 9.4, Table 9.5, and Table 9.6.

LDVs are also influenced by the method used to correct for the different solvent properties of wet and dry octanol. This correction is, in principle, always necessary to construct a consistent data set that includes K_{OW} data measured with wet octanol and K_{OA} and/or S_O measured with dry octanol. If the correction is not applied to our selected LDVs for PCBs, then the averages of the corresponding misclosure errors for the partitioning properties increase to 0.586 and 0.438 from 0.231 and 0.083, respectively. Therefore, there is more evidence of bias in the property data if the correction is not applied. No general method has yet been proposed to address the problem of the different properties of wet and dry octanol. Beyer et al. (2002) and Li et al. (2003) derived different corrections from data gathered for their compounds of interest; Xiao et al. (2004) and Shen and Wania (2005) did not apply a correction.

We suggest that the most sensible way of dealing with the problem of the different solvent properties of wet and dry octanol is to perform future measurements of K_{OA} and S_O with water-saturated octanol rather than dry octanol. This would eliminate the source of the inconsistency between these properties and K_{OW}. We believe this approach is advantageous because most empirical relationships between partitioning to octanol and partitioning to organic matter are derived from data based on K_{OW}, and thus, wet octanol. Even the often-cited Finizio et al. (1997) relationship between K_{OA} and the gas-particle partition coefficient is based partially on wet octanol, since some K_{OA} values used in the regression were calculated as the ratio of K_{OW}/K_{AW} without correcting for the different solvent properties of

wet and dry octanol. As measurements of K_{OA} and S_O based on wet octanol become available, it will be possible to perform three-solubility analyses of property data using a fully consistent set of solvents: wet octanol, water, and air.

In summary, the new least-squares adjustment procedure allows the calculation of internally consistent property values that are optimally adjusted from the LDVs. Because of the more stringent and explicit requirements of the least-squares method, it is now possible to more thoroughly evaluate the quality of LDVs and to identify and correct bias in property values prior to adjustment. The method also makes quantitative propagation of uncertainty through the adjustment procedure possible. We believe that the method will contribute to improved data quality for organic chemicals through (a) improving the best estimate of the chemical properties' true value, (b) providing insight into the quality of the experimental data, and (c) enabling quantitative analysis of uncertainty in the property values. Property data of higher quality − including accuracy, internal consistency and quantitative uncertainty ranges – will in turn support more reliable environmental fate and exposure modeling.

2.5 Acknowledgments

We thank Bertrand Merminod for literature recommendations, Werner Stahel for discussions about statistical issues, and Fabio Wegmann for helpful comments on the manuscript.

2.6 Supporting Information

Supporing Information is available in the appendix, chapter 9.1.

Chapter 3:

Including Degradation Products of Persistent Organic Pollutants in a Global Multi-Media Box Model

Urs Schenker, Martin Scheringer, Konrad Hungerbühler

Institute for Chemical and Bioengineering, ETH Zurich, CH-8093 Zurich, Switzerland

Keywords: arctic contamination potential; degradation products; environmental fate modeling; hazard assessment; organochlorine pesticides; persistence; spatial range; transformation products.

Reproduced from:
Environmental Science and Pollution Research, 2007
Volume 14, Issues 3, pages 145-152
DOI: http://dx.doi.org/10.1065/espr2007.03.398

Abstract

Goal, Scope and Background

Global multi-media box models are used to calculate the fate of persistent organic chemicals in a global environment and assess long-range transport or Arctic contamination. Currently, such models assume substances to degrade in one single step. In reality however, intermediate degradation products are formed. If those degradation products have a high persistence, bioaccumulation potential and / or toxicity, they should be included in environmental models. The goal of this project was to gain an overview of the general importance of degradation products for environmental fate models, and to expand existing exposure-based hazard indicators to take degradation products into account.

Methods

The environmental fate model CliMoChem was modified to simultaneously calculate a parent compound and several degradation products. The three established hazard indicators of persistence, spatial range and arctic contamination potential were extended to include degradation products. Five well-known pesticides were selected as example chemicals. For those substances, degradation pathways were calculated with CATABOL, and partition coefficients and half-lives were compiled from literature.

Results

Including degradation products yields a joint persistence value that is significantly higher than the persistence of the parent compound alone: in the case of heptachlor an increase of the persistence by a factor of 58 can be observed. For other substances, the increase is much smaller (4% for α-HCH). The spatial range and the arctic contamination potential (ACP) can increase significantly, too: for 2,4-D and heptachlor, an increase by a factor of 2.4 and 3.5 is seen for the spatial range. However, an important increase of the persistence does not always lead to a corresponding increase in the spatial range: the spatial range of aldrin increases by less than 50%, although the persistence increases by a factor of 20 if the degradation products are included in the assessment. Finally, the arctic contamination potential can increase by a factor of more than 100 in some cases.

Discussion

Influences of parent compounds and degradation products on persistence, spatial range and ACP are discussed. Joint persistence and joint ACP reflect similar characteristics of the total environmental exposure of a substance family (i.e., parent compound and all its degradation products).

Conclusions

The present work emphasizes the importance of degradation products for exposure-based hazard indicators. It shows that the hazard of some substances is underestimated if the degradation products of these substances are not included in the assessment. The selected hazard indicators are useful to assess the importance of degradation products.

Recommendations and Perspectives

It is suggested that degradation products be included in hazard assessments to gain a more accurate insight into the environmental hazard of chemicals. The findings of this project could also be combined with information on the toxicity of degradation products. This would provide further insight into the importance of degradation products for environmental risk assessments.

3.1 Introduction

Persistent organic pollutants (POPs) are chemicals that are persistent in the environment, subject to long-range transport, bioaccumulate in humans and animals, and impact human health and the environment. In the Stockholm Convention on Persistent Organic Pollutants (United Nations Environmental Program, 2008), some of the most dangerous POPs are regulated.

Multi-media box models have been developed to understand and possibly predict the behavior of existing and new chemicals in the environment (Mackay and Paterson, 1991, Wania and Mackay, 1995, Scheringer, 1996). Such models simulate how chemicals behave in the different environmental media, and aim at predicting how long such substances will be present in the environment. Degradation in such models is generally the main removal pathway, and is usually assumed to take place in one step. In reality, however, degradation is known to occur in a series of transformations. Intermediate degradation products are formed and often have similar properties as the original substances (persistence, bioaccumulation potential, toxicity). Depending on the dynamics of the different transformation processes, such intermediate degradation products may accumulate in the system. If a degradation product is, at the same time, present in the environment in relevant quantities, has high bioaccumulation potential and toxicity, not taking this degradation product into account might lead to an underestimation of the hazard and risk of the parent compound (Boxall et al., 2004).

There are some multimedia box models currently available that include degradation products (Fenner et al., 2000, Fenner, 2001, Cahill et al., 2003). All of those are one-region models, i.e. they can be used for a regional environment only, or look at the whole globe as one single box with homogeneous properties. However, many chemicals are known to be distributed over large scales, and can be found in various regions of the globe, in particular in the Arctic (Arctic Monitoring and Assessment Program, 1998). It has been shown that the behavior of such chemicals is strongly influenced by the variable climatic conditions on earth: in the cold Arctic climates, degradation is slower, and vapor pressure lower, so that the chemicals accumulate in these regions (a behavior called ‘cold condensation’). To accurately reproduce such phenomena, unit world models are not suited, and zonally averaged models like CliMoChem (Scheringer et al., 2000, Wegmann, 2004) or GloboPOP (Wania and Mackay,

1995) and Global Circulation Models (Koziol and Pudykiewicz, 2001, Dachs et al., 2002, Leip and Lammel, 2004) have been developed.

However, none of these models take into account the impact of degradation products so far. As mentioned above, it is thus possible that the hazard and risk of such substances are not correctly identified. This is particularly important for substances like DDT or aldrin that are known to be globally distributed, and have degradation products that are known to be persistent, too: DDE, a known degradation product of DDT is frequently measured in the Arctic environment and biota, and often present at higher concentrations than the parent compound. Therefore, there is a strong need for a model that includes degradation products in the assessment of chemicals.

Here, we have integrated degradation products into the environmental fate model CliMoChem. Three established exposure-based hazard indicators have been expanded to include degradation products. With the example of five well-known insecticides and herbicides, it is shown that degradation products can contribute significantly to the overall hazard score of the parent compounds.

3.2 Material and Methods

3.2.1 Information on Degradation Pathways and Property Data of Degradation Products

Information on substance properties is generally scarce, especially when it comes to substances that have not been assessed in detail. This is particularly true for degradation products that are not produced and therefore less frequently studied. To reduce problems with data availability for this study, it was decided to rely on relatively well known substances. In addition, the substances had to be known to be globally distributed; otherwise an assessment with a simpler unit-world model would be sufficient. To fulfill these two conditions, we have selected five insecticides and herbicides that have been frequently used in the past and have been found at remote places in the global environment: DDT, aldrin, and heptachlor are three insecticides that have known, persistent degradation products (see following section for details), whereas α-HCH and 2,4-D, an insecticide and a herbicide, are not known to degrade into persistent degradation products.

For much of the input data used in this study we rely on QSAR software. It has been shown that results from QSAR models can be associated with considerable uncertainty. We are aware that this potential inaccuracy could lead to severely biased conclusions in this study if we tried to reproduce the exact behavior of a specific chemical in the real environment, or quantify the importance of a specific degradation product. Therefore, we do not attempt to make statements for individual substances here: our study aims at giving a general overview and at stressing the general importance of degradation products. For these purposes, the uncertainties of QSAR results are less problematic.

To describe the degradation pathways in the model, Fenner et al. (2000) have introduced the notion of 'fraction of formation', *ff*. The *ff* is the amount of a given degradation product that is formed from the degradation of a given amount of the parent compound. If one mole of DDT is degraded into one mole of DDE, then the *ff* for the DDT – DDE degradation would be one. If DDT is equally degraded into DDE and DDD, then the two *ff* would be 0.5 each. If 10% of the DDT is directly mineralized and the rest forms DDE, then the *ff* for DDT – DDE would be 0.9. Finally, if a molecule is split in two (for instance the two benzene rings might be separated), the sum of the fractions of formation can also be bigger than one. For this study, substances were usually degraded into one degradation product at a given step of the degradation, and therefore we have assumed the *ff* to be 0.9. Exceptions are DDT and aldrin, which both have *ff*s of 0.5 in water and soil, standing for equal degradation into DDE and DDD and into dieldrin and ald-deg1, respectively.

For each of the substances investigated, the degradation pathways had to be determined. Where possible, literature information was used. This was often the case only for the substances with known degradation products. For the substances without known degradation products, and to complement literature information, QSAR programs were used to predict the degradation pathways.

CATABOL (Jaworska et al., 2002) predicts possible transformation products formed by biodegradation of the parent compound. The CATABOL outputs have been very useful to determine the degradation pathways for poorly known substances. This information was completed by the MSU database (Schmidt, 1996, Ellis et al., 2006) which also predicts the most probable biodegradation products. A degradation pathway is usually a long sequence of transformations. It would theoretically be possible to include every single degradation step until the full mineralization. However, it has been shown for unit world models (Fenner,

2001) that, in most of the cases, only the first two generations of degradation products have a significant impact on the overall hazard of the chemicals. Therefore, when deciding how many substances we should include in the degradation pathway, we have relied on the 'probabilities to be stable' output given by CATABOL. In the degradation pathways that we have selected for this assessment, we have retained only substances for which this probability was greater than 0. This was the case for between six (aldrin) and two (heptachlor) substances. The selected degradation pathways in soil are shown in Figure 3.1. Degradation pathways predicted by CATABOL are subject to considerable uncertainty. For aldrin, e.g., Paasivirta et al. (1988) have identified transformation products that are not indicated by CATABOL. We have, in this case, changed the pathways predicted by CATABOL to include pentachlorodieldrin, as suggested by Paasivirta et al. (1988).

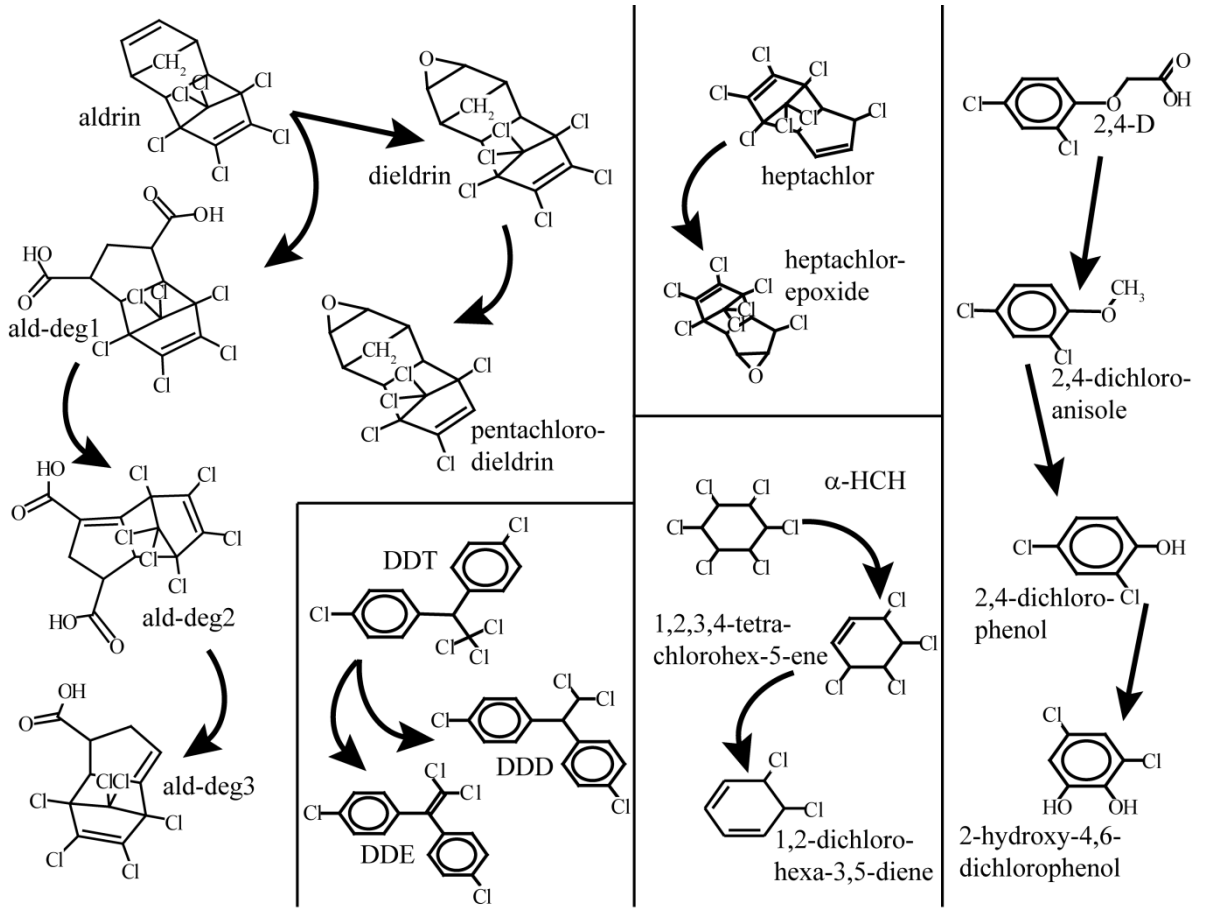

Figure 3.1: Degradation pathways for the five substances in this study.

Biodegradation is representative for the degradation processes in soil, and to a certain amount also in water and vegetation. In the atmosphere, OH radical reactions are the most important degradation pathway, and they do not necessarily form the same products as biodegradation. Unfortunately, there is to our knowledge no QSAR software available that would predict the

substances formed after OH radical reactions. Therefore, if no literature information was available, we have assumed that OH radical reactions always lead to total mineralization of the substance. This leads to an underestimation of the total hazard caused by those chemicals. This meant that α-HCH and 2,4-D were directly mineralized in atmosphere, and that the degradation products of dieldrin were mineralized in atmosphere, too. Aldrin, DDT, and heptachlor were degraded into dieldrin, DDE and heptachlor-epoxide with a fraction of formation of 0.9 (Crosby and Moilanen, 1977, Zepp et al., 1977, Buser and Müller, 1993, Bandala et al., 2002).

In addition to the degradation pathways degradation half-lives for all the substances had to be found for the different media. Sometimes such values are measured and reported (Mackay et al., 1997), but this is not usually the case for degradation products. Therefore, QSAR software was used to predict degradation half-lives if no reported values were available. AOPWin and BIOWin from the EPIWin software (U.S. Environmental Protection Agency, 2004) were used to calculate OH reaction rates and biodegradation half-lives. The degradation classes given by BIOWin were transformed into half-lives with the estimation procedure suggested by Arnot et al. (2005).

Table 3.1: Degradation half-lives ($T_{1/2}$), partition coefficients ($\log K_{OW}$, $\log K_{AW}$) and their temperature dependencies (ΔU_{OW}, ΔU_{AW}) for the substances used in this study.

	$T_{1/2}$ air (d)	$T_{1/2}$ water (d)	$T_{1/2}$ soil (d)	$\log K_{OW}$ (–)	$\log K_{AW}$ (–)	ΔU_{OW} (J/mol)	ΔU_{AW} (J/mol)
2,4-D	1.6	5	11	2.62	-6.08	-20’000	88’514
2,4-dichloroanisole	4.0	19	38	3.63	-1.70	-20’000	57’855
2,4-dichlorophenol	6.0	6	12	2.80	-4.33	-20’000	63’355
2-hydroxy-4,6-dichlorophenol	0.92	18	36	2.32	-8.06	-20’000	88’614
α-HCH	18.66	664	1327	3.88	-3.59	-20’000	73’164
1,2,3,4-tetrachlorohex-5-ene	0.32	36	71	3.68	-1.44	-20’000	59’352
1,2-dichlorohexa-3,5-diene	0.10	16	33	3.11	-0.70	-20’000	45’828
aldrin	0.36	80	160	6.25	-2.01	-20’000	98’023
dieldrin	1.1	238	475	5.49	-3.35	-20’000	105’214
pentachlorodieldrin	0.53	228	455	4.96	-3.13	-20’000	89’768
ald-deg1	1.0	78	157	3.67	-10.33	-20’000	137’538
ald-deg2	0.30	79	157	3.72	-10.62	-20’000	138’328
ald-deg3	0.15	140	279	4.99	-5.98	-20’000	109’893
DDT	15	844	1688	6.41	-3.31	-15’262	72’609
DDE	1.4	810	1621	6.94	-2.77	-50’815	47’125
DDD	2.5	804	1608	6.30	-3.74	-18’479	61’637
heptachlor	0.18	2444	4888	5.96	-1.78	-20’000	75’079
heptachlor-epoxide	2.1	1620	3239	5.40	-3.22	-20’000	82’382

Finally, partitioning information for all the substances had to be found. K_{OW} and K_{AW} values have been measured for a large number of substances, and such data has been assembled for pesticides by various authors (Beyer et al., 2002, Xiao et al., 2004, Shen and Wania, 2005). Here, we have taken an improved compilation of partitioning data and their temperature dependency by Schenker et al. (2005a). Again, partitioning data is usually unavailable for degradation products that were not known to be persistent. We have relied on QSAR software from the EPIWin package to extract raw values of K_{OW} and K_{AW}. Those values were adjusted with the least-squares adjustment procedure (Schenker et al., 2005a). Temperature dependencies were estimated with a method suggested by MacLeod et al. (2007).

Figure 3.1 shows the degradation pathways of the selected substances and Table 3.1 gives the degradation half-lives and the partitioning properties for the selected substances as they were used for the calculations in this paper. As mentioned above, DDT is simultaneously degraded into DDE and DDD in soil and water. In atmosphere, DDT is degraded into DDE only. Aldrin can be degraded in two different ways: either into dieldrin and then pentachlorodieldrin, or it can be degraded in three steps to more polar substances (ald-deg1 to ald-deg3). Heptachlor is degraded into heptachlor epoxide, and α-HCH is de-chlorinated in two steps. Finally, 2,4-D degrades into 2,4-dichloroanisole, and then in two steps into 2-hydroxy-4,6-dichlorophenol.

3.2.2 The CliMoChem Model

CliMoChem (Scheringer et al., 2000, Scheringer et al., 2004, Wegmann, 2004, Wegmann et al., 2006) is a zonally averaged multi-media box model. The model assembles a variable number of zones in the North-South direction (see Figure 3.2). Each of the zones represents one latitudinal band around the globe and is composed of an ocean-water, atmosphere, bare-soil, vegetation-soil and vegetation compartment. The model assumes a homogeneous distribution of the chemicals in the East-West direction. The model calculates environmental processes such as diffusive exchange between phases (partitioning), advective exchange between phases (wet deposition, runoff), transport between zones (wind, ocean-currents), and degradation. For each box (a compartment in a zone), mass-balance equations can be written to describe the exchange, transport, emission, and degradation processes (for details, see Scheringer et al., 2000). The mass-balance equations for a given substance in all the boxes can be summarized in a single differential equation with a square-matrix **S**, see eq. 3.1. **S** stores all the above mentioned processes for all the boxes in the model and has the size

(n_{zones} × $n_{compartments}$) × (n_{zones} × $n_{compartments}$); **c(t)** and d**c(t)**/dt are vectors with (n_{zones} × $n_{compartments}$) elements.

$$\frac{d\mathbf{c}(t)}{dt} = \mathbf{S} \cdot \mathbf{c}(t) \qquad \text{(eq. 3.1)}$$

Fenner et al. (2000) have shown how a series of chemicals can simultaneously be calculated with the above equations for a unit world model. This procedure can be applied as such for the case of a zonally averaged model and is reconstructed briefly here. For each substance *X*, the mass balance equations have to be established as mentioned above, leading to a series of $\mathbf{S}_X$ matrixes. To link the substances with each other, the $\mathbf{S}_X$ matrixes have to be written as blocks on the diagonal of a new $\mathbf{S}_{BIG}$ matrix. The non-diagonal blocks of the $\mathbf{S}_{BIG}$ matrix have to be filled with source matrixes. Those source matrixes contain on their diagonals the k_i degradation coefficients multiplied by the respective fractions of formation $ff_{i->j}$ (for the degradation of the parent compound *i* into the degradation product *j*, as described in the previous section).

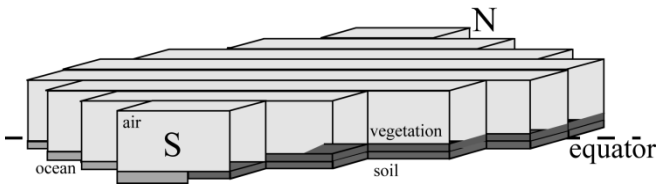

Figure 3.2: The geometry of the CliMoChem Model

3.2.3 Expanding Exposure-Based Hazard Indicators to Take Degradation Products into Account

Exposure-based hazard indicators have been developed to classify chemical substances according to their persistence, long-range transport potential and probability to accumulate in the Arctic.

At steady-state (with continuous emissions of a parent compound of *m*, in kg/day), the primary persistence (PP), as defined in Scheringer (1996), is the total mass of the parent compound in the system divided by the emission rate *m*. The primary persistence represents the overall residence time of the chemical in the system. In analogy, Fenner et al. (2000) have defined the joint persistence (JP) as the overall residence time of the parent compound and all its degradation products in the system. At steady-state, it can be calculated as the sum of the mass of the parent compound and all the degradation products divided by the emission rate *m* (of the parent compound). The 'contribution to joint persistence' (CJP) of the degradation products, finally, is the steady-state mass of a given degradation product, divided by *m*. It can easily be seen that the sum of the contributions to joint persistence of all the degradation

products, plus the primary persistence of the parent compound is equal to the joint persistence ($PP + \Sigma_i CJP_i = JP$). These concepts are equally valid for pulse emissions that we have worked with in this project.

The spatial range (Scheringer, 1997) serves to classify chemicals according to their long-range transport potential. It is defined as the 95% interquantile range of the geographical distribution of the time-integrated mass on a north−south transect of the earth, after an emission at the equator. A high spatial range signifies that a substance is highly mobile and will be transported far away from the usage areas. It has been shown that this concept can be expanded for degradation products, too (Quartier and Müller-Herold, 2000). In analogy to the joint persistence, we define here the joint spatial range as the 95% interquantile range of the sum of the time-integrated mass of the parent compound and all the degradation products. In analogy to the 'contribution to joint persistence', we define an indicator for the individual degradation products, too: the 'apparent spatial range' is defined as the 95% interquantile range of a given degradation product after the emission of the parent compound. This 'apparent spatial range' of a degradation product is not equal to the spatial range of the same substance if it were directly emitted at the equator. It can be shown that the joint spatial range must lie within the minimum and the maximum of the spatial range of the parent compound and the apparent spatial ranges of all the degradation products.

The arctic contamination potential (ACP) has been introduced to identify chemicals that are likely to accumulate in the Arctic (Wania, 2003). In the current project, we work with the exposure-ACP (eACP), as opposed to the mass-ACP (mACP) (see Wania, 2004). The eACP has been defined as the ratio of the mass of a chemical that is present in the Arctic surface media (excluding atmosphere), divided by the total emissions of the substance, after 1 year (eACP-1), and after 10 years (eACP-10). The emissions of the substances occur proportionally to the latitudinal population distribution over the globe. In analogy to the joint persistence and the joint spatial range, we define the joint eACP as the ratio of the total mass of the parent compound and the mass of all the degradation products, divided by the total emissions of the parent compound. Like the contribution to the joint persistence, the contribution to the joint eACP can be calculated for the degradation products. The joint eACP is again the sum of the eACP of the parent compound and the contributions to joint eACP of all the degradation products.

Table 3.2: Overview of the indicators for parent compounds, degradation products, and combined indicators for all the substances in the degradation pathway.

	indicator for the parent compound	indicator for a given degradation product	combined indicator for all substances in degradation pathway
persistence	primary persistence (PP)	contribution to joint persistence (CJP)	joint persistence (JP)
long-range transport potential	spatial range (SR)	apparent spatial range (ASR)	joint spatial range (JSR)
arctic contamination potential	eACP	contribution to eACP (CeACP)	joint eACP (JeACP)

All described indicators are sensitive to the medium to which the substance is emitted. In our case, all emissions were into atmosphere. An overview of the nomenclature of the different indicators for parent compounds, individual degradation products, and entire substance families is given in Table 3.2.

3.3 Results

3.3.1 Impact of Degradation Products on the Temporal Evolution of Concentrations

The temporal evolution of all the substances follows a similar pattern. As an example, Figure 3.3 displays the evolution of DDT and its degradation products DDE and DDD. It can be seen how the concentration of DDT decreases immediately after the pulse emission, and continues to decrease exponentially. The two degradation products DDE and DDD are present at low concentrations at the beginning and accumulate in the first years, as a result of the degradation of DDT. After about 3−4 years, their concentration has reached a peak, and they start to decrease, too, although at a slower rate than DDT. Eventually (after about 10 years), DDE and DDD are present at higher concentrations than DDT.

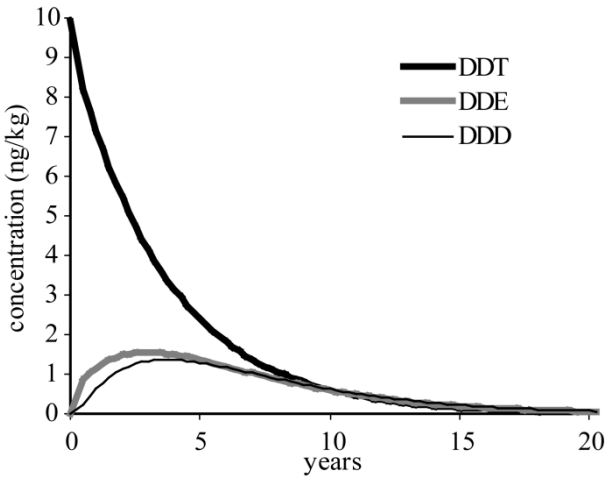

Figure 3.3: Evolution of the concentration of DDT and its degradation products after a pulse emission. The plot shows the evolution in the emission zone at the equator in soil as a function of time (in years).

For the other substance families, a similar behavior can be observed: for heptachlor, for instance, the degradation product is present at higher concentrations than the parent compound already after only a few months, because the half-life of heptachlor-epoxide is so much longer than the one of the parent compound. Later on, the concentration of the degradation product is several magnitudes higher than the concentration of the parent compound. In the environment, this would mean that the degradation product would be present in much higher concentrations than the parent compound (a finding that is confirmed, for instance, for measurements in Arctic atmosphere (Hung et al., 2005) or in temperate agricultural soils (Harner et al., 1999)).

3.3.2 Persistence

Figure 3.4 gives the persistence for the five parent compounds and their degradation products, and the joint persistence. It is clearly visible that the persistence of aldrin and heptachlor is significantly increased if their degradation products are included. The impact is still significant for the herbicide 2,4-D, but for DDT and especially α-HCH, the increase of the persistence is of less than a factor two. This is consistent for the case of α-HCH (a substance that is not known to have persistent degradation products), but surprising for DDT, as DDE is often cited as an example for an important degradation product. One reason why the hazard of DDE might be underestimated in our study is that the half-life in atmosphere for DDE is based on only one QSAR value from AOPWin (1.4 days). For DDT, in addition to the AOPWin value, several estimated and measured atmospheric half-lives were available (Moltmann et al., 1999, Liu et al., 2005, Mueller, 2005). These alternative values suggest a much slower degradation (20.9 days on average) than indicated by the AOPWin value for DDT (that is similar to the QSAR result of DDE: 3.1 days), and therefore the atmospheric half-life of DDT in our study is much higher than the one of DDE, see Table 3.1. If alternative values for the half-life of DDE were available, they would probably be significantly higher than the AOPWin value, too. This would significantly increase the contribution to joint persistence for DDE.

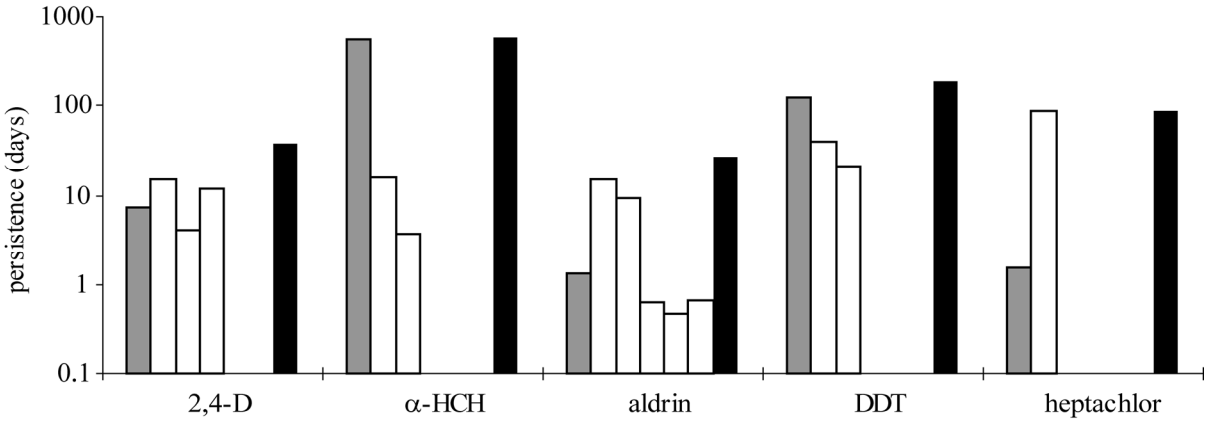

Figure 3.4: Persistence (in a log-scale) of the studied substances: parent compounds have gray bars, their degradation products white bars, and the joint persistence of the whole substance family is given in black bars.

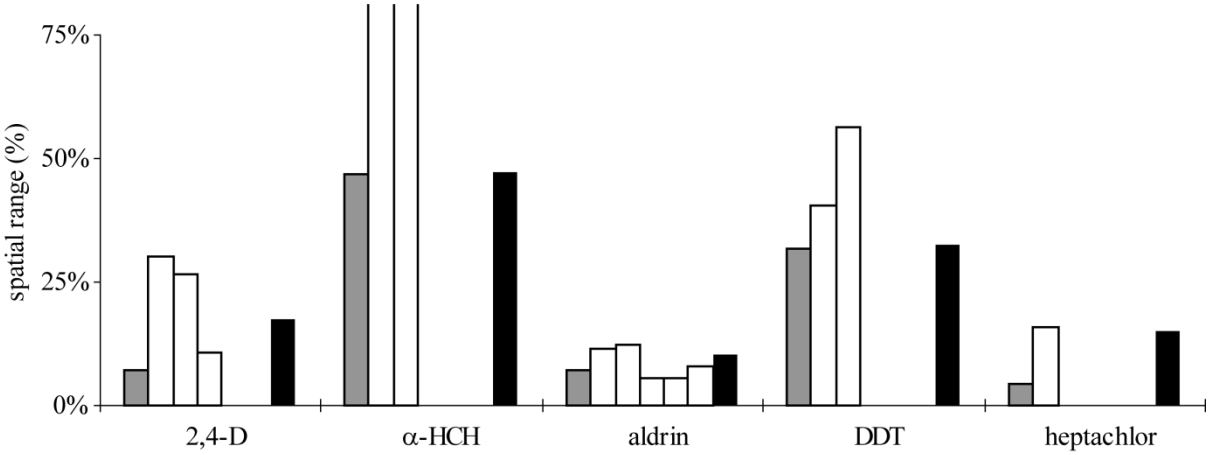

Figure 3.5: Spatial Range of the studied substances. The spatial range of the parent compound is given in gray, the apparent spatial range of the degradation products in white, and the joint spatial range in black. The apparent spatial ranges of the two α-HCH degradation products are 96 and 98% and are not completely displayed in the figure.

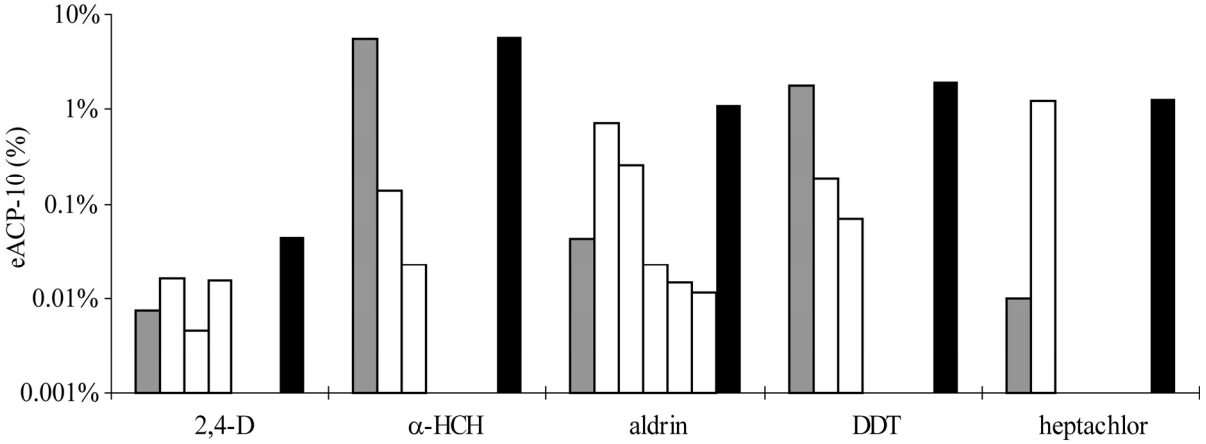

Figure 3.6: Arctic contamination potential after 10 years (eACP-10), for the parent compound (gray), the degradation products (white), and the joint ACP for the whole substance family (black). The scale is a log-scale and gives the eACP-10 in percents.

3.3.3 Spatial Range

Figure 3.5 shows that the apparent spatial range of many degradation products exceeds the spatial range of the parent compound. This effect is very significant for the α-HCH, heptachlor, 2,4-D, and DDT substance families, but less pronounced for the aldrin substance family. The joint spatial range of α-HCH (and DDT) is almost uninfluenced by the degradation products, although those have very high apparent spatial ranges (especially for the case of α-HCH). This will be analyzed in detail in the discussion part.

3.3.4 Arctic Contamination Potential

As could already be seen for the persistence, the degradation products of aldrin and heptachlor considerably increase the eACP-10 of their parent compounds (Figure 3.6). For α-HCH and DDT, the effects are much less pronounced.

3.4 Discussion

The contribution of degradation products to persistence has previously been assessed with unit world models (Fenner et al., 2000). Our study confirms the findings from the previous work: for some substances (such as heptachlor and aldrin), the impact of the degradation products is very important, as the joint persistence is much higher than the primary persistence of the parent compound (a factor of 20 for aldrin and 58 for heptachlor). For other substances, like DDT and especially α-HCH, the impact is much lower, for α-HCH the increase is only by 4%. This is because the two degradation products of α-HCH, 1,2,3,4-tetrachlorohex-5-ene and 1,2-dichlorohexa-3,5-diene, are chemicals that degrade quite readily in the environment. These results show that the persistence of the parent compound alone is not a good indicator for the joint persistence of the whole substance family.

Many degradation products have a higher apparent spatial range than the parent compound. This can be explained by the fact that the parent compound is emitted as a pulse emission at the equator, whereas the degradation products occur continuously on the whole globe, as a result of the transport of the parent compound. The joint spatial range for heptachlor and 2,4-D is much higher than the spatial range of their parent compounds (a factor of 3.5 and 2.4). This shows again that the spatial range of the parent compound is not a good indicator for the long-range transport potential of the whole substance family.

Interestingly, for aldrin, DDT, and α-HCH, the joint spatial range is almost equal to the one of the parent compound, although the apparent spatial ranges of the degradation products are much higher. This is due to the fact that the contribution to joint persistence of those intermediate degradation products is very low: they are present in the system in relatively small quantities. The joint spatial range, as it is defined, is mainly determined by the substance that is present at the highest concentrations, which is the parent compound for the case of α-HCH. In the case of heptachlor, the degradation product is present at much higher concentrations, and therefore, the joint spatial range is determined by the degradation product. It can therefore be said if persistent degradation products that are subject to long-range transport exist, that the joint spatial range will be significantly higher than the spatial range of the parent compound.

The arctic contamination potential shows a behavior similar to the one for joint persistence: for aldrin and heptachlor, an important increase of the eACP-10 can be observed, while the difference is only minor for DDT and α-HCH. This stresses again the fact that the eACP-10 of the parent compound can, in some cases even severely, underestimate the overall hazard of a substance family: including heptachlor-epoxide in the eACP-10 of heptachlor increases the eACP-10 by a factor of more than 100.

In the current study, we have heavily relied on estimation methods to determine substance parameters and degradation pathways. Our conclusions can therefore only highlight the general importance of degradation products, especially with respect to the three indicators investigated. To confirm the accuracy of the predictions of our model, and to be able to draw conclusions on a specific substance, more thorough studies are required that have to include a comprehensive investigation of the degradation pathways and the substance properties as well as detailed comparisons of model results and measurements in various environmental media and regions of the world. For DDT, we are presently working on such a study (Schenker et al., 2008), taking into account historical emissions, measured data on chemical properties and degradation kinetics, and conducting a detailed comparison of model results and concentrations measured in the field. This study on DDT demonstrates that the CliMoChem model yields results that are in good agreement with field data.

3.5 Conclusion

The importance of degradation products for the hazard assessment of organic chemicals has clearly been shown. Taking into account only the parent compounds can lead to a severe underestimation of the persistence, the spatial range and also the arctic contamination potential. Furthermore, for regulatory purposes, chemicals are often ranked according to their score for persistence, spatial range or arctic contamination potential. The goal of this is to identify the most harmful substances. If such a ranking is uniquely based on the score of the parent compound, it is well possible that substances with low scores for their parent compounds, but high scores for the degradation products would not be identified, whereas substances with a high score for the parent compound, but low very score for the degradation products would be flagged as problematic.

It is suggested that degradation products be included in hazard assessments to gain a more accurate insight into the environmental hazard of chemicals. The findings of this project could also be combined with information on the toxicity of degradation products. This would provide further insight into the importance of degradation products for environmental risk assessments.

3.6 Acknowledgment

We gratefully acknowledge the help of Mark Bonnell, Lukas Gasser and Kathrin Fenner in the compilation of the degradation pathways, and thank Fabio Wegmann for interesting comments on the project.

Chapter 4:

Contribution of Volatile Precursor Substances to the Flux of Perfluorooctanoate to the Arctic

Urs Schenker[1], Martin Scheringer[1], Matthew MacLeod[1], Jonathan W. Martin[2], Ian T. Cousins[3], Konrad Hungerbühler[1]

[1] Institute for Chemical and Bioengineering, ETH Zurich, CH-8093 Zurich, Switzerland
[2] Division Analytical & Environmental Toxicology, Department of Laboratory Medicine & Pathology, University of Alberta, Edmonton, AB T6G 2G3, Canada
[3] Department of Applied Environmental Science (ITM), Stockholm University, SE-10691 Stockholm, Sweden

Keywords: fluorotelomer alcohol, perfluoroalkanesulfonamido ethanol, perfluorooctanoic acid, environmental fate model

Reproduced with permission from:
Environmental Science and Technology, 2008
Volume 42, Issue 10, pages 3710-3716
DOI: http://dx.doi.org/10.1021/es703165m

Abstract

Perfluorooctanoate (PFO) has recently been found in remote ocean water and Arctic samples, despite not having been used in significant quantities in remote areas. Two main scenarios for the contamination of the Arctic by PFO have been suggested: (i) direct emissions of PFO and oceanic transport to the Arctic and (ii) emissions of volatile precursor substances that are transported and oxidized in the atmosphere to form PFO, which is subsequently deposited to the Arctic. Focusing on the atmospheric transport pathway, we compare the importance of fluorotelomer alcohols (FTOHs) and perfluorooctyl sulfonamidoethanols (FOSEs) for PFO deposition to the Arctic. Using a global scale multispecies mass balance model, we simultaneously calculate the transport, degradation, partitioning, and deposition of precursor substances, intermediate degradation products, and PFO and compare model results to field measurements. Prior to 2002, the modeled deposition fluxes of PFO to the Arctic originating from FOSEs and FTOHs are of a similar magnitude, and total estimated deposition compares well with deposition measurements for Arctic ice cores. However, the model underpredicts recent measurements of FOSEs in Arctic air, indicating that there may be additional emissions not taken into account. Using Monte Carlo calculations we quantify the uncertainties in our model results and identify that emission estimates, degradation yields, and degradation rate constants are the most influential input parameters controlling the estimated deposition of PFO to the Arctic.

4.1 Introduction

Perfluorooctanoate (PFO) has been found in the environment and biota worldwide, including in remote environments such as the Arctic (Arctic Monitoring and Assessment Program, 2004, Houde et al., 2006). Since perfluorooctanoic acid has a low pKa value of 2.8 (Brace, 1962) or perhaps lower (Goss, 2008), it will be mainly present in its dissociated, involatile, and water soluble ionic form at environmentally relevant pH. Therefore oceanic transport of directly emitted PFO has been hypothesized to be an important pathway for global distribution and transport to the Arctic Ocean (Yamashita et al., 2005, Armitage et al., 2006). However, there is also considerable evidence from laboratory and field studies that volatile precursors of PFO are transported in the atmosphere to remote locations, where they degrade to PFO, and are deposited (Ellis et al., 2003, Ellis et al., 2004, Wallington et al., 2006). Fluorotelomer alcohols (FTOHs) (Ellis et al., 2003, Ellis et al., 2004, Wallington et al., 2006) and substances derived from perfluorooctylsulfonyl fluoride (POSF-based substances) (D'Eon et al., 2006, Martin et al., 2006) have been suggested to be important precursors for PFO. Major POSF-based precursors include the following: N-ethyl (or N-methyl) perfluorooctane sulfonamide (N-EtFOSA or N-MeFOSA, respectively) and N-ethyl (or N-methyl) perfluorooctanesulfonamidoethanol (N-EtFOSE or N-MeFOSE, respectively).

Several studies have recently aimed at quantifying the importance of FTOH atmospheric transport and oxidation to Arctic contamination with PFO (Wallington et al., 2006, Wania, 2007, Yarwood et al., 2007). A modeling study by Wallington et al. (2006) suggested that FTOH-derived PFO is deposited to the latitude range 65−90° N at a rate of up to 400 kg/year. This result was based on relatively high estimated FTOH emissions of 1000 t/year. The oceanic transport of directly emitted PFO into the Arctic Ocean has been estimated to be much higher: 9–20 tonnes/year (Wania, 2007) for the years 2000–2005. Therefore, in terms of overall mass the atmospheric transport route is currently estimated to be between 1 and 2 orders of magnitude less important to overall Arctic contamination than transport of directly emitted PFO. However, for remote terrestrial and inland freshwater ecosystems, the atmospheric transport pathway is expected to be the dominant source of PFO (Stock et al., 2007, Young et al., 2007). Atmospherically deposited PFO may also contribute to exposure of organisms in marine ecosystems when seasonal snowmelt enters the top-ocean layers, but it is not clear to what extent (Butt et al., 2007).

POSF-based substances such as N-EtFOSE ($C_8F_{17}SO_2N(C_2H_5)C_2H_4OH$) and N-MeFOSE ($C_8F_{17}SO_2N(CH_3)C_2H_4OH$) have so far received less attention than FTOHs as volatile precursors of PFO. The contribution of POSF-based substances to PFO in the Arctic was estimated by Prevedouros et al. (2006) in a study where the main objectives were to identify sources of PFO in the environment. They estimated that POSF-based substances contributed about six times less to total perfluorocarboxylic acids (PFCAs) than FTOHs, assuming a yield of PFO of 1% from POSF-based substances (Prevedouros et al., 2006). However, in two smog chamber experiments (D'Eon et al., 2006, Martin et al., 2006) performed after the study by Prevedouros et al., significantly higher total PFCA yields (10−45%) were detected during the degradation of perfluoroalkylsulfonamides. Armitage et al. (2006), in a study focusing on oceanic transport, used these higher yields for the amount of PFCA generated from POSF-based precursor degradation. An additional consideration that has not been taken into account by past modeling exercises is that POSF-based substances, and their intermediate degradation products, have lower vapor pressures than FTOHs. It is thus possible that they may be removed from the atmosphere before reaching remote locations (Atkinson, 2000, Martin et al., 2006), which would reduce their importance as a source of PFO to the Arctic.

Here we employ the global-scale "Climate Zone Model for Chemicals", CliMoChem, to simultaneously describe the environmental fate of PFO and its precursor compounds. We explicitly model selected intermediate degradation products of the precursor substances, including their deposition prior to reaching the Arctic. Using best available emission estimates for PFO, FTOH, and POSF-based substances, we estimate the contribution of these substances to levels and fluxes of PFO in the Arctic. The focus of this work is on semivolatile precursor substances of PFO which are believed to be responsible for atmospheric deposition fluxes to land. The modeled PFO deposition fluxes are compared with calculated fluxes from ice-core measurements and model predictions from other studies.

The model applied here uses many simplifications to arrive at a tractable quantitative description of the relationship between emissions of PFO and its precursor substances, and concentrations measured in the global environment. We have used Monte Carlo techniques to assess the implications of the high uncertainties associated with some of the model input parameters. This analysis has been used to quantify the uncertainties in the model's description of different pathways for Arctic contamination, and to estimate their relative

importance to total contamination levels. The resulting information is expected to be useful for directing future field and laboratory investigations into the global sources of PFO.

4.2 Methods

4.2.1 The CliMoChem Model

CliMoChem is a temporally resolved global-scale multimedia contaminant fate model that has been developed to investigate the fate of semivolatile organic compounds in the environment (Scheringer et al., 2002, Wegmann, 2004). Recently, the model has been extended to simultaneously describe parent compounds and their degradation products (Schenker et al., 2007). In our study, the model represents the global environment as a set of 10 latitudinally averaged zones, and our focus is on describing south-north migration of contaminants. Each zone consists of bare soil, vegetation-covered soil, vegetation, ocean water, and atmosphere compartments. The model simulates advective and diffusive exchange processes between these compartments and interzonal transport in ocean water and atmosphere. Environmental parameters such as temperature, OH-radical concentrations, and soil organic matter content are zone- and season-specific, and a temporal resolution of four seasons is used. A description of the exchange processes between atmosphere and surface media is given in the Supporting Information.

Compared to models like IMPACT or CAMx that have previously been used to investigate the fate of fluorinated substances (Wallington et al., 2006, Yarwood et al., 2007), the treatment of chemical reactions in the gas-phase of CliMoChem is highly simplified. Instead of modeling a large number of chemical reactions involving many chemical species, CliMoChem only explicitly accounts for substances that have a sufficiently long atmospheric lifetime to be subject to long-range transport and/or deposition and wash-out.

To identify those intermediates that are sufficiently long-lived to be transported and/or deposited, information from smog chamber experiments (D'Eon et al., 2006, Martin et al., 2006) and detailed models of atmospheric chemistry (Wallington et al., 2006) has been used. Intermediates that undergo rapid transformation are not modeled explicitly although they are essential elements of the reaction scheme. This simplification of the reaction scheme allows a more detailed treatment of other processes in the model, such as inclusion of other environmental media like ocean water, vegetation, and soils and reduces calculation time,

which allows Monte Carlo simulations to be performed with CliMoChem. The degradation scheme is described in more detail further below.

4.2.2 Emission Scenario

In previous modeling studies, precursor substances alone were simulated (Ellis et al., 2004, Wallington et al., 2006) or the amount of PFO generated from the degradation of precursor substances was estimated and added to the direct emissions of PFO at the source regions (Prevedouros et al., 2006) and only the fate of PFO in the environment was calculated. Our model goes beyond that and uses separate emissions of PFO and the precursor substances (POSF-based substances and FTOHs) as inputs. The degradation of the precursor substances is explicitly calculated by the model and competes with other processes such as deposition or transport of the precursor substances from emission areas to the Arctic.

Emissions of PFO were taken from the inventory compiled by Prevedouros et al. (2006), which also has been used in other modeling exercises (Armitage et al., 2006, Wania, 2007). Emissions of precursor substances are highly uncertain, because percentages of unreacted raw materials present in the final products are only roughly known. Lower and upper limits for unreacted raw material content were assumed to be 1 and 2% for FTOHs, and 0.1 and 3% for POSF-based substances, on the basis of information provided in Prevedouros et al. (2006). It was further assumed that all unreacted raw materials are emitted in the year of production of the final product. Production data for products with FTOH and POSF-based substances present as unreacted residuals were estimated from the Supporting Information of Prevedouros et al. (2006) and Wania (2007). These emission inventories result in total emissions between 1951 and 2005 of about 750–1500 tonnes of total FTOH, 82–2480 tonnes of POSF-based substances, and about 3800 tonnes of PFO. Details of these inventories are given in the Supporting Information.

4.2.3 Fate of Precursor Substances in the Atmosphere

The degradation scheme of precursor substances into PFO (Ellis et al., 2004, D'Eon et al., 2006, Martin et al., 2006, Wallington et al., 2006) can be described in two parts (see Figure 4.1A). First, the functional group of the precursor substance undergoes various reactions until only the $F(CF_2)_x$ radical remains (green, red, purple, and blue molecules and arrows in Figure 4.1A). In the second part (black molecules and arrows), PFCAs of shorter perfluorinated chain lengths are formed by one of two mechanisms initiated by reaction with alkyl peroxy

radicals; either the intact $F(CF_2)_x$ radical is transformed into the corresponding PFCA, or it begins to "unzip" (i.e., its chain length is reduced by sequential loss of COF_2), before possibly exiting the unzipping cycle and forming a PFCA with a chain length shorter than *x*. For POSF-based substances, $x = 8$, whereas for FTOHs more than eight fluorinated carbons are also possible. While the first part of the degradation scheme is different for POSF-based and FTOH precursor substances, the second part (black arrows) is the same.

Fluorotelomer alcohols undergo reaction with OH radicals (blue molecules and arrows, Figure 4.1A). This results in the formation of two sequential intermediate degradation products, the fluorotelomer aldehyde (FTAL) and the perfluorinated aldehyde (PFAL) (Ellis et al., 2004, Wallington et al., 2006). The fate of PFAL includes formation of PFCAs by various mechanisms, but the relative importance of each mechanism remains uncertain. For example, it is unclear to what extent the PFAL species $F(CF_2)_8CHO$ degrades to perfluorononanoic acid (PFNA) relative to PFO and shorter PFCAs. Wallington et al. (2006) considered decomposition of PFAL by (i) direct photolysis ($\Phi = 0.02$ quantum yield), leading to PFO and shorter PFCAs, and (ii) OH radical decomposition. The OH radical decomposition pathway can yield PFNA by subsequent reaction of the acyl peroxy radical with HO_2 (which we have not considered in the present work), or PFO and shorter PFCAs by reaction of the acyl peroxy radical with NO. More recently, Chiappero et al. (2006) suggested that PFAL photolysis quantum yields may be higher than those predicted by Wallington et al. (2006). Waterland and Dobbs (2007) also argued that perfluoroacyl radicals can readily decompose. These new data would both serve to decrease the relative extent of PFNA formation, while increasing the relative yield of PFO and shorter PFCAs, compared to the assumptions of Wallington et al. (2006). On the other hand, Andersen et al. (2006) recently described a hydration mechanism that would serve to increase the PFNA yield and decrease the PFO and shorter PFCA yield predicted by Wallington et al. (2006). Because the cumulative influence of these opposing assertions has not yet been resolved, none have been taken into account in the present work nor have they been considered in any previous models to our knowledge.

After two unzipping cycles, 10:2 FTOH degrades into PFO, while 8:2 FTOH degrades into PFO without perfluorinated chain unzipping. Both precursor substances are expected to be important contributors to PFO in the environment. Because our emission data are for total

FTOH, we have modeled 10:2 and 8:2 FTOH as a single "block" with average properties and degradation yield into PFO.

The degradation mechanisms of POSF-based substances have received less attention than those of FTOHs. Two general reaction pathways have been described. The first involves OH radical addition to the sulfur atom and subsequent cleavage of either the S−C or S−N bond (D'Eon et al., 2006) (green arrows and molecules in Figure 4.1A). This mechanism may produce perfluorooctane sulfonic acid (PFOS) by cleavage of the S-N bond or can lead to the unzipping cycle that will ultimately result in PFO and shorter PFCAs (cleavage of the S-C bond). There are no known stable intermediates from this OH addition mechanism. The second general set of reactions for POSF-based substances (red molecules and arrows) involves abstraction of hydrogen from the alkyl substituents, R^1, R^2, or R^3 (Martin et al., 2006). These reactions may result in N-dealkylation, but the resulting intermediate degradation products can also include various ketones and aldehydes. In general, all of the intermediate products are more resistant to further OH radical reactions than the starting POSF-based material. More reactions and intermediates might occur than shown in Figure 4.1A, in particular reactions of N-EtFOSE and N-MeFOSE might also occur on the R^1 side chain prior to the dealkylation leading to N-EtFOSA and N-MeFOSA; this is not shown here to facilitate comparison of the present scheme with the scheme in D'Eon et al. (2006) and Martin et al. (2006). The dashed purple arrows indicate reactions that have not yet been reported but are possible additional pathways; see below.

4.2.4 Establishing the Degradation Scheme for Model Applications

For implementation into the CliMoChem model, the degradation pathways presented in Figure 4.1A were simplified to include only chemical species that are stable for at least several hours so that deposition processes competing with further degradation and atmospheric transport might influence concentrations. The degradation scheme used in the model is presented in Figure 4.1B. For the FTOH degradation pathway, radicals were excluded but FTAL and PFAL were modeled. For the POSF-based degradation pathway, similar substances were grouped into distinct substance "blocks". Grouping substances with similar properties in one block and modeling their fate with an average set of properties is an established approach for modeling complex mixtures (MacLeod et al., 2004). The alcohols, N-EtFOSE and N-MeFOSE, were grouped in the xFOSE block, whereas the N-alkyl compounds, N-EtFOSA and N-MeFOSA, were grouped in the xFOSA block. We summarize

all other intermediate degradation products in one substance block called “INT”, as shown in Figure 4.1B. Intermediate substances formed subsequent to the unzipping cycle (black molecules and arrows in Figure 4.1A) were excluded because previous modeling (Wania, 2007) indicated that their half-lives are short enough that competing deposition to the surface would not influence the yield of PFO. Furthermore, only the C8-PFCA (PFO) was tracked in the output of the model.

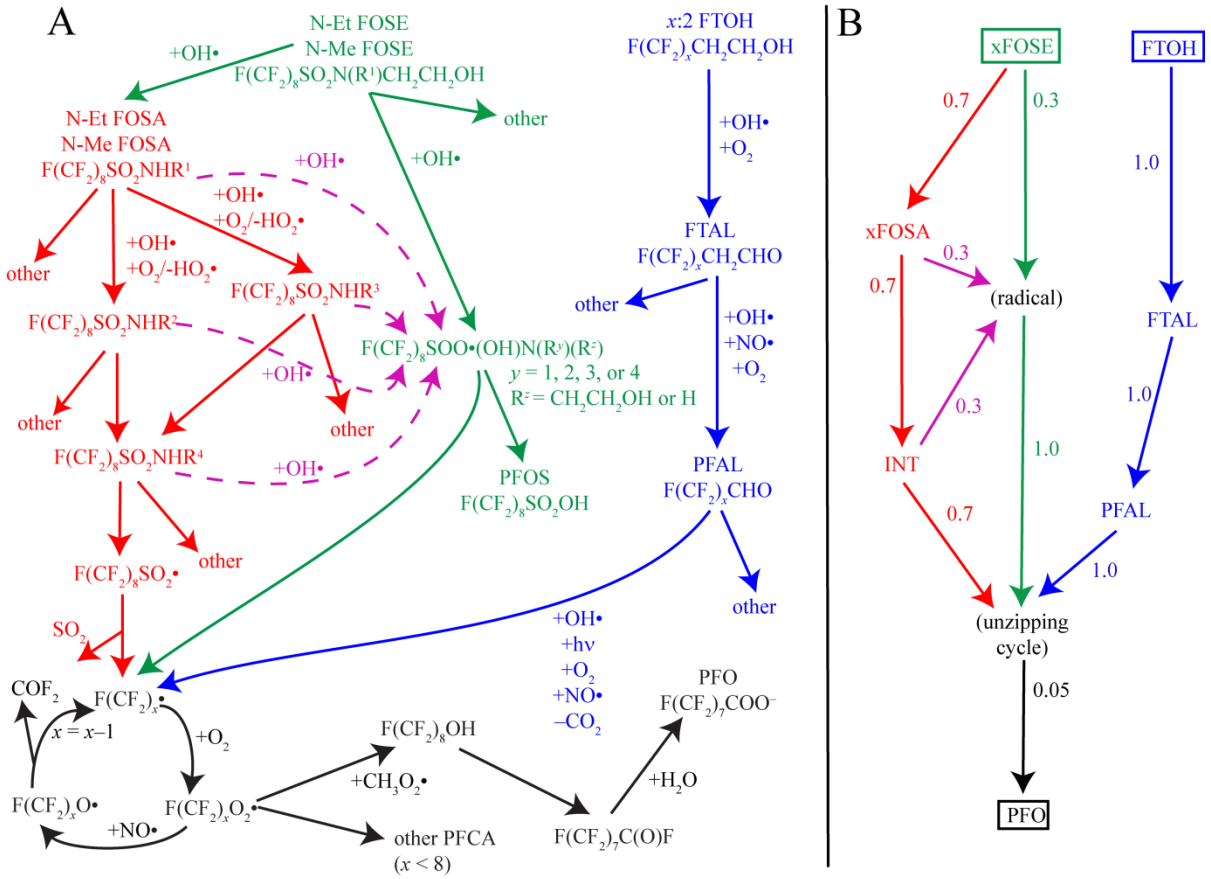

Figure 4.1: Degradation scheme of precursor substances into PFO in air. (A) Summary of the most important reactions. Some arrows represent a series of reactions; R^1, methyl or ethyl; R^2-R^4, various substituents of the intermediate degradation products. (B) Simplified reaction scheme used in our model calculations. Substances in parentheses have not been modeled and are only included to facilitate reading of the scheme. Substances in rectangles have direct emissions into the model environment. Numbers at the arrows indicate fractions of formations. For details, see text.

D’Eon et al. (*10*) observed PFOS as a degradation product of xFOSE and proposed an “OH addition pathway” as the mechanism (Figure 4.1A). Although the analogous OH addition reactions for xFOSA and the various INT species (Figure 4.1A, dashed purple arrows) have not been demonstrated experimentally, we included the OH addition pathway for xFOSA and INT in Figure 4.1B (purple arrows) on the basis of the assumption that their reactivities at the sulfonyl moiety would be similar to xFOSE. With the same splitting ratio as that for xFOSE,

inclusion of the OH addition pathway from xFOSA increased PFO deposition from POSF-based precursors by only 4%; thus, this pathway was included for completeness but did not significantly impact the overall result.

The overall yield of PFO from the degradation of FTOH has been estimated to be around 5% (1–10%), as modeled by Wallington et al. (2006). Here we have also assumed a 5% yield for the formation of PFO from POSF-based precursors, on the basis of the following reasoning: in their analysis of FTOH degradation, Wallington et al. (2006) estimated that yields of shorter PFCAs are similar to those of PFO. We interpret this to mean that the total PFCA yield from FTOH is approximately between 15 and 30%. In the degradation of POSF-based substances, smog-chamber studies have shown between 10 (D'Eon et al., 2006) and 45% (Martin et al., 2006) total PFCA yield. Because the total PFCA yield from Wallington et al. is similar to the PFCA yield measured for POSF-based substances (D'Eon et al., 2006, Martin et al., 2006), and because the reaction pathway to PFO from the unzipping cycle is identical for FTOH and POSF-based substances, we assume that the yield of PFO, as one component of total PFCAs, is similar to the PFO yield reported by Wallington et al., i.e., 5%. Our reasoning thus rests on the assumption that the yield of the $F(CF_2)_8$ radical from FTOH and POSF-based substances is approximately equal.

In the model, the yield of PFO formation is represented by a fraction of formation (the relative amount of a transformation product that is formed from the degradation of a parent compound) of 5% for the transformation of $F(CF_2)_8$ radicals from the unzipping cycle to PFO. All other fractions of formation (except for the branching reactions discussed below; see Figure 4.1B) are assumed to be one. Further information on this assumption is provided in the Supporting Information.

The importance of the “OH addition pathway” (green and purple arrows/molecules Figure 4.1) as compared to the “H abstraction pathway” (red arrows/molecules in Figure 4.1) for xFOSE had to be specified in the model. There is little information about the relative importance of the two pathways; however, H abstraction is believed to be more important than OH addition. The AOPWin software (U.S. Environmental Protection Agency, 2004), for instance, predicts H abstraction reactions for N-EtFOSE to be more than 2 orders of magnitude faster than OH addition, although this software cannot account for the influence of the perfluoroalkylsulfonamide moiety. In the absence of other information, we therefore assumed that the reactivity due to H abstraction lies between 50 and 90% of the total

reactivity. For the deterministic calculations, we have chosen 70%. This parameter is highly uncertain, and the chosen value is admittedly a best guess. However, results from Monte Carlo simulations (see the Supporting Information), where this parameter has been uniformly varied between 50 and 90%, show that its impact on the model output is relatively low.

4.2.5 Degradation Rate Constants

Atmospheric degradation half-lives have been reported for FTOHs (Ellis et al., 2003), for FTAL and for PFAL (Wallington et al., 2006), and values have been suggested for N-Et-/N-MeFOSE and N-Et-/N-MeFOSA on the basis of measurements with analogous substances (D'Eon et al., 2006, Martin et al., 2006). These have been used here for the xFOSE and xFOSA substance blocks. For the substances contained in the INT block, no literature information is available on the half-lives. We have assumed the same half-life for the INT block as for the xFOSA block. Quantitative structure-property relationship (QSPR) information from AOPWin (U.S. Environmental Protection Agency, 2004) suggests that degradation for the different species in the INT block is between 1 magnitude faster and 1 magnitude slower than degradation of substances in the xFOSA block. PFO is assumed to be stable in the atmosphere, and all substances are assumed to be stable in surface compartments. All degradation rate constants that we have used are listed in Table 9.24 in the Supporting Information.

4.2.6 Partition Coefficients

The partition coefficients of the substance blocks included in the model were taken from the literature where possible or estimated on the basis of structurally similar substances (Table 9.24 in the Supporting Information). Since we describe substance blocks instead of individual substances, the properties sometimes do not represent particular substances (e.g., 10:2 FTOH is represented by the properties of 8:2 FTOH). For FTOH and PFO, the partitioning data used by Wania (2007) have been selected. The $\log K_{AW}$ of xFOSE has been estimated from measured and estimated information (Arp et al., 2006) on N-EtFOSE and N-MeFOSE. This value lies 1.5 log units below the $\log K_{AW}$ for FTOHs, indicating that the POSF-based substances are less likely to partition from water to air than FTOHs. For xFOSA, no measured information on $\log K_{AW}$ was available. We have therefore selected the same value as that for xFOSE because QSPR information (Arp et al., 2006) did not indicate that $\log K_{AW}$ differed significantly from the one for xFOSE. No measured $\log K_{AW}$ was available for the

substances summarized in the INT block. Their logK_{AW} was chosen to be 0.5 log unit higher than for xFOSE and xFOSA, because QSPR estimations with EPIWin (U.S. Environmental Protection Agency, 2004) indicate that these substances might be slightly more volatile than their precursors. The logK_{OC} has not been measured for any of the substances in the POSF-based degradation pathway. Therefore, we have selected the same values as those for FTOH. QSPR results for logK_{OW} of xFOSE and xFOSA do not differ significantly from logK_{OW} of the FTOHs.

4.2.7 Uncertainty Calculations

Uncertainties in the input parameters for fluorinated substances are generally large and arise from various sources. Because concentrations and fluxes calculated by the model scale linearly with emissions, we have calculated scenarios using minimal and maximal estimates of precursor emissions (see Emission Scenario above). However, to take into account uncertainties of several input parameters in combination, minimum and maximum values are not an appropriate approach. Instead, we have performed Monte Carlo simulations using a best guess of uncertainties in the most important input parameters (partition coefficients, atmospheric degradation half-lives, and ratios and yields in the degradation pathway). Distributions of input parameters have been established mainly on the basis of expert judgment; they should be viewed as estimations of the possible upper and lower bounds of input parameter values. For the analysis of results, the input parameters of both pathways have been summarized in three groups: (a) atmospheric degradation half-lives of parent compounds and intermediates, (b) degradation yield and ratio between OH abstraction and H addition in the degradation pathway of POSF-based precursors, and (c) partition coefficients. A complete list of the parameters in these groups and the distribution types and parameters of all input values is given in Table 9.26 in the Supporting Information. We have performed 10000 Monte Carlo runs and tracked the deposition flux of PFO to the Arctic in the year 2000. In these calculations, the emissions were set to one single value: the geometric mean of the minimal and maximal emissions presented above.

4.3 Results and Discussion

4.3.1 Atmospheric Concentrations of Precursor Substances

Figure 4.2A shows levels of FTOHs (red) and xFOSE (blue) as predicted by our model for the years 1998–2005, assuming geometric means (bold lines) and minimal and maximal values (bands) for the content of unreacted raw material (as described in Methods). Calculated levels of FTOHs increase throughout this period, whereas calculated levels of xFOSE decrease strongly after the year 2000. Both results are attributable to changes in the emissions of the two substances; estimated emissions of FTOH increase between 1998 and 2005, whereas estimated emissions of xFOSE decrease strongly in the same period due to a phase-out by their primary manufacturer.

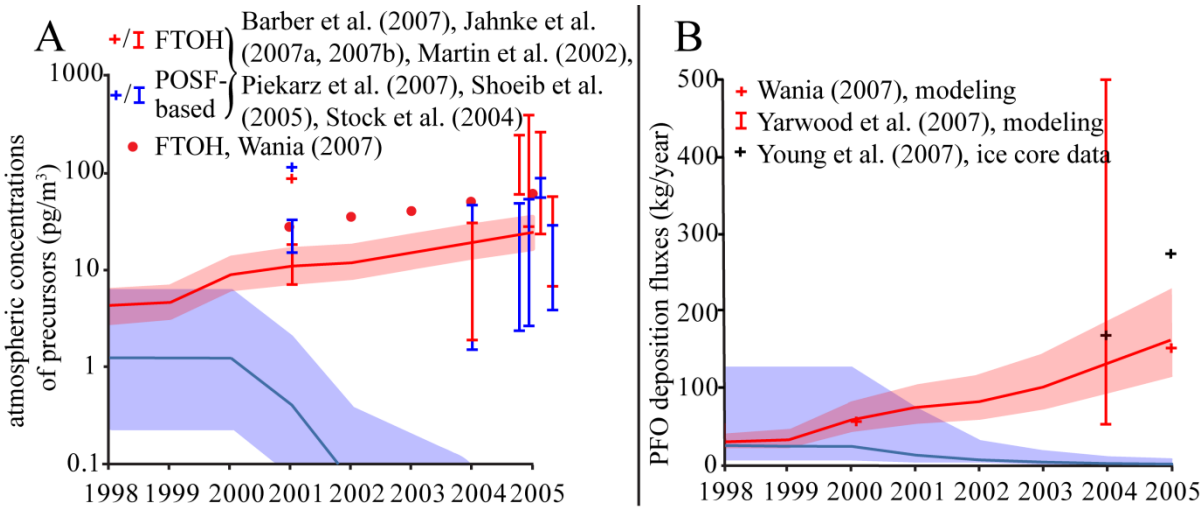

Figure 4.2: (A) Concentrations of FTOHs (red) and xFOSE (blue) in air in the northern midlatitudes (36° N to 54° N) derived with our model (bold lines and bands), measured by various authors (crosses and bars), and modeled by Wania (2007) (dots). Modeled atmospheric concentrations of xFOSE are below 0.1 pg/m^3 after 2002. (B) PFO deposition fluxes from the atmosphere to the Arctic (65° N to 90° N) due to the degradation of FTOHs (red) and xFOSE (blue) calculated by our model (bold lines and bands) and modeled by others (red crosses and bars). Black crosses: extrapolated deposition fluxes from ice core measurements, representing the sum of PFO deposition from both FTOH and POSF-based precursor degradation.

Figure 4.2A also shows measured (Martin et al., 2002, Stock et al., 2004, Shoeib et al., 2005, Barber et al., 2007, Jahnke et al., 2007a, Jahnke et al., 2007b, Piekarz et al., 2007) and modeled (Wania, 2007) concentrations of FTOHs and xFOSE in air in the midlatitudes of the northern hemisphere. Levels of FTOHs are generally well-reproduced by our model (measured concentrations generally overlap with the band of model results). Conversely,

modeled levels of xFOSE decrease strongly after 2000, whereas measured xFOSE concentrations show no strong decreasing trend between 2001 and 2005 and lie several orders of magnitude above model results. Furthermore, even xFOSE measurements from the years 2004/2005 lie at least 1 order of magnitude above model results for the years 1998–2000, when calculated levels show their maximum. Possible reasons for this discrepancy are as follows: (a) estimates of historical emissions may be too low because important source categories are omitted (e.g., xFOSE emissions during production or degradation of the large quantities of POSF-based polymers stored in landfills) or because assumptions about historical production volumes or fractions of POSF-based precursors in products are too low; (b) emissions may continue from products after phase-out of manufacture if the product lifetimes are long (e.g., carpets); (c) other manufacturers may have continued to produce or increased their production of POSF-based polymer products in response to continued demand after the phase-out by the primary manufacturer. These factors, possibly contributing to higher emissions of POSF-based precursors, have not been incorporated into our model because they are rather speculative and difficult to quantify. For example, it is known that numerous companies have continued to make POSF-based products (Risk and Policy Analysts LTD, 2004, Organization for Economic Co-ordination and Development, 2006) since the major manufacturer phased out production in 2002, but there is little quantitative information on production volumes and types of products.

4.3.2 Estimated Deposition Fluxes to the Arctic

Figure 4.2B shows calculated atmospheric deposition fluxes of PFO into the Arctic. The red-shaded area represents PFO deposition fluxes from FTOH degradation, the blue shaded area represents PFO deposition fluxes from POSF-based precursor degradation. The model indicates that until the year 2000 atmospheric fluxes from POSF-based substances had a similar importance as fluxes from FTOHs. If emissions of POSF-based substances have not decreased since 2000 (as suggested by environmental measurements), PFO deposition from the degradation of POSF-based substances may be equally important as that from FTOHs, even today.

According to our analysis, the historical and potentially also the current atmospheric flux of PFO into the Arctic from POSF-based substances is comparable to the flux from FTOHs, despite the fact that the K_{AW} of the POSF-based substances and related intermediate degradation products is more than 1 order of magnitude below that of the FTOHs and their

intermediate degradation products. This finding is significant, because it takes into account the fact that POSF-based substances (and their intermediate degradation products) have lower vapor pressures than FTOHs and can undergo deposition prior to reaching the Arctic. Our results support the estimation by Armitage et al. (2006) that POSF-based substances and FTOHs contribute a similar amount of PFCAs in the global environment. The goal of their study was, however, not to explicitly model the behavior of the precursor substances in the environment. It was therefore unclear if POSF-based substances could be transported to remote locations like the Arctic or if deposition would prevent their long-range transport. Our results indicate that deposition of intermediates does not markedly reduce the amount of PFO reaching the Arctic. In the Supporting Information, we further analyze to what extent intermediate degradation products contribute to the deposition and wash-out of precursors during transport to the Arctic.

4.3.3 Comparison with Other Modeling Studies and Measurements

Direct emissions of PFO and subsequent transport in oceans has been suggested to be an important pathway for the Arctic contamination with PFO (Wania, 2007). In the Supporting Information we show that our calculated concentrations in oceans and water-borne fluxes into the Arctic originating from direct emissions of PFO are about 2 orders of magnitude higher than the sum of concentrations and fluxes originating from degradation of the precursor substances, in good agreement with results from Wania (2007).

Our modeled concentrations of PFO can be compared with the results of Wania (2007). For 2005, Wania predicts PFO concentrations in ocean water of 0.4 pg/L from FTOH degradation, similar to the CliMoChem model yielding between 0.21 and 0.42 pg/L PFO from FTOH degradation (2005). The deposition flux of PFO from the atmosphere to the Arctic from the degradation of FTOH is given as 57 and 154 kg/year in 2000 and 2005, respectively, by Wania (red crosses in Figure 4.2B), whereas our results are 41–83 and 113–226 kg/year, respectively. FTOHs have also been modeled by Yarwood et al. (2007). If their estimation for PFO deposition flux in remote areas (units of ng/m^2) is multiplied by the surface area of the Arctic north of 65° N (26.4 million km^2), between 50 and 500 kg/year of PFO is deposited into the Arctic from FTOH (red bar in Figure 4.2B), which is consistent with our estimates. Wallington et al. (2006) have predicted annual PFO deposition fluxes of 400 kg into the Arctic from FTOH (not shown in Figure 4.2B). Young et al. (2007) have extrapolated PFO deposition fluxes from concentrations in ice cores in the high Arctic. They

predict 167 and 271 kg/year of PFO in 2004 and 2005, respectively, for the whole Arctic (black crosses in Figure 4.2B), in good agreement with the 92–192 (2004) and 113–231 kg/year (2005) from our calculations (sum of deposition due to FTOHs and POSF-based substances). Scott et al. (2006) measured PFO in precipitation at various locations in North America. At remote locations, they report deposition fluxes of PFO in precipitation of 50–300 ng/m^2 PFO in 2002. Our model suggests precipitation deposition rates of 9.2–21.2 ng/m^2 of PFO for the same year, which is up to 1 order of magnitude below the measurements of Scott et al. In summary, our model results for PFO deposition to the Arctic agree reasonably well with previous model results and measurements from ice cores, whereas disagreements of up to 1 order of magnitude exist for deposition fluxes from precipitation.

4.3.4 Uncertainty Calculations

To characterize the influence of uncertain chemical properties on the model results, we have calculated quantiles of the output distribution of PFO deposition in 2000. The 2.5, 50, and 97.5% quantiles for PFO deposition are 21, 75, and 149 kg/year, respectively. The deposition fluxes from our deterministic calculations (assuming geometric mean, minimal, and maximal values for unreacted raw material content) are 81, 45, and 207 kg/year. This suggests that the combined uncertainty of substance properties results in an uncertainty that is as important as the one from the emission estimates.

To identify model parameters that contribute most to uncertainties in the outputs, the contribution to variance of groups of input parameters has been calculated (Figure 9.2 in the Supporting Information). Parameters belonging to the FTOH pathway contribute the most to the variance of modeled PFO deposition. This is because in a model run based on the geometric mean of the emission estimates (bold lines in Figure 4.2B), FTOHs are responsible for the majority of PFO deposition in 2000. Degradation half-lives in air are the dominant source of uncertainty, followed by the FTOH degradation yield. Partition coefficients have a surprisingly low importance for PFO deposition fluxes. This indicates that further information on atmospheric degradation half-lives and degradation yields would help to improve the overall picture obtained by our analysis.

The CliMoChem model links emissions and chemical properties with environmental concentrations and mass fluxes. Results obtained with the model show agreement with field data for concentrations of FTOH in air and total deposition of PFO to surface media in the

Arctic. The calculated concentrations of POSF-based precursors in air, however, deviate from levels measured in the environment. To overcome this disagreement, two elements are needed: (i) emissions of POSF-based precursors have to be higher than in our current assumptions (global emissions below 5 tonnes/year after 2000; see Table 9.25 in the Supporting Information); (ii) if calculated levels of POSF-based precursors are higher than in the current model results (Figure 4.2A), this leads to deposition fluxes of PFO in the Arctic that are higher than indicated by ice core measurements (Figure 4.2B). On the basis of recent smog chamber experiments, it may be hypothesized that the yield of PFO formation from POSF-based precursors is lower than the 5% that we assumed in the present calculations. If this is the case, calculated PFO deposition fluxes may well be in agreement with field data even under the assumption of significantly higher emissions of POSF-based precursors. We see these two aspects – emissions and atmospheric degradation pathways of POSF-based precursors – as priority topics for further research to reduce uncertainties in the global mass balance of perfluorooctanoate.

4.4 Acknowledgments

We thank Bob Buck, Mark Russell, James Armitage, Costas Prevedouros, David Trudel, and Fabio Wegmann for valuable comments.

4.5 Supporting Information

Supporting Information is available in the appendix, chapter 9.2.

Chapter 5:

Modeling the Environmental Fate of Polybrominated Diphenyl Ethers (PBDEs): the Importance of Photolysis for the Formation of Lighter PBDEs

Urs Schenker, Fabian Soltermann, Martin Scheringer, Konrad Hungerbühler

Institute for Chemical and Bioengineering, ETH Zurich, CH-8093 Zurich, Switzerland

Keywords: debromination, environmental fate modeling, deca-BDE, penta-BDE

Abstract

A global multi-media model is used to calculate the fate of polybrominated diphenyl ethers (PBDEs) in the environment. Special emphasis is given to the importance of direct photolysis that was shown to be an important degradation mechanism for highly brominated PBDEs, and is believed to result in the formation of lower brominated PBDEs. We show that the inclusion of direct photolysis decreases the overall persistence and long-range transport potential of most PBDEs (in particular the heavier ones). We develop a PBDE emission inventory and calculate realistic concentrations of different PBDEs. Differences between predicted concentrations and field data are assessed, and possible reasons for these differences discussed. The importance of debromination of deca-BDE is compared to direct emissions of lower brominated PBDEs. The model predicts that about 10% of penta- and about 2% of tetra-BDE homologues found in the environment arise from the degradation of deca-BDE. Uncertainties of our predictions are quantified and their implications for the findings of our study discussed.

5.1 Introduction

Polybrominated diphenyl ethers (PBDEs) are widely used as flame retardants in textiles and polymer products (Rahman et al., 2001, de Wit, 2002). Given their beneficial effects in reducing fire hazards, their use has strongly increased in the past decades. Recently, however, concern has risen about lower brominated PBDEs, because their concentrations in remote regions and in human milk have increased strongly (Meironyte et al., 1999, Ikonomou et al., 2002). Therefore, the European Union has phased-out the commercial penta- and octa-BDE mixtures, allowing only the highly brominated deca-BDE mixture to be used (European Commission, 2003). Highly brominated BDEs have created less concern: because of their high K_{OW} and low vapor pressure they are believed to be immobile and strongly sorbed to soil and sediments. Furthermore, toxicological studies have shown that highly brominated PBDEs are less toxic than the lighter ones (European Chemicals Bureau, 2002).

There is, however, some evidence of deca-BDE transported to remote locations (Su et al., 2007), and it has been suggested that heavy PBDEs sorbed to aerosol particles may be subject to long-range transport. Furthermore, deca-BDE might also be degraded into lighter PBDEs: deca-BDE in organic solvents and on mineral surfaces that was exposed to sunlight has been shown to degrade quickly into lighter PBDEs, including penta-BDE (Watanabe and Tatsukawa, 1987, da Rosa et al., 2003, Eriksson et al., 2004, Soderstrom et al., 2004). These, in turn, seem to be more stable under the influence of sunlight. However, other researchers have questioned whether one can extrapolate from the processes identified under optimized laboratory conditions to the environment (Rothenbacher, 2007).

Model calculations can be used to characterize the behavior of chemicals in the environment, to identify relevant processes, and to quantify mass fluxes. Several researchers have calculated the fate of PBDEs in the environment. Their focus has been on the determination of the long-range transport potential of the different PBDE congeners (Wania and Dugani, 2003, Breivik et al., 2006) and the quantification of exchange processes between atmosphere and surface media (Gouin and Harner, 2003). To our knowledge, there have not been any modeling studies that predict the amount of heavier PBDEs that might degrade into lighter ones, or compare this amount with direct emissions of lighter PBDEs. Furthermore, modeling studies that aim to predict the long-range transport behavior of PBDEs have, until now, not

taken into account the possible impact of direct photolysis on the fate of PBDEs in the environment.

In a first step, we characterize the behavior of PBDEs in the global environment. The importance of direct photolysis for the fate of different PBDEs is quantified, and results are compared to previous modeling studies. In a second step, we develop and apply a global emission inventory to calculate realistic PBDE concentrations and mass fluxes. Concentrations are compared to field data, and the importance of the formation of lower brominated PBDEs by debromination of deca-BDE is compared to direct emissions of lower brominated PBDEs.

5.2 Methods

We summarize the 209 PBDE congeners into groups with an equal number of bromine atoms (homologues). Substance properties and emissions of homologues in our model are representative of the average or sum of the properties or emissions of individual congeners. This type of simplification has proven successful in modeling studies of other substance categories (MacLeod et al., 2004).

5.2.1 Degradation Rate Constants

Direct photolysis has been identified as an important degradation process for highly brominated PBDEs (da Rosa et al., 2003, Eriksson et al., 2004, Soderstrom et al., 2004). Raff and Hites (2007) have determined photolytic degradation rate constants for PBDE congeners and compared them to OH radical reaction rate constants. They show that atmospheric degradation half-lives of all congeners from the tri- to deca-BDE homologues are determined by direct photolysis.

We have taken the photolysis rate constants measured in isooctane and cyclohexane by Raff and Hites (2007) and combined this information with measurements in other organic solvents and silica gel from additional studies (e. g. da Rosa et al., 2003, Eriksson et al., 2004, Soderstrom et al., 2004, further information is given in the Supporting Information). From the average of these measured degradation rate constants we have extrapolated degradation rate constants for PBDEs in the gas phase and sorbed to aerosol particles.

Because diffusion in the gas phase is faster than in solvents, the likelihood that fragments generated by photolysis recombine to form the original molecule ("cage effect") is decreased. Raff and Hites have derived a quantum-yield of 0.5 in cyclohexane, which indicates that degradation in organic solvents is by a factor two slower than in the gas phase (if a the maximum quantum-yield of 1 is assumed for the gas phase). Therefore, we select photolysis in the gas phase to occur two times faster than in organic solvents.

For the degradation rate constant on aerosol particles, we base our extrapolation on results from Behymer et al. (1988), who have measured photolysis rate constants on black and clear aerosol particles. They found that on average, photolysis rate constants on black aerosol particles were 62.4 times below the values on clear aerosol particles. Assuming that organic solvents and silica gel have similar properties as clear aerosol particles, we estimate photolysis rate constants on aerosols to be 62.4 times below the average value measured in organic solvents and silica gel. This is in contradiction to Raff and Hites (2007), who have assumed that no photolysis occurs on aerosols. The implications of this difference are discussed in the results section.

OH radical reactions were calculated from EPIWin data (U.S. Environmental Protection Agency, 2004), and it was assumed that no OH radical reactions occur on particles, as in (Raff and Hites, 2007).

Photolytic degradation might also occur in the uppermost layer of surface compartments which is penetrated by sunlight (Ciani et al., 2005, Kuivikko et al., 2006). We made calculations to take into account these processes. Because they were unimportant for the overall fate of PBDEs in the model system, they were ignored in the present calculations. Microbial degradation processes, however, are relevant in surface compartments, and have been estimated using data from the EPIWin software package (U.S. Environmental Protection Agency, 2004) and an estimation method by Arnot et al. (2005). A table with the degradation rate constants is given in the Supporting Information.

5.2.2 Degradation Pathways

Direct photolysis has been reported to result in a number of debromination steps (Watanabe and Tatsukawa, 1987, da Rosa et al., 2003, Eriksson et al., 2004, Soderstrom et al., 2004, see Supporting Information) that result in lower brominated PBDEs. The median of observed debromination yields was 70% (for each individual degradation step). For highly brominated

PBDEs, the likelihood of debromination is higher than for lighter PBDEs. Therefore, the debromination yield of photolysis was set to 80% for each degradation step for deca- to hexa-BDE homologues, and 50% for lower brominated PBDEs. OH radical reactions in atmosphere (Raff and Hites, 2006) and microbial degradation (for instance in soils, Gerecke et al., 2005) are not reported to result in a significant debromination.

Uncertainties in the debromination yields are relatively high. In particular, the debromination of light PBDEs are less frequently reported, and might be below 50%. There is, however, considerable measurement evidence that concentrations of tri-BDE in air are increased relative to tetra-BDE (Jaward et al., 2004a, Lee et al., 2004, Jaward et al., 2005), which cannot be explained by the higher vapor pressure of the tri-BDE homologue alone. The only other mechanism that might result in higher levels of tri-BDE in the environment is debromination. Therefore, we believe that debromination is an important degradation pathway for the lighter homologues, too. A more detailed assessment of the implications of uncertainties in the debromination yields is given in the Supporting Information.

5.2.3 The CliMoChem Model

The "Climatic zone Model for Chemicals" (CliMoChem) is a temporally resolved, global zonally averaged multi-media model (Scheringer et al., 2000, Wegmann, 2004, Wegmann et al., 2004). CliMoChem calculates the time-dependent concentration of a parent compound and selected transformation products in 10 latitudinal zones (assumed to be homogeneous in the east west direction) with a temporal resolution of three months. Each zone is composed of an ocean-water, atmosphere, bare-soil, vegetation-covered-soil, and vegetation compartment. The model simulates advective and diffusive exchange processes between compartments in the same zone (e. g. rain, evaporation), and exchange processes between the atmosphere and ocean-water compartments of neighboring zones (due to wind or ocean currents). Degradation processes are simulated in each compartment.

For the present project, a modified model version was employed that takes into account direct photolysis. Direct photolysis is dependent on the light intensity, which is in turn dependent on the climatic zone and the season. Light intensity data has been used from Lohmann et al. (2006b) and takes into account cloud cover and seasonal variations in day-length. Photolysis is calculated in the model by multiplying a second-order reaction rate constant k'_{photo} ($m^2/d/kW$) with the light intensity L (kW/m^2), for details see Supporting Information.

5.2.4 Emission Scenario

PBDE emissions have been estimated for Switzerland (Morf et al., 2007), Japan (Sakai et al., 2006a, Sakai et al., 2006b), and Denmark (Danish Environmental Protection Agency, 1999). Prevedouros et al. (Prevedouros et al., 2004) have, furthermore, estimated penta-BDE emissions into air in Europe. We have calculated time-dependent PBDE emissions of all homologues for the different climatic zones of the model and the different environmental media. To estimate global PBDE production, the method by Prevedouros et al. (2004) has been used; to predict emissions into different compartments the same method as used by Morf et al. (2007) has been applied to the global environment.

One of the important mass fluxes in the emission calculations arises from open burnings of waste containing PBDEs in countries with economies in transition (Chen et al., 2006, Leung et al., 2007). The only available measurement (Sakai et al., 2006b) of the amount of PBDEs that are released from open burnings predicts 10% of all PBDEs contained in the waste to be released to air. The same study claims that a high fraction of these 10% will undergo debromination during the combustion process. However, from other studies (Chen et al., 2006, Leung et al., 2007) there is strong evidence for high concentrations of deca-BDE in the surroundings of PBDE recycling and burning sites in China, whereas concentrations of typical debromination products of deca-BDE (such as nona- and octa-BDE) have not been measured at higher concentrations. When wind blows from recycling sites toward the measuring site, even particularly high concentrations of deca-BDE in air have been measured (Chen et al., 2006). We think this indicates that a significant part of deca-BDE from the recycled material is released without debromination during the combustion process. Therefore we assume that 10% of the total PBDE is released during combustion, and that none of this is debrominated during combustion. The details of all other mass fluxes are described in the Supporting Information.

Uncertainties are associated with the emission scenario because important emission factors are poorly known, and assumptions underlying some of the emission scenarios can be questioned. In the results section we describe the implications of these uncertainties.

5.2.5 Model Measurement Comparison

Using the emission scenario described above, realistic concentrations of PBDEs are calculated with CliMoChem, and the results are compared to field data. The goal of this comparison is not to confirm the model or its input parameters; this has previously been done for other substances for which more field data are available and emission scenarios are better known than for PBDEs, e. g. DDT (Schenker et al., 2008). For PBDEs, uncertainties on emissions, degradation pathways, and degradation rate constants are much higher, which impedes accurate predictions of present or future levels of PBDEs in the environment. However, a semi quantitative comparison of model results with field data still helps to identify model results that are in general agreement with field data, and in which some confidence may be placed.

Model results from CliMoChem are representative of average concentrations of large areas and can, therefore, only be compared to background measurements. For PBDEs, background measurements are widely available only for concentrations in air, and hence we have limited our comparison to the air compartment in the temperate region. In addition, in the CliMoChem model, measurements should be representative of average concentrations of a whole latitudinal zone. This is a strong limitation in the case of PBDEs, because the congener pattern of PBDE emissions differs between North America, Europe, and Japan (which all lie in the same CliMoChem zone). In particular, because penta-BDE has been phased-out in Europe, its usage is close to zero, whereas it is still frequently used in North America (Rahman et al., 2001). On the other hand, deca-BDE is by percentage less frequently used in North America, but the most abundant compound in Asia. Therefore, measurements of PBDEs are expected to differ strongly between continents, and we have tried to select measurement studies from different continents to obtain a picture that is representative of a whole zone of the CliMoChem model.

5.3 Results and Discussion

5.3.1 Fate of Various PBDE Homologues in the Environment

Table 5.1 shows values of the overall persistence (P_{OV}, units: days) and spatial range (R, a measure of long-range transport potential, units: percent of the pole-to-pole distance) (Scheringer, 1996) for four PBDE homologues. In the base scenario, photolysis is included as

described above. In an alternative scenario, all photolysis rate constants were set to zero, to quantify the importance of the photolytic degradation mechanism, and to reproduce the setting of previous modeling studies. In the base scenario, the overall persistence in the environment of highly brominated compounds considerably exceeds the persistence of lighter homologues. The spatial ranges, on the other hand, are higher for the lighter homologues (> 30%), whereas deca-BDE has a spatial range of only 10%. Both findings can be explained by the substance properties (see Tables S2, S18, and S19 in the Supporting Information) of heavier and lighter PBDEs: in soil and water, where the majority of the PBDE mass is stored, half-lives of heavier PBDEs are greater than those of lighter PBDEs, resulting in a higher overall persistence for the heavier PBDEs than for the lighter PBDEs. Half-lives in air, on the other hand, are shorter for the heavier PBDEs than for the lighter ones and, in addition, heavier PBDEs have lower vapor pressures than lighter PBDEs and are more efficiently washed-out from the atmosphere. The combination of these effects results in a shorter long-range transport potential for the heavier PBDEs than for the lighter PBDEs.

In previous studies (Gouin and Harner, 2003, Breivik et al., 2006, Raff and Hites, 2007) it was often stated that the dominant removal process of PBDEs from air is deposition, in particular for heavier PBDEs. In our model, this is not the case: for the hepta- to deca-BDE homologues, degradation in the atmosphere of the emission zone is responsible for 45% of the loss processes, deposition only for 30%. For hexa- and penta-BDE, all three processes have similar importance. For tetra-BDE, transport amounts to 42% of all loss processes, deposition to only 28%. The reason for these differences between previous studies and our results is that direct photolysis is included in our calculations as an additional degradation mechanism. If photolysis is switched off, atmospheric life-times of PBDEs (in particular of the heavier ones) increase considerably, and the dominant removal processes of all PBDE compounds from temperate atmosphere are deposition (40-60%) and transport (40-50%) but no longer degradation. This is in agreement with previous modeling studies that did not take into account photolysis (Gouin and Harner, 2003, Breivik et al., 2006). The implications of this degradation mechanism on the environmental fate of PBDEs will be analyzed in the following section.

Table 5.1 Persistence (P_{OV}, in days) and spatial range (R, in percent of the pole-to-pole distance) of different PBDE homologues in the base scenario (with photolysis as described in the methods section) and under the assumption that no photolysis takes place. For these calculations, a peak emission was assumed into atmosphere of zone 5 (0° N to 18° N) of the CliMoChem model.

indicator	photolysis	tetra-BDE	penta-BDE	octa-BDE	deca-BDE
P_{OV} (d)	yes	33	70	126	183
	no	90	355	1259	1552
R (%)	yes	23%	15%	11%	10%
	no	33%	32%	30%	30%

5.3.2 The Importance of Direct Photolysis

The influence of direct photolysis on persistence and spatial range is shown in Table 5.1: if photolysis is switched off in the model, the persistence of all compounds increases strongly, in particular for the highly brominated compounds. The same is observed for the spatial range: if photolysis is switched off, the spatial range of all PBDE homologues increases, and the spatial range of deca-BDE reaches a value close to those of tetra- and penta-BDE. This is in disagreement with measurement studies that generally find deca-BDE to be less mobile than the lighter homologues (Wang et al., 2005, Breivik et al., 2006).

The importance of photolysis can also be seen if the model results from CliMoChem are compared to model calculations presented by Breivik et al. (2006): in their results (from the CoZMo-POP model, not taking into account photolysis), the long-range transport potential of heavier PBDEs is higher than that of lighter ones. They also present model results from the TaPL3 and ELPOS models (that do not take into account photolysis either), which suggest a lower long-range transport potential for the heavier PBDE congeners than for the lighter ones. Breivik et al. explain the difference between CoZMo-POP and TaPL3/ELPOS with the fact that CoZMo-POP takes into account intermittent rainfall: in TaPL3 and ELPOS, rain is assumed to occur permanently and to constantly wash out chemicals from atmosphere, thereby limiting their potential for long-range transport. In reality, however, periods of dry weather appear and result in episodes of efficient long-range transport, as described by Hertwich (2001). The CoZMo-POP model takes into account periods of dry weather, which results in a high long-range transport potential for the heavier PBDEs. Because a higher persistence in air is assumed for these chemicals in CoZMo-POP (no photolysis), heavier PBDEs bound to aerosols may travel far before they are degraded or deposited under dry conditions.

The CliMoChem model also features a module that takes into account intermittent rainfall (according to the parameterization suggested by Jolliet et al. (2005)) that was used in our base scenario. If this module is switched off, the spatial range of all PBDEs remains almost constant. This shows that intermittent rainfall has no influence on the behavior of PBDEs if photolysis is taken into account. This is different if we model PBDEs without photolysis (to mimic the behavior of the models presented by Breivik et al. (2006)): switching off the module on intermittent rainfall results in a decrease of the spatial range of deca-BDE from 30% to 25%. This is in agreement with the findings from Breivik et al. The higher half-life in air in this model parameterization makes deca-BDE more sensitive to modifications in the rain deposition settings of the model. As opposed to the TaPL3 / ELPOS models, the spatial range of deca-BDE in CliMoChem is still in the same range as that of penta-BDE, even if the module on intermittent rainfall is switched off. This shows that photolysis needs to be taken into account in CliMoChem to adequately model the long-range transport potential of PBDE homologues.

In our calculations, photolysis takes place in the gas-phase and on aerosols, as described in the methods section, whereas Raff and Hites (2007) assume that photolysis occurs only in the gas-phase. The importance of the particle-bound phase for the overall fate of PBDEs in the environment depends on the fraction of PBDEs that is bound to aerosol particles. Raff and Hites (2007) assume that 99.999% of deca-BDE is bound to particles. With this assumption, degradation of the particle-bound fraction is a highly influential process: if no photolysis is assumed in the particle-bound fraction, the atmospheric degradation life-time of deca-BDE is about 250 days (Table 1 in Raff and Hites, 2007). However, if photolysis is assumed to take place and the photolysis rate constant of the particle-bound fraction is assumed to be 125 times lower than in the gas phase (the ratio used in our calculations), the degradation half-life of deca-BDE decreases to only 0.31 days. With this constellation, photolysis of deca-BDE will be the dominant removal pathway. Compared to the results of Raff and Hites, the deposition fluxes of deca-BDE are then considerably lower, and the emission fluxes leading to the observed atmospheric concentration would be higher than estimated by Raff and Hites. In our calculations with the CliMoChem model, the particle-bound fraction of deca-BDE is between 99.1 and 99.98%, which is lower than assumed by Raff and Hites. Therefore, deca-BDE photolysis on particles is approximately equally important as in the gas phase in the CliMoChem model. In summary, the value of the particle-bound fraction, which is a function

of temperature and other parameters (for details, see Götz et al., 2008), determines if photolysis on aerosols is an important degradation pathway.

5.3.3 Realistic Concentrations of PBDEs

To compare model results with field data, we have calculated geometric means of measured concentrations from different studies (see Supporting Information). Of these means from different studies, the median, minimal, and maximal values are displayed in Figure 5.1 (crosses, squares, and dots with vertical bars), together with model results (diamonds).

In Europe (ter Schure et al., 2004) and Asia (Wang et al., 2005), average deca-BDE concentrations of about 3.7pg/m3 have been measured. In North America average concentrations of about 0.88 pg/m3 have been reported (Strandberg et al., 2001, ter Schure et al., 2004, Hoh and Hites, 2005, Gouin et al., 2006). Our model results suggest an atmospheric deca-BDE concentration of about 0.15 pg/m3 in the northern temperate region, which is about one order of magnitude below the field data.

More measurements than in the case of deca-BDE are available for penta- and tetra-BDE homologues, and levels in Northern America and Europe are more similar. The most frequently measured congeners are BDE-47 for the tetra-BDE homologue, and BDE-99 and BDE-100 for the penta-BDE homologue. Average levels of about 5.3 pg/m3 have been measured for the sum of tetra-BDE congeners, and 2.9 pg/m3 for the sum of penta-BDE congeners (Strandberg et al., 2001, Jaward et al., 2004a, Lee et al., 2004, ter Schure et al., 2004, Hoh and Hites, 2005, Jaward et al., 2005, Wang et al., 2005, Gouin et al., 2006). Model results for tetra-BDE suggest concentrations of about 0.18pg/m3 in 2002 in the temperate atmosphere, and 0.08pg/m3 for penta-BDE. Model concentrations are again at least one order of magnitude below measurements.

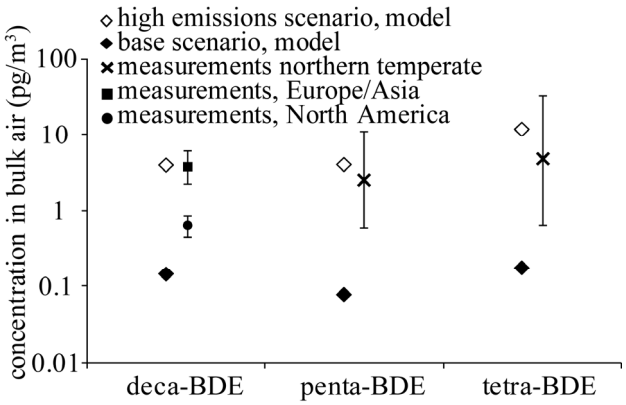

Figure 5.1: Atmospheric concentrations measured in the Northern temperate regions, and predicted by the model. The modifications in the emission scenario increase predicted concentrations by the model to levels close to measurements.

The relative order of the homologues is correctly reproduced: the CliMoChem model yields highest concentrations of the tetra-, followed by deca- and penta-BDE homologues. In the measurements, tetra-BDE congeners are measured in higher concentrations than the penta-BDE congeners (Figure 5.1). Depending on the continent in which measurements took place, deca-BDE concentrations are above (for instance in Sweden in ref. (ter Schure et al., 2004)) or below (in North America in ref. (Strandberg et al., 2001, Hoh and Hites, 2005)) the sum of tetra- and penta-BDE congeners. Latitudinal differences are correctly reproduced by the model on a qualitative basis: concentrations of all PBDE homologues in the model decrease from the temperate zone toward the Arctic, and the decrease is stronger for the heavier PBDEs than for the lighter ones. This is consistent with atmospheric deposition data extrapolated from sediments (Breivik et al., 2006), and atmospheric measurements for deca-, penta-, and tetra-BDE congeners in the Pacific and Arctic Ocean (Wang et al., 2005).

The model underestimates levels of PBDEs in the environment. This could, among other reasons, be due to errors in the emission inventory or in the degradation rate constants. Whereas lower degradation rate constants might increase PBDE levels in the environment slightly, we believe that the main reason for the discrepancy visible in Figure 5.1 is that we have underestimated PBDE emissions. If some of the assumptions underlying the emission scenario are modified, the model yields results that are close to the field data. In the alternative emission scenario "high emissions", we attribute maximal values to three factors of the emissions scenario: (a) PBDE production in our study is between two to three times below values suggested in other sources (e. g. (Rahman et al., 2001)). Therefore, we increase the amount of PBDE production by a factor of three. (b) Emission factors from the use phase (evaporation or washout of PBDEs) are highly uncertain. Therefore, the emission factors of all PBDE homologues have been increased by a factor of 25, the difference between the value in the base-scenario and the maximal value for these factors suggested in refs. (European Chemicals Bureau, 2000, Alcock et al., 2003, Prevedouros et al., 2004). (c) A significant source of PBDE emissions in developing countries are emissions from open burnings of waste containing PBDEs, in particular electronic waste (Leung et al., 2007). Electronic waste from industrialized countries is sent for treatment into developing countries, where it is often burnt and leads to even higher emissions (Widmer et al., 2005). The amount of waste containing PBDEs that burn in open fires is uncertain and varies strongly between countries. In the "high-emissions" scenario, we set the part of waste that is burnt in open fires to 50% in developing countries, and to 25% in countries in transition (five times higher than in our base

scenario). In addition, we assume that 25% of the PBDEs in polymer products in industrialized countries are sent for waste treatment to developing countries (zero in the base scenario).

The results of the alternative model runs are indicated by open diamonds in Figure 5.1. Modeled concentrations with the "high-emissions" scenario are much higher than previously and lie above the median of the field data.

5.3.4 The Importance of deca-BDE for Lighter PBDEs in the Environment

To assess the importance of the deca-BDE mixture for concentrations of the lower brominated compounds, the share of the concentrations caused by emissions of the deca-mixture alone is calculated. The results suggest that about 50% of the hepta- and hexa-BDE homologues in the environment originate from emissions of the deca-BDE mixture. For the lower brominated compounds, this ratio decreases quickly: about 13% of the penta- and only 2.5% of the tetra-BDE homologues in the environment originate from the deca-BDE mixture. The octa-BDE mixture is responsible for another 11% of the penta- and 2% of tetra-BDE homologues (see Supporting Information for details). This means that the main contributor to levels of penta-BDE in the environment is direct emissions of the commercial penta-BDE mixture. On the other hand, if the commercial penta-BDE mixture was phased-out on a global scale, levels of penta-BDE measured in the environment would decrease by a factor of ten, but penta-BDE would not completely disappear from the environment, because it is constantly regenerated from the degradation of deca-BDE.

The fraction of deca-BDE mixture use is much higher in Asia than elsewhere (Rahman et al., 2001), and we expect the levels of penta-BDE in Asia to be more strongly influenced by emissions of deca-BDE than predicted by our zonally averaged model. On the other hand, in North America, where penta-BDE emissions are more important than in the rest of the world (Rahman et al., 2001), the importance of deca-BDE for levels of penta-BDE are less important than in our prediction.

5.3.5 Uncertainties of the Predicted Importance of Debromination

If emissions of penta-BDE were lower or emissions of deca-BDE higher than assumed in our emission inventory, the importance of the deca-BDE mixture as a source of penta-BDE might be higher than calculated above. As stated in previous measurement studies (Lee et al., 2004),

the congener pattern of penta-BDEs found in the environment is consistent with the congener pattern of the commercial penta-BDE mixture and differs from the congeners that are frequently identified in debromination studies of deca-BDE. This indicates that direct emissions of penta-BDE are responsible for a majority of penta-BDE found in the environment, and it appears unlikely that debromination of deca-BDE is responsible for more than 10% of the penta-BDE levels. If emissions of penta-BDE were higher or emissions of deca-BDE lower, on the other hand, the deca-BDE mixture might be responsible for a smaller part of the total penta- and tetra-BDE in the environment. In the comparison of the model results with field data (see Figure 5.1), the ratio of penta- to deca-BDE in the model was similar to that observed in the field data. This suggests that the ratio of emissions of the two homologues is approximately correct, although a small bias in the emissions might be masked by a bias in the degradation rate constants, or by the selection of measurement data to which we have compared our model results. It is therefore possible that the contribution of deca-BDE to levels of penta-BDE in the environment is below 10%. It is, however, unlikely that the bias in degradation rate constants and the selection of measurement data masks a bias in the emissions larger than a factor of five, and therefore we believe that the lower limit of the importance of deca-BDE as a source of lighter PBDEs is 2%.

Deca-BDE contributes up to 10% of penta-BDE levels in the environment. If penta-BDE is phased-out completely, the importance of deca-BDE as a source of penta-BDE will increase, and penta-BDE will still be present in the environment, yet in lower concentrations than today. If deca-BDE use increases in the future due to an increasing demand in countries in transition (Wang et al., 2007), levels of penta-BDE might decrease less strongly. To reduce levels of deca-BDE in the environment, our model suggests that improving waste-management methods might be an efficient measure, because a majority of deca-BDE originates from the waste-management phase. To improve the reliability of the present model calculations, more information on PBDE emission factors in the use- and waste-management-phases should be gained. In addition, the behavior of PBDEs in atmosphere, in particular the debromination yields of lighter homologues, should be better characterized.

5.4 Acknowledgments

We thank Markus Bläuenstein, Andreas Buser, Thomas Peter, Ulrich Krieger, Claudia Marcolli, Christian Bogdal, Andreas Gerecke, Martin Kohler, and Peter Schmid for help with the emission scenario, field data, degradation processes, and debromination yields.

5.5 Supporting Information

Supporting Information is available in the appendix, chapter 9.3.

Chapter 6:

Investigating the Global Fate of DDT: Model Evaluation and Estimation of Future Trends

Urs Schenker, Martin Scheringer, Konrad Hungerbühler

Institute for Chemical and Bioengineering, ETH Zurich, CH-8093 Zurich, Switzerland

Keywords: pesticide hazard assessment, model confirmation, realistic emission inventory, multimedia box modeling

Reproduced with permission from:
Environmental Science and Technology, 2008
Volume 42, Issue 4, pages 1178-1184
DOI: http://dx.doi.org/ 10.1021/es070870h

Abstract

The global environmental fate model CliMoChem has been used to calculate concentrations of dichlorodiphenyltrichloroethane (DDT) and its degradation products in the environment. To this end, best available physicochemical properties of DDT have been assembled, and a realistic DDT emission scenario covering the period from 1940 to 2005 has been generated. Results from the model are temporally and geographically resolved concentrations of DDT, dichlorodiphenyldichloroethylene (DDE), and dichlorodiphenyldichloroethane (DDD) in various environmental media. To confirm model results with measurements, we have developed a method for a qualitative and quantitative comparison of model and measurements. The agreement between the model and measurements is good, especially in the temporal dimension, and in the soil and air compartments. Using estimated DDT emissions for the future, we predict environmental concentrations in the next 50 years. The results show that, if emissions continue at a low level, concentrations will decrease by a factor of 30 in temperate regions and by a factor of 100 in the Arctic, as compared to the concentrations in the 1960s and 1970s. In the tropics, levels decrease by a factor of 5 to 10, only. Whereas environmental concentrations and estimated future emissions are at steady-state after about 10 years in temperate and tropical regions, this takes over 50 years in the Arctic.

6.1 Introduction

Environmental fate models have widely been used to determine the exposure of humans and the environment to chemicals (Mackay and Paterson, 1991, Scheringer, 1996). They are a necessary complement to measurements in the environment, because they provide insights into how and why some chemicals accumulate in given media of the environment. However, the major drawback of models is that they are, by their very nature, only representations of the environment, and that it is often unclear whether these representations are valid. Therefore, it is crucial that models be confirmed by comparison with measurements.

Results from multimedia fate models have been compared with field data in earlier studies: for atmospheric and oceanic α-HCH concentrations globally by Wania et al. (1999), for α-HCH and γ-HCH concentrations in and around the Baltic Sea in various media by Breivik and Wania (2002), and Shen et al. (2005) have compared measured distributions of various substances with model-derived transport distances in North America. However, no guidelines for comparing model results with environmental measurements have yet been suggested. Because field data and model results often differ in their temporal and spatial resolution and in the environmental media, geographic regions, and time periods that are sampled/modeled, guidance is needed for model measurement comparisons.

In this publication, we present a new method that compares results from a global environmental fate model to measurements in the environment. We have applied this method to the environmental fate model CliMoChem (climatic zone model for chemicals) with DDT as an example. DDT has been selected because it is frequently measured in the environment, has fairly reliable substance properties, and emission inventories are available. We compare model results from CliMoChem for DDT and the transformation products DDE and DDD on a large scale to past and present measurements in various environmental media and geographic regions.

DDT has extensively been used as a pesticide for agricultural and public health purposes (to combat the malaria vector, the anopheles mosquito). Because of the human health and environmental hazards that are associated with DDT, it has been regulated under the Stockholm Convention (United Nations Environmental Program, 2008) and can legally only be used for vector control. Recently, the World Health Organization has announced that it will rely more heavily on DDT for malaria vector combat programs in the future (World

Health Organization, 2006). Based on the confirmation of our model with measurements from the past, we have attempted to predict levels of DDT that may be expected from such uses in the future. To this end, we use two scenarios: a base scenario, in which emissions continue on a certain level for malaria combat purposes, and an alternative scenario where emissions cease in 2005. We have assessed the environmental concentrations that have to be expected in the next 50 years in various media of the Arctic, temperate zones, and the Tropics.

6.2 Materials and Methods

6.2.1 CliMoChem Model

To calculate pollutant dynamics, the temporally resolved, zonally averaged multimedia box model CliMoChem has been used (Scheringer et al., 2000, Wegmann, 2004). This model has been developed in our institute; a freely available version is in preparation. For the present calculations, CliMoChem is used with 30 latitudinal zones, each of which covers 6° latitude. Each zone contains five environmental media: bare soil, vegetation-covered soil (with a higher organic matter content than bare soil), vegetation, top layer ocean water, and tropospheric air. The model simulates diffusive and advective phase exchange processes within a zone, and describes interzonal transport with eddy-diffusion coefficients in ocean and atmosphere. A model version capable of simulating parent compounds and degradation products simultaneously was used (Schenker et al., 2007).

6.2.2 Substance Property Data

The CliMoChem model requires information on substance half-lives in the media, phase partitioning data, and the temperature dependencies of those properties. While partitioning and half-life information for DDT is available in the literature (Mackay et al., 1997, Schenker et al., 2005a), there is much less information available on the degradation products DDE and DDD, in particular about degradation half-lives. If no literature information was available, we extracted degradation half-lives from QSAR software (Jaworska et al., 2002, U.S. Environmental Protection Agency, 2004), or applied existing extrapolation methods based on QSAR values (Arnot et al., 2005). A detailed description of these methods and a table with the substance properties used for DDT, DDE, and DDD is given in the Supporting Information. We did not distinguish between the p,p´- and o,p´- isomers of DDT, DDE, and

DDD. Instead, we used averaged substance properties, e.g., for biodegradation, and tracked the sum of the two isomers in field data.

6.2.3 Emission Scenario Construction

Several DDT emission inventories have previously been compiled. Semeena and Lammel (2003) relied on agricultural usage data reported to the Food and Agriculture Organization (FAO), Wegmann (2004) based his inventory on production data from various sources, and Li and co-workers (Arctic Monitoring and Assessment Program, 2004, Li and Macdonald, 2005, Li et al., 2006) partially published an emission inventory based on a large number of sources on agricultural and public health usage. We compared the three independently compiled inventories to each other, and found only small differences (Schenker et al., 2006). From these three inventories, a "most probable" inventory was compiled and adapted to the CliMoChem model to calculate environmental concentrations between 1940 and 2005 (see the Supporting Information). For calculations of future concentrations, two scenarios were assumed: in the base scenario, DDT emissions in the tropics continue at a low level. In this scenario, about 15000 tonnes of DDT are emitted per year. This is about 10% of the annual emissions in the 1960s and would be sufficient to treat at least 15 million households against the anopheles mosquito (for details on this calculation, see the Supporting Information). In the alternative scenario, emissions cease in 2005, representing a complete ban of DDT.

6.2.4 Measurement Data

Measurement data from 54 sources (peer-reviewed journal publications, books, reports, personal communications, and online-databases) have been used to compare model results with measurements. For reasons of brevity, the complete list and a more detailed description of studies that we have used is relegated to the Supporting Information. Here, a summarized description of the most important studies is presented.

6.2.4.1 Air and Water

Frequent background measurements exist for the Arctic atmosphere (Bailey et al., 2000, Hjellbrekke, 2007). Iwata et al. (1993) have studied DDT in the oceanic atmosphere on ship cruises. The atmosphere in temperate regions has been intensely studied (for instance Hoff et al., 1996, Shen et al., 2005, Hjellbrekke, 2007). Iwata et al (1993) have measured concentrations in water on a north−south transect in the Pacific and Indian Oceans from the

Chukchi Sea to the oceans surrounding the Antarctic. More measurements are available for water (see Supporting Information), but ocean water clearly is the medium in which measurements are least frequent, especially in recent years.

6.2.4.2 Soils and Sediment

DDT levels have been determined in background soils in temperate regions by various authors (Dimond and Owen, 1996, Harner et al., 1999). In addition, a global study has also sampled background soils in arctic and tropical regions (Kurt-Karakus, 2006). Various authors have measured DDT concentrations in sediment (Jonsson et al., 2000). These measurements have usually been made in lakes or shallow ocean water of temperate zones (see Supporting Information). We have used those studies for comparison with the temporal evolution of DDT concentrations in our model. In addition to these sediment studies, the temporal evolution of DDT has also been measured in some long-term soil measurements (Dimond and Owen, 1996, among others).

For reasons of consistency and transparency, some studies on DDT in the environment could not be included. All measurement studies that we used had to provide at least basic information on quality assessment of their measurements. Because the CliMoChem model consists of ocean water, atmosphere, soil, and vegetation, only data for these media were considered. Bioaccumulation studies had to be excluded, as they cannot be compared to results from CliMoChem. Furthermore, the results generated by the CliMoChem model are representative of background DDT concentrations and cannot be compared to areas where DDT has (recently) been applied. Therefore, several studies assessing evaporation of DDT from sprayed fields had to be excluded.

Bignert et al. (1998) pointed out that summarizing measurements from various sources is a challenging task from a methodological point of view. They describe three potential factors that can bias the summarized measurement data: measurement methods and protocols (including detection limits and sensitivities) can differ between studies; seasonal variations in concentrations have to be taken into account when geographical or long-term temporal comparisons are made; only background measurements allow statements on long-range transport of pollutants. The Supporting Information gives more detailed information on how we dealt with these issues.

6.2.5 Model Measurement Comparisons

Model results can be compared to measurements in four dimensions: zonal distribution, partitioning between environmental phases, temporal evolution of concentrations, and relative amount of parent compound and transformation products. To perform the actual comparison, a method was developed that is based on three levels: on the first level, only qualitative information extracted from the measurements is compared with qualitative information from the model. On this level, the general behavior of the model can be evaluated. On the second level, indicators calculated from the model are quantitatively compared with indicators calculated from measurements. Examples of such indicators are the ratio between concentration in atmosphere and soil, or the year of maximum concentration. Indicators allow conclusions about certain aspects of the model and whether they are consistent with what can be seen in the environment: for instance, if the DDT/DDE ratio in air differs from measured values, there could be a problem with the degradation half-lives of either DDT or DDE in air. Finally, on the third level, absolute values (concentrations) from the model can be compared with environmental concentrations. We suggest that the comparison on these three levels be made in sequence: if the comparison on the first level suggests a poor agreement of the model with measurements, modifications of the model or reinterpretations of measurements can be made before the more labor-intensive second and third level comparisons are attempted.

In the DDT case, a comparison in all four dimensions is not possible on all levels: insufficient measurements are available for the comparison of absolute concentrations before 1985 and for the degradation products of DDT. Therefore, absolute values are only compared for the last 20 years and only for DDT. Furthermore, the zonal resolution has been reduced to three regions (instead of the 30 zones of the model): the Arctic (north of 54° N), the temperate belt (36° N to 48° N), and the Tropics (24° N to 24° S). Very few measurements exist for the southern hemisphere and, therefore, we have not compared model results with measurements in the southern temperate and polar zones.

In the quantitative comparisons between model and measurements (second and third level), the data points from publications in the literature have been aggregated to measurement series. From some publications, only one measurement series was created if the total amount of data points was small. From other publications, typically measurement databases, several measurement series were created (for details, see the Supporting Information). For each

measurement series, a median or average was determined. Then, for each environmental medium, geographical region, and substance, the median of the medians of these measurement series was calculated. To obtain information on the variability of the measured concentrations, 25th and 75th percentiles of the measurement series were derived for the comparison on the third level.

6.3 Results and Discussion

6.3.1 Levels Measured in the Environment

Temporal trends of DDT from sediments in Europe and North America reveal that DDT concentrations in the environment increased from about 1940 on and reached a peak between 1965 and 1970 (dots in Figure 6.1). Since then, concentrations have been decreasing. The average concentration between 1965 and 1970 was about 3 times higher than the average concentration in 1990. The two long-term studies in soils (open circles in Figure 6.1) indicate that, from 1965 on, DDT concentrations have been decreasing (no soil studies prior to 1965 were available). The average concentration between 1965 and 1970 was between 4 and 10 times higher than concentrations in 1990.

Measurements show (e. g. Iwata et al., 1993) that in all environmental media, DDT concentrations decrease from the tropical regions to the temperate and Arctic environments. The decrease seems to be stronger for the atmosphere than for soil and water. In most measurement studies, DDT was the dominant substance (e. g. Iwata et al., 1993, Dimond and Owen, 1996, Kurt-Karakus, 2006), although in the atmosphere DDE was present at similar concentrations (Hoff et al., 1996). In water, DDD was present at higher concentrations than DDE, whereas in atmosphere and soil, DDE is usually more abundant than DDD by a factor of 3-5.

6.3.2 Model Comparison

In the following, we compare the model results with measured data using the method described above.

6.3.2.1 First Level

On a qualitative basis, the model reproduces measurements fairly well: concentrations in the model increase until about 1965, come to a peak, and decrease afterward (see Figure 6.1). The zonal distribution shows highest atmospheric and soil concentrations around the equator and decreasing concentrations toward the pole (not shown). In ocean water, however, concentrations in the Arctic are slightly higher than in the tropical and in the temperate regions, see Figure 6.2. This difference from the measured data is analyzed in more detail in the following section. DDT is found in the highest concentrations as compared to its degradation products in all media of the model.

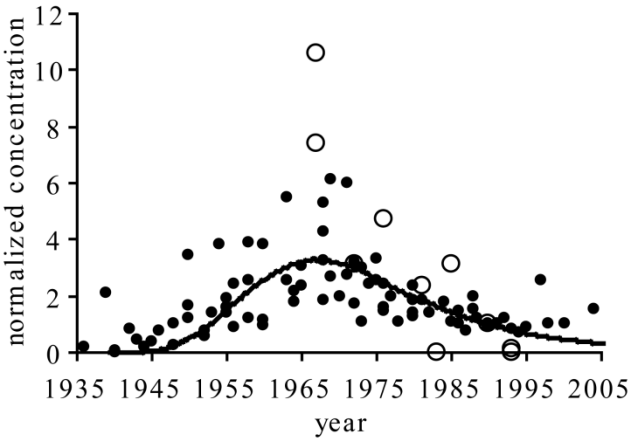

Figure 6.1: Evolution of concentrations in the model in soil of the temperate regions (line) and deduced from various sediment (dots) and soil studies (open circles) (data from Dimond and Owen, 1996, van Metre et al., 1997, Jonsson et al., 2000, Olsson et al., 2000, Meijer et al., 2001, Stern et al., 2005, van Metre and Mahler, 2005, Bogdal et al., 2007). To allow comparisons between different studies, all concentrations from a given study were normalized to the concentration that was reported in this study for 1990.

6.3.2.2 Second Level

On the second level, model and measurements are compared in terms of various indicators. For each of the dimensions of the model results (temporal dimension, zonal dimension, environmental phases, fractions of substances), indicators are shown in Table 6.1. These show that, first, the model is in close agreement with measurements for the temporal evolution: the maximal concentration appears at about the same time, and the magnitude of the maximal concentration, as compared to the concentration in 1990, is similar, too. Second, the model is in relatively good agreement with the zonal distribution of the measurements expressed as concentration ratios between the Arctic, temperate, and tropical regions. The

difference between the measurements and the model is around a factor of 2. The measurements suggest a stronger decrease of concentrations toward the Arctic. Third, for DDT the model reproduces well the partitioning between phases (expressed as concentration ratios between atmosphere, water, and soils). For DDE and especially DDD, the corresponding ratios differ by 1 or 2 orders of magnitude. On the one hand this is because DDE concentrations in atmosphere are underestimated in the model, as discussed further below. On the other hand, the number of measurements available for DDE and DDD is small, and the values of the empirical concentration ratios are uncertain. Finally, the fraction of the parent compound and the degradation products is well reproduced by the model in water and soils. In the atmosphere, the fraction of DDE is too low and the fraction of DDT too high. Again, possible reasons for this discrepancy will be given in the following section.

Table 6.1: Level two comparison (indicators) for model results (left part of table) and measurements (right part of table). The selected indicators are displayed in the rows of the table.

	model results			**measurements**		
	temporal evolution					
year of maximum	1966			~ 1968		
maximum / 1990	5.9			~ 4		
	zonal distribution					
	atmosphere	non-volatile phases		atmosphere	non-volatile phases	
Arctic/tropic ratio	0.21	0.82		0.10	0.37	
temp/tropic ratio	0.55	0.87		0.25	1.11	
	partitioning between phases					
	DDT	DDE	DDD	DDT	DDE	DDD
c_{air} / c_{water}	1.6×10^{-3}	4.4×10^{-4}	5.7×10^{-6}	3.6×10^{-3}	3.5×10^{-3}	8.8×10^{-5}
c_{air} / c_{soil}	2.3×10^{-9}	4.1×10^{-10}	3.0×10^{-12}	4.2×10^{-9}	1.2×10^{-8}	-
	fractions of parent compounds and degradation products					
	soil	atmosphere	water	soil	atmosphere	water
DDT	49%	91%	65%	42%	58%	59%
DDE	25%	9%	21%	50%	16%	32%
DDD	26%	0%	14%	8%	27%	9%

6.3.2.3 Third Level

Figure 6.2 compares absolute concentrations of DDT (without degradation products) between 1985 and 2005 in the model with measurements from the same period of time. The green dots represent the median values from measurements. The green bars represent the 25th and 75th percentiles of the measurements in cases where four or more measurement series were available. If only one measurement series was available, no bars are displayed, and if two or three measuement series were available, all values are displayed by bars with dashed lines.

The large red dots display the concentrations predicted by the model; the small red dots show variability in the model results obtained from different model scenarios, see below and in the Supporting Information.

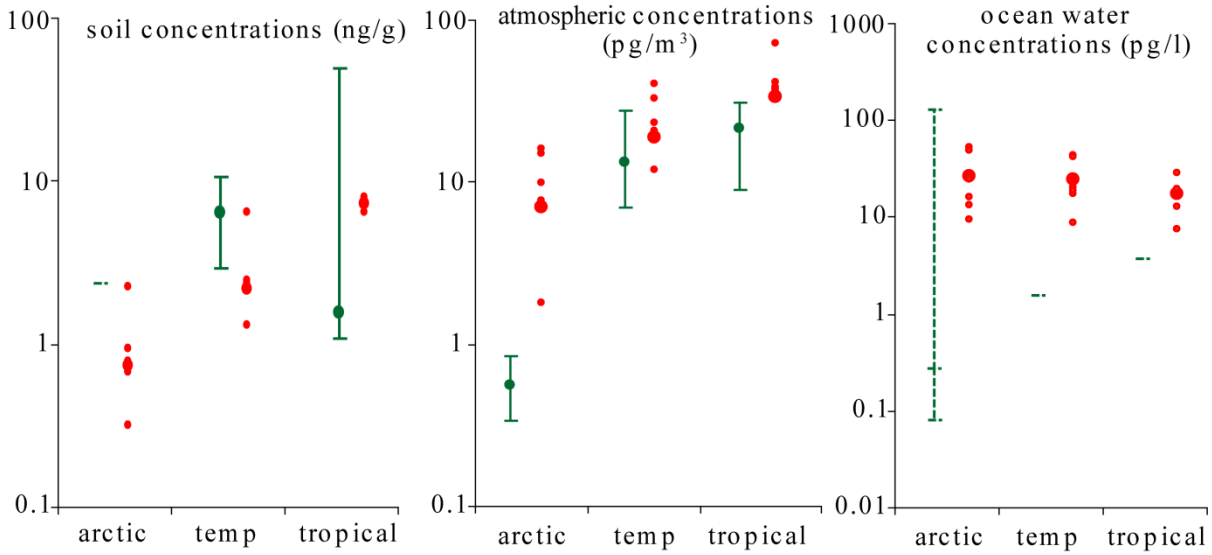

Figure 6.2: Measured (green dots and bars) and modeled (red dots) DDT concentrations (without degradation products) between 1985 and 2005. For the measurements, 25th and 75th percentiles are displayed as green bars, indicating variability among different measurement series. If dashed lines are used for the bars, fewer than four measurement series were available, and the bars display the individual values. If no bars are given, only one measurement series was available. For the model, the concentrations from the standard run are displayed as large red dots. The small red dots are results from runs with modified model settings, as described in the Supporting Information. The *y* scales are logarithmic; each medium has different units.

Modeled and measured concentrations are in good agreement for soil. Atmospheric concentrations are in good agreement in the tropical and temperate regions. In the Arctic, the model predicts atmospheric concentrations that are about 1 order of magnitude above the measurements. In ocean water, the modeled concentrations on average seem to be higher than measurements. However, it is unclear whether the available measurements actually represent background values since in both, temperate and tropical regions, only one ocean measurement study was available. In the Arctic region, where three studies were available, the minimal and maximal values span more than 3 orders of magnitude, suggesting a high variability of DDT concentrations in oceans.

6.3.3 Findings from Model Measurement Comparison

From the above comparison on the three levels, a number of elements can be identified where the model and measurements are in good agreement: the temporal evolution of concentrations is well reproduced by the model; the zonal distribution predicted by the model is relatively close to the measurements (within about a factor of 2, see Table 6.1), indicating that the model reproduces the general pattern of long-range transport and deposition of DDT; the partitioning between atmosphere, water, and soils is very well reproduced for DDT; the fractions of DDT and its degradation products correspond well in water and soils. This is encouraging because our model setting has not been fitted to the measurements in any way; all model input parameters have been taken from the literature as they were reported, no adaptations have been made.

On the other hand, there are several elements where the model and the measurements show a disagreement: Absolute levels in the Arctic atmosphere exceed measurements by a factor of 10 (see Figure 6.2); DDE levels in atmosphere are underestimated; DDT levels in air are overestimated; DDE partitioning between air and soils differs by 2 orders of magnitudes between measurements and the model (the model predicts a lower volatility); the zonal distribution in water in the model suggests constant or slightly increasing concentrations toward the pole, whereas measured concentrations decrease, but are based on very few measurements.

6.3.4 Possible Reasons for Disagreements

There are three possible reasons that could explain these disagreements.

(a) Chemical substance properties and emission data that are used as inputs for the model are subject to considerable uncertainties and may lead to incorrect results. We believe that this might be the reason for underestimated DDE levels in the atmosphere. No measured half-lives for DDE in air are available, and therefore we relied on OH radical reaction rate constants predicted with AOPWin (U.S. Environmental Protection Agency, 2004). In the case of DDT, in contrast, there are also measured degradation rate constants and the AOPWin predictions are about 1 order of magnitude higher than the measured values, suggesting that AOPWin might predict atmospheric degradation half-lives that are too short (see the Supporting Information).

(b) Relevant environmental processes might be reproduced incompletely in the model. This might explain part of the discrepancies in the zonal distribution in ocean water: Lohmann et

al. (2006a) have shown that deep water formation in the North Atlantic is the most important removal pathway for many PCB congeners. This process has not been considered in the model setting. As we show in the Supporting Information, including this process, together with other modifications in the ocean compartments, can decrease DDT concentrations in the Arctic ocean by about 60%.

(c) Measurements might poorly represent actual background levels, especially if only few measurements are available. This probably applies to the concentrations in ocean water; the data we used in our comparison is based on only three measurement studies. Other studies were excluded from the comparison because they were performed before 1985. These older studies show DDT concentrations in ocean water that are much higher than the low values in Figure 6.2. The review by Fowler et al. (1990) with data from 1972 to 1980 and a north−south transect in the Pacific and Indian Ocean from 1980 to 1981 (Tanabe et al., 1982) report concentrations that are about 1000 times higher than those from Iwata et al. (1993), which is our data basis for the temperate and tropical regions. In our opinion, this discrepancy cannot be caused by the decrease of DDT concentrations in Arctic ocean water alone but also indicates spatial variability in DDT levels. Figure 6.1 and Figure 6.3 (below) indicate that average DDT levels in the environment did not decrease by more than a factor of 5 in the 1980s. A high spatial variability of oceanic DDT concentrations is also confirmed by the pronounced differences between the measurements in the Arctic from Iwata (1993) and Strachan et al. (2001).

It is possible to change the model setting to achieve a better fit between the model results and the measurements. To illustrate the variability of the model results, we have compiled six model runs with alternative settings. A detailed description of these model runs is given in the Supporting Information. We have included the results from these runs in Figure 6.2 as small red dots. It has to be kept in mind that these points do not indicate confidence intervals or quartiles. Moreover, the combination of two modifications can lead to lower or higher concentrations than indicated by the small red dots in Figure 6.2. It would be desirable to perform a more complete sensitivity and uncertainty analysis for the model to gain more information on the confidence intervals of model results. This is, however, beyond the scope of the present study and will be investigated in a future project.

In conclusion, the fate and transport model CliMoChem has been shown to be capable of adequately reproducing the spatial distribution and temporal evolution of DDT concentrations and, to some extent, absolute levels of DDT and its degradation products in the environment.

The model performs best when indicators are assessed: the ratio between water and atmosphere, or the year of maximal concentration in the environment is reproduced with high accuracy. The model produces acceptable results if absolute concentrations are assessed; soils are the compartment in which measured levels are reproduced best. To evaluate the model performance for concentrations in water, more measured data would be required.

6.3.5 Predicting Future Levels with CliMoChem

To assess the utility of CliMoChem for future temporal evolutions, we have analyzed the sensitivity of model results with regard to the six model modifications used in the previous section (small red dots in Figure 6.2) and presented in detail in the Supporting Information. It shows that the ratio of the DDT concentration in 1990 and in 2040 varies by less than 20% (in any compartment) among the six model settings (see Supporting Information). This means that the prediction of future trends with the model is relatively reliable.

We have tracked the mass of the sum of DDT, DDE, and DDD (denoted by ΣDDT in the following) in the model. Assessing ΣDDT instead of DDT alone takes into account that degradation products can significantly contribute to environmental and human exposure to chemicals (Schenker et al., 2007). Figure 6.3, left, displays the temporal evolution of DDT emissions (bars, right *y* axis) and of ΣDDT normalized to the mass of ΣDDT in the 1970s for the Arctic, temperate, and tropical regions (lines, left *y* axis). In the past, the highest levels in the tropical and temperate regions (red and green lines) occurred with a lag-time of 5 to 10 years after the peak of the emissions, and about 5 years before the highest levels in the Arctic (blue line). When the peak concentrations in the environment were reached, emissions were already decreasing.

For the future evolution of DDT emissions, two scenarios are assumed: either emissions continue at a low level (light-gray bars, resulting levels in the environment in full lines), or they cease in 2005 (dark-gray bars, resulting levels in the environment in dashed lines). The future evolution of ΣDDT levels in the environment differs strongly between the Arctic and the tropics. With continuing emissions, ΣDDT levels have reached a steady-state in the tropics in 2020. In the Arctic, however, levels are still declining, and a steady-state is not reached until about 2090 (not shown in figure). It can also be seen that a stop of emissions affects environmental levels in a significant way only in the tropical regions. In the temperate

regions, the difference between the full and the dashed line remains below a factor of 2 for 20 years, in the Arctic for about 50 years.

The overall mass in the model environment is dominated by the soil compartment: typically, about 95% of the ΣDDT are contained in soils. It is interesting to consider also the ocean compartment, which is important for marine food chains. The right side of Figure 6.3 displays the temporal evolution of ΣDDT in oceans with the two emission scenarios. The ocean compartment reacts much more quickly than the soil compartment; with ongoing emissions, a steady-state is reached by 2030 in all regions. Ceasing emissions result in an immediate and significant reduction of ΣDDT in the ocean water in all three regions. Within less than twenty years, a difference of at least a factor of 2 appears between the two scenarios. The behavior of the atmosphere (not shown) is very similar to the ocean compartment.

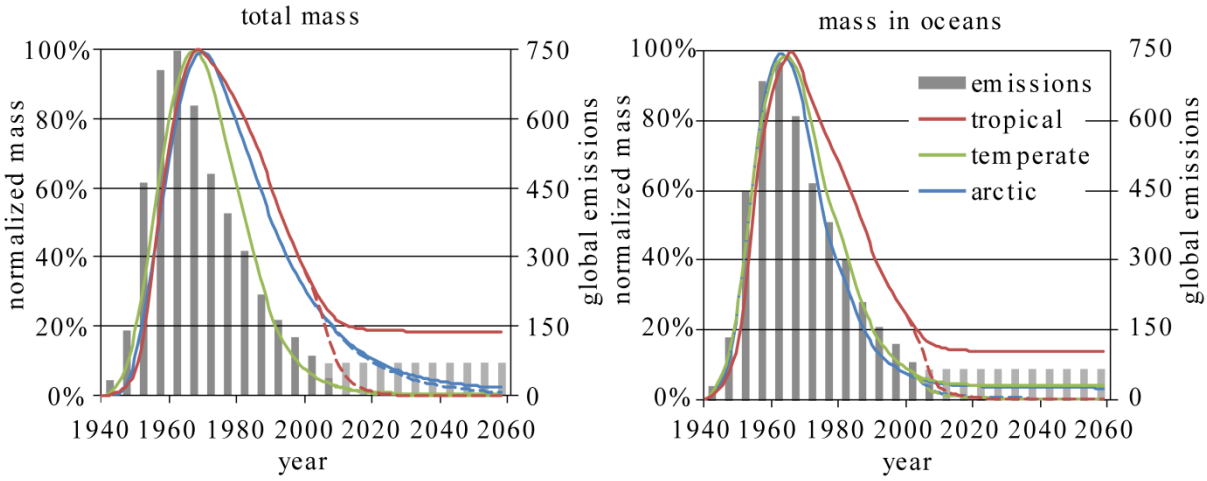

Figure 6.3: Relationship between emissions (bars, scale on the right *y* axis, in 1000 tonnes, each bar indicates the sum of the emissions of 5 years) and amounts of ΣDDT (DDT and degradation products) in the environment (left *y* axis, as a percentage of maximal amounts). The full line represents the base scenario (emissions continue for malaria vector combat after 2005, as given by light-gray bars), the dashed line represents the alternative scenario in which emissions stop in 2005 (dark gray bars). Mass in all media (left) and in ocean water (right).

These findings lead to different implications for different geographical regions. Model results for the soil compartment indicate that a stop of DDT emissions would result in only small reductions of ΣDDT levels in Arctic soils in the next 50 years. A significant effect on levels in Arctic soils can be expected only on the long-term (>100 years). In ocean water, a stop of emissions results in a significant reduction within a few years in the Arctic. In the tropical region, the impact of an emission stop is clearly visible within a few years in all media. If

emissions continue, the steady-state concentration in the Arctic and temperate regions will be between 30 and 100 times lower than the levels in the 1970s, whereas this decrease is only a factor of 5 in the tropical regions.

Further research is required to compare the risks associated to ongoing DDT emissions with the benefits from DDT use in the tropical regions. This should include a more detailed assessment of the exposure of the population in spraying areas, and a comparison of predicted exposure (daily uptake) with effect concentrations for long-term DDT exposure.

In addition, our results suggest that the temporal evolution of pollutants in Arctic soils should be investigated. Most of the measurements today are performed in the atmosphere, and a relatively rapid decrease of DDT levels is observed for the recent years in these measurements. Our model indicates that levels in Arctic regions may decrease more slowly in soils. If this could be confirmed by measurements, this would indicate a reservoir of DDT (and similar compounds) that may lead to secondary emissions if temperatures increase as a consequence of climate change.

6.4 Acknowledgments

We thank Fabio Wegmann, Yi-Fan Li, Kathrin Fenner, Mark Bonnell, Martin Kohler, Peter Schmid, Christian Bogdal, Kevin Jones, Perihan Kurt-Karakus, Rainer Lohmann, Ivan Holubek, Roland Kallenborn, and the Norwegian Institute for Air Research (NILU) for sharing unpublished data and for interesting discussions.

6.5 Supporting Information

Supporting information is available in the appendix, chapter 9.4.

Chapter 7:

Using Information on Uncertainty to Improve Environmental Fate Modeling: A Case Study on DDT

Urs Schenker[1], Martin Scheringer[1], Michael D. Sohn[2], Randy L. Maddalena[2], Thomas E. McKone[2,3], Konrad Hungerbühler[1]

[1] Institute for Chemical and Bioengineering, ETH Zurich, CH-8093 Zurich, Switzerland
[2] Indoor Environment Department, Lawrence Berkeley National Laboratory, Berkeley, California 94720, USA
[3] School of Public Health, University of California at Berkeley, Berkeley, California 94720, USA

Keywords : Monte Carlo simulation, Bayesian updating, substance property data, probabilistic modeling

Abstract

Present and future concentrations of DDT are calculated with a global multi-media model. Monte Carlo simulations are used to assess the importance of uncertainties in substance property data, emission rates, and model parameterization for model results. Uncertainties in the different model outputs expressed as 95% confidence intervals of DDT concentrations in various matrices, in different geographical locations, and at different moments in time are typically between one and two orders of magnitude. An analysis of rank correlations between model inputs and predicted DDT concentrations indicates that emission estimates and degradation rate constants, in particular in the atmosphere, are the most influential model inputs. For DDT levels in the Arctic, temperature dependencies of substance properties are also important contributors to uncertainty. A Bayesian Monte Carlo approach is used to update uncertain model inputs based on field observations. The assessment suggests an alternate value for half-life in atmosphere and a reduced range of uncertainty for K_{OW} of DDT. The updated model results are closer to observations and uncertainties of the model predictions are reduced. The combined sensitivity analysis and Bayesian Monte Carlo approach provide new insight into important processes that might be controlling the global fate and persistence of this contaminant.

7.1 Introduction

Dichlorodiphenyltrichloroethane (DDT) is an insecticide that has been used worldwide since the 1940s for controlling agricultural pests and to combat vectors of insect-borne diseases, such as typhus or malaria. DDT is hydrophobic and resistant to biotic and abiotic degradation, causing it to be very persistent in the environment. For this reason, it has been banned for agricultural uses under the Stockholm Convention (United Nations Environmental Program). Its global emission inventory (Li and Bidleman, 2003, Li et al., 2004, Li and Macdonald, 2005, Li et al., 2006), partitioning properties (Schenker et al., 2005a, Shen and Wania, 2005), and degradation rate constants (Aislabie et al., 1997, Mackay et al., 1997, Krüger et al., 2005, Liu et al., 2005) are measured intensively. Yet considerable uncertainty and variability remains in properties inferred from these measurements, particularly in the degradation and partitioning properties, owing to DDT's highly hydrophobic behavior. The extent to which these knowledge gaps affect estimates of the global fate of DDT may be significant. For example, Schenker et al. (2008), used past emissions and DDT property data to predict DDT concentrations in various matrices of the environment with a global contaminant fate model. Modeled concentrations corresponded well with measurements, although several disagreements were identified. For example, the model underpredicted atmospheric concentrations of DDT in the Arctic. Schenker et al. (2008), indicated that the disagreements are likely due to uncertainties in certain model inputs, such as the octanol−water partition coefficient (K_{OW}). Pontolillo and Eganhouse (2001) showed that the K_{OW} may vary by more than three orders of magnitude among different studies.

When model predictions differ from measurements, researchers often attribute these difference to uncertainties in model inputs, as was the case for Schenker et al. (2008). However, without a detailed and systematic uncertainty analysis it is unclear that the attribution is correct. Model developers are making progress on this front, with several recent papers reporting on efforts to assess the relative contribution of different model inputs to uncertainty in model results (McKone, 1994, Hertwich et al., 1999, Maddalena et al., 2001, MacLeod et al., 2002, Fenner et al., 2003, Luo and Yang, 2007, Meyer and Wania, 2007). However, most of these studies are limited to a local scale or rely on analytical uncertainty calculations (Slob, 1994) to reduce the calculation time of the uncertainty assessment. MacLeod et al. (2002) suggest the use of more general Monte Carlo methods (Morgan et al., 1990) when performing chemical-specific fate, exposure, and/or risk assessments. These

methods make possible the assessment of uncertainties in non-linear systems and of model inputs with complex and sometimes correlated uncertainty distributions. In addition, a systematic comparison of model results with field data can improve estimates of uncertain model inputs and provide valuable insight into the performance of environmental models. Our review of the current literature reveals that Monte Carlo type uncertainty assessments and techniques to update model inputs based on field data have not been applied to characterize and reduce uncertainties in results from global environmental fate models.

In this paper, we apply Monte Carlo uncertainty assessment methods to the DDT case study presented in Schenker et al. (2008). We calculate the importance of uncertainties from different types of model inputs (substance properties, emission rates, model parameters of the CliMoChem model) on time-dependent model results. Rank correlations between model inputs and outputs are used to identify important processes governing the behavior of DDT in the environment. Using field data, we apply a quantitative method to update model inputs and subsequent model predictions. Uncertainties in the updated model results decrease strongly, and predicted DDT concentrations are closer to field data. The updated model inputs, in particular substance properties are presented along with possible explanations for differences between original and updated values.

7.2 Methods

7.2.1 The CliMoChem Model

The CliMoChem model (Scheringer et al., 2000, Wegmann, 2004) has been used to calculate the behavior of chemicals in the environment. For the present calculations, we use a version of the model with 30 latitudinal zones. The model calculates diffusive and advective exchange processes between environmental compartments (atmosphere, ocean water, vegetation, vegetation-covered soil, and bare soil) and across regions on a global scale. We calculated time dependent DDT concentrations between 1940 and 2040 using the historic DDT emission scenario presented in Schenker et al. (2008). For the time after 2005, we assumed that emissions continue at a rate of approximately 15000 tonnes per year, according to the base scenario presented earlier (Schenker et al., 2008).

7.2.2 Monte Carlo Simulations

Monte Carlo Simulation is a technique that is used to construct a distribution of model outcomes for complex, non-linear systems with a large number of uncertain and sometimes correlated inputs (Morgan et al., 1990). First, a series of model input data sets are randomly generated from the domain of possible input values according to the selected uncertainty distributions. Then, model realizations are calculated for each of the model input data sets. From each realization, the modeled output is stored for analysis. Correlation between the model outcome distribution and model input values used in a Monte Carlo Simulation can be used to identify important parameters, assumptions and processes in the model. In the application that follows, we use the CrystalBall software (CrystalBall, 2008a) to run 5000 realizations. We tested summary statistics to ensure sufficient sampling.

We tracked 90 model outputs in the uncertainty analysis: concentrations in atmosphere, ocean-water, and vegetation-covered soil in the Arctic, the temperate, and the tropical regions (nine boxes), every ten years from 1945 to 2035 (10 times).

7.2.3 Prior Uncertainty Distributions

We modeled uncertainty using probability distributions for 47 model inputs (see Supporting Information for a table giving all model inputs, the corresponding probability distributions, and the methods used to estimate them). For degradation rate constants and partition properties, we assumed log-normal distributions and determined geometric means and geometric standard deviations of each property based on available measurements. Activation energies of degradation reactions and energies of phase change for partition coefficients (describing the temperature dependence of these properties) were assigned log-normal and normal distributions, respectively. Uncertainty of DDT emissions was characterized using two scaling factors for past and future emissions (which have higher uncertainties). Both scaling factors were assigned log-normal distributions around the geometric mean of one. As in Schenker et al. (2008), 90% of the emissions are into soil and a triangular distribution from 80% to 100% was used for the simulations. We did not account for uncertainty of the location and time where DDT emissions occurred, because the model outputs are relatively insensitive to these variables (Schenker et al., 2006).

The CliMoChem model also uses a number of intrinsic model parameters that are uncertain (e. g. OH radical concentrations in a given zone, organic matter content of a given soil type,

wind speed, etc.) for which we have estimated uncertainty distributions based on previous assessments (Hertwich et al., 1999, Maddalena et al., 2001, McKone et al., 2001, MacLeod et al., 2002). We have found the model to be somewhat insensitive to these parameters relative to other model inputs, as has been diagnosed previously (Hertwich et al., 1999, MacLeod et al., 2002, Fenner et al., 2003, Luo and Yang, 2007). The Supporting Information has further details about the magnitude and uncertainty distributions of these parameters. We have assumed that none of the model inputs are correlated, as asserted in previous studies (Hertwich et al., 1999, Maddalena et al., 2001, MacLeod et al., 2002, Fenner et al., 2003, Luo and Yang, 2007).

7.2.4 Using Rank Correlations for Sensitivity Analysis

The rank correlation between a model input and model outcome from a Monte Carlo Simulation can be useful for identifying model sensitivities. CrystalBall computes a Pearson Correlations Coefficient (CrystalBall, 2008b) which was used for the present calculations. Positive rank correlations indicate that an increase of a given model input with all other inputs unchanged will result in an increase of a model output, whereas negative rank correlations indicate the opposite. The magnitude of the absolute value of a rank correlation for a particular input indicates the importance of that input to the model outcome. In addition to providing insight into importance of specific model inputs, the rank correlations can highlight important processes in the model structure, for example, inputs related to the ocean water compartment have a high rank correlation for concentrations in ocean water, but much less for concentrations in soils. It is also important to note that model sensitivity to specific inputs can change over time.

7.2.5 Bayesian Monte Carlo Approach

We use Bayesian updating (Brand and Small, 1995, Sohn et al., 2000) to update model parameter and output uncertainties. The specific method used is Bayes Monte Carlo (BMC), an empirical and somewhat computationally intensive approach to updating, rather than Markov Chain Monte Carlo because it is simple to implement and model computations are fast. The approach also facilitates other types of studies, such as value-of-information analyses.

In the BMC approach, a posterior probability (p'_k) is calculated by assessing the level of agreement between each Monte Carlo run k and the measurements (O). The likelihood

function, $p(O|Y_k)$, is the probability of observing O given the model prediction Y_k, and $p(Y_k)$ is the prior probability of model run k. U is the total number of all Monte Carlo runs:

$$p'_k = \frac{p(O|Y_k) \cdot p(Y_k)}{\sum_{i=1}^{U} p(O|Y_i) \cdot p(Y_i)} \qquad \text{(eq. 7.1)}$$

We update on multiple independent observations from various environmental media and geographical regions, so $p(O|Y_k)$ represents the probability of observing all observations simultaneously (S = number of independent observations, in the present case $S = 6$):

$$p(O|Y_k) = \prod_{s=1}^{S} p_s(O_s|Y_k) \qquad \text{(eq. 7.2)}$$

We assume a Normal distribution for the likelihood function, as used by others (for instance in Sohn et al., 2000) and because we do not have sufficient data to suggest an alternative:

$$p(O|Y_k) = \frac{1}{\sqrt{2 \cdot \pi} \cdot \sigma_\varepsilon} \exp\left(-\frac{1}{2} \cdot \left[\frac{O - Y_k}{\sigma_\varepsilon} \right]^2 \right) \qquad \text{(eq. 7.3)}$$

where σ_ε is the standard deviation of the measurement errors in O.

The posterior mean of all model inputs and outputs (V') can be calculated from the posterior probability of each model run (p'_k) and the prior value V_k of the corresponding model input or output value in each of the U model runs:

$$V' = \sum_{k=1}^{U} p'_k \cdot V_k \qquad \text{(eq. 7.4)}$$

The standard deviation of each of the model inputs and outputs can be found with:

$$\sigma'_V = \sqrt{\sum_{k=1}^{U} p'_k \cdot (V_k - V')^2} \qquad \text{(eq. 7.5)}$$

To respect the condition that our probability function (eq. 7.3 above) holds true for normally-distributed measurement errors only, measurements in the environment were converted into log-values and the standard deviations of the log-values were estimated. The concentrations from the model were also converted into log-values and used for the updating. Equally, when calculating updated model inputs, log-values where compiled for the log-normally distributed model inputs.

7.2.6 Measurement Data Used for Bayesian Monte Carlo Assessment

For the BMC assessment, we used the DDT measurements reported in Schenker et al. (2008), (Figure 2 therein). These concentrations of DDT in atmosphere, ocean water, and soils of the Arctic, the temperate, and the tropical regions are based on several individual measurement studies. We calculated empirical measurement errors (σ_ε in eq. 7.3) from the variation in the data between studies. Because measurements in temperate and tropical ocean water and Arctic soils are based on a single measurement each, no empirical measurement errors could be calculated. As a result, these media were excluded from the BMC assessment.

7.3 Results and Discussion

7.3.1 Uncertainties of Model Results

Figure 7.1 shows the predicted evolution of DDT concentrations in the Arctic atmosphere (left, in pg/m^3) and tropical soil (right, in ng/g). We see that DDT concentrations increase until 1965 and start decreasing afterward. The slope of the decreasing concentration is greater in the Arctic atmosphere than in the tropical soils. We attribute this to a longer half-life in soil as compared to the air and because DDT emissions continue in the tropical regions.

Vertical bars in Figure 7.1 show the two-sided 95% confidence intervals. The confidence intervals are larger in the Arctic atmosphere than in tropical soils. We show later that this is because of the uncertainties that are associated with temperature dependent substance properties. We note that in the Arctic, ambient temperatures are much lower than temperatures in the laboratory settings where substance properties are determined. As a result substance properties have to be extrapolated from the measured values, using measured temperature dependencies. This results in additional uncertainties for Arctic regions as compared to the tropical regions because laboratory conditions under which substance properties are measured are typically more closely related to tropical temperatures. Furthermore it can be seen that uncertainties increase after 2005 because uncertainties of future emissions are higher than uncertainties of past emissions, as mentioned previously. Plots of all concentrations as a function of time with associated uncertainties for all media in all regions are given in the Supporting Information.

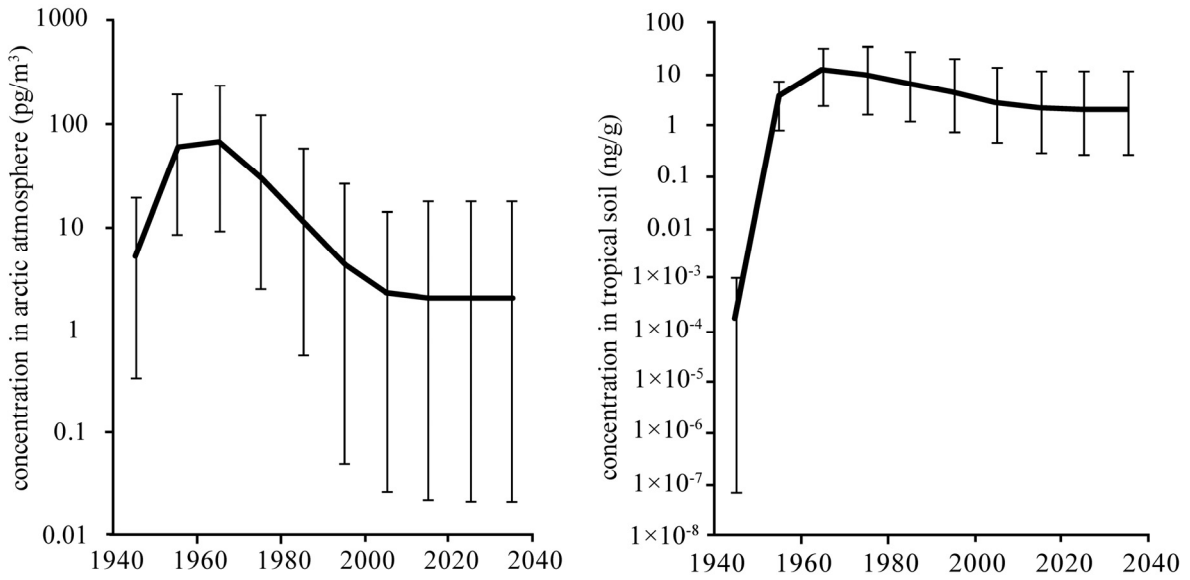

Figure 7.1: Evolution of DDT concentrations in arctic atmosphere (left) and tropical soils (right). Error bars represent 95% confidence intervals.

7.3.2 Sensitivity Analysis

Figure 7.2 (left) shows the sum of the absolute rank correlation coefficients in temperate soils for five groups of model inputs: degradation half-lives (4 inputs), partition coefficients (2 inputs), temperature dependencies of half-lives and partition coefficients (6 inputs), emissions (3 inputs), and model parameters (32 inputs). We see that the rank correlation, and thus the model sensitivity, decreases for emissions related inputs over time as emissions shift away from the temperate zones. In contrast, sensitivity of the model to the degradation rate constants and temperature dependencies increase as transport into the temperate zone of newly emitted DDT and degradation of stocks from previous emissions become the dominant processes. In the Supporting Information, graphs showing the rank correlations with concentrations in all media and in all geographic regions over time are given. It can be seen from these graphs that temperature dependence is much more important for the concentrations in the Arctic than in temperate regions, and is almost negligible in the tropics. This supports the notion that properties measured in the laboratory are more relevant to temperate and tropical regions because the experimental conditions are more closely related to these regions.

Figure 7.2 (right) shows the temporal evolution of the highest rank correlations (RC) between model inputs and concentrations in the tropical atmosphere. Up to 2005, the atmospheric degradation rate constant (k'_{air}) is the most sensitive model input (RC = −0.94); it influences long-range transport from temperate regions into the tropics, and also the residence time of DDT in tropical atmosphere. The scaling factor for past emissions (until 2005) has a high importance (RC = 0.17). The model is also sensitive to logK_{OW} (RC = −0.18), which is used to estimate partitioning into soil and particles in the atmosphere and oceans. After 2005, the importance of the scaling factor for past emissions (S_{past}) decreases strongly, and the importance of the scaling factor for future emissions (S_{future}) increases correspondingly (RC = 0.54). Given that the future emissions occur inside the tropics, its rank correlation is

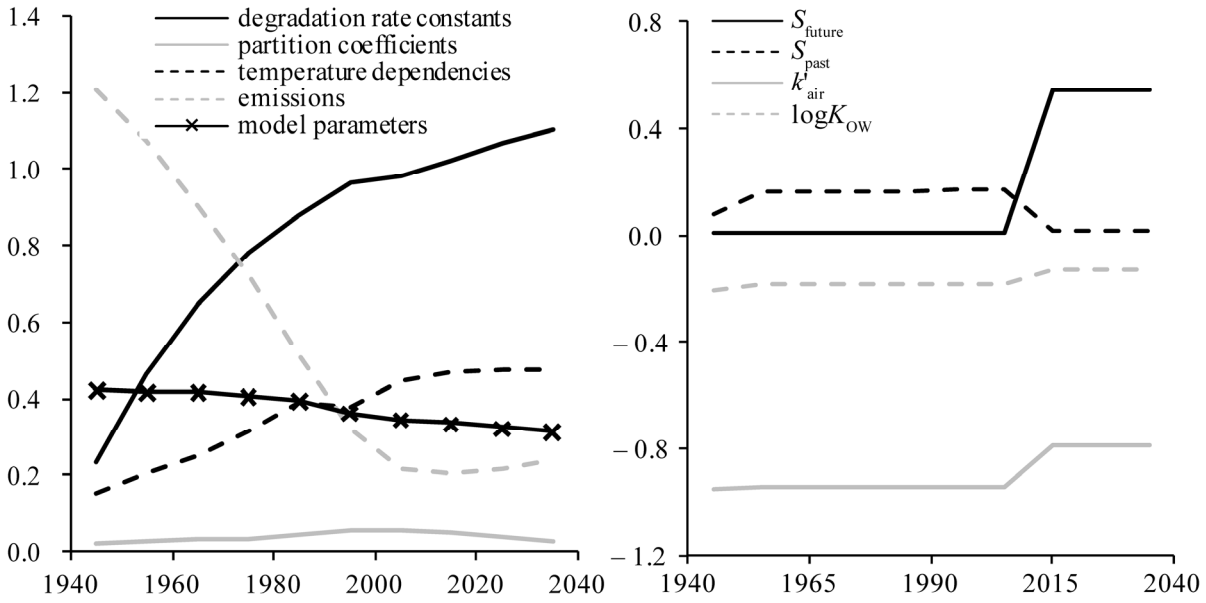

Figure 7.2: Sum of absolute values of rank correlation coefficients for groups of model inputs to concentration in temperate soils (left) and the rank correlations of the model inputs with highest correlations to concentrations in tropical atmosphere (right) over time .

considerably higher than that of the scaling factor for past emissions, because no transport intervenes between the emissions and the modeled concentrations in the tropics. As a consequence, the importance of the atmospheric degradation rate constant (k'_{air}) also decreases slightly after 2005 (RC = −0.78).

Plots of the model inputs with the highest rank correlations for all media and geographical regions are given in the Supporting Information. In all of these plots the future emissions become one of the most important contributors to model outcome uncertainty after 2005, even for the Arctic. The rank correlation of the scaling factor for future emissions (S_{future}) for

concentrations in atmosphere (in all climatic regions) increases sharply in 2005 and remains constant from 2015 to 2035. This shows that DDT concentrations in air are strongly influenced by future emissions immediately after their occurrence. A similar behavior can be observed for oceans, although the increase in the rank correlation between the scaling factor for future emissions and concentrations in oceans is not as sharp as for concentrations in the atmosphere. The rank correlation between the scaling factor of future emissions and concentrations in soils continues to increase until after the end of the simulation period. This shows that past emissions influence concentrations in soil for much longer than in atmosphere and ocean water. In accordance, the rank correlation between past emission (S_{past}) and concentrations in soils continues to decrease for several years after past emissions have ceased.

7.3.3 Bayesian Updating of the Most Important Model Inputs

Table 7.1 shows prior and posterior statistics for some of the most sensitive model inputs. Half-lives in soils (k_{soil}) and ocean water (k_{water}) remain fairly unchanged (indicating that literature data on degradation half-lives is well suited to explain measured DDT concentrations in the environment). The scaling factor for past emissions (S_{past}), the ratio of emissions into soil (R_{soil}), and the logK_{AW} also do not differ appreciable even though the sensitivity analysis indicated they were important to the model. This again indicates that the distribution of values in the literature is appropriate for this type of assessment.

The posterior DDT degradation rate constant in the atmosphere (k'_{air}) is approximately three times faster than previously assumed (Schenker et al., 2008). Quantitative Structure Property Relationship (QSPR) data from the AOPWin software (U.S. Environmental Protection Agency, 2004) predicts that DDT degrades very quickly in atmosphere (even faster than the posterior estimate), but to establish the prior value for the atmospheric degradation rate constant, data from AOPWin was combined with measurements derived from smog chambers studies (Krüger et al., 2005, Liu et al., 2005), which suggest longer half-lives for DDT in the atmosphere. Based on inconsistencies in the modeled fraction of DDE and DDT in atmosphere, we previously found that the atmospheric degradation rate constant for DDE might have to be reduced relative to that of DDT (Schenker et al., 2008). However, the Bayesian Monte Carlo assessment suggests that the degradation rate constant of DDT might have to be increased, and the value initially given for DDE (from AOPWin) might be more appropriate.

The median of the posterior logK_{OW} of DDT is 0.2 log units higher than the prior, suggesting that DDT might be only slightly more hydrophobic than previously assumed. The prior for logK_{OW} was estimated from a large number of direct but highly variable measurements. Pontolillo and Eganhouse (2001) indicated values for logK_{OW} to be between 3 and 7. However, based on additional knowledge from DDT field data, we find posterior uncertainty to be significantly tighter with the 95% interquantile range only about +/- 0.85. Values of the logK_{OW} below 5.16 thus do not seem to be well suited to explain DDT field data with the CliMoChem model. This might indicate that the lower part of the range of logK_{OW} values found by Pontolillo and Eganhouse is attributed to experimental difficulties measuring logK_{OW} for highly lipophilic chemicals.

Finally, temperature dependencies of all properties (Ea_{soil} for degradation rate constants in soil, ΔU_{AW} and ΔU_{OW} for logK_{AW} and logK_{OW}, respectively) were increased by the BMC approach. Temperature dependencies are fairly uncertain so it is possible that they were all underestimated. However, this could also indicate that the temperature profile in the CliMoChem model, as used in (Schenker et al., 2008), should be steeper. In other words, real temperatures in the Arctic could be below the current values assumed in the model. The increase in the temperature dependencies of substance properties corresponds to decreasing the temperature in the Arctic by 2-3° C. Further study is needed to determine the implications of this result since we do not think that the temperature data used for this input is that erroneous (given that temperature measurements are fairly simple and should not be subject to uncertainties above +/- 0.5° C). One explanation may be that some processes in the environment take place at temperatures that are below the ones we use in our model (e. g. degradation in atmosphere might take place in the high atmosphere under temperatures significantly below the ones at the earth's surface).

Table 7.1: The most important model inputs as they were initially used for the Monte Carlo simulations (columns "prior"), and after adjustment with the BMC approach (columns "posterior").

	prior			posterior		
	2.5%	**50%**	**97.5%**	**2.5%**	**50%**	**97.5%**
S_{past} (–)	0.77	1	1.29	0.76	0.99	1.26
R_{soil} (–)	0.82	0.9	0.98	0.82	0.9	0.97
k_{soil} (d^{-1})	2.32×10^{-4}	6.77×10^{-4}	1.97×10^{-3}	2.63×10^{-4}	5.83×10^{-4}	1.13×10^{-3}
k_{water} (d^{-1})	4.66×10^{-4}	1.35×10^{-3}	3.95×10^{-3}	5.00×10^{-4}	1.69×10^{-3}	4.29×10^{-3}
k'_{air} (cm^3/d/molecule)	5.17×10^{-9}	8.98×10^{-8}	1.55×10^{-6}	2.67×10^{-8}	2.64×10^{-7}	6.30×10^{-7}
$\log K_{AW}$ (–)	–3.55	–3.35	–3.15	–3.56	–3.36	–3.14
$\log K_{OW}$ (–)	5.16	6.01	6.86	5.34	6.21	7.03
Ea_{soil} (kJ/mol)	13.6	30.0	66.2	15.5	35.8	74.4
ΔU_{AW} (kJ/mol)	33.4	72.6	112	35.4	74.4	112
ΔU_{OW} (kJ/mol)	–54.2	–15.3	23.9	–58.3	–20.0	19.4

In the comparison of model results with measurement data in Schenker et al. (2008), several disagreements were highlighted, and possible reasons for the disagreement discussed. Under the new evidence gained from the sensitivity analysis and the Bayesian Monte Carlo assessment, it is useful to reconsider these points. The model results presented in Schenker et al. (2008) showed atmospheric concentrations in the Arctic that were about one order of magnitude above measurements. It also showed that DDT concentrations were constant along latitudinal zones, or even increasing toward the poles, whereas field data showed a decreasing trend toward the poles (although the data was based on very few measurements). The increased temperature dependence of $\log K_{AW}$ that was suggested by the BMC approach will result in a more efficient scavenging of DDT by rain from the atmosphere, and will thus tend to reduce DDT concentrations (and travel distances) in the atmosphere, in particular in the Arctic. Also the increased degradation rate constant in air reduces DDT concentrations in atmosphere, yet this applies to all regions. The zonal distribution of DDT in ocean water is not expected to be significantly modified by the BMC approach, because the measurement data in oceans is subject to high uncertainties and does therefore not contribute to the updating notably. The effects of the BMC approach on model results are assessed in the following section.

7.3.4 Bayesian Updating of the Model Results

Figure 7.3 shows the cumulative distribution functions of measurements, prior model results, and posterior model results (after the BMC approach) in 1995. As an example, we show concentrations in Arctic atmosphere and temperate soils. The posterior values for model inputs from the BMC approach result in model predictions that are closer to the measurements than are the initial Monte Carlo simulation results in both cases. Notably, in Arctic atmosphere, the DDT concentration predicted by the model (the median of the results from the BMC approach) is within a factor of three of the median of the measurement data, as compared to about one order of magnitude difference prior to the BMC approach. The Bayesian updating has thus considerably reduced the divergence between model results and measurements identified in Schenker et al. (2008). Similarly, in temperate soils, the median of the BMC model results lies between the median of the original model results and the measurement data. Improved model fit was not consistently observed across all regions and phases. In the temperate atmosphere, the posterior model output shifted away from the measurements (see Figure 9.10 in the Supporting Information). This is likely because the reduction in the corresponding deviations between measurements and model results in other compartments were quantitatively more important.

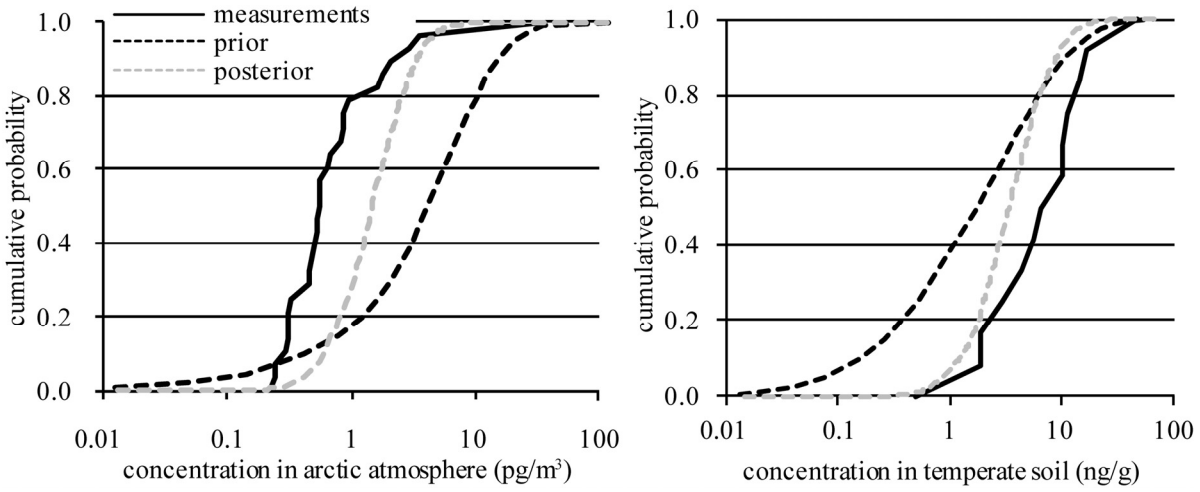

Figure 7.3: Cumulative Distribution Functions (CDFs) for measurements, prior-, and posterior-model results in arctic atmosphere (left) and temperate soils (right) in 1995. The *y* axis shows the probability that the corresponding results (measurements or model data) are below or equal to a given value on the *x* axis.

The graphs with the temporal evolution of DDT (Figure 7.1) can be redrawn with the results from the BMC approach (see Supporting Information). Uncertainties in the model results decrease due to the additional information that has been gained from the measurement data. Furthermore, it can be seen that concentrations in soils (in particular in the temperate region and the Arctic) seem to decrease more slowly than originally predicted. The reason for this can be found in the increased temperature dependencies of partition properties and the half-life in soil. This suggests that DDT might be more persistent in the Arctic and temperate soils than initially predicted.

The methods presented above demonstrate how uncertainties of model results from a global contaminant fate model can be better characterized. Substance properties and emission data were identified as the most important sources for uncertainty. The Bayesian updating provides insight on how to select and restrict model inputs. For example the values of degradation rate constants in ocean-water and soils, the emission data, and the $\log K_{AW}$ have not been modified by the method, suggesting that the selected values are suitable to model the behavior of DDT in the environment given the available observations. This is particularly encouraging in the case of past emission rates. There is very little information available on DDT emissions (only two different studies were used to construct the emission scenario presented in Schenker et al. (2008)). Yet, the scaling factor for past emissions has not been markedly modified by the BMC approach, indicating that these studies probably catch the amount of DDT emitted relatively well. Furthermore, the Bayesian updating suggests that uncertainties in the value of $\log K_{OW}$ might be less than previous estimates. In the case of the atmospheric degradation rate constant, additional information has been gained that might help to select the optimal degradation rate constant among different suggestions from measurement or QSPR data. When modeling other substances in the future, we suggest using Bayesian updating techniques to take advantage of all available observations to better characterize uncertainties in model inputs. Finally, we have illustrated that differences between DDT field data and model results were reduced with Bayesian updating. The reduced range of uncertainties of future DDT concentrations increases confidence in model predictions and may facilitate decisions that policy makers have to take on future DDT usage.

7.4 Acknowledgments

We thank Fabio Wegmann and Matt MacLeod for valuable comments on the manuscript. Sohn, Maddalena and McKone were supported in part by the US Environmental Protection Agency through Interagency Agreement DW-988-38190-01-0 carried out through the US Department of Energy contract Grant No. DE-AC02-05CH11231.

7.5 Supporting Information

Supporting information is available in the appendix, chapter 9.5.

Chapter 8:

Conclusion and Outlook

8.1 Significance of Degradation Products for the Assessment of POPs under a Global Perspective

Substance properties of transformation products are challenging to obtain, and the least-squares adjustment procedure (chapter 2) has proven to be a useful tool to gain as much information as possible from a limited number of studies of solubility and partitioning coefficients. The least-squares adjustment procedure allows correcting measured data for random errors, but also helps to detect biased substance data. Both features improve the overall reliability of substance properties.

In the third chapter of this thesis, the importance of degradation products has been demonstrated with the example of a series of pesticides. It could be seen that in some situations, the ranking of chemicals according to hazard indicators may change if intermediate degradation products are taken into account (chapter 3.3). The effect of intermediate degradation products is particularly important in the case of pesticides: today, pesticides are designed to develop their activity only once they are taken up by the target organism (the plant or insect), to increase the efficiency of the substance, and to decrease the occurrence of side effects. Often, the original substance undergoes some transformation reaction during this process, for instance to increase its solubility. Therefore, the first transformation reaction of currently used pesticides takes place readily in the environment, but the first degradation product might be as persistent (and also toxic) as the original substance (possibly even more). A good example is trinexapac-ethyl (Health Canada, 2001), a plant growth regulator which is in itself not biologically active. Its first transformation product, trinexapac-acid, is readily formed from the degradation of trinexapac-ethyl inside the plant, and is the biologically active component. It is expected that this effect occurs for other substances that have not been assessed here, too. Pesticides that degrade into stable, and possibly mobile and toxic intermediate degradation products have been brought together previously (Boxall et al., 2004, Gasser et al., 2007). In other substance classes, for instance pharmacological products, such substances certainly exist, too. When assessing a chemical for its hazard or risk, it is therefore suggested to perform at least screening-level assessments on the fate of its degradation products. If the joint persistence, for instance, is significantly above the persistence of the parent compound alone, intermediate degradation products should be taken into account in detail.

In the case of DDT (chapter 6), the principal biologically active component is the parent compound. Although the degradation of DDT is relatively slow, DDE (one of the main transformation products) is today present at high concentrations in the environment, because it is very persistent itself. DDE also causes the most concern because of its toxic effects on birds and reptiles. In this case, the biologically active ingredient can be transformed into another substance that is even more hazardous than the original compound. Again, it has to be expected that a large number of substances exist for which degradation products are more hazardous than the parent compounds themselves. In a modeling study of these products, the inclusion of degradation products therefore is crucial.

A global model that includes degradation products can also be used to compare direct emissions of a pollutant to emissions, transport, and degradation of precursor substances (chapters 4 and 5). In the case of the PFO (chapter 4), direct emissions of PFO and oceanic transport into the Arctic were compared to emissions of fluorotelomer alcohols (FTOHs) and perfluorooctylsulfonamido ethanols (FOSEs), long-range transport in atmosphere, and degradation of FTOHs and FOSEs into PFO and deposition in the Arctic. In the case of PBDEs (chapter 5), direct emissions of penta-BDE were compared to emissions and debromination of deca-BDE. There probably exist other substances categories where emissions of a precursor substance and degradation into a given substance compete with direct emissions of this substance. In such a situation, the CliMoChem model might be useful to calculate the relative share of levels due to direct emissions and degradation of precursors.

In chapter 7, uncertainties of the CliMoChem model have been assessed with Monte Carlo simulations. Uncertainties in DDT concentrations over time were high (Figure 7.1): the 95% interquantile range spreads over two to three orders of magnitude. Substance properties and emissions of DDT are fairly well known, and therefore it has to be expected that uncertainties of model results for other chemicals might even be higher. In the case of DDT, the Bayesian updating procedure successfully reduced these uncertainties by weighting model runs from the Monte Carlo simulations according to their level of agreement with field data. This method would be useful to reduce uncertainties in other substance classes, too. The three levels of comparison between field data and model results that have been presented in chapter 6.2.5 could thus be extended by a forth level, in which field data is used to update model results with a Bayesian updating procedure.

8.2 Limitations

When intermediate degradation products shall be included in modeling studies, the identification of possible degradation products of a chemical is a challenge in itself: for substances that are not suspected to be a threat to human health or the environment, degradation products are generally not known at all. Therefore it is close to impossible to include degradation products systematically when assessing new chemicals. There is some QSAR software that predicts which degradation products are formed: CATABOL (Jaworska et al., 2002) and the University of Minnesota Biocatalysis / Biodegradation Database (Schmidt, 1996, Ellis et al., 1999) have been used for this purpose in chapter 3. Unfortunately, the predictions by both programs are only representative for biodegradation, and have sometimes resulted in predictions that were not very accurate (degradation pathways reported in literature for aldrin were not predicted by the model, see chapter 3.2.1). A more thorough assessment of the usability of QSAR software for the prediction of degradation products (Gasser et al., 2007) has shown that the current performance of such programs is insufficient to be used in the context of risk assessments.

Once intermediate degradation products of chemicals are identified, it has to be determined what percentage of the parent compound degrades into the different degradation products. To quantify the amount of degradation products that are formed from the degradation of the parent compound, fractions of formation (see chapter 3.2.1) have to be determined. These are not frequently measured, and have to be estimated based mainly on expert judgment, which may yield biased results. No reliable QSAR software is available today for this task.

Furthermore, substance properties like partition coefficients and degradation half-lives are scarce for degradation products. In the case of the intermediate degradation products of fluorotelomer alcohols and perfluorooctylsulfonamido ethanols, no substance properties were available. Fortunately, QSPR software is available for the most important substance properties, and the performance of EPIWin (U.S. Environmental Protection Agency, 2004) in predicting many model inputs is sufficient for screening-level assessments (as those performed in chapter 3). EPIWin failed to predict accurate atmospheric degradation half-lives for PBDEs, because it does not take into account direct photolysis (believed to be relatively unimportant for the majority of POPs (Atkinson, 1987)).

In the case of PBDEs, the spatial resolution of CliMoChem has reached its limits. Given that the congener pattern of PBDE emissions differs strongly between North America and Asia (Rahman et al., 2001), and because the heavier PBDEs have fairly low long-range transport potentials, the assumption of a zonal homogeneity in CliMoChem is not valid any more. The concentrations predicted by CliMoChem are representative of zonal averages, but it is very difficult to compare these concentrations with measurements, because neither measurements in North America, nor measurements in Asia are representative of the zonal average concentration. In such a situation, a model with an East-West resolution (like BETR – Toose et al., 2004) should be preferred. In the case study on fluorinated substances, a similar problem arises in oceans: emissions of PFCAs mainly occur in Europe and the Eastern US. Therefore, measured concentrations in the Atlantic are much higher than in the Pacific Ocean. In CliMoChem, however, there is no difference between the Pacific and Atlantic Oceans; concentrations represent zonal averages. Again, model results are not representative of either, the Atlantic or the Pacific, and an alternative model with a spatial resolution in the East-West direction should be preferred (for instance the BETR model, Toose et al., 2004).

In the light of the findings from this thesis and under consideration of the limitations that still exist when performing risk assessments of chemicals and their degradation products, a decision guideline can be established to guide researchers. The aim is to give advice to adequately include transformation products and simultaneously minimize the additional effort that has to be spent.

The guideline (Figure 8.1) starts with a screening-level assessment of the importance of degradation products for the chemical under consideration. This may be done, for instance, by comparing the joint persistence and the primary persistence (Fenner, 2001). If degradation products turn-out to be relatively unimportant, modeling without degradation products is appropriate. If degradation products might be important, the potential for long-range transport of the parent compound and the degradation products have to be assessed, for instance by comparing the spatial range to the joint spatial range (see chapter 3). If no significant long-range transport potential is identified, the methods suggested by Fenner (2001) in a previous thesis are sufficient. If there is a potential for long-range transport for the chemical under consideration or its degradation products, the fate of these chemicals should be assessed with the CliMoChem model. Furthermore, it has to be tested whether the assumption of zonal homogeneity of the CliMoChem model is valid. If emissions occur homogeneously into the

zones of CliMoChem, the concepts presented in this thesis are sufficient. On the other hand, if emissions differ strongly between continents, it is suggested that a model with an East-West resolution that also takes into account degradation products is used. No such model exists today, and it is therefore suggested that the results from the CliMoChem model (under the assumption of zonal homogeneity) be compared to results from a model with a spatial resolution in the East-West direction (for instance, the BETR model (Toose et al., 2004)) without the inclusion of degradation products.

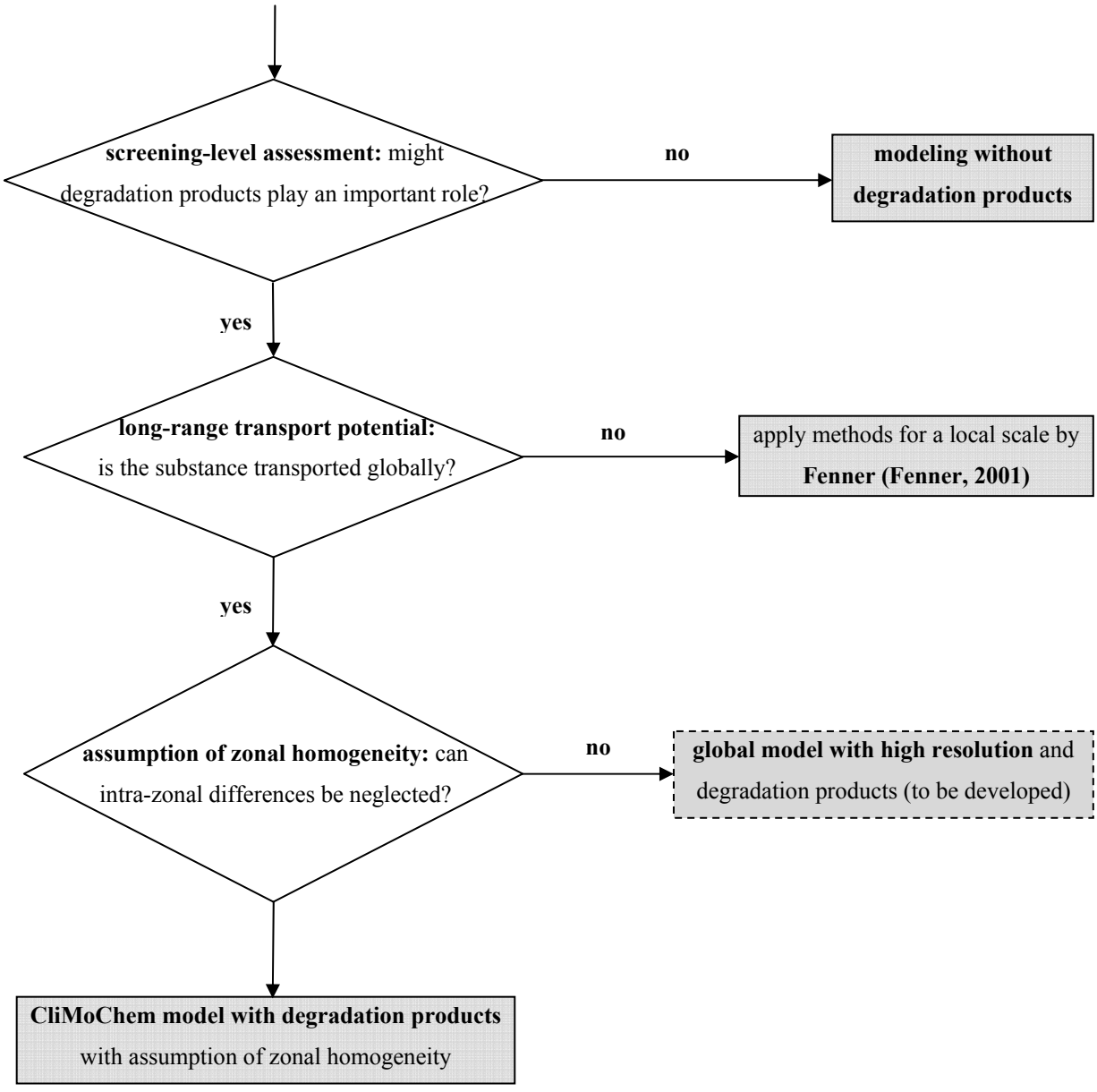

Figure 8.1: Decision scheme to assess chemicals under consideration of their degradation products.

8.3 Outlook

The framework for the inclusion of intermediate degradation products developed herein for the CliMoChem model can also be integrated into more highly resolved models. In chapter 5, differences between emission patterns of PBDEs in Asia and North America could not be taken into account, because the CliMoChem model assumes zonal homogeneity of concentrations. Therefore, the comparison of model results with field data was difficult. This could be overcome if degradation products were calculated in a model with a zonal resolution in the East-West direction. It has to be kept in mind, however, that calculation times will increase significantly if several substances are modeled simultaneously in a highly resolved model, and that modifications to the model structure are probably necessary if many substances have to be modeled simultaneously, or if an assessment of uncertainties is required.

The methods developed during this thesis can also be applied to other substance categories in the future:

- Elevated concentrations of perfluorooctane sulfonate (PFOS) have been detected in the Arctic ocean-water and biota. The origin of these could be characterized with the CliMoChem model. Similarly to the situation of PFO (described in chapter 4), direct emissions of PFOS compete with emissions and degradation of precursor substances.
- Polybrominated dibenzofurans (PBDFs) and –dioxins (PBDDs) are frequently measured from the degradation of polybrominated diphenyl ethers (PBDEs) (chapter 5). In particular for the lower brominated PBDEs, most of the degradation products might be PBDFs and PBDDs. It is expected that their toxicity is higher than that of PBDEs, and although their persistence might be lower than for PBDEs, they might contribute significantly to the hazard of PBDEs.

To overcome shortcomings related to uncertainties in the model inputs, and to fully take advantage of field data, modeling methods that take into account uncertainties could be applied more frequently in the future. In particular, in the present project, the uncertainty calculations (chapter 7) were not applied to the degradation products of DDT. The ratios of DDT to its degradation products are measured frequently in the environment, and their consideration could give additional information on the accuracy of the selected substance properties, for instance the relative half-lives of the DDT, DDE, and DDD. Furthermore, the uncertainties that arise from the emission scenario could be integrated into a Bayesian

updating procedure in the case studies on PFO and PBDEs: In the case of PFO, concentrations of perfluorinated sulfonamido ethanols (FOSEs) in atmosphere have not decreased in recent years, despite the fact that FOSEs emissions are supposed to have decreased recently. If the disagreement between model results and field data suggests that recent emissions should be increased, the Bayesian Monte Carlo approach might be capable of finding a more accurate level of emissions. In the case of PBDEs, underestimated emission factors from incineration in open fires and evaporation from textiles and polymer products seem to be responsible for the underestimation of PBDE levels in the model. Again, if emission factors were included as uncertain model inputs, these could be changed by the Bayesian Monte Carlo approach to take into account the high levels of PBDEs measured in the environment.

Finally, the CliMoChem model does only calculate the fate of degradation products in the environment. Calculating not only the environmental fate of degradation products, but also their accumulation in the food-chain, and their uptake by humans would add an additional important dimension to the hazard score of degradation products. To accurately characterize the risk of chemicals and their degradation products for humans requires not only knowledge on levels of these substances in the environment, but also knowledge on whether they bioaccumulate, how easily they are taken up by humans, how quickly they are excreted from our bodies, and how toxic they are. The coupling of an environmental fate model like CliMoChem with a bioaccumulation and a pharmacokinetic model would give a much more complete picture on the risk of chemicals and their degradation products for humans. In particular, the risk score of the degradation products might take into account not only the persistence of the different degradation products, but also their bioaccumulation potential, and toxicity. Furthermore, by comparing predicted concentrations in blood or fatty tissue of biota with field data, and inclusion of additional exposure pathways for humans (for instance through food) would also allow to compare predicted concentrations in human blood or urine to field data. This would allow model results to be confirmed on an additional level with field data. Finally, a series of integrated fate, hazard, and risk indicators for chemicals and their degradation products could be developed and would enable researchers to gain a much better image of the significance of chemicals and their degradation products for the protection of the environment and human health.

Chapter 9:

Appendixes

9.1 Supporting Information for Chapter 2: *Improving Data Quality for Environmental Fate Models: A Least-Squares Adjustment Procedure for Harmonizing Physicochemical Properties of Organic Compounds*

A spreadsheet to apply the least-squares adjustment procedure, including property data for PCBs, hexachlorocyclohexane and organochlorine pesticides (Li et al., 2003, Xiao et al., 2004, Shen and Wania, 2005) is also available from http://www.sust-chem.ethz.ch/.

9.1.1 Mathematical Development of the Equations for the Least-Squares Adjustment when all Partitioning Properties Are Given

The least-squares adjustment procedure is based on a method used in geodesy. The relevant paragraphs in geodesy textbooks are pages 161–167 in Niemeier (2001), pages 137–159 in Mikhail and Ackermann (1976), and pages 139–144 in Hoepcke (1980).

As mentioned in the main text (eq. 2.13 to eq. 2.15), when all partitioning properties are known, the thermodynamic constraints can be written in three equations:

$$\log(S_A) - \log(S_W) - \log(K_{AW}) = w_1 \qquad \text{(eq. 9.1)}$$

$$\log(S_A) - \log(S_O) + \log(K_{OA}) = w_2 \qquad \text{(eq. 9.2)}$$

$$\log(S_W) - \log(S_O) + \log(K_{OW}{}^*) = w_3 \qquad \text{(eq. 9.3)}$$

It is convenient to express eq. 9.1 to eq. 9.3 in matrix form:

$$\mathbf{B} \cdot \mathbf{l} = \mathbf{w} \qquad \text{(eq. 9.4)}$$

where the **l** vector represents the LDVs and the **w** vector the misclosure errors of the equations. **B**, **l**, and **w** have the following form:

$$\mathbf{B} = \begin{pmatrix} 1 & -1 & 0 & -1 & 0 & 0 \\ 1 & 0 & -1 & 0 & 0 & 1 \\ 0 & 1 & -1 & 0 & 1 & 0 \end{pmatrix} \qquad \mathbf{l} = \begin{pmatrix} \log(S_A) \\ \log(S_W) \\ \log(S_O) \\ \log(K_{AW}) \\ \log(K_{OW}{}^*) \\ \log(K_{OA}) \end{pmatrix} \qquad \mathbf{w} = \begin{pmatrix} w_1 \\ w_2 \\ w_3 \end{pmatrix}$$

By analogy to eq. 2.7 to eq. 2.9 in the main text, we introduce a **v** vector that contains the corrections of the LDVs so that the FAVs are given by:

$$\bar{\mathbf{l}} = \mathbf{l} - \mathbf{v} \qquad \text{(eq. 9.5)}$$

To find the **v** vector, the Lagrange equation (eq. 2.11 in the main text) is written in matrix form (Hoepcke, 1980):

$$\Omega = \mathbf{v}^{\mathrm{T}} \cdot \mathbf{Q}^{-1} \cdot \mathbf{v} - 2 \cdot \mathbf{k}^{\mathrm{T}} \cdot (\mathbf{B} \cdot \mathbf{v} - \mathbf{w}) \qquad \text{(eq. 9.6)}$$

Q is the cofactor matrix (for details, see Mikhail and Ackermann, 1976, pages 64-65). If the measurements of the LDVs are independent, **Q** is a diagonal matrix containing the relative variances of the LDVs on its diagonal.

By analogy to the simple case with only one constraint (see main text, eq. 2.12), **v** can be found:

$$\mathbf{v} = \mathbf{Q} \cdot \mathbf{B}^{\mathrm{T}} \cdot (\mathbf{B} \cdot \mathbf{Q} \cdot \mathbf{B}^{\mathrm{T}})^{-1} \cdot \mathbf{w} \qquad \text{(eq. 9.7)}$$

For a step-by-step derivation of this expression, see Niemeier (2001), pages 156/157 or Mikhail and Ackermann (1976), pages 112/113. The FAVs then follow from eq. 9.5.

9.1.2 Development of Uncertainty Propagation with the Least-Squares Method

The derivation of the following equation is given in Mikhail and Ackermann (1976) or Niemeier (2001):

$$\overline{\mathbf{Q}} = \mathbf{Q} - \left(\mathbf{Q} \cdot \mathbf{B}^{\mathrm{T}} \cdot \left(\mathbf{B} \cdot \mathbf{Q} \cdot \mathbf{B}^{\mathrm{T}}\right)^{-1} \cdot \mathbf{B} \cdot \mathbf{Q}\right) \qquad \text{(eq. 9.8)}$$

$\overline{\mathbf{Q}}$ is the matrix of the adjusted cofactors. On its diagonal appear the relative variances of the properties to be adjusted, whereas the other elements contain their relative covariances (see Mikhail and Ackermann, 1976, pages 64–65 and 76–79). As an illustration, we can imagine the simple case presented in eq. 2.6 of the main text, where only one equation links the three partitioning properties

$$\overline{\log(K_{\mathrm{AW}})} - \overline{\log(K_{\mathrm{OW}}^{*})} + \overline{\log(K_{\mathrm{OA}})} = 0 \qquad \text{(eq. 9.9)}$$

If the relative variance of $\log(K_{\mathrm{OW}}^{*})$ is twice as high as that of $\log(K_{\mathrm{AW}})$ and $\log(K_{\mathrm{OA}})$, then **B** and **Q** have the following form:

$$\mathbf{B} = \begin{pmatrix} 1 & -1 & 1 \end{pmatrix}; \qquad \mathbf{Q} = \begin{pmatrix} 1 & 0 & 0 \\ 0 & 2 & 0 \\ 0 & 0 & 1 \end{pmatrix}$$

Using eq. 9.8, one obtains $\overline{\mathbf{Q}} = \begin{pmatrix} 0.75 & 0.5 & -0.25 \\ 0.5 & 1 & 0.5 \\ -0.25 & 0.5 & 0.75 \end{pmatrix}$. The relative variances of the three adjusted logarithms of the partition coefficients are therefore 0.75, 1, and 0.75, respectively. The covariances can be used to predict in what way a measurement error in the LDV of one property affects the FAVs of the other properties: If the first LDV (log K_{AW}) is measured with an error of +1 (one log-unit), then the adjusted values $\overline{\log(K_{AW})}$, $\overline{\log(K_{OW}*)}$, and $\overline{\log(K_{OA})}$ will be erroneous by +0.75, +0.5, and –0.25 respectively (the first line in the $\overline{\mathbf{Q}}$ matrix). If the second parameter, log K_{OW}*, is measured with an error of +2 (its variance on the diagonal of the **Q** matrix), the adjusted values $\overline{\log(K_{AW})}$, $\overline{\log(K_{OW}*)}$, and $\overline{\log(K_{OA})}$ will be erroneous by +0.5, +1, and +0.5 respectively (the second line in the $\overline{\mathbf{Q}}$ matrix). In the case where six chemical properties exist, the $\overline{\mathbf{Q}}$ matrix has the size 6×6. Then, if the LDV of the *i*-th property is measured with an error of $+\sigma_i^2$ (its variance in the **Q** matrix), the FAV of the *j*-th property is erroneous by the value in the *i*-th line and *j*-th column of the $\overline{\mathbf{Q}}$ matrix.

9.1.3 Comparison of the Beyer Analytical and Iterative Adjustment Procedure

The differences between the analytical and iterative adjustment procedure are described by Beyer et al. in (2002). The two procedures give very similar results if fewer than six chemical properties are known. However, if six chemical properties are known, the differences become very important: sometimes, the two methods apply corrections into opposite directions (log S_A and K_{AW} of DDT in the data set of Beyer et al., for instance).

We believe that the analytical adjustment procedure, as it is presented in the Excel-spreadsheet (available from http://www.usf.uos.de/projects/elpos/download/adjust.en.html), is erroneous for the case when six measured properties have to be adjusted. Line 182 of the VisualBasic code that was used for the calculations in Beyer et al. is programmed as follows:

```
corr0 = uncert(0)/2*(epsilon1/uncert1+epsilon2/uncert2)
```

We believe that the plus should be replaced by a minus:

```
corr0 = uncert(0)/2*(epsilon1/uncert1-epsilon2/uncert2)
```

If this correction is made, the two adjustment procedures also give very similar results for six available measurements. For three example chemicals from the Beyer et al. data set, the

differences between the iterative adjustment procedure, the original and the corrected analytical adjustment procedure are displayed in Table 9.1, Table 9.2, and Table 9.3.

Table 9.1: Original and corrected properties of PCB-52 calculated with the iterative and analytical adjustment procedure.

	$\log S_A$	$\log S_W$	$\log S_O$	$\log K_{AW}$	$\log K_{OW}$*	$\log K_{OA}$	Σv^2
original values	–5.188	–3.488	2.871	–1.885	6.274	8.220	
A: iterative adjustment	–5.257	–3.434	2.886	–1.823	6.320	8.143	0.0196
B: original analytical adjustment	–5.192	–3.443	2.884	–1.749	6.326	8.076	0.0441
C: corrected analytical adjustment	–5.246	–3.443	2.884	–1.803	6.326	8.129	0.0231
difference B – A	0.065	–0.009	–0.003	0.074	0.006	–0.068	
difference C – A	0.012	–0.009	–0.003	0.020	0.006	–0.014	

Table 9.2: Original and corrected properties of p,p'-DDT calculated with the iterative and analytical adjustment procedure.

	$\log S_A$	$\log S_W$	$\log S_O$	$\log K_{AW}$	$\log K_{OW}$*	$\log K_{OA}$	Σv^2
original values	–6.905	–3.621	3.208	–3.277	6.818	9.809	
A: iterative adjustment	–6.843	–3.621	3.145	–3.222	6.765	9.988	0.0458
B: original analytical adjustment	–6.955	–3.621	3.155	–3.334	6.776	10.110	0.1013
C: corrected analytical adjustment	–6.853	–3.621	3.155	–3.233	6.776	10.009	0.0493
difference B – A	–0.112	0.000	0.011	–0.112	0.011	0.122	
difference C – A	–0.010	0.000	0.011	–0.010	0.011	0.021	

Table 9.3: Original and corrected properties of γ-HCH calculated with the iterative and analytical adjustment procedure.

	$\log S_A$	$\log S_W$	$\log S_O$	$\log K_{AW}$	$\log K_{OW}$*	$\log K_{OA}$	Σv^2
original values	–4.885	–0.735	3.197	–3.845	3.432	7.843	
A: iterative adjustment	–4.776	–0.696	3.049	–4.080	3.745	7.825	0.1887
B: original analytical adjustment	–4.874	–0.703	3.074	–4.171	3.776	7.947	0.2521
C: corrected analytical adjustment	–4.794	–0.703	3.074	–4.092	3.776	7.868	0.2043
difference B – A	–0.098	–0.007	0.025	–0.091	0.031	0.122	
difference C – A	–0.018	–0.007	0.025	–0.012	0.031	0.043	

9.1.4 Final Adjusted Values (FAVs) of the Chemicals Reported by Beyer et al.

Table 9.4: FAVs of the chemical properties reported by Beyer et al. Only the least-squares adjustment procedure is applied. All data is in log-units, units of S_A, S_W, and S_O are mol/m^3, partition coefficients are dimensionles.

	logS_A	logS_W	logS_O	logK_{AW}	logK_{OW}*	logK_{OA}
PCB-15	–4.56	–2.36	3.11	–2.20	5.47	7.67
PCB-29	–4.67	–2.73	3.36	–1.94	6.09	8.03
PCB-31	–4.94	–2.98	3.04	–1.96	6.02	7.98
PCB-44	–5.29	–3.24	2.99	–2.05	6.23	8.28
PCB-52	–5.27	–3.41	2.88	–1.86	6.29	8.16
PCB-61	–5.43	–3.45	3.18	–1.98	6.63	8.60
PCB-77	–6.29	–3.84	3.12	–2.45	6.96	9.41
PCB-101	–5.84	–3.87	3.13	–1.97	7.01	8.98
PCB-153	–6.71	–4.72	2.86	–1.99	7.58	9.57
p,p'-DDT	–6.83	–3.61	3.12	–3.22	6.73	9.95
p,p'-DDE	–5.93	–3.05	3.40	–2.88	6.45	9.33
a-HCH	–4.39	–0.79	2.99	–3.59	3.79	7.38
g-HCH	–4.75	–0.68	3.01	–4.07	3.69	7.76
1,2,4,5-chlorobenzene	–2.47	–1.24	3.23	–1.23	4.47	5.70
1,2,3,5-chlorobenzene	–2.44	–1.30	3.32	–1.14	4.62	5.76
pentachlorobenzene	–3.43	–2.05	3.01	–1.39	5.05	6.44
hexachlorobenzene	–4.59	–3.02	2.79	–1.58	5.80	7.38
naphthalene	–1.80	0.02	3.18	–1.83	3.15	4.98
biphenyl	–2.77	–0.78	3.10	–1.98	3.88	5.87
acenaphthene	–3.08	–0.85	3.00	–2.23	3.85	6.08
fluorene	–3.59	–1.08	3.13	–2.51	4.21	6.72
phenanthrene	–4.41	–1.55	3.14	–2.85	4.69	7.55
anthracene	–4.82	–1.84	2.87	–2.98	4.71	7.69
fluoranthene	–5.64	–2.36	3.10	–3.28	5.46	8.74
pyrene	–5.31	–2.03	3.41	–3.29	5.44	8.73
benzo(a)pyrene	–8.60	–3.94	2.53	–4.66	6.47	11.13
chrysene	–7.37	–2.98	2.83	–4.38	5.81	10.19
2,3,7,8-cl-furan	–6.16	–3.07	3.72	–3.09	6.79	9.87
1,2,3,4-cl-dioxin	–6.46	–3.70	3.43	–2.77	7.13	9.90

Table 9.5: FAVs of the chemical properties reported by Beyer et al. Only the least-squares adjustment procedure is applied. Here, K_{OW} is given instead of K_{OW}*.

	P (Pa)	S_W (mol/m^3)	S_O (mol/m^3)	K_{AW}	K_{OW}	K_{OA}
PCB-15	6.80×10^{-2}	4.34×10^{-3}	1.28×10^{3}	6.32×10^{-3}	1.67×10^{5}	4.67×10^{7}
PCB-29	5.27×10^{-2}	1.85×10^{-3}	2.29×10^{3}	1.15×10^{-2}	4.82×10^{5}	1.08×10^{8}
PCB-31	2.85×10^{-2}	1.05×10^{-3}	1.11×10^{3}	1.09×10^{-2}	4.29×10^{5}	9.64×10^{7}
PCB-44	1.26×10^{-2}	5.71×10^{-4}	9.76×10^{2}	8.92×10^{-3}	6.13×10^{5}	1.92×10^{8}
PCB-52	1.32×10^{-2}	3.88×10^{-4}	7.60×10^{2}	1.37×10^{-2}	6.77×10^{5}	1.43×10^{8}
PCB-61	9.25×10^{-3}	3.52×10^{-4}	1.50×10^{3}	1.06×10^{-2}	1.20×10^{6}	4.01×10^{8}
PCB-77	1.28×10^{-3}	1.45×10^{-4}	1.32×10^{3}	3.55×10^{-3}	2.12×10^{6}	2.56×10^{9}
PCB-101	3.57×10^{-3}	1.33×10^{-4}	1.36×10^{3}	1.08×10^{-2}	2.30×10^{6}	9.45×10^{8}
PCB-153	4.88×10^{-4}	1.92×10^{-5}	7.30×10^{2}	1.02×10^{-2}	6.09×10^{6}	3.71×10^{9}
p,p'-DDT	3.69×10^{-4}	2.45×10^{-4}	1.31×10^{3}	6.06×10^{-4}	1.43×10^{6}	8.83×10^{9}
p,p'-DDE	2.90×10^{-3}	8.96×10^{-4}	2.52×10^{3}	1.31×10^{-3}	8.86×10^{5}	2.15×10^{9}
a-HCH	1.02×10^{-1}	1.60×10^{-1}	9.87×10^{2}	2.56×10^{-4}	9.48×10^{3}	2.40×10^{7}
g-HCH	4.42×10^{-2}	2.08×10^{-1}	1.02×10^{3}	8.57×10^{-5}	8.01×10^{3}	5.71×10^{7}
1,2,4,5-chlorobenzene	8.34	5.71×10^{-2}	1.69×10^{3}	5.89×10^{-2}	3.04×10^{4}	5.03×10^{5}
1,2,3,5-chlorobenzene	9.03	5.02×10^{-2}	2.10×10^{3}	7.27×10^{-2}	3.93×10^{4}	5.77×10^{5}
pentachlorobenzene	9.11×10^{-1}	8.99×10^{-3}	1.02×10^{3}	4.09×10^{-2}	8.22×10^{4}	2.77×10^{6}
hexachlorobenzene	6.35×10^{-2}	9.65×10^{-4}	6.15×10^{2}	2.66×10^{-2}	2.95×10^{5}	2.40×10^{7}
naphthalene	3.89×10	1.05	1.50×10^{3}	1.49×10^{-2}	3.21×10^{3}	9.55×10^{4}
biphenyl	4.25	1.65×10^{-1}	1.27×10^{3}	1.04×10^{-2}	1.12×10^{4}	7.37×10^{5}
acenaphthene	2.04	1.41×10^{-1}	9.97×10^{2}	5.84×10^{-3}	1.05×10^{4}	1.21×10^{6}
fluorene	6.41×10^{-1}	8.32×10^{-2}	1.34×10^{3}	3.11×10^{-3}	1.94×10^{4}	5.20×10^{6}
phenanthrene	9.75×10^{-2}	2.82×10^{-2}	1.39×10^{3}	1.40×10^{-3}	4.44×10^{4}	3.54×10^{7}
anthracene	3.75×10^{-2}	1.45×10^{-2}	7.37×10^{2}	1.05×10^{-3}	4.54×10^{4}	4.87×10^{7}
fluoranthene	5.74×10^{-3}	4.40×10^{-3}	1.27×10^{3}	5.26×10^{-4}	1.64×10^{5}	5.47×10^{8}
pyrene	1.20×10^{-2}	9.40×10^{-3}	2.58×10^{3}	5.17×10^{-4}	1.58×10^{5}	5.31×10^{8}
benzo(a)pyrene	6.24×10^{-6}	1.15×10^{-4}	3.37×10^{2}	2.19×10^{-5}	9.14×10^{5}	1.34×10^{11}
chrysene	1.06×10^{-4}	1.04×10^{-3}	6.70×10^{2}	4.14×10^{-5}	2.98×10^{5}	1.56×10^{10}
2,3,7,8-cl-furan	1.72×10^{-3}	8.54×10^{-4}	5.21×10^{3}	8.14×10^{-4}	1.57×10^{6}	7.49×10^{9}
1,2,3,4-cl-dioxin	8.55×10^{-4}	2.01×10^{-4}	2.72×10^{3}	1.71×10^{-3}	2.83×10^{6}	7.88×10^{9}

Table 9.6: Relative variances of the FAVs in Table 9.5 (in log units). The corresponding uncertainty factors (i.e., relative variances) of the LDVs are 1 for all properties. All data is in log-units, units of S_A, S_W, and S_O are mol/m^3, partition coefficients are dimensionles.

	logS_A	logS_W	logS_O	logK_{AW}	logK_{OW}*	logK_{OA}
PCB-15	0.62	0.62	1.00	0.50	0.62	0.62
PCB-29	0.62	0.62	1.00	0.50	0.62	0.62
PCB-31	0.62	0.62	1.00	0.50	0.62	0.62
PCB-44	0.62	0.62	1.00	0.50	0.62	0.62
PCB-52	0.50	0.50	0.50	0.50	0.50	0.50
PCB-61	0.50	0.50	0.50	0.50	0.50	0.50
PCB-77	0.62	0.62	1.00	0.50	0.62	0.62
PCB-101	0.62	0.62	1.00	0.50	0.62	0.62
PCB-153	0.62	0.62	1.00	0.50	0.62	0.62
p,p'-DDT	0.50	0.50	0.50	0.50	0.50	0.50
p,p'-DDE	0.62	0.62	1.00	0.50	0.62	0.62
a-HCH	0.62	0.62	1.00	0.50	0.62	0.62
g-HCH	0.50	0.50	0.50	0.50	0.50	0.50
1,2,4,5-chlorobenzene	0.50	0.50	0.50	0.50	0.50	0.50
1,2,3,5-chlorobenzene	0.62	0.50	0.62	0.62	0.62	1.00
pentachlorobenzene	0.50	0.50	0.50	0.50	0.50	0.50
hexachlorobenzene	0.50	0.50	0.50	0.50	0.50	0.50
naphthalene	0.62	0.50	0.62	0.62	0.62	1.00
biphenyl	0.62	0.50	0.62	0.62	0.62	1.00
acenaphthene	0.62	0.50	0.62	0.62	0.62	1.00
fluorene	0.50	0.50	0.50	0.50	0.50	0.50
phenanthrene	0.50	0.50	0.50	0.50	0.50	0.50
anthracene	0.62	0.50	0.62	0.62	0.62	1.00
fluoranthene	0.50	0.50	0.50	0.50	0.50	0.50
pyrene	0.50	0.50	0.50	0.50	0.50	0.50
benzo(a)pyrene	0.62	0.50	0.62	0.62	0.62	1.00
chrysene	0.62	0.50	0.62	0.62	0.62	1.00
2,3,7,8-cl-furan	0.62	0.62	1.00	0.50	0.62	0.62
1,2,3,4-cl-dioxin	0.62	0.62	1.00	0.50	0.62	0.62

9.1.5 Literature-Derived Values (LDVs) and Final Adjusted Values (FAVs) of the PCB Data Reported by Li et al.

Table 9.7: LDVs of the chemical properties after van Noort correction (applied to S_A, S_W, S_O). All data is in log-units. Log K_{AW}, log K_{OW}* and log K_{OA} are identical to the ones reported by Li et al. (2003). FAVs after the adjustment with the least-squares method can be found in the main text (Table 2.1).

	logS_A	logS_W	logS_O	logK_{AW}	logK_{OW}*	logK_{OA}
PCB-3	–3.74	–1.79	3.10	–1.84	4.57	6.82
PCB-8	–4.30	–2.15		–1.98	5.26	7.40
PCB-15	–4.71	–2.48	3.02	–2.24	5.63	7.65
PCB-28	–5.02	–3.01		–1.87	5.80	7.93
PCB-29	–4.74	–2.76	2.81	–1.88	6.02	7.80
PCB-31	–5.01	–3.08		–1.83	6.08	7.93
PCB-52	–5.37	–3.21	2.83	–1.94	6.34	8.22
PCB-61	–5.56	–3.48	2.89	–2.08	6.52	8.64
PCB-101	–6.02	–4.05		–1.90	6.50	8.90
PCB-105	–6.45	–4.01		–1.87	7.03	10.01
PCB-118	–6.44	–4.09		–1.89	6.89	9.82
PCB-138	–6.66	–4.71		–1.80	7.48	9.76
PCB-153	–6.67	–4.49		–2.00	7.14	9.52
PCB-155	–5.91	–4.49		–1.51	7.90	8.89
PCB-180	–7.27	–4.76		–2.63	7.81	10.14
PCB-194	–8.08	–5.25		–2.56	8.26	11.31

Table 9.8: LDVs of the energies of phase transition reported by Li et al. (2003) with the new ΔU_{AW} values, and after the van Noort correction of S_A, S_W, and S_O. Data for ΔU_{OW} and ΔU_{OA} are identical to the values given in Li et al. FAVs after adjustment with the least-squares method can be found in Table 2.2 in the main text.

	ΔU_A (kJ/mol)	ΔU_W (kJ/mol)	ΔU_O (kJ/mol)	ΔU_{AW} (kJ/mol)	ΔU_{OW} (kJ/mol)	ΔU_{OA} (kJ/mol)
PCB-3	70.6	14.5		53.5	–20.0	–66.4
PCB-8	70.6			56.5	–21.0	–73.1
PCB-15	75.4	22.6	–7.40	56.5	–21.0	–75.9
PCB-28	77.1			50.0	–22.0	–80.2
PCB-29	74.2	18.1		59.4	–22.0	–84.3
PCB-31	77.0			59.4	–22.0	–80.2
PCB-52	77.7			52.0	–23.0	–83.1
PCB-61	85.2	19.1		62.3	–24.0	–96.6
PCB-101	86.2	15.8		64.8	–24.0	–83.5
PCB-105	88.6			64.8	–24.0	–89.6
PCB-118	90.4			64.8	–24.0	–89.9
PCB-138	93.9			67.0	–25.0	–86.3
PCB-153	91.8			67.0	–25.0	–95.1
PCB-155	93.7	21.0		67.0	–25.0	–81.3
PCB-180	94.1			68.9	–26.0	–95.3
PCB-194	101			70.9	–27.0	–95.1

Table 9.9: FAVs of the chemical properties after van Noort correction and the least-squares adjustment procedure. These data are derived from the LDVs in Table 9.7 and are the non-log-values for Table 2.1 given in the main text.

	P (Pa)	S_W (mol/m^3)	S_O (mol/m^3)	K_{AW}	K_{OW}	K_{OA}
PCB-3	4.38×10^{-1}	2.01×10^{-2}	1.03×10^{3}	8.78×10^{-3}	4.09×10^{4}	5.84×10^{6}
PCB-8	1.39×10^{-1}	6.48×10^{-3}	1.26×10^{3}	8.66×10^{-3}	1.29×10^{5}	2.25×10^{7}
PCB-15	4.95×10^{-2}	2.95×10^{-3}	1.09×10^{3}	6.76×10^{-3}	2.25×10^{5}	5.46×10^{7}
PCB-28	2.58×10^{-2}	8.97×10^{-4}	7.46×10^{2}	1.16×10^{-2}	4.52×10^{5}	7.16×10^{7}
PCB-29	4.49×10^{-2}	1.38×10^{-3}	1.15×10^{3}	1.31×10^{-2}	4.51×10^{5}	6.33×10^{7}
PCB-31	2.54×10^{-2}	7.57×10^{-4}	8.89×10^{2}	1.35×10^{-2}	6.08×10^{5}	8.67×10^{7}
PCB-52	1.15×10^{-2}	4.27×10^{-4}	7.73×10^{2}	1.09×10^{-2}	8.83×10^{5}	1.66×10^{8}
PCB-61	6.41×10^{-3}	3.12×10^{-4}	9.37×10^{2}	8.29×10^{-3}	1.37×10^{6}	3.62×10^{8}
PCB-101	2.15×10^{-3}	1.03×10^{-4}	5.90×10^{2}	8.39×10^{-3}	2.38×10^{6}	6.80×10^{8}
PCB-105	8.98×10^{-4}	8.95×10^{-5}	1.50×10^{3}	4.05×10^{-3}	6.01×10^{6}	4.13×10^{9}
PCB-118	8.88×10^{-4}	8.22×10^{-5}	9.85×10^{2}	4.36×10^{-3}	4.51×10^{6}	2.75×10^{9}
PCB-138	5.33×10^{-4}	2.00×10^{-5}	1.00×10^{3}	1.07×10^{-2}	1.55×10^{7}	4.67×10^{9}
PCB-153	5.51×10^{-4}	3.01×10^{-5}	6.22×10^{2}	7.38×10^{-3}	7.20×10^{6}	2.80×10^{9}
PCB-155	3.20×10^{-3}	3.14×10^{-5}	1.65×10^{3}	4.11×10^{-2}	1.61×10^{7}	1.28×10^{9}
PCB-180	1.32×10^{-4}	1.72×10^{-5}	7.83×10^{2}	3.10×10^{-3}	1.43×10^{7}	1.47×10^{10}
PCB-194	2.12×10^{-5}	5.08×10^{-6}	1.16×10^{3}	1.68×10^{-3}	5.74×10^{7}	1.36×10^{11}

Table 9.10: Relative variances of the chemical properties of the PCBs after the adjustment procedure (in log units). The relative variances of the LDVs, given in Li et al, are higher by a factor of about 2 compared to those of the FAVs presented here.

	$\log S_A$	$\log S_W$	$\log S_O$	$\log K_{AW}$	$\log K_{OW}$*	$\log K_{OA}$
PCB-3	0.58	0.58	0.50	0.83	0.58	0.58
PCB-8	1.55	1.35	1.87	0.97	0.77	1.10
PCB-15	0.63	0.75	0.59	0.82	0.63	0.75
PCB-28	1.17	1.17	2.21	0.69	1.45	1.31
PCB-29	1.25	1.17	1.66	1.37	1.30	1.77
PCB-31	1.45	1.75	2.40	1.54	1.75	1.45
PCB-52	1.10	1.35	1.41	0.75	1.35	1.10
PCB-61	1.30	1.27	1.55	1.78	1.81	1.94
PCB-101	1.45	1.75	2.06	1.54	1.78	0.86
PCB-105	1.59	2.43	3.05	1.96	1.55	2.21
PCB-118	1.59	2.43	3.05	1.96	1.55	2.21
PCB-138	1.58	2.38	2.86	1.87	2.38	1.58
PCB-153	1.44	1.73	2.65	1.48	2.18	1.55
PCB-155	1.31	0.83	2.91	1.44	2.51	2.67
PCB-180	1.57	2.34	2.29	1.79	2.07	0.88
PCB-194	1.60	2.52	3.55	2.14	2.18	2.71

Table 9.11: Relative variances of the energies of phase transition (ΔU) of the PCBs after the adjustment procedure. The relative variances of the LDVs, given in Li et al., are higher by a factor of about 2 compared to those of the FAVs presented here.

	ΔU_A (kJ/mol)	ΔU_W (kJ/mol)	ΔU_O (kJ/mol)	ΔU_{AW} (kJ/mol)	ΔU_{OW} (kJ/mol)	ΔU_{OA} (kJ/mol)
PCB-3	0.85	1.62	2.18	1.56	2.22	1.56
PCB-8	2.00	4.55	3.64	2.55	2.73	1.64
PCB-15	1.41	2.13	2.23	2.01	2.43	2.19
PCB-28	2.00	3.56	3.56	1.56	2.22	1.56
PCB-29	1.49	1.85	3.72	1.82	2.95	2.95
PCB-31	2.00	4.55	3.64	2.55	2.73	1.64
PCB-52	2.00	3.56	3.56	1.56	2.22	1.56
PCB-61	1.49	1.85	3.72	1.82	2.95	2.95
PCB-101	1.46	1.78	2.12	1.62	1.96	0.88
PCB-105	2.00	4.40	2.90	2.40	2.50	0.90
PCB-118	2.00	4.40	2.90	2.40	2.50	0.90
PCB-138	2.00	4.40	2.90	2.40	2.50	0.90
PCB-153	2.00	4.40	2.90	2.40	2.50	0.90
PCB-155	0.85	1.69	3.35	1.67	2.92	2.92
PCB-180	2.00	4.77	4.77	2.77	3.08	2.77
PCB-194	2.00	4.86	5.21	2.86	3.21	3.21

9.1.6 Two Parameter Regressions for the PCB Data set Using new FAVs

As described in the text, two-parameter (molar mass and number of orthochlorines) regressions can improve the correlation coefficients for the QSPRs of some properties. The parameters that should be used in such equations are given below. The equations must have the following form:

property = intercept + <Molar Mass> × slope

for one parameter regressions taking into account molar mass (in g/mol) only, or

property = intercept + <Molar Mass> × slope 1 + <# Orthochlorines> × slope 2

for two parameter regressions taking into account molar mass and number of orthochlorines.

It can be seen that a correlation with $R^2 \geq 0.95$ cannot be obtained for all the properties: only 5 properties (shaded in light grey) have a R^2 higher than 0.95, and four more have a R^2 higher than 0.5. If no significant increase in the correlation can be obtained with an additional parameter, it should be omitted.

Table 9.12: Summary of the regressions for mass and number of orthochlorines.

	only mass				mass and number of orthochlorines				
	intercept	**slope**	R^2	$R^2_{adjusted}$	**intercept**	**slope 1**	**slope 2**	R^2	$R^2_{adjusted}$
log$P$	2.74	-1.67×10^{-2}	0.94	0.94	3.38	-2.06×10^{-2}	3.85×10^{-1}	0.99	0.99
logS_W	9.07×10^{-1}	-1.49×10^{-2}	0.98	0.98	9.08×10^{-1}	-1.49×10^{-2}	3.54×10^{-3}	0.98	0.97
logS_O	3.02	-1.09×10^{-4}	0.00	–0.07	3.07	-3.79×10^{-4}	2.63×10^{-2}	0.02	–0.13
logK_{AW}	–1.56	-1.76×10^{-3}	0.15	0.09	-9.21×10^{-1}	-5.67×10^{-3}	3.82×10^{-1}	0.83	0.80
logK_{OW}	2.37	1.28×10^{-2}	0.97	0.96	2.41	1.25×10^{-2}	2.08×10^{-2}	0.97	0.96
logK_{OA}	3.68	1.66×10^{-2}	0.94	0.94	3.07	2.02×10^{-2}	-3.59×10^{-1}	0.98	0.98
ΔU_A	4.23×10^{1}	1.37×10^{-1}	0.94	0.94	4.01×10^{1}	1.50×10^{-1}	–1.29	0.95	0.94
ΔU_W	5.86	5.39×10^{-2}	0.64	0.61	4.85	6.00×10^{-2}	-5.98×10^{-1}	0.65	0.59
ΔU_O	-1.04×10^{1}	3.08×10^{-2}	0.24	0.19	–8.53	1.95×10^{-2}	1.11	0.27	0.16
ΔU_{AW}	3.65×10^{1}	8.28×10^{-2}	0.78	0.77	3.53×10^{1}	8.99×10^{-2}	-6.92×10^{-1}	0.79	0.76
ΔU_{OW}	-1.62×10^{1}	-2.30×10^{-2}	0.19	0.13	-1.34×10^{1}	-4.05×10^{-2}	1.71	0.29	0.18
ΔU_{OA}	-5.27×10^{1}	-1.06×10^{-1}	0.79	0.77	-4.87×10^{1}	-1.30×10^{-1}	2.40	0.83	0.80

All quantities are obtained in the following units: P in (Pa), S_W and S_O in (mol/m^3), partition coefficients are dimensionless, and all ΔU in (kJ/mol).

9.1.7 Literature-Derived Values (LDVs) and Final Adjusted Values (FAVs) of the Data Reported by Xiao et al.

Table 9.13: LDVs of the chemical properties reported by Xiao et al. (2004). All data is in log-units, solubilities in mol/m^3. These data are identical to the values given in the original publication.

	logS_A	logS_W	logS_O	logK_{AW}	logK_{OW}*	logK_{OA}
α-HCH	–4.00	–0.53	3.48	–3.58	3.81	7.61
β-HCH	–4.61	0.07		–4.82	3.84	8.87
γ-HCH	–4.51	–0.63	3.29	–3.96	3.70	7.84

Table 9.14: FAVs of the chemical properties reported by Xiao et al. (2004). Only the least-squares adjustment procedure was applied. All data is in log-units, solubilities in mol/m^3.

	logS_A	logS_W	logS_O	logK_{AW}	logK_{OW}*	logK_{OA}
α-HCH	–4.04	–0.45	3.44	–3.59	3.88	7.48
β-HCH	–4.67	0.16	4.07	–4.83	3.91	8.74
γ-HCH	–4.54	–0.58	3.18	–3.96	3.76	7.72

Table 9.15: Relative variance of the chemical properties after the adjustment procedure (in log units, solubilities in mol/m^3). The relative variances of the LDVs, given in Xiao et al., are higher by a factor of about 2 compared to those of the FAVs presented here.

	$\log S_A$	$\log S_W$	$\log S_O$	$\log K_{AW}$	$\log K_{OW}$*	$\log K_{OA}$
α-HCH	1.25	1.37	1.77	1.17	1.30	1.66
β-HCH	2.02	2.26	3.65	1.66	2.11	2.52
γ-HCH	0.69	0.65	1.08	0.82	0.75	1.18

Table 9.16: LDVs of the energies of phase transition reported by Xiao et al. These data are identical to the values given in the original publication.

	ΔU_A (kJ/mol)	ΔU_W (kJ/mol)	ΔU_O (kJ/mol)	ΔU_{AW} (kJ/mol)	ΔU_{OW} (kJ/mol)	ΔU_{OA} (kJ/mol)
α-HCH	63.3		4.9	58.2	–7.20	–61.9
β-HCH	65.7			63.7	–5.80	–94.5
γ-HCH	72.0	14.4	1.6	53.8	–10.4	–58.0

Table 9.17: New FAVs of the energies of phase transition reported by Xiao et al. Only the least-squares adjustment procedure is applied.

	ΔU_A (kJ/mol)	ΔU_W (kJ/mol)	ΔU_O (kJ/mol)	ΔU_{AW} (kJ/mol)	ΔU_{OW} (kJ/mol)	ΔU_{OA} (kJ/mol)
α-HCH	64.5	7.7	2.43	56.9	–5.2	–62.1
β-HCH	65.7	–2.2	–18.38	67.9	–16.2	–84.1
γ-HCH	71	16.2	6.59	54.3	–9.6	–64.0

9.1.8 Literature-Derived Values (LDVs) and Final Adjusted Values (FAVs) of the Data Reported by Shen and Wania

Table 9.18: LDVs of the data reported by Shen and Wania (2005). All data is in log-units, solubilities in mol/m^3. These data are identical to ones reported in the original publication.

	logS_A	logS_W	logS_O	logK_{AW}	logK_{OW}*	logK_{OA}
hexachlorobenzene	–0.85	–3.02		–1.68	5.52	7.38
pentachlorobenzene	0.08	–1.96		–1.53	5.08	6.90
p,p'-DDT	–3.25	–3.57		–3.35	6.28	9.81
p,p'-DDE	–2.48	–3.09		–2.77	6.96	9.69
p,p'-DDD	–3.01	–2.55		–3.57	6.22	10.10
cis-chlordane	–2.10	–2.96		–2.62	6.10	8.91
trans-chlordane	–1.89	–2.96		–2.62	6.22	8.86
heptachlor	–0.89	–2.46		–1.92	6.10	7.64
heptachlor epoxide	–1.89	–1.74		–3.07	5.40	8.62
aldrin	–1.21	–2.54		–2.22	6.50	8.07
dieldrin	–1.80	–1.92		–3.39	5.40	8.89
endrin	–2.28	–2.57		–3.59	5.20	8.13
α-endosulfan	–2.22	–2.38		–3.54	4.74	8.63
β-endosulfan	–2.37	–1.10		–4.79	4.78	

Table 9.19: New FAVs of the chemical properties reported by Shen and Wania (2005).Only the least-squares adjustment procedure was applied. All data is in log-units, solubilities in mol/m^3.

	logS_A	logS_W	logS_O	logK_{AW}	logK_{OW}*	logK_{OA}
hexachlorobenzene	–1.00	–2.88	2.73	–1.51	5.61	7.12
pentachlorobenzene	0.02	–1.83	3.32	–1.54	5.15	6.69
p,p'-DDT	–3.31	–3.39	3.02	–3.31	6.41	9.72
p,p'-DDE	–2.47	–3.10	3.84	–2.77	6.94	9.70
p,p'-DDD	–2.96	–2.61	3.70	–3.74	6.30	10.05
cis-chlordane	–2.14	–2.88	3.31	–2.65	6.19	8.84
trans-chlordane	–1.97	–2.82	3.45	–2.54	6.27	8.82
heptachlor	–0.86	–2.47	3.49	–1.78	5.96	7.74
heptachlor epoxide	–1.69	–1.86	3.54	–3.22	5.40	8.62
aldrin	–1.19	–2.58	3.67	–2.01	6.25	8.26
dieldrin	–1.82	–1.87	3.62	–3.35	5.49	8.84
endrin	–2.41	–2.52	2.48	–3.28	5.00	8.28
α-endosulfan	–2.34	–2.17	2.75	–3.56	4.93	8.49
β-endosulfan	–2.40	–1.05	3.73	–4.75	4.78	9.53

Table 9.20: Relative variance of the chemical properties after the adjustment procedure (in log units, solubilities in mol/m^3). The relative variances of the LDVs, given in Shen and Wania, are higher by a factor of about 2 compared to those of the FAVs presented here.

	$\log S_A$	$\log S_W$	$\log S_O$	$\log K_{AW}$	$\log K_{OW}$*	$\log K_{OA}$
hexachlorobenzene	0.73	0.73	1.31	0.92	0.81	1.27
pentachlorobenzene	0.79	1.15	1.61	1.09	0.82	1.36
p,p'-DDT	0.83	1.47	1.98	1.28	1.66	1.40
p,p'-DDE	2.01	2.01	3.41	2.03	2.67	2.16
p,p'-DDD	2.01	2.01	3.41	2.03	2.67	2.16
cis-chlordane	2.18	2.71	3.60	2.14	2.41	2.11
trans-chlordane	2.18	2.71	3.60	2.14	2.41	2.11
heptachlor	1.86	1.49	2.97	1.84	2.32	2.05
heptachlor epoxide	2.66	2.16	3.75	2.00	2.16	2.66
aldrin	0.83	1.32	2.39	1.48	2.20	1.99
dieldrin	0.82	1.29	2.54	1.41	2.43	2.07
endrin	2.38	1.58	3.30	1.87	2.32	2.06
α-endosulfan	2.15	2.63	3.59	1.93	2.34	2.07
β-endosulfan	2.25	2.92	6.92	2.67	4.00	6.67

Table 9.21: LDVs of the energies of phase transition reported by Shen and Wania. These data are identical to the values given in the original publication.

	ΔU_A	ΔU_W	ΔU_O	ΔU_{AW}	ΔU_{OW}	ΔU_{OA}
hexachlorobenze	67.6	9.5		47.7	-24.4	-75.5
pentachlorobenze	61.7	12.1		40.6	-22.8	-71.3

Table 9.22: New FAVs of the energies of phase transition reported by Shen and Wania. Only the least-squares adjustment procedure was applied.

	ΔU_A	ΔU_W	ΔU_O	ΔU_{AW}	ΔU_{OW}	ΔU_{OA}
hexachlorobenze	66.0	14.1	-9.9	51.9	-24.0	-75.9
pentachlorobenze	60.6	15.3	-9.1	45.3	-24.4	-69.7

The FAVs calculated with the least-squares adjustment procedure differ by the FAVs reported by Shen and Wania by about 5-10% on average in non-log scales. Some values can differ by up to 25% with the exception of octanol solubility which can be up to 40% different since it is inferred from data on other properties in all cases.

9.1.9 Analysis of the Impact of the Correction Suggested by van Noort on the Chemicals Reported by Li et al.

Table 9.23: Fugacity ratios reported by Li et al. (2003) and calculated according to van Noort (2004) at 25° C. In the last three columns, the new values for vapor pressure (P), solubility in water (S_W), and solubility in octanol (S_O), referring to the subcooled liquid, are listed, but only if the original values were based on the solid state. Empty cells for vapor pressure mean that this value was already derived from measurements based on the subcooled liquid state. For solubility in octanol, only five values are available.

	F (Li et al.) (–)	F (van Noort) (–)	P (Pa)	S_W (mol/m^3)	S_O (mol/m^3)
PCB-3	0.450	0.479	4.47×10^{-1}	1.61×10^{-2}	1.27×10^{3}
PCB-8	0.651	0.654		7.03×10^{-3}	
PCB-15	0.058	0.088	4.88×10^{-2}	3.30×10^{-3}	1.05×10^{3}
PCB-28	0.474	0.485		9.89×10^{-4}	
PCB-29	0.255	0.271		1.75×10^{-3}	6.50×10^{2}
PCB-31	0.410	0.423		8.25×10^{-4}	
PCB-52	0.319	0.349	1.05×10^{-2}	6.23×10^{-4}	6.72×10^{2}
PCB-61	0.163	0.181	6.89×10^{-3}	3.28×10^{-4}	7.79×10^{2}
PCB-101	0.325	0.346	2.36×10^{-3}	8.99×10^{-5}	
PCB-105	0.125	0.155		9.67×10^{-5}	
PCB-118	0.147	0.176		8.14×10^{-5}	
PCB-138	0.295	0.316		1.97×10^{-5}	
PCB-153	0.172	0.200		3.24×10^{-5}	
PCB-155	0.200	0.244	3.02×10^{-3}	3.23×10^{-5}	
PCB-180	0.140	0.170		1.72×10^{-5}	
PCB-194	0.051	0.080		5.57×10^{-6}	

9.2 Supporting Information for Chapter 4: *Contribution of Volatile Precursor Substances to the Flux of Perfluorooctanoate to the Arctic*

9.2.1 Atmospheric Deposition Processes in the CliMoChem Model

The CliMoChem model takes into account four atmospheric deposition processes: dry gasous deposition (diffusion), wet gaseous deposition (rain washout), dry particle deposition (particle deposition), and wet particle deposition (particle washout). These processes are described in detail in Wegmann (2004); a short summary is given below.

Dry gaseous deposition is part of the diffusion processes between soil and atmosphere, parameterized according to the Jury et al. (1983). The deposition flux from atmosphere to soil can be simplified and written in the form

$$\frac{dc_A(t)}{t} = (1-\Phi)\cdot v_{as}^{diff}\cdot\frac{A}{V_A}\cdot c_A(t) \qquad \text{(eq. 9.10)}$$

where $c_A(t)$ (kg/m^3) is the time-dependent concentration in air, Φ (−) the particle-bound fraction, and v_{as}^{diff} (numerical value 24 m/d) the velocity of diffusive transfer from air to soil, A (m^2) the exchange surface area, and V_A (m^3) the volume of the air compartment (both depending on the latitudinal zone).

Wet gaseous deposition is parameterized according to

$$\frac{dc_A(t)}{t} = (1-\Phi)\cdot\frac{v^{rain}}{K_{AW}}\cdot\frac{A}{V_A}\cdot c_A(t) \qquad \text{(eq. 9.11)}$$

where v_{rain} (global averaged numerical value: 2.33×10^{-3} m/d) is the precipitation velocity and K_{AW} (−) the air−water partition coefficient (depending on the substance).

Dry particle deposition is given by

$$\frac{dc_A(t)}{t} = \Phi\cdot v^{dry}\cdot\frac{A}{V_A}\cdot c_A(t) \qquad \text{(eq. 9.12)}$$

where v^{dry} (numerical value 260 m/d for bare soil, variable for vegetation and vegetation-covered soil) is the dry particle deposition velocity.

Finally, the wet particle deposition velocity can be written by

$$\frac{dc_A(t)}{t} = \Phi \cdot v^{rain} \cdot Q \cdot \frac{A}{V_A} \cdot c_A(t) \qquad \text{(eq. 9.13)}$$

where Q (numerical value $2\times10^5(-)$) is the scavenging ratio.

9.2.2 Importance of NO_X Concentrations for Yields in the Degradation of FTOHs

NO_x concentrations are known to reduce the PFO yield during the degradation of FTOH in the atmosphere (Ellis et al., 2004). Given that NO_x concentrations are low in the Arctic, the PFO yield is expected to be higher than in temperate regions, where emissions from industry and transport result in higher NO_x concentrations. In the present study, no zonal differences in NO_x have been taken into account. The degradation yield of 5% is representative of Arctic regions (Wallington et al., 2006) that are most interesting in this context. Given that our results are similar to those of Wania (2007) (who used zone-specific degradation yields), we think that this simplification is justified.

9.2.3 Fractions of Formation and General Importance of Intermediate Degradation Products

As stated in the main text, many of the fractions of formation (*fof*) were assumed to be equal to one (e.g. in the degradation of FTAL to PFAL). It is known that during these reactions other substances are formed as well and the *fof*s are in reality not equal to one. One could argue that this would reduce the PFO yield and should be reflected by *fof* values below one for these first transformation reactions. However, such an adjustment is not needed, because we have calibrated the product of all *fof*s to result in a known overall transformation yield (5% PFO yield from Wallington et al., 2006). Whether the fraction of formation is applied only to the last step of the degradation scheme (as in the present calculations), or distributed among the different steps of the degradation (e.g. 50% *fof* for degradation from xFOSE to xFOSA, 50% from xFOSA to INT and 20% from INT to PFO; 50%×50%×20% = 5%) does not have any influence on the amount of PFO that is formed, as long as the product of all *fofs* remains constant.

To assess the importance of the formation of intermediate degradation products, we compare in the following the base-case with maximal formation of intermediate degradation products (presented above and used in the main text), with an alternative case where no intermediate degradation products are represented in the model but still with the same overall yield of the

transformation pathway. To this end, the temporal evolution of deposition fluxes of PFO into the Arctic was calculated after generic peak emissions of fluorotelomer alcohols and POSF-based substances into the temperate zone, with and without intermediate degradation products. The overall degradation yields were the same in both scenarios. The differences between the scenario with and without intermediate degradation products are thus only due to deposition and wash-out of the intermediate degradation products.

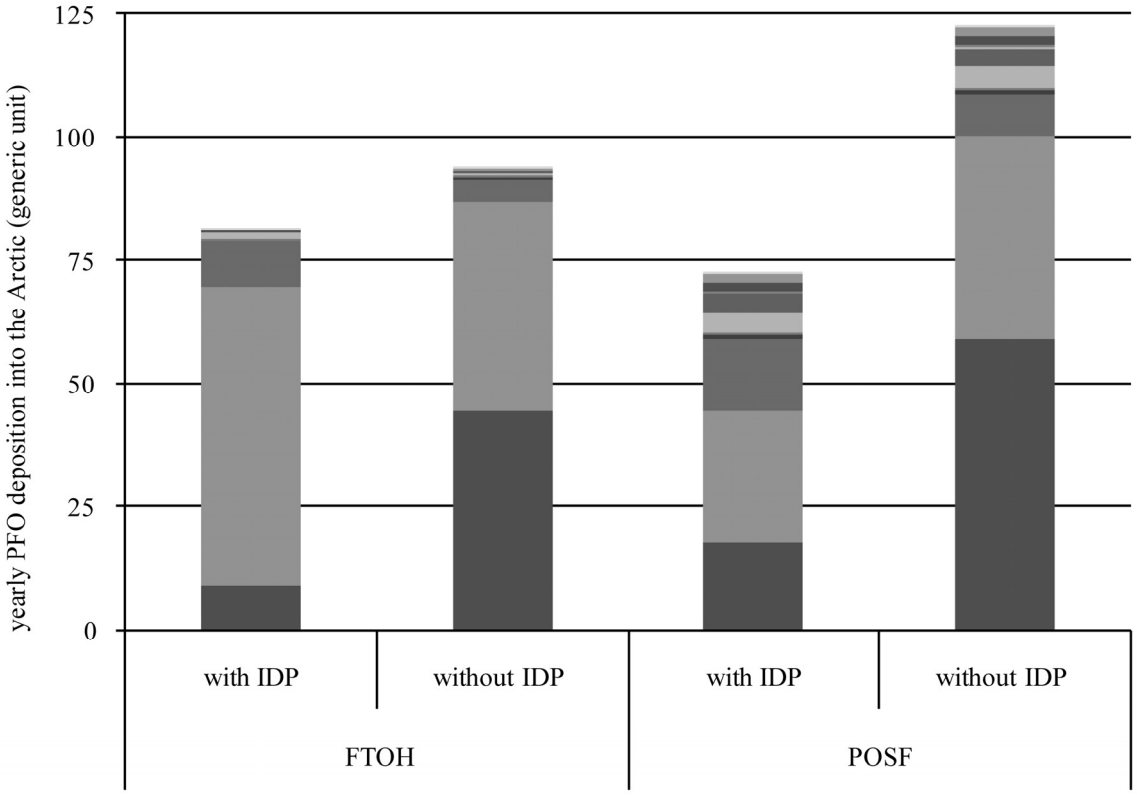

Figure 9.1: PFO deposition fluxes into the Arctic from FTOHs and POSF-based substances, with and without intermediate degradation products (IDP). The stacked bars are deposition fluxes from the first 12 seasons (equal to 3 years) after the peak emission, the first season being represented by the lowermost (deep-blue) bar, the second season by the second-bar from the bottom (brown) and so on. Fluxes decrease strongly over time, and become negligible after three years.

Whereas in the case of the POSF-based substances, the degradation of intermediate products is slower than the degradation of the parent compound (by about one order of magnitude), the degradation products of FTOH degrade faster than their parent compound. Furthermore, the vapor pressure of the intermediate degradation products of POSF-based substances is relatively low (as compared to the FTOH) and, therefore, these transformation products could be deposited, or scavenged by rain and snowfall more efficiently. Both effects suggest that PFO levels originating from POSF-based substances should be influenced more significantly

by wash-out and deposition of intermediate degradation products than PFO levels originating from FTOHs.

Results presented in Figure 9.1 show that for both, FTOHs and POSF-based substances, formation of PFO with intermediate degradation products leads to lower deposition fluxes to the Arctic than PFO formation without intermediate degradation products, because intermediate degradation products are deposited, which reduces the overall amount of PFO that is formed. Results show that for FTOHs this effect is less pronounced than for POSF-based substances: if degradation with intermediate degradation products is assumed, the deposition flux of PFO decreases by 12% for the FTOH and by 40% for the POSF-based substances. This is due to the fact that the intermediate degradation products of FTOHs are more volatile and have shorter lifetimes than those of the POSF-based substances, which are washed-out more efficiently. Another interesting effect can be observed for the FTOHs: the deposition in the first season (deep-blue bar) is strongly reduced if intermediate degradation products are taken into account. In the second season, however, deposition is higher with intermediate degradation products, suggesting that these have not been washed-out, but only delayed the transformation of FTOH into PFO by about one season (90 days).

As a conclusion it can be said that wash-out of intermediate degradation products occurs, but does not reduce the amount of PFO that reaches the Arctic by more than a factor of two (in the case of POSF-based substances). The influence is even smaller for the more volatile and shorter lived fluorotelomer alcohols.

There is the possibility that POSF-based substances and their intermediate degradation products are deposited into the Arcitc due to their low vapor pressures, as compared to FTOH, and are subsequently degraded in surface media to form PFO. There is very little quantitative information about this process available today, but given that deposition fluxes of the POSF-based substances and their intermediate degradation products into Arctic surface media are about ten times higher than deposition fluxes of PFO, this process might play an important role. The degradation half-lives in surface media would have to be shorter than about one year in the Arctic surface media for the two processes to have similar importance.

9.2.4 Selected Partition Coefficients and Degradation Half-Lives

Table 9.24: Second order rate constants for atmospheric degradation are transformed into average $t_{1/2}$ (in days), assuming OH radical concentrations of 7.5×10^5 molecules/cm^3 (only for illustration purposes – calculations in the model were done on zone- and season-specific OH radical concentrations as stated in the main text). Degradation in water and soil were assumed to be equal to zero for all substances. Atmospheric degradation half-lives for FTOH, FTAL, and PFAL are taken from Wallington et al. (2006), for xFOSE from D'Eon et al. (2006) and xFOSA from Martin et al. (2006). Partition coefficients for FTOH and PFO are from Wania (2007), for xFOSE from Arp et al. (2006). Note that the logK_{AW} for PFO is probably very low (PFO is mostly present in the ionic form in the environment, and is thus involatile), and that the value selected by Wania (logK_{AW} = –6.5) is the lowest value that Wania's model is able to calculate without becoming numerically unstable. We have selected a value that is 1.5 log-units lower to further decrease the volatility of the PFO ion. No measurements were available for all other properties, which were therefore based on properties of similar compounds, as described in the main text. Temperature dependencies were taken into account with energies of phase transition (ΔU_{AW} = 71,600 J/mol, ΔU_{OW} = 0 J/mol) for all partitioning properties and activation energies (E_A = 15,000 J/mol) for all atmospheric degradation rate constants. Wallington et al. (2006) suggest for FTOH E_A = 8300 J/mol, but we have retained the default value in CliMoChem that is based on a number of different substances (Atkinson et al., 1989, Anderson and Hites, 1996), as described in Scheringer et al. (2000). The influence of this parameter on the results is small.

	FTOH	FTAL	PFAL	xFOSE	xFOSA	INT	PFO
k_{air}' (cm^3/d/molecule)	9.24×10^{-8}	2.89×10^{-7}	4.91×10^{-8}	5.0×10^{-7}	3.23×10^{-8}	3.23×10^{-8}	0
average $t_{1/2}$ (d)	10.0	3.3	20.0	1.8	28.6	28.6	–
logK_{OC} (–)	5.48	5.48	5.48	5.48	5.48	5.48	1.54
logK_{AW} (–)	0.58	0.58	0.58	–1.0	–1.0	–0.5	–8.0

9.2.5 Further Information on Emission Inventories

In the present project, the emission data provided in Prevedouros et al. (2006) has been reinterpreted. Prevedouros et al. distinguish between direct PFO emissions that occur during the manufacture and use of PFO, and indirect PFO emission from precursor products that were not intended to contain PFO. There are three possible indirect PFO sources for both types of precursor substances, fluorotelomer alcohols and POSF-based substances:

- PFO impurities in products that are made from precursor substances
- precursor substances that degrade into PFO
- aqueous fire fighting foams based on precursor substances that contain impurities of PFO

For our calculations, we need to distinguish between emissions of PFO, and emission of precursor substances that degrade into PFO in the environment. Therefore, in our model, PFO emissions are the sum of direct PFO emissions in Prevedouros et al., and PFO residual impurities in precursor products and fire fighting foams from indirect emissions. Precursor substances that degrade into PFO are emitted as precursor substances in the CliMoChem model, and degrade into PFO in the model environment. The amount of precursor emissions is based on data reported in the Supporting Information in Prevedouros et al. (their Tables S12 and S15).

The data presented in the following table is based on the geometric mean of available information on unreacted raw-material content in polymers (as described in the main text). For the results shown in Figure 4.2 in the main text, geometric means, minimal, and maximal values have been used (as described in the main text). All emissions occurred into zone three of CliMoChem (36° N to 54° N). The receiving media were atmosphere for the precursor substances, and 55% ocean water, 31% atmosphere, and 14% soils for the direct emissions of PFO, as suggested in Wania (2007).

The following table gives global yearly emissions (in tonnes/year) of direct emission of PFO and the two precursor substances, FTOH and POSF-based substances.

Table 9.25: Global emissions of PFO, FTOH, and POSF-based substances in tonnes/year. Total emissions between 1951 and 2005 are about 3,800 t for PFO, about 1,100 t for FTOH, and about 450 t for POSF-based substances.

	PFO	FTOH	POSF-b.		PFO	FTOH	POSF-b.
1951	8.3	0.0	0.0	1981	92.5	21.2	16.4
1952	8.3	0.0	0.0	1982	92.5	21.2	16.4
1953	8.3	0.0	0.0	1983	92.5	21.2	16.4
1954	8.3	0.0	0.0	1984	92.5	21.2	16.4
1955	8.3	0.0	0.0	1985	92.5	21.2	16.4
1956	8.3	0.0	0.0	1986	92.5	21.2	16.4
1957	8.3	0.0	0.0	1987	92.5	21.2	16.4
1958	8.3	0.0	0.0	1988	92.5	21.2	16.4
1959	8.3	0.0	0.0	1989	92.5	21.2	16.4
1960	9.6	0.0	2.5	1990	92.5	21.2	16.4
1961	9.6	0.0	2.5	1991	92.5	21.2	16.4
1962	9.6	0.0	2.5	1992	92.5	21.2	16.4
1963	9.6	0.0	2.5	1993	92.5	21.2	16.4
1964	9.6	0.0	2.5	1994	92.5	21.2	16.4
1965	35.7	0.0	2.5	1995	167.8	22.6	24.6
1966	35.7	0.0	2.5	1996	167.8	24.7	24.6
1967	35.7	0.0	2.5	1997	167.8	25.5	24.6
1968	35.7	0.0	2.5	1998	167.8	26.9	24.6
1969	35.7	0.0	2.5	1999	230.7	29.7	24.6
1970	35.7	0.0	2.5	2000	231.7	60.1	24.6
1971	35.7	0.0	2.5	2001	160.6	70.7	7.7
1972	35.7	0.0	2.5	2002	149.3	77.8	1.1
1973	35.7	0.0	2.5	2003	139.2	99.0	0.5
1974	35.7	7.1	2.5	2004	124.2	127.3	0.3
1975	32.1	7.1	2.5	2005	53.7	155.6	0.1
1976	32.1	7.1	2.5	2006	26.9	77.8	0.1
1977	32.1	7.1	2.5	2007	13.4	38.9	0.0
1978	32.1	7.1	2.5	2008	6.7	19.4	0.0
1979	32.1	7.1	2.5	2009	3.4	9.7	0.0
1980	92.5	21.2	16.4	2010	1.7	4.9	0.0

9.2.6 Distributions of Input Parameters for Uncertainty Calculations – Figure Showing Parameters that Contribute the most to Variance of PFO Deposition

Table 9.26: Distribution types and parameters for Monte Carlo Simulations. μ and σ stand for the mean and standard deviation in a normal distribution, μ and GSD for geometric mean and geometric standard deviation in a log-normal distribution, (min – mode – max) for the minimal value, most probable value (mode), and maximal value in a triangular distribution, and (min-max) stands for the minimal and maximal value in a uniform distribution.

half-lives FTOH		
k_{air}'(FTOH) (cm^3/d/molecule)	log-normal	$\mu=-9.24\times10^{-8}$, GSD=1.0
k_{air}'(FTAL) (cm^3/d/ molecule)	log-normal	$\mu=-2.89\times10^{-7}$, GSD=1.0
k_{air}'(PFAL) (cm^3/d/ molecule)	log-normal	$\mu=-4.91\times10^{-8}$, GSD=1.0
half-lives POSF		
k_{air}'(xFOSE) (cm^3/d/ molecule)	log-normal	$\mu=-5\times10^{-7}$, GSD=1.5
k_{air}'(xFOSA) (cm^3/d/ molecule)	log-normal	$\mu=-3.23\times10^{-8}$, GSD=1.5
k_{air}'(INT) (cm^3/d/ molecule)	log-normal	$\mu=-3.23\times10^{-8}$, GSD=2.0
degradation yield		
PFO yield from precursor degradation (-)	triangular	(min/mode/max) = (0.03/0.05/0.1)
partitioning FTOH		
logK_{OC} (FTOH) (–)	normal	μ=5.48, σ=0.75
logK_{OC} (FTAL) (–)	normal	μ=5.48, σ=0.75
logK_{OC} (PFAL) (–)	normal	μ=5.48, σ=0.75
logK_{AW} (FTOH) (–)	normal	μ=0.58, σ=0.75
logK_{AW} (FTAL) (–)	normal	μ=0.58, σ=0.75
logK_{AW} (PFAL) (–)	normal	μ=0.58, σ=0.75
partitioning POSF		
logK_{OC} (xFOSE) (–)	normal	μ=5.48, σ=0.75
logK_{OC} (xFOSA) (–)	normal	μ=5. 48, σ=0.75
logK_{OC} (INT) (–)	normal	μ=5. 48, σ=1.5
logK_{AW} (xFOSE) (–)	normal	μ=–1.0, σ=0.75
logK_{AW} (xFOSA) (–)	normal	μ=–1.0, σ=0.75
logK_{AW} (INT) (–)	normal	μ=–0.5, σ=1.5
partitioning PFO		
logK_{OC} (PFO) (–)	normal	μ=1.54, σ=0.75
logK_{AW} (PFO) (–)	normal	μ=–8.0, σ=0.75

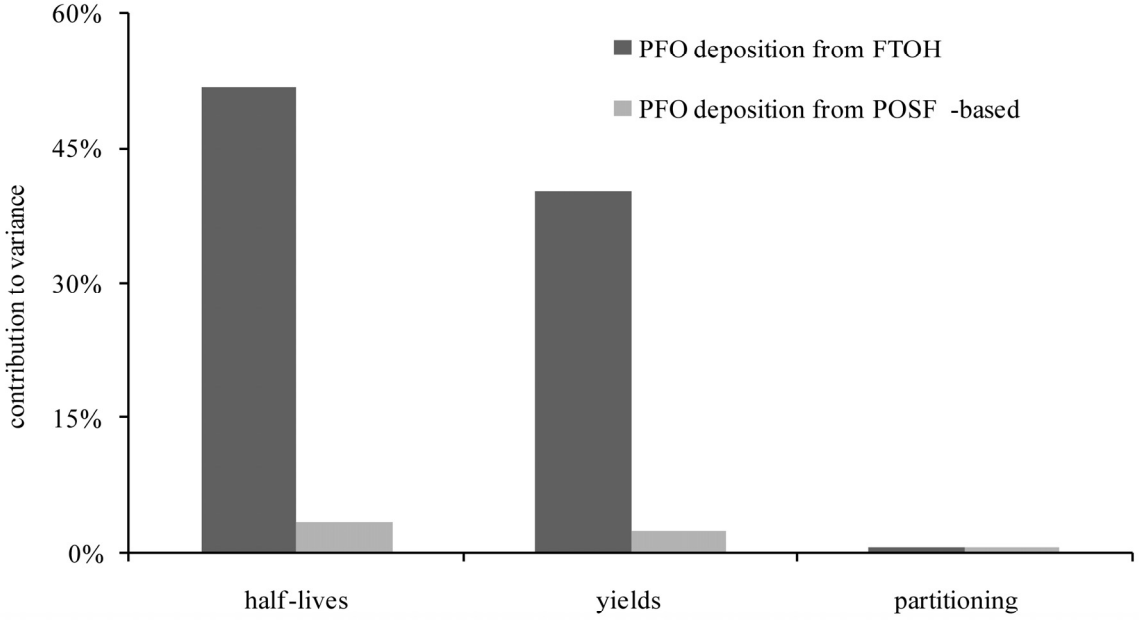

Figure 9.2: Parameter groups contributing the most to deposition of PFO.

9.2.7 Comparison of Levels and Fluxes of PFO from Direct Emissions and from Degradation of Precursor Substances

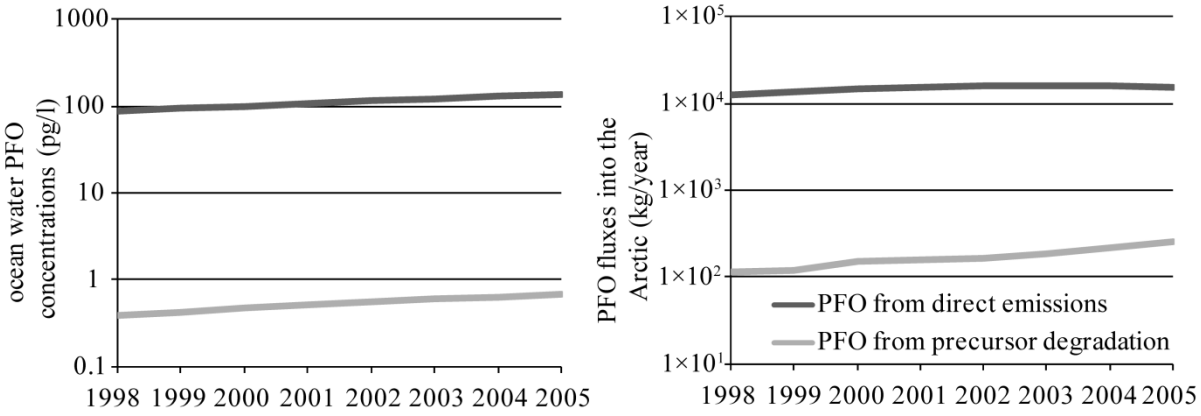

Figure 9.3: PFO concentrations in Arctic Ocean water and fluxes to the Arctic from direct emissions and precursor degradation.

9.3 Supporting Information for Chapter 5: *Modeling the Environmental Fate of Polybrominated Diphenyl Ethers (PBDEs): the Importance of Photolysis for the Formation of Lighter PBDEs*

9.3.1 Degradation Rate Constants

Photolysis rate constants for different PBDE congeners in atmosphere have been measured by Raff and Hites (2007). We have amended their data with additional measurements in various media. Photolysis rate constants in different media differ strongly, because of the properties of these media (light penetration depth, diffusion properties, etc.). To extrapolate photolysis rate constants in the gas phase and on aerosols, only measurements in organic solvents (or silica gel) are suited. Such measurements are scarce for congeners other than deca-BDE. It has frequently been found that the logarithm of photolysis rate constants (or atmospheric lifetimes due to photolysis) correlates linearly with the number of bromine atoms of different PBDE homologues (da Rosa et al., 2003, Eriksson et al., 2004, Palm et al., 2004, Raff and Hites, 2007). The slope of this regression is not expected to differ between different media, because it is determined only by the overlap of the solar spectrum with the absorption spectrum of the PBDE homologues (da Rosa et al., 2003, Palm et al., 2004). Therefore, we

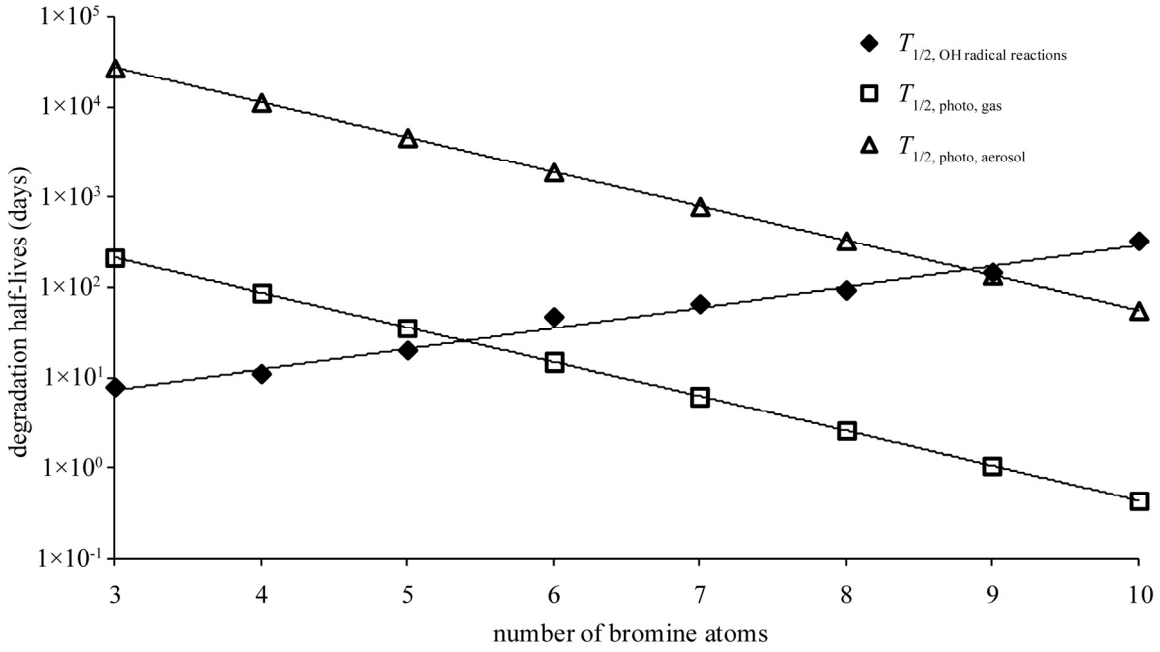

Figure 9.4: Comparison of atmospheric degradation half-lives in the northern temperate zone due to OH radical reactions, direct photolysis in the gas-phase, and direct photolysis in the particle-bound phase for different PBDE homologues.

have used ref. (da Rosa et al., 2003, Peterman et al., 2003, Bezares-Cruz et al., 2004, Eriksson et al., 2004, Raff and Hites, 2006) to calculate the slope of the logarithm of PBDE photolysis constants as a function of their number of bromine atoms, and ref. (da Rosa et al., 2003, Bezares-Cruz et al., 2004, Eriksson et al., 2004, Soderstrom et al., 2004, Raff and Hites, 2007) (which only contain measurements in organic solvents or silica gel) to extrapolate the photolysis rate constant of deca-BDE. Based on these data, photolysis rate constants for all PBDE homologues were calculated for organic solvents, and extrapolated to degradation rate constants in the gas phase and on aerosols, as described in the main text. OH radical reaction rates are also calculated, based on predicted values by the AOPWin software (U.S. Environmental Protection Agency, 2004). Photolysis rate constants and OH radical reactions (that occur only in the gas phase) are compared in Figure 9.4 and Table 9.27. Degradation rate constants in surface compartments are calculated based on BioWin (U.S. Environmental Protection Agency, 2004) and an estimation procedure by Arnot et al. (2005). Table 9.27 gives an overview over all degradation rate constants.

9.3.1.1 Summary on Degradation Rate Constants

Table 9.27: Half-lives and corresponding degradation rate constants for PBDE homologues in different media. The photolysis half-lives are representative of photolysis in the gas-phase. Degradation in the particle-bound phase is 124.8 times slower than in the gas-phase (as described in the main text).

	k_{soil} (d^{-1})	$T_{1/2,soil}$ (d)	k_{wat} (d^{-1})	$T_{1/2,wat}$ (d)	k_{OH} (cm^3/d/OH)	$T_{1/2,OH}$ (d)	$k_{photo,gas}$ (m^2/d/kW)	$T_{1/2,photo,gas}$ (d)
tri-BDE	3.32×10^{-3}	209	6.64×10^{-3}	104	1.22×10^{-7}	7.6	8.43×10^{-3}	207
tetra-BDE	1.80×10^{-3}	385	3.61×10^{-3}	192	8.67×10^{-8}	11	2.04×10^{-2}	86
penta-BDE	9.80×10^{-4}	707	1.96×10^{-3}	354	4.75×10^{-8}	19	4.95×10^{-2}	35
hexa-BDE	5.30×10^{-4}	1308	1.06×10^{-3}	654	2.00×10^{-8}	46	1.20×10^{-1}	15
hepta-BDE	3.94×10^{-4}	1759	7.88×10^{-4}	880	1.44×10^{-8}	64	2.90×10^{-1}	6.0
octa-BDE	3.24×10^{-4}	2139	6.49×10^{-4}	1068	1.02×10^{-8}	91	7.03×10^{-1}	2.5
nona-BDE	2.68×10^{-4}	2586	5.35×10^{-4}	1296	6.53×10^{-9}	142	1.70	1.0
deca-BDE	2.19×10^{-4}	3165	4.38×10^{-4}	1583	2.91×10^{-9}	318	4.13	0.42

9.3.2 Debromination Yields

Table 9.28: Debromination yields measured in different studies.

debromination yield (per step)	for debromination from	measured in	reference / note
85%	deca to nona	methanol/water	minimal yield, see text in Eriksson et al. (2004)
40%	deca to nona	toluene	UV-AB and UV-ABC light (Olsman et al., 2006)
100%	deca to octa	hexane	from figure 7 in Bezares-Cruz et al. (2004), corrected for mass balance > 1
75%	deca to hepta	hexane	from figure 4 in Watanabe and Tatsukawa (1987)
70%	deca to hepta	kaolinit, montmorillonite	from figure 3 in Ahn et al. (2006), only few deca had reacted, high variation in the measurements
90%	deca to hepta	toluene	from figure 2 in da Rosa et al. (2003)
90%	deca to hexa	silica gel	from figure 2 in Soderstrom et al. (2004)
85%	hexa to penta	polymethyl-siloxane fibers	minimal yield, table 3 in Sanchez-Prado et al. (2005)
50%	hexa to penta	distilled water	minimal yield, see text in Rayne et al. (2006)
20%	hexa to penta	acetonitrile	minimal yield, see text in Rayne et al. (2006)
10%	hexa to penta	THF	see text in Zetzsch et al. (2004)
75%	penta to tetra	polymethyl-siloxane fibers	minimal yields, table 3 in Sanchez-Prado et al. (2005)
80%	penta to di	THF	from figure 1 in Zetzsch et al. (2004)
100%	tetra to di	THF	from figure 2 in Palm et al. (2004)
69%	**average**		

As mentioned in the main text, the debromination yield of photolysis was set to 80% for each degradation step for deca- to hexa-BDE homologues, and 50% for lower brominated PBDEs (based on the data from the table above). Debromination yields for lighter homologues are less certain than for the heavier ones. Therefore, we have calculated an alternative scenario "reduced debromination" with a debromination yield for penta- and tetra-BDE of only 10%. In the "reduced debromination" scenario, the rate of tetra- to tri-BDE in air increases to 4.4 (2.6 in the base scenario). In field data (Jaward et al., 2004b, Lee et al., 2004, Jaward et al., 2005) the ratio of tetra- to tri-BDE was found to be 1.0, closer to the base scenario. Furthermore, the share of tri-BDE of the total PBDEs (without the deca-BDE congener) in the "reduced debromination" scenario is 9% (15% in the standard scenario), as compared with >20% in field data (Lee et al., 2004). In another study (Chen et al., 2006), the share of BDE-28 (one of the dominant tri-BDEs) was more than 10% of the total PBDEs (without the nona- and octa-BDE congeners). All these data indicate that the "reduced debromination" scenario is less suited to match the field data.

Furthermore, ter Schure et al. (2004), who detected BDE-17 far away from sources, but not close to urbanized areas (Agrell et al., 2004, Butt et al., 2004), suggest that "it is likely that

this compound is a breakdown product from atmospheric debromination processes", which also suggests that debromination plays an important role for lighter PBDEs.

Finally, other degradation products of PBDEs such as polybrominated dibenzo dioxins and -furans (Watanabe and Tatsukawa, 1987), monobromo-polychlorinated dibenzo dioxins and -furans (Hayakawa et al., 2004), hydroxilated PBDEs (Ueno et al., 2008), and polybrominated 2-hydroxybiphenyls (Rayne et al., 2006) have been measured in small concentrations or detected during degradation experiments. The assumptions on debromination rates of PBDEs that we have used in our standard scenario do not exclude the formation of small amounts of the above mentioned substances. In summary, we believe that it is likely that debromination occurs in significant amounts for the lower brominated congeners, too.

9.3.3 Light Intensity in the CliMoChem Model

To include direct photolysis in the CliMoChem model, solar light intensity had to be implemented into the model. Therefore, spatially and temporally resolved data from the "International Satellites for Ionosphere Studies" project was used. The data has been published in Lohmann et al. (2006b). This high-resolution data takes into account seasonal and zonal variations in day length, seasonal and zonal variations in light intensity due to the angle of the incoming sunlight, and light extinction by clouds and aerosols.

Based on measured photolysis reaction rate constants (k_{photo} (d^{-1})), pseudo second order reaction rate constants k'_{photo} ($m^2/d/kW$) were derived by dividing the reaction rate constants for the gas phase and the particle bound phase by the light intensity under which the initial photodissociation experiments took place (~ $0.85 kW/m^2$). In the model, this second order reaction rate constant is multiplied by the light intensity.

9.3.4 PBDE Emission Estimation

We have created a mass-flux scheme to estimate the temporal evolution of PBDE emissions into the different environmental compartments of the latitudinal zones in the CliMoChem model. Emissions of PBDE homologues are estimated in two steps: in a first step the produced amount of the different PBDE homologues is estimated following the method suggested by Prevedouros et al. (2004). In a second step the mass fluxes of the different PBDE homologues in the production, use, and waste-management phases are simulated, and emissions into the environment are estimated, using the same method as Morf et al. (2007)

for Switzerland, adapted to the whole globe. Whereas production of PBDEs is found almost solely in industrialized countries (emissions from the production phase thus occur mainly to the Northern temperate zone), emissions from the use and waste-management phase occur throughout the world. Three groups of countries were established based on their score in the human development index (United Nations, 2006), namely industrialized countries, countries with economies in transition, and developing countries, see Table 9.29. Details on this method have been described by Soltermann (2007). Given that waste-management techniques vary strongly with the degree of economic development of a country, the emissions from the use and waste management phases are calculated separately for the three groups of countries. We assume that the PBDE use per person is six times higher in industrialized countries than in developing countries, and three times higher in countries in transition than in developing countries (to represent the influence of stricter fire regulation and higher consumption of developed industries).

Table 9.29: Population density of three groups of countries in the different latitudinal zones of CliMoChem. PBDE emissions are assigned to the different zones according to population density. Units: %.

	industrialized countries	countries in transition	developing countries
zone 1 (72° N to 90° N)	0	0	0
zone 2 (54° N to 72° N)	2	10	0
zone 3 (36° N to 54° N)	45	31	4
zone 4 (18° N to 36° N)	50	15	49
zone 5 (0° to 18° N)	0	24	31
zone 6 (18° S to 0°)	0	12	13
zone 7 (36° S to 18° S)	2	8	3
zone 8 (54° S to 36° S)	1	0	0

9.3.4.1 PBDE Production

According to the method suggested by Prevedouros et al. (2004), the production of PBDEs can be estimated in three steps: based on bromine production figures, the production volume of brominated flame retardants can be estimated. Then, the amount of PBDE production as a subgroup of all brominated flame retardants can be estimated, and finally the percentage of the different commercial PBDE mixtures is estimated (see Table 9.30). Emissions from PBDE production are assumed to occur only in the industrialized countries, where they are distributed among the CliMoChem zones according to population density (Table 9.29).

Table 9.30: Estimated PBDE consumption worldwide (in tonnes). Bold values are derived from literature, other values are linear interpolations of literature values.

	PBDE-production			share of different PBDE - mixtures		
year	world bromine production (t/y)[1]	BFR production / bromine production (%)[1]	PBDE production / BFR production (%)	deca-BDE mixture (%)	octa-BDE mixture (%)	penta-BDE mixture (%)
1970	**210000**	**1.0**	1.0	75.0	15.0	10.0
1971	**219000**	**1.0**	1.0	75.0	15.0	10.0
1972	**237000**	**1.0**	2.0	75.0	15.0	10.0
1973	**278000**	**1.0**	3.0	75.0	15.0	10.0
1974	**292000**	**1.0**	4.0	75.0	15.0	10.0
1975	**278000**	**1.0**	5.0	75.0	15.0	10.0
1976	**297000**	**1.0**	6.0	75.0	15.0	10.0
1977	**307000**	**1.0**	7.0	75.0	15.0	10.0
1978	**309000**	**1.0**	8.0	75.0	15.0	10.0
1979	**346000**	**1.0**	9.0	75.0	15.0	10.0
1980	**295000**	2.9	10.0	75.0	15.0	10.0
1981	**353000**	4.8	11.0	75.0	15.0	10.0
1982	**381000**	6.7	12.0	75.0	15.0	10.0
1983	**363000**	8.6	13.0	75.0	15.0	10.0
1984	**388000**	10.5	14.0	75.0	15.0	10.0
1985	**379000**	12.4	15.0	75.0	15.0	10.0
1986	**371000**	14.3	16.0	75.0	15.0	10.0
1987	**384000**	16.2	17.0	75.0	15.0	10.0
1988	**405000**	18.1	18.0	75.0	15.0	10.0
1989	**420000**	20.0	19.0	75.0	15.0	10.0
1990	**440000**	21.9	20.0	75.0	15.0	10.0
1991	**400000**	23.8	21.0	75.0	15.0	10.0
1992	**370000**	25.7	22.0	75.0	15.0	10.0
1993	**390000**	27.6	23.0	75.0	15.0	10.0
1994	**410000**	29.5	24.0	75.0	**15.0**[2]	**10.0**[2]
1995	**430000**	31.4	25.0	76.2	13.7	10.1
1996	**450000**	33.3	**26.0**[3]	77.3	12.4	10.3
1997	**470000**	35.2	21.0	78.5	11.1	10.4
1998	**510000**	37.1	16.0	79.6	9.8	10.6
1999	**530000**	**39.0**	**11.0**[4]	80.8	8.5	10.7
2000	**542000**	40.0	11.0	81.9	7.2	10.9
2001	**540000**	**41.0**	11.0	83.0	**6.0**[5]	**11.0**[5]
2002	540000	43.3	11.0	83.0	6.0	11.0
2003	550000	45.5	11.0	83.0	6.0	11.0
2004	560000	47.8	11.0	83.0	6.0	11.0
2005	580000	50.0	11.0	83.0	6.0	11.0

[1] data from Prevedouros et al. (2004), updated by Morf et al. (2007)
[2] data from Law et al. (2006)
[3] data from Frost et al. (1997) cited in (Danish Environmental Protection Agency, 1999)
[4] data from IAL Consultants (1999), cited in (Danish Environmental Protection Agency, 1999)
[5] data from chapter 4 of Paasivirta and Asplund (2000)

Table 9.31: Homologue composition of different commercial PBDE mixtures. Data from ref. (World Health Organization, 1994). Units: %.

	deca-BDE mixture	octa-BDE mixture	penta-BDE mixture
tri-BDE			1
tetra-BDE			34
penta-BDE			57
hexa-BDE		11	8
hepta-BDE		44	
octa-BDE		34	
nona-BDE	3	10	
deca-BDE	97	1	

9.3.4.2 Emissions from Production, Use Phase and Waste Management

PBDEs are used as flame retardants in two product groups: polymer materials (75%) and textiles (25%) (European Chemicals Bureau, 2002, European Chemicals Bureau, 2007). The emission characteristics of PBDEs from these two product groups in the use phase differ strongly. Therefore, the two product groups are modeled separately. Both product groups have an estimated lifetime of 10 years in the use phase (Sakai et al., 2006b, Morf et al., 2007). In the waste management phase, residence times in landfills were assumed to be 10 years. Transfer factors (Table 9.32) describe mass fluxes between the use phase and several pathways in the waste management phase. Emission factors from the production, use-, and waste-management phase are described in Table 9.33.

Table 9.32: Transfer factors for PBDEs between the use phase and different waste-management options. "Waste water" and "landfills" both emit waste water into waste water treatment plants. Sewage sludge from waste water treatment plants treating "waste water" is mainly used for soil amendments, whereas sewage sludge from waste water treatment plants treating water from "landfills" is not used for soil amendments in industrialized countries (see last two rows of the table).

	industria-lized coun-tries (ic)	countries in transition (ct)	developing countries (dc)	reference
use phase to open fire combustion	0.0020	0.050	0.10	ic: (Breivik et al., 2002), ct: own estimation, dc: (United Nations, 2006)
use phase to controlled incineration	0.10	0.050	0.0	ic:(Voorspoels et al., 2003), others: own estimation
use phase to landfill	0.90	0.90	0.90	ic: (Voorspoels et al., 2003), others: own estimation
waste water to waste water treatment plant	0.70	0.40	0.050	ic: (European Chemicals Bureau, 2002) and (European Chemicals Bureau, 2007), others: own estimation
landfill to waste water treatment plant	1.0	0.50	0.0	own estimation
landfill to surface water	0.0	0.50	1.0	own estimation
waste water treatment plant to surface water	0.060	0.060	-	(Rayne and Ikonomou, 2005)
waste water treatment plant to sewage sludge	0.94	0.94	-	(Rayne and Ikonomou, 2005)
sewage sludge (from waste water) to soil	0.90	1.0	-	own estimation
sewage sludge (from landfills) to soil	0.0	0.50	-	own estimation

Table 9.33: Emission factors used for different PBDE homologues

Process	compartment	Deca-BDE	Nona-BDE	Octa-BDE	Hepta-BDE	Hexa-BDE	Penta-BDE	Tetra-BDE	Tri-BDE
production	air[1]	2.4×10^{-5}	5.5×10^{-5}	5.5×10^{-5}	5.5×10^{-5}	5.5×10^{-5}	1.3×10^{-4}	1.3×10^{-4}	1.3×10^{-4}
	waste water[2]	2.8×10^{-4}	2.8×10^{-4}	2.8×10^{-4}	2.8×10^{-4}	2.8×10^{-4}	2.8×10^{-4}	2.8×10^{-4}	2.8×10^{-4}
	soil	0	0	0	0	0	0	0	0
use polymer	air[3]	3.9×10^{-8}	2.3×10^{-7}	1.4×10^{-6}	7.9×10^{-6}	4.6×10^{-5}	2.7×10^{-4}	1.6×10^{-3}	9.3×10^{-3}
	waste water[4]	5.3×10^{-7}	5.3×10^{-7}	5.3×10^{-7}	5.3×10^{-7}	5.3×10^{-7}	5.3×10^{-7}	5.3×10^{-7}	5.3×10^{-7}
	soil[4]	1.6×10^{-6}	1.6×10^{-6}	1.6×10^{-6}	1.6×10^{-6}	1.6×10^{-6}	1.6×10^{-6}	1.6×10^{-6}	1.6×10^{-6}
use textiles	air[5]	9.5×10^{-5}	1.2×10^{-4}	1.6×10^{-4}	2.0×10^{-4}	2.6×10^{-4}	3.3×10^{-4}	4.2×10^{-4}	5.4×10^{-4}
	waste water[6]	3.2×10^{-6}	3.2×10^{-6}	3.2×10^{-6}	3.2×10^{-6}	3.2×10^{-6}	0	0	0
	soil	0	0	0	0	0	0	0	0
incineration	air[7]	6.0×10^{-7}	6.0×10^{-7}	6.0×10^{-7}	6.0×10^{-7}	6.0×10^{-7}	6.0×10^{-7}	6.0×10^{-7}	6.0×10^{-7}
	waste water	0	0	0	0	0	0	0	0
	soil	0	0	0	0	0	0	0	0
open fire	air[4]	9.1×10^{-2}	9.1×10^{-2}	9.1×10^{-2}	9.1×10^{-2}	9.1×10^{-2}	9.1×10^{-2}	9.1×10^{-2}	9.1×10^{-2}
	waste water	0	0	0	0	0	0	0	0
	soil	0	0	0	0	0	0	0	0
landfill	air[8]	6.1×10^{-6}	6.1×10^{-6}	6.1×10^{-6}	6.1×10^{-6}	6.1×10^{-6}	6.1×10^{-6}	6.1×10^{-6}	6.1×10^{-6}
	waste water[9]	5.0×10^{-4}	5.0×10^{-4}	5.0×10^{-4}	5.0×10^{-4}	5.0×10^{-4}	5.0×10^{-4}	5.0×10^{-4}	5.0×10^{-4}
	soil	0	0	0	0	0	0	0	0

[1] linear regression of the logarithmic values based on the deca- and penta-BDE homologues. The emission factor for deca-BDE is the geomean from refs. Sakai et al. (2005) and European Chemicals Bureau (2002), the one for penta-BDE is taken from Alcock et al. (2003).
[2] geomean of data calculated using (European Chemicals Bureau, 2002, Sakai et al., 2005, Morf et al., 2007)
[3] linear regression of the logarithmic values based on the deca- and penta-BDE homologues. The emission factor for deca-BDE is the geomean from Sakai et al. (2006b) and European Chemicals Bureau (2002). The emission factor for penta-BDE is taken from Alcock et al. (2003) and Morf et al. (2007)
[4] data from European Chemicals Bureau (2007)
[5] linear regression of the logarithmic values based on the deca- and penta-BDE homologues. The emission factor for deca-BDE is taken from European Chemicals Bureau (2007) citing Stevens et al. (2004). The emission factor for penta-BDE is derived from Alcock et al. (2003) and Morf et al. (2007)
[6] geomean of data from Morf et al. (2007) and European Chemicals Bureau (2007)
[7] data from Sakai et al. (2006a)
[8] data from Morf et al. (2007)
[9] own estimation: polymer materials are decomposed within 20 years, 1% of the PBDE is leached upon degradation

9.3.5 Partition Coefficients

We have compiled measurements of partition coefficients and solubilities of eight PBDE congeners with different degrees of bromination. Insufficient property data measurements were found for the mono-, octa-, and nonaBDE congeners.

According to the three solubilities approach (Cole and Mackay, 2000), the solubilities in water and octanol, vapor pressure, and the partition coefficients are internally consistent if they fulfill the following three equations:

$$\log(S_A) - \log(S_W) - \log K_{AW} = 0 \quad \text{(eq. 9.14)}$$

$$\log(S_A) - \log(S_O) + \log K_{OA} = 0 \quad \text{(eq. 9.15)}$$

$$\log(S_W) - \log(S_O) + \log K_{OW} = 0 \quad \text{(eq. 9.16)}$$

The least-squares adjustment method (Schenker et al., 2005a) adjusts LDVs for internal consistency and results in a set of minimally adjusted (according to the theory of least-squares) final adjusted values (FAVs). To take into account that different LDVs may be known with different degrees of certainty, the weighted sum of squares of the adjustments is minimized. Therefore, the least-squares adjustment method requires the relative variance (RV, as a measure of the uncertainty) of the LDVs as an additional input.

A semi-quantitative method was used to estimate relative variances for substance properties of the different congeners: The relative variance was set to four (the highest degree of uncertainty) if only one measurement was available, or if several measurements differed by more than one order of magnitude. The relative variance was set to two if three or more measurements were available, and they differed by less than 0.5 orders of magnitude, or if two measurements were available differing by less than 0.25 orders of magnitude. In all other cases, the relative variance was set to three. The selected values for the relative variance (RV) are given as notes to the LDVs in the tables below.

Solubilities in water were converted from the solid state to the subcooled liquid state if literature data was given as solid state; to this end, the fugacity ratios given in (Wania and Dugani, 2003) were used. For the energies of dissolution in water (ΔU_W), the values obtained from the literature represent the inner energy for the transition from the solid to the dissolved state. The value needed in the least-squares adjustment is the inner energy for the transition from the liquid to the dissolved state. This value was calculated by subtracting the inner

energy of fusion (solid to liquid state) from the inner energy from solid to dissolved state. The inner energy of fusion was obtained from measurements by (Kuramochi et al., 2007).

Table 9.34: Measurements, LDVs and FAVs for BDE-15. The relative variance (RV) used in the least-squares adjustment are given as notes to the LDVs.

name	4,4'-dibromodiphenyl ether
formula	$C_{12}H_8Br_2O$
molecular weight (g/mol)	328

Vapor pressure (Pa)			**ΔU_{vap} (kJ/mol)**		
used values	**reference**	**note**	**used values**	**reference**	**note**
1.73×10^{-2}	(Tittlemier et al., 2002)		65.1	(Tittlemier et al., 2002)	
1.55×10^{-2}	(Watanabe, 1989)		75.5	(Wong et al., 2001)	
9.84×10^{-3}	(Wong et al., 2001)				
1.38×10^{-2}	LDV	(RV=2)	70.3	LDV	(RV=3)
1.37×10^{-2}	FAV		70.3	FAV	
rejected values	**reference**	**note**	**rejected values**	**reference**	**note**
none			none		
Water solubility (subcooled liquid, mol/m^3)			**ΔU_w (kJ/mol)**		
used values	**reference**	**note**	**used values**	**reference**	**note**
8.21×10^{-4}	(Tittlemier et al., 2002)		20.9	(Kuramochi et al., 2007)	
1.38×10^{-3}	(Kuramochi et al., 2007)				
1.06×10^{-3}	LDV	(RV=2)	20.9	LDV	(RV=4)
1.07×10^{-3}	FAV		20.9	FAV	
rejected values	**reference**	**note**	**rejected values**	**reference**	**note**
none			none		
logK_{OW} (-)			**ΔU_{OW} (kJ/mol)**		
used values	**reference**	**note**	**used values**	**reference**	**note**
5.86	(Kuramochi et al., 2007)		none		
5.03	(Watanabe, 1989)				
5.45	LDV	(RV=3)			
5.44	FAV				
rejected values	**reference**	**note**	**rejected values**	**reference**	**note**
5.55	(Tittlemier et al., 2002)	based on PCDEs and fragment const. for Br	none		
logK_{AW} (-)			**ΔU_{AW} (kJ/mol)**		
used values	**reference**	**note**	**used values**	**reference**	**note**
-2.25	(Lau et al., 2006)		none		
-2.33	(Lau et al., 2006)				
-2.29	LDV	(RV=2)			
-2.29	FAV				

rejected values	reference	note	rejected values	reference	note
-2.07	(Tittlemier et al., 2002)	calc. from vapour pres. and water solubility	none		
-2.78	(Wania and Dugani, 2003)	based on other lit. values, adjustments			
-1.83	(Lau et al., 2003)	unreliable measurement method			
logK_{OA} (-)			**ΔU_{OA} (kJ/mol)**		
used values	**reference**	**note**	**used values**	**reference**	**note**
none			none		
rejected values	**reference**	**note**	**rejected values**	**reference**	**note**
8.79	(Harner and Shoeib, 2002)	calculated from relative retention time	none		

Table 9.35: Measurements, LDVs and FAVs for BDE-28. The relative variance (RV) used in the least-squares adjustment are given as notes to the LDVs.

name	2,4,4'-tribromodiphenyl ether
formula	$C_{12}H_7Br_3O$
molecular weight (g/mol)	406.9

Vapor pressure (Pa)			**ΔU_{vap} (kJ/mol)**		
used values	**reference**	**note**	**used values**	**reference**	**note**
2.19×10^{-3}	(Tittlemier et al., 2002)		77.2	(Tittlemier et al., 2002)	
2.08×10^{-3}	(Watanabe, 1989)				
2.13×10^{-3}	LDV	(RV=2)	77.2	LDV	(RV=4)
2.11×10^{-3}	FAV		77.2	FAV	
rejected values	**reference**	**note**	**rejected values**	**reference**	**note**
1.60×10^{-3}	(Wong et al., 2001)	calculated	none		
Water solubility (subcooled liquid, mol/m^3)			**ΔU_W (kJ/mol)**		
used values	**reference**	**note**	**used values**	**reference**	**note**
4.16×10^{-4}	(Tittlemier et al., 2002)		none		
4.16×10^{-4}	LDV	(RV=4)			
4.27×10^{-4}	FAV				
rejected values	**reference**	**note**	**rejected values**	**reference**	**note**
none			none		
logK_{OW} (-)			**ΔU_{OW} (kJ/mol)**		
used values	**reference**	**note**	**used values**	**reference**	**note**
5.94	(Braekevelt et al., 2003)		none		
5.53	(Watanabe, 1989)				
5.73	LDV	(RV=3)			
5.92	FAV				
rejected values	**reference**	**note**	**rejected values**	**reference**	**note**
5.98	(Tittlemier et al., 2002)	based on values from PCDEs	none		

$\log K_{AW}$ (-)			ΔU_{AW} (kJ/mol)		
used values	**reference**	**note**	**used values**	**reference**	**note**
-2.71	(Cetin and Odabasi, 2005)		61.7	(Cetin and Odabasi, 2005)	
-2.28	(Lau et al., 2006)				
-2.43	(Lau et al., 2006)				
-2.53	LDV	(RV=2)	61.7	LDV	(RV=4)
-2.70	FAV		61.7	FAV	
rejected values	**reference**	**note**	**rejected values**	**reference**	**note**
-2.69	(Tittlemier et al., 2002)	cal. from vapour pres. and water solubility	none		
-3.11	(Wania and Dugani, 2003)	based on other lit. values, adjustments			
-2.22	(Lau et al., 2003)	unreliable measurement method			

$\log K_{OA}$ (-)			ΔU_{OA} (kJ/mol)		
used values	**reference**	**note**	**used values**	**reference**	**note**
9.50	(Harner and Shoeib, 2002)		-72.8	(Harner and Shoeib, 2002)	
9.50	LDV	(RV=4)	-72.8	LDV	(RV=4)
9.16	FAV		-72.8	FAV	
rejected values	**reference**	**note**	**rejected values**	**reference**	**note**
none			none		

Table 9.36: Measurements, LDVs and FAVs for BDE-47. The relative variance (RV) used in the least-squares adjustment are given as notes to the LDVs.

name	2,2',4,4'-tetrabromodiphenyl ether
formula	$C_{12}H_6Br_4O$
molecular weight (g/mol)	485.82

Vapor pressure (Pa)			ΔU_{vap} (kJ/mol)		
used values	**reference**	**note**	**used values**	**reference**	**note**
1.86×10^{-4}	(Tittlemier et al., 2002)		92.1	(Tittlemier et al., 2002)	
2.92×10^{-4}	(Watanabe, 1989)		89.5	(Wong et al., 2001)	
3.19×10^{-4}	(Wong et al., 2001)				
2.59×10^{-4}	LDV	(RV=2)	90.8	LDV	(RV=3)
2.40×10^{-4}	FAV		86.7	FAV	
rejected values	**reference**	**note**	**rejected values**	**reference**	**note**
8.18×10^{-5}	(Palm et al., 2002)	based on linearization of lit. data	none		

Water solubility (subcooled liquid, mol/m^3)			ΔU_W (kJ/mol)		
used values	**reference**	**note**	**used values**	**reference**	**note**
1.16×10^{-4}	(Kuramochi et al., 2007)		14.9	(Kuramochi et al., 2007)	
1.17×10^{-4}	(Tittlemier et al., 2002)				
1.17×10^{-4}	LDV	(RV=2)	14.9	LDV	(RV=4)
1.26×10^{-4}	FAV		20.4	FAV	
rejected values	**reference**	**note**	**rejected values**	**reference**	**note**
7.35×10^{-5}	(Palm et al., 2002)	based on extrapolation from other lit. data	none		
logK_{OW} (-)			**ΔU_{OW} (kJ/mol)**		
used values	**reference**	**note**	**used values**	**reference**	**note**
6.81	(Braekevelt et al., 2003)		none		
6.78	(Kuramochi et al., 2007)				
6.19	(Tomy et al., 2004)				
6.02	(Watanabe, 1989)				
6.45	LDV	(RV=3)			
6.53	FAV				
rejected values	**reference**	**note**	**rejected values**	**reference**	**note**
6.67	(Palm et al., 2002)	based on extrapolation from other lit. data	none		
7.4	(Ellinger et al., 2003)	based on correl. with PCB cong.			
6.55	(Tittlemier et al., 2002)	based on PCDEs and fragment const. for Br			
logK_{AW} (-)			**ΔU_{AW} (kJ/mol)**		
used values	**reference**	**note**	**used values**	**reference**	**note**
-3.5	(Cetin and Odabasi, 2005)		60.9	(Cetin and Odabasi, 2005)	
-2.64	(Lau et al., 2006)				
-2.59	(Lau et al., 2006)				
-3.06	LDV	(RV=3)	60.9	LDV	(RV=4)
-3.12	FAV		66.4	FAV	
rejected values	**reference**	**note**	**rejected values**	**reference**	**note**
-3.22	(Tittlemier et al., 2002)	calc. from vapour pres. and water solubility	none		
-3.35	(Wania and Dugani, 2003)	based on other lit. values, adjustments			
-1.77	(Lau et al., 2003)	unreliable measurement method			
logK_{OA} (-)			**ΔU_{OA} (kJ/mol)**		
used values	**reference**	**note**	**used values**	**reference**	**note**
10.53	(Harner and Shoeib, 2002)		-97.0	(Harner and Shoeib, 2002)	
10.53	LDV	(RV=4)	-97.0	LDV	(RV=4)
10.39	FAV		-97.0	FAV	
rejected values	**reference**	**note**	**rejected values**	**reference**	**note**
none			none		

Table 9.37: Measurements, LDVs and FAVs for BDE-99. The relative variance (RV) used in the least-squares adjustment are given as notes to the LDVs.

name	2,2',4,4',5-pentabromodiphenyl ether
formula	$C_{12}H_5Br_5O$
molecular weight (g/mol)	564.7

Vapor pressure (Pa)			**ΔU_{vap} (kJ/mol)**		
used values	**reference**	**note**	**used values**	**reference**	**note**
1.76×10^{-5}	(Tittlemier et al., 2002)		106	(Tittlemier et al., 2002)	
4.63×10^{-5}	(Watanabe, 1989)		97.8	(Wong et al., 2001)	
6.82×10^{-5}	(Wong et al., 2001)				
3.82×10^{-5}	LDV	(RV=3)	102	LDV	(RV=3)
3.92×10^{-5}	FAV		94.8	FAV	
rejected values	**reference**	**note**	**rejected values**	**reference**	**note**
7.64×10^{-6}	(Palm et al., 2002)	based on linearisation of lit. values	none		

Water solubility (subcooled liquid, mol/m^3)			**ΔU_W (kJ/mol)**		
used values	**reference**	**note**	**used values**	**reference**	**note**
1.98×10^{-5}	(Stenzel and Markley, 1997)	cited in (Wania and Dugani, 2003)	3.10	(Kuramochi et al., 2007)	
3.60×10^{-5}	(Kuramochi et al., 2007)				
7.71×10^{-5}	(Tittlemier et al., 2002)				
3.80×10^{-5}	LDV	(RV=3)	3.10	LDV	(RV=4)
3.70×10^{-5}	FAV		12.3	FAV	
rejected values	**reference**	**note**	**rejected values**	**reference**	**note**
8.40×10^{-6}	(Palm et al., 2002)	based on extrapolation from other lit. data	none		

logK_{OW} (-)			**ΔU_{OW} (kJ/mol)**		
used values	**reference**	**note**	**used values**	**reference**	**note**
7.32	(Braekevelt et al., 2003)		none		
7.39	(Kuramochi et al., 2007)				
6.53	(Tomy et al., 2004)	cited in (Wania and Dugani, 2003)			
6.72	(Watanabe, 1989)				
6.99	LDV	(RV=3)			
7.00	FAV				
rejected values	**reference**	**note**	**rejected values**	**reference**	**note**
7.42	(Palm et al., 2002)	based on extrapolation from other lit. data	none		
7.90	(Ellinger et al., 2003)	based on correlation with PCB congeners			
7.13	(Tittlemier et al., 2002)	based on PCDEs and fragment const. for Br			

$\log K_{AW}$ (-)			ΔU_{AW} (kJ/mol)		
used values	**reference**	**note**	**used values**	**reference**	**note**
-3.62	(Cetin and Odabasi, 2005)		73.3	(Cetin and Odabasi, 2005)	
-2.92	(Lau et al., 2006)				
-3.20	(Lau et al., 2006)				
-3.34	LDV	(RV=3)	73.3	LDV	(RV=4)
-3.37	FAV		82.5	FAV	
rejected values	**reference**	**note**	**rejected values**	**reference**	**note**
-4.03	(Tittlemier et al., 2002)	calc. from vapour pres. and water solubility	none		
-3.67	(Wania and Dugani, 2003)	based on other lit. values, adjustments			
$\log K_{OA}$ (-)			ΔU_{OA} (kJ/mol)		
used values	**reference**	**note**	**used values**	**reference**	**note**
11.31	(Harner and Shoeib, 2002)		-91.1	(Harner and Shoeib, 2002)	
11.31	LDV	(RV=4)	-91.1	LDV	(RV=4)
11.29	FAV		-91.1	FAV	
rejected values	**reference**	**note**	**rejected values**	**reference**	**note**
none			none		

Table 9.38: Measurements, LDVs and FAVs for BDE-100. The relative variance (RV) used in the least-squares adjustment are given as notes to the LDVs.

name	2,2',4,4',6-pentabromodiphenyl ether
formula	$C_{12}H_5Br_5O$
molecular weight (g/mol)	564.7

Vapor pressure (Pa)			ΔU_{vap} (kJ/mol)		
used values	**reference**	**note**	**used values**	**reference**	**note**
2.86×10^{-5}	(Tittlemier et al., 2002)		99.5	(Tittlemier et al., 2002)	
4.63×10^{-5}	(Watanabe, 1989)				
3.64×10^{-5}	LDV	(RV=2)	99.5	LDV	(RV=4)
6.01×10^{-5}	FAV		99.5	FAV	
rejected values	**reference**	**note**	**rejected values**	**reference**	**note**
none			none		
Water solubility (subcooled liquid, mol/m^3)			ΔU_W (kJ/mol)		
used values	**reference**	**note**	**used values**	**reference**	**note**
3.96×10^{-4}	(Tittlemier et al., 2002)		none		
3.96×10^{-4}	LDV	(RV=4)			
1.45×10^{-4}	FAV				
rejected values	**reference**	**note**	**rejected values**	**reference**	**note**
none			none		

$\log K_{OW}$ (-)			ΔU_{OW} (kJ/mol)		
used values	**reference**	**note**	**used values**	**reference**	**note**
7.24	(Braekevelt et al., 2003)		none		
6.30	(Tomy et al., 2004)	cited in (Wania and Dugani, 2003)			
6.72	(Watanabe, 1989)				
6.75	LDV	(RV=3)			
6.68	FAV				
rejected values	**reference**	**note**	**rejected values**	**reference**	**note**
7.80	(Ellinger et al., 2003)	based on correl. with PCB cong.	none		
6.86	(Tittlemier et al., 2002)	based on PCDEs and fragment const. for Br			

$\log K_{AW}$ (-)			ΔU_{AW} (kJ/mol)		
used values	**reference**	**note**	**used values**	**reference**	**note**
-4.03	(Cetin and Odabasi, 2005)		56.6	(Cetin and Odabasi, 2005)	
-2.91	(Lau et al., 2006)				
-2.93	(Lau et al., 2006)				
-3.47	LDV	(RV=4)	56.6	LDV	(RV=4)
-3.78	FAV		56.6	FAV	
rejected values	**reference**	**note**	**rejected values**	**reference**	**note**
-4.56	(Tittlemier et al., 2002)	calc. from vapour pres. and water solubility	none		
-3.81	(Wania and Dugani, 2003)	based on other lit. values, adjustments			

$\log K_{OA}$ (-)			ΔU_{OA} (kJ/mol)		
used values	**reference**	**note**	**used values**	**reference**	**note**
11.13	(Harner and Shoeib, 2002)		-105	(Harner and Shoeib, 2002)	
11.13	LDV	(RV=4)	-105	LDV	(RV=4)
11.26	FAV		-105	FAV	
rejected values	**reference**	**note**	**rejected values**	**reference**	**note**
none			none		

Table 9.39: Measurements, LDVs and FAVs for BDE-153. The relative variance (RV) used in the least-squares adjustment are given as notes to the LDVs.

name	2,2',4,4',5,5'-hexabromodiphenyl ether
formula	$C_{12}H_4Br_6O$
molecular weight (g/mol)	643.6

Vapor pressure (Pa)			**ΔU_{vap} (kJ/mol)**		
used values	**reference**	**note**	**used values**	**reference**	**note**
2.09×10^{-6}	(Tittlemier et al., 2002)		108	(Tittlemier et al., 2002)	
6.31×10^{-6}	(Watanabe, 1989)		105	(Wong et al., 2001)	
8.43×10^{-6}	(Wong et al., 2001)				
4.81×10^{-6}	LDV	(RV=3)	106	LDV	(RV=3)
4.33×10^{-6}	FAV		97.2	FAV	
rejected values	**reference**	**note**	**rejected values**	**reference**	**note**
none			none		
Water solubility (subcooled liquid, mol/m^3)			**ΔU_W (kJ/mol)**		
used values	**reference**	**note**	**used values**	**reference**	**note**
1.74×10^{-6}	(Kuramochi et al., 2007)		8.40	(Kuramochi et al., 2007)	
3.00×10^{-5}	(Tittlemier et al., 2002)				
7.22×10^{-6}	LDV	(RV=4)	8.40	LDV	(RV=4)
8.29×10^{-6}	FAV		20.5	FAV	
rejected values	**reference**	**note**	**rejected values**	**reference**	**note**
none			none		
logK_{OW} (-)			**ΔU_{OW} (kJ/mol)**		
used values	**reference**	**note**	**used values**	**reference**	**note**
7.90	(Braekevelt et al., 2003)		none		
8.05	(Kuramochi et al., 2007)				
6.87	(Tomy et al., 2004)	cited in (Wania and Dugani, 2003)			
7.39	(Watanabe, 1989)				
7.55	LDV	(RV=4)			
7.36	FAV				
rejected values	**reference**	**note**	**rejected values**	**reference**	**note**
8.3	(Ellinger et al., 2003)	based on correlation with PCB congeners	none		
7.9	(Tittlemier et al., 2002)	based on PCDEs and fragment const. for Br			

$\log K_{AW}$ (-)			ΔU_{AW} (kJ/mol)		
used values	**reference**	**note**	**used values**	**reference**	**note**
-4.00	(Cetin and Odabasi, 2005)		64.6	(Cetin and Odabasi, 2005)	
-4.00	LDV	(RV=4)	64.6	LDV	(RV=4)
-3.68	FAV		76.7	FAV	
rejected values	**reference**	**note**	**rejected values**	**reference**	**note**
-4.57	(Tittlemier et al., 2002)	calc. from vapour pres. and water solubility	none		
-3.86	(Wania and Dugani, 2003)	based on other lit. values, adjustments			
$\log K_{OA}$ (-)			ΔU_{OA} (kJ/mol)		
used values	**reference**	**note**	**used values**	**reference**	**note**
11.82	(Harner and Shoeib, 2002)		-98.2	(Harner and Shoeib, 2002)	
11.82	LDV	(RV=4)	-98.2	LDV	(RV=4)
12.08	FAV		-98.2	FAV	
rejected values	**reference**	**note**	**rejected values**	**reference**	**note**
none			none		

Table 9.40: Measurements, LDVs and FAVs for BDE-183. The relative variance (RV) used in the least-squares adjustment are given as notes to the LDVs.

name	2,2',3,4,4',5,6-heptabromodiphenyl ether
formula	$C_{12}H_3Br_7O$
molecular weight (g/mol)	722.5

Vapor pressure (Pa)			ΔU_{vap} (kJ/mol)		
used values	**reference**	**note**	**used values**	**reference**	**note**
4.68×10^{-7}	(Tittlemier et al., 2002)		116	(Tittlemier et al., 2002)	
4.68×10^{-7}	LDV	(RV=4)	116	LDV	(RV=4)
1.87×10^{-6}	FAV		116	FAV	
rejected values	**reference**	**note**	**rejected values**	**reference**	**note**
none			none		
Water solubility (subcooled liquid, mol/m^3)			ΔU_W (kJ/mol)		
used values	**reference**	**note**	**used values**	**reference**	**note**
5.81×10^{-5}	(Tittlemier et al., 2002)		none		
5.81×10^{-5}	LDV	(RV=4)			
1.45×10^{-5}	FAV				
rejected values	**reference**	**note**	**rejected values**	**reference**	**note**
none			none		

$\log K_{OW}$ (-)			ΔU_{OW} (kJ/mol)		
used values	**reference**	**note**	**used values**	**reference**	**note**
8.27	(Braekevelt et al., 2003)		none		
7.14	(Tomy et al., 2004)	cited in (Wania and Dugani, 2003)			
7.71	LDV	(RV=4)			
7.26	FAV				
rejected values	**reference**	**note**	**rejected values**	**reference**	**note**
none			none		
$\log K_{AW}$ (-)			ΔU_{AW} (kJ/mol)		
used values	**reference**	**note**	**used values**	**reference**	**note**
none			none		
rejected values	**reference**	**note**	**rejected values**	**reference**	**note**
-5.52	(Tittlemier et al., 2002)	calculated from vapour pressure and water solubility	none		
-4.27	(Cetin and Odabasi, 2005)	calculated value			
$\log K_{OA}$ (-)			ΔU_{OA} (kJ/mol)		
used values	**reference**	**note**	**used values**	**reference**	**note**
11.96	(Harner and Shoeib, 2002)		-89.5	(Harner and Shoeib, 2002)	
11.96	LDV	(RV=4)	-89.5	LDV	(RV=4)
12.56	FAV		-89.5	FAV	
rejected values	**reference**	**note**	**rejected values**	**reference**	**note**
none			none		

Table 9.41: Measurements, LDVs and FAVs for BDE-209. The relative variance (RV) used in the least-squares adjustment are given as notes to the LDVs.

name	decabromodiphenyl ether
formula	$C_{12}Br_{10}O$
molecular weight (g/mol)	959.2

Vapor pressure (Pa)			ΔU_{vap} (kJ/mol)		
used values	**reference**	**note**	**used values**	**reference**	**note**
none			145	(Tittlemier et al., 2002), (Wong et al., 2001)	linear regression of the values from (Tittlemier et al., 2002) and (Wong et al., 2001) versus bromine number
			145	LDV	(RV=4)
			145	FAV	

rejected values	reference	note	rejected values	reference	note
4.63×10^{-6}	(Norris et al., 1973)	measured the commercial product	none		
2.95×10^{-9}	(Wong et al., 2001)	based on linearisation of literature values			
5.42×10^{-11}	(Palm et al., 2002)	based on linearisation of literature values			

Water solubility (subcooled liquid, mol/m^3)			ΔU_W (kJ/mol)		
used values	reference	note	used values	reference	note
2.33×10^{-6}	(Wania and Dugani, 2003)		none		
2.33×10^{-6}	LDV	(RV=4)			
2.33×10^{-6}	FAV				
rejected values	reference	note	rejected values	reference	note
7.57×10^{-9}	(Palm et al., 2002)	based on extrapolation from other literatur data	none		
1.34×10^{-2}	(Norris et al., 1973)	measured the commercial product			

logK_{OW} (-)			ΔU_{OW} (kJ/mol)		
used values	reference	note	used values	reference	note
9.97	(Watanabe, 1989)		none		
9.97	LDV	(RV=4)			
9.97	FAV				
rejected values	reference	note	rejected values	reference	note
11.15	(Palm et al., 2002)	based on extrapolation from other literatur data	none		
9.30	(Ellinger et al., 2003)	based on correlation with PCB congeners			
8.70	(Wurl et al., 2006a)	calculated			

logK_{AW} (-)			ΔU_{AW} (kJ/mol)		
used values	reference	note	used values	reference	note
-4.81	(Cetin and Odabasi, 2005)		65.7	(Cetin and Odabasi, 2005)	
-4.81	LDV	(RV=4)	65.7	LDV	(RV=4)
-4.81	FAV		65.7	FAV	
rejected values	reference	note	rejected values	reference	note
none			none		

$\log K_{OA}$ (-)			ΔU_{OA} (kJ/mol)		
used values	**reference**	**note**	**used values**	**reference**	**note**
none			none		
rejected values	**reference**	**note**	**rejected values**	**reference**	**note**
14.40	(Harner and Shoeib, 2002)	extrapol. from other cong.	none		

Table 9.42: Summary table of all FAVs (final adjusted values). Values in italic have been deduced by using the three equations of the three solubility approach (eq. 9.14 – eq. 9.16 above), because an insufficient number of properties was available to perform an adjustment.

congener	Vapor pressure (Pa)	Water solubility (subcooled liquid, mol/m³)	$\log K_{AW}$ (-)	$\log K_{OW}$ (-)	$\log K_{OA}$ (-)	ΔU_{vap} (kJ/mol)	ΔU_W (kJ/mol)	ΔU_{AW} (kJ/mol)	ΔU_{OA} (kJ/mol)
BDE-15	1.37×10^{-2}	1.07×10^{-3}	*-2.29*	5.44	*8.09*	*70*	*21*	*49*	
BDE-28	2.11×10^{-3}	4.27×10^{-4}	-2.70	5.92	9.16	*77*	16	*62*	*-73*
BDE-47	2.40×10^{-4}	1.26×10^{-4}	-3.12	6.53	10.4	87	20	66	*-97*
BDE-99	3.92×10^{-5}	3.70×10^{-5}	-3.37	7.00	11.3	95	12	82	*-91*
BDE-100	6.01×10^{-5}	1.45×10^{-4}	-3.78	6.68	11.3	*100*	43	*57*	*-105*
BDE-153	4.33×10^{-6}	8.29×10^{-6}	-3.68	7.36	12.1	97	21	77	*-98*
BDE-183	1.87×10^{-6}	1.45×10^{-5}	*-4.28*	7.26	12.6	*116*			*-90*
BDE-209	*9.03×10^{-8}*	*2.33×10^{-6}*	*-4.81*	*9.97*	*16.8*	*145*	80	*66*	

Based on the FAVs for PBDE congeners, substance properties were estimated for the different PBDE homologues. For the penta-BDE homologue, the average between BDE-99 and BDE-100 was taken, for the octa- and nona-BDE homologues, substance properties were estimated based on the substance properties of other PBDE homologues: for the solubilities and partition coefficients, a linear regression was determined to calculate substance properties of octa- and nona-BDE as a function of the number of bromine atoms. In the case of energies of phase-change, less data is available, and the correlations between measured energies of phase change and the number of bromines in a homologue group is not always very good. Therefore, linear regression was only performed for the energy of vaporization (ΔU_{vap}). Instead of a linear regression, the geometric mean of the FAVs was taken for ΔU_{AW} and ΔU_{OA} (no strong correlation could be found for the number of bromine atoms and ΔU_{AW} or ΔU_{OA}). Finally, for ΔU_W, ΔU_O, and ΔU_{OW}, missing values were calculated with the equations given by the three solubilities approach (eq. 9.14 – eq. 9.16, as discussed above).

Table 9.43: Property data for PBDE homologues. Values in italic have been derived from a linear regression based on other PBDE homologues.

PBDE homologues	P_A (Pa)	S_W (mol/m^3)	S_O (mol/m^3)	logK_{AW} (–)	logK_{OW} (–)	logK_{OA} (–)
di-BDE	1.37×10^{-2}	1.07×10^{-3}	6.76×10^{2}	-2.29	5.44	8.09
tri-BDE	2.11×10^{-3}	4.27×10^{-4}	1.23×10^{3}	-2.70	5.92	9.16
tetra-BDE	2.40×10^{-4}	1.26×10^{-4}	2.40×10^{3}	-3.12	6.53	10.3
penta-BDE	4.85×10^{-5}	7.53×10^{-5}	3.72×10^{3}	-3.58	6.84	11.3
hexa-BDE	4.33×10^{-6}	8.29×10^{-6}	2.14×10^{3}	-3.68	7.36	12.1
hepta-BDE	1.88×10^{-6}	1.45×10^{-5}	2.75×10^{3}	-4.28	7.26	12.6
octa-BDE	*6.76×10^{-7}*	*6.31×10^{-6}*	*5.37×10^{4}*	*-4.36*	*8.48*	*14.3*
nona-BDE	*1.48×10^{-7}*	*2.88×10^{-6}*	*1.29×10^{5}*	*-4.68*	*9.01*	*15.3*
deca-BDE	9.03×10^{-8}	2.33×10^{-6}	2.14×10^{6}	-4.81	9.97	16.8
Linear regression [a)]						
R^2	0.965	0.921	0.739	0.966	0.944	0.986
Slope	-0.662	-0.341	0.377	-0.320	0.528	1.042
Intercept	-0.875	-2.472	1.715	-1.798	4.255	5.954

a) Linear regression y = (slope) × x + (intercept), where x stands for the number of bromines in the homologue group, and y is the log10 of a solubility or partition coefficient.

Table 9.44: Energies of phase change for PBDE homologues. Values in italic have been derived from a linear regression based on other PBDE homologues. If the correlation between the number of bromines and the energy of phase change was weak, the average of the energies of phase change of other homologues was used (indicated with an asterisk *). Some values of ΔU_W, ΔU_O, and ΔU_{OW} (indicated with a $^+$) were calculated with the equations of the three solubilities approach (eq. 9.14 – eq. 9.16 above). Units: kJ/mol.

	ΔU_{vap}	ΔU_W	ΔU_O	ΔU_{AW}	ΔU_{OW}	ΔU_{OA}
di-BDE	70.3	20.9	-21.9^+	49.4	-42.8^+	-92.3*
tri-BDE	77.2	15.5	4.42	61.7	-11.1	-72.8
tetra-BDE	86.7	20.4	-10.3	66.4	-30.6	-97.0
penta-BDE	97.1	27.6	-90.5	69.6	-28.5	-98.1
hexa-BDE	97.2	20.5	-95.8	76.7	-21.5	-98.2
hepta-BDE	116	49.9^+	26.0	65.6*	-23.9^+	-89.5
octa-BDE	*124*	58.2^+	31.5^+	65.6*	-26.7^+	-92.3*
nona-BDE	*133*	67.5^+	40.8^+	65.6*	-26.7^+	-92.3*
deca-BDE	145	79.3	52.8^+	65.7	-26.6^+	-92.3*
Linear regression [b)]						
R^2	0.98					
Slope	9’311					
Intercept	49’244					

b) Linear regression y = (slope) × x + (intercept), where x stands for the number of bromines in the homologue group, and y is the energy of phase change in J/mol.

9.3.6 Measurements of PBDE Congeners in the Environment

The following table provides the measurement data that has been considered for the comparison of model results with field data. For tri-, tetra-, and penta-BDE, only selected congeners are generally measured. Because the results from CliMoChem are representative of the sum of all congeners in a homologue group, the sum of the measured congeners was multiplied by a correction factor to account for unmeasured congeners. The correction factor is calculated based on the study of Lee et al. (2004) who have measured the highest number of congeners of all studies considered here. The sum of the measured congeners in each study was scaled by the inverse of the ratio of these congeners to all congeners measured in Lee et al. This assumes that the sum of the congeners measured by Lee et al. is representative of the sum of all congeners in a homologue group, and that the difference between the congener pattern measured in Lee et al. and that of other studies is small. Correction factors were around 1.33 for tetra-BDE and 1.07 for penta-BDE. Because very large corrections would have to be considered for tri-BDE (between 3 and 7), and only few measurements are available, we have not considered tri-BDE for the comparison of model results with field data.

Table 9.45: PBDE measurements considered in the comparison of model results to field data. Concentrations are corrected for congeners that have not been measured (as mentioned above).

		tri-BDE	tetra-BDE	penta-BDE	deca-BDE
Wang et al. (2005)	East Asia[1)]	<0.2	32.75	16.96	2.25
ter Schure et al. (2004)	Sweden		1.52	1.03	6.10
ter Schure et al. (2004)	UK		20.67	11.43	
ter Schure et al. (2004)	North America		28.18	21.33	
Strandberg et al. (2001)	North America[2)]		5.51	3.68	<DL[3)]
Gouin et al. (2006)	North America		1.70	<DL[3)]	6.19
Lee et al. (2004)	UK	2.23	3.32	2.64	
Hoh and Hites (2005)	North America		6.32	3.65	0.88
Jaward et al. (2005)	Asia	10.54	4.29	1.28	
Jaward et al. (2004b)	Norway / UK	0.41	0.65	0.60	
geomean	**world**		**5.25**	**2.93**	**2.30**
geomean	**North America**		**6.39**	**6.60**	**0.88**
geomean	**Europe / Asia**		**4.61**	**2.72**	**3.70**

1) measurements in the North Pacific Ocean and the Arctic were not considered, because they lay outside the temperate region
2) measurements from Chicago were not considered, Chicago is not a background station (see main text)
3) to account for values below the detection limit (DL), the value <DL and the highest measured concentration in the same homologue were not considered in calculation of the medians, minima, and maxima.

9.3.7 Contribution of the Commercial penta-, octa-, and deca-BDE Mixtures to Levels of Lower Brominated PBDE Compounds

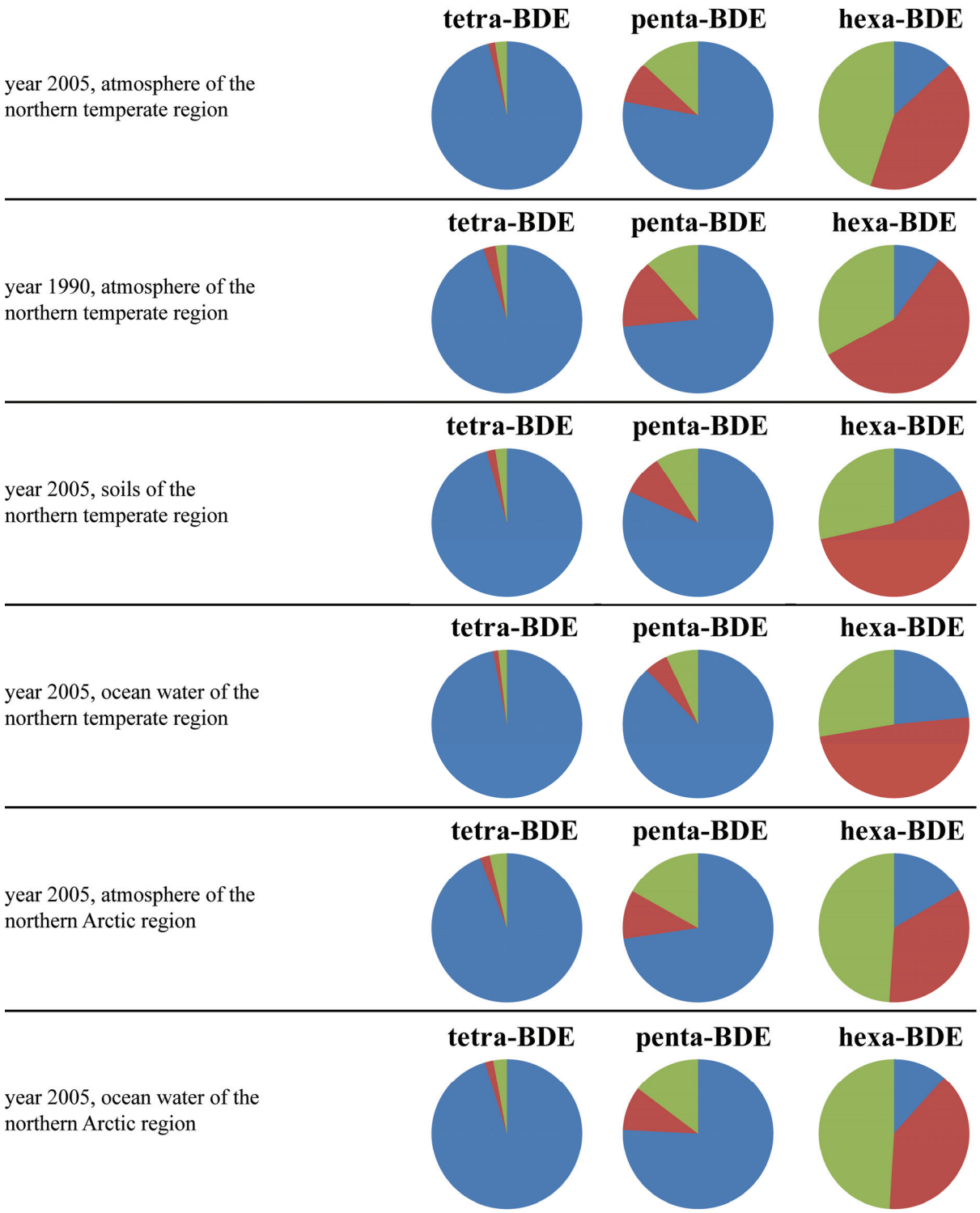

Figure 9.5: Contribution of the commercial penta- (blue), octa- (red), and deca-BDE (green) mixtures to levels of tetra-, penta-, and hexa-BDE in various compartments of the environment.

9.4 Supporting Information for Chapter 6: *Investigating the Global Fate of DDT: Model Evaluation and Estimation of Future Trends*

9.4.1 Substance Properties

Partitioning properties for DDT and its degradation products have been reported frequently; Shen and Wania (2005) have summarized a large number of research papers that report such data. To obtain partitioning data, we have adjusted the data from Shen and Wania with the least-squares adjustment procedure developed by Schenker et al. (2005a). For DDT, DDE, and DDD, temperature dependent information on vapor pressure, water solubility and K_{OA} is available in Shen et al., too (for individual studies only). From these data we have calculated energies of phase transition (ΔU_A, ΔU_W, ΔU_{OW}) with linear regressions of log(X) against the inverse of temperature, where X stands for the vapor pressure, the water solubility, and the K_{OA}. From these values we have calculated ΔU_{OW} and ΔU_{AW} with the least-squares adjustment procedure. Final adjusted values for the partition coefficients and the energies of phase transition are given in Table 9.46 below.

For environmental half-lives of DDT, three different sources have been considered:

- summarized biodegradation half-lives in soils given in handbooks (Howard, 1991, Mackay et al., 1997).
- individual publications about DDT levels at various geographic locations provide additional information on temperature dependence of DDT biodegradation (Samuel et al., 1988, Nair et al., 1992, Agarwal et al., 1994, Andrea et al., 1994, Boul et al., 1994, Espinosagonzalez et al., 1994, Helling et al., 1994, Hussain et al., 1994, Lalah et al., 1994, Sjoeib et al., 1994, Stephens et al., 1994, Varca and Magallona, 1994, Zayed et al., 1994, Boul, 1995, Boul, 1996, Dimond and Owen, 1996, Arisoy, 1998, Roberts and Hutson, 1998, Corona-Cruz et al., 1999).
- Arnot et al. (2005) have developed a method to extract half-lives from the raw output of the BioWin software.

We have combined the three sources and extracted a best estimate of the biodegradation half-live for soils.

For DDE and DDD, only the handbook and BioWin data (treated with the approach of Arnot et al.) were available. We have therefore taken the geometric mean of these two values. For all three compounds, it is assumed that biodegradation half-lives in water are by a factor of

two shorter than in soil. For degradation in the atmosphere, rate constants for reaction with OH radicals from AOPWin (U.S. Environmental Protection Agency, 2004) have been combined with measured rate constants and results from other QSAR software for DDT (Moltmann et al., 1999, Krüger et al., 2005, Liu et al., 2005, Mueller, 2005). For DDE and DDD, only AOPWin data were available. For all degradation half-lives, temperature dependence is taken into account with activiation energies in CliMoChem. We have selected 30'000 J/mol as the activation energy in soils, water, and vegetation, and 15'000 J/mol in the atmosphere. Table 9.47 compares measured and predicted OH reaction rate constants for DDT, DDE, and DDD.

Table 9.46: Substance property data (degradation half-lives, partition coefficients, and energies of phase transition) used in the present modeling study.

substance name	$t_{1/2}$ soil (d)	$t_{1/2}$ water (d)	$t_{1/2}$ air (d)	logK_{OW} (–)	logK_{AW} (–)	ΔU_{OW} (J/mol)	ΔU_{AW} (J/mol)
DDT	1025	512	10	6.41	–3.31	–15'262	72'609
DDE	858	429	1.4	6.94	–2.77	–50'815	47'125
DDD	916	458	2.5	6.30	–3.74	–18'479	61'637

Table 9.47: Comparison of predicted and measured OH reaction rate constants for DDT, DDE, and DDD. Predicted OH reaction rate constants from AOPWin (U.S. Environmental Protection Agency, 2004) for DDT suggest much higher degradation rate constants than measurements. Therefore, it has to be expected that also OH reaction rate constants predicted by AOPWin for DDE and DDD might be too high.

substance Name	AOPWin predicted reaction rate constant (cm^3/molecule*sec)	measured reaction rate constant (Liu et al., 2005) (cm^3/molecule*sec)
DDT	3.44×10^{-12}	5.00×10^{-13}
DDE	7.43×10^{-12}	
DDD	4.34×10^{-12}	

9.4.2 Emission Scenario

9.4.2.1 Emission Scenario for the Years from 1940 to 2005

Three emission inventories have been compiled for DDT: Li and coworkers (Li and Bidleman, 2003, Li et al., 2004, Li and Macdonald, 2005, Li et al., 2006) have published parts of their emission inventory that is still under construction. Their emission inventory is based on usage data from various sources. Wegmann (2004) has based his inventory on production data. Finally, Semeena and Lammel (2003) have used an emission inventory for agricultural DDT usage that comes from usage reporting to the Food and Agriculture

Organization (FAO). Those three inventories have been compared with each other, and the importance of the differences on the results of the CliMoChem model has been assessed (Schenker et al., 2006). Here, selected results from Schenker et al. (2006) are given.

Table 9.48 displays the total amounts of DDT emitted in different regions. Whereas the inventories by Semeena and Lammel and the one by Wegmann are based on continents, this information was not available for the Li et al. inventory, because some of the emissions are attributed to "other coutries". For the comparison of the three inventories, we have attributed 50% of the emissions from "other countries" to South America, and 25% each to Asia and Africa.

The values from Semeena and Lammel cannot directly be compared to the two other inventories, because they represent only agricultural DDT usage. The other two inventories are, however, surprisingly close, given the fact that they were compiled from completely different sources (use data for Li et al, production data for Wegmann). In Schenker et al. (2006), we show that the remaining differences have little impact on the final results of the model, especially when compared to impacts of degradation half-lives or partition properties.

Based on the above information, we have compiled an emission inventory that is adapted to the latitudinal zones of CliMoChem. Therefore, emissions from different countries were attributed to the zones of CliMoChem in which DDT was most likely used. Similarly, emissions from countries were attributed to the years in which DDT was most likely used. The resulting country-to-zone and country-to-year distributions were combined and resulted in a table giving DDT emission per year and zone (Table 9.49). The sum of these emissions from 1945 to 2005 for each latitudinal zone is displayed in Figure 9.6. The media receiving the emissions are vegetation-soil (90%) and atmosphere (10%); emissions take place as a continuous release over the whole year. No emissions to water occur because the CliMoChem model does not contain a freshwater compartment, and emissions to ocean water are not to be expected.

9.4.2.2 Future Emissions

The most efficient way of DDT usage against the anopheles mosquito is indoor house spraying. It is generally recommended (WWF, 1998, Walker, 2000) that DDT be applied with a dosage of 2 g (active ingredient) per square meter of indoor walls. Spraying is needed twice per year. If one assumes 250 square meters to be sprayed per house (one room of 8

times 8 meters, no internal walls, 2 meters high), the DDT usage per house would be 1 kg per year.

Therefore, yearly DDT emissions of 15'000 tonnes (equal to 10% of the maximal emissions, and about 50% of what was used in 1998 (WWF, 1998)), would allow the treatment of 15 million households, which would equal about 74 million persons (assuming a household size of 4.9 (United Nations Statistics Division, 1995)). The financial resources required to spray 15'000 tonnes of DDT are estimated to be $25–150 million (based on estimations in Walker, 2000, Brown, 2006).

Table 9.48: DDT emissions in kg for different geographical regions (total for 1945 to 1990).

Region	Semeena and Lammel	Li et al.	Wegmann
N-America	5.8×10^{8}	8.4×10^{8}	6.7×10^{8}
S-America	1.2×10^{8}	1.1×10^{9}	8.9×10^{8}
Europe	4.0×10^{7}	3.2×10^{8}	2.4×10^{8}
Asia, Australia, Oceania	2.4×10^{8}	1.3×10^{9}	1.2×10^{9}
Africa	2.1×10^{8}	4.9×10^{8}	3.1×10^{8}
Total	1.2×10^{9}	4.1×10^{9}	3.3×10^{9}

Table 9.49: Zonal – yearly DDT emissions in tonnes/year. No emissions occur in zones 1-3 and 21-30.

	zone 4	zone 5	zone 6	zone 7	zone 8	zone 9	zone 10	zone 11	zone 12
1941	0	0	0	0	2.1×10^{2}	4.2×10^{2}	1.1×10^{3}	4.2×10^{2}	0
1942	0	0	0	0	4.2×10^{2}	8.5×10^{2}	2.1×10^{3}	8.5×10^{2}	0
1943	0	0	0	0	6.4×10^{2}	1.3×10^{3}	3.2×10^{3}	1.3×10^{3}	0
1944	0	0	0	0	8.5×10^{2}	1.7×10^{3}	4.2×10^{3}	1.7×10^{3}	0
1945	0	0	0	0	1.1×10^{3}	2.1×10^{3}	5.3×10^{3}	2.1×10^{3}	0
1946	4.2×10	6.2×10	1.0×10^{2}	5.2×10^{2}	2.3×10^{3}	2.9×10^{3}	6.6×10^{3}	2.8×10^{3}	1.8×10^{2}
1947	8.3×10	1.2×10^{2}	2.1×10^{2}	1.0×10^{3}	3.5×10^{3}	3.6×10^{3}	7.9×10^{3}	3.4×10^{3}	3.7×10^{2}
1948	1.2×10^{2}	1.9×10^{2}	3.1×10^{2}	1.6×10^{3}	4.7×10^{3}	4.4×10^{3}	9.3×10^{3}	4.1×10^{3}	5.5×10^{2}
1949	1.7×10^{2}	2.5×10^{2}	4.1×10^{2}	2.1×10^{3}	6.0×10^{3}	5.1×10^{3}	1.1×10^{4}	4.7×10^{3}	7.3×10^{2}
1950	2.1×10^{2}	3.1×10^{2}	5.2×10^{2}	2.6×10^{3}	7.2×10^{3}	5.9×10^{3}	1.2×10^{4}	5.4×10^{3}	9.2×10^{2}
1951	2.4×10^{2}	3.7×10^{2}	6.1×10^{2}	3.1×10^{3}	8.5×10^{3}	7.0×10^{3}	1.4×10^{4}	7.4×10^{3}	2.7×10^{3}
1952	2.8×10^{2}	4.2×10^{2}	7.0×10^{2}	3.5×10^{3}	9.8×10^{3}	8.2×10^{3}	1.7×10^{4}	9.4×10^{3}	4.4×10^{3}
1953	3.2×10^{2}	4.8×10^{2}	8.0×10^{2}	4.0×10^{3}	1.1×10^{4}	9.4×10^{3}	1.9×10^{4}	1.1×10^{4}	6.2×10^{3}
1954	3.6×10^{2}	5.3×10^{2}	8.9×10^{2}	4.4×10^{3}	1.2×10^{4}	1.1×10^{4}	2.2×10^{4}	1.3×10^{4}	7.9×10^{3}
1955	3.9×10^{2}	5.9×10^{2}	9.8×10^{2}	4.9×10^{3}	1.4×10^{4}	1.2×10^{4}	2.4×10^{4}	1.5×10^{4}	9.7×10^{3}
1956	4.1×10^{2}	6.1×10^{2}	1.0×10^{3}	5.1×10^{3}	1.4×10^{4}	1.2×10^{4}	2.4×10^{4}	1.6×10^{4}	1.0×10^{4}
1957	4.2×10^{2}	6.3×10^{2}	1.0×10^{3}	5.2×10^{3}	1.4×10^{4}	1.2×10^{4}	2.5×10^{4}	1.7×10^{4}	1.1×10^{4}
1958	4.3×10^{2}	6.5×10^{2}	1.1×10^{3}	5.4×10^{3}	1.5×10^{4}	1.2×10^{4}	2.5×10^{4}	1.7×10^{4}	1.1×10^{4}
1959	4.5×10^{2}	6.7×10^{2}	1.1×10^{3}	5.6×10^{3}	1.5×10^{4}	1.3×10^{4}	2.5×10^{4}	1.8×10^{4}	1.2×10^{4}
1960	4.6×10^{2}	6.9×10^{2}	1.1×10^{3}	5.7×10^{3}	1.6×10^{4}	1.3×10^{4}	2.6×10^{4}	1.8×10^{4}	1.2×10^{4}
1961	4.4×10^{2}	6.6×10^{2}	1.1×10^{3}	5.5×10^{3}	1.5×10^{4}	1.2×10^{4}	2.5×10^{4}	1.8×10^{4}	1.3×10^{4}
1962	4.2×10^{2}	6.3×10^{2}	1.1×10^{3}	5.3×10^{3}	1.4×10^{4}	1.2×10^{4}	2.4×10^{4}	1.8×10^{4}	1.3×10^{4}
1963	4.0×10^{2}	6.0×10^{2}	1.0×10^{3}	5.0×10^{3}	1.4×10^{4}	1.2×10^{4}	2.4×10^{4}	1.8×10^{4}	1.3×10^{4}
1964	3.8×10^{2}	5.8×10^{2}	9.6×10^{2}	4.8×10^{3}	1.3×10^{4}	1.2×10^{4}	2.3×10^{4}	1.8×10^{4}	1.4×10^{4}
1965	3.7×10^{2}	5.5×10^{2}	9.1×10^{2}	4.6×10^{3}	1.3×10^{4}	1.1×10^{4}	2.3×10^{4}	1.8×10^{4}	1.4×10^{4}
1966	3.3×10^{2}	5.0×10^{2}	8.3×10^{2}	4.1×10^{3}	1.2×10^{4}	1.1×10^{4}	2.2×10^{4}	1.8×10^{4}	1.4×10^{4}
1967	3.0×10^{2}	4.5×10^{2}	7.4×10^{2}	3.7×10^{3}	1.1×10^{4}	1.0×10^{4}	2.1×10^{4}	1.7×10^{4}	1.3×10^{4}
1968	2.6×10^{2}	4.0×10^{2}	6.6×10^{2}	3.3×10^{3}	9.5×10^{3}	1.0×10^{4}	2.0×10^{4}	1.7×10^{4}	1.3×10^{4}
1969	2.3×10^{2}	3.4×10^{2}	5.7×10^{2}	2.9×10^{3}	8.5×10^{3}	9.5×10^{3}	1.9×10^{4}	1.7×10^{4}	1.3×10^{4}
1970	2.0×10^{2}	2.9×10^{2}	4.9×10^{2}	2.4×10^{3}	7.5×10^{3}	9.0×10^{3}	1.8×10^{4}	1.6×10^{4}	1.3×10^{4}
1971	1.7×10^{2}	2.5×10^{2}	4.2×10^{2}	2.1×10^{3}	6.5×10^{3}	8.2×10^{3}	1.7×10^{4}	1.6×10^{4}	1.3×10^{4}
1972	1.4×10^{2}	2.1×10^{2}	3.5×10^{2}	1.7×10^{3}	5.5×10^{3}	7.4×10^{3}	1.5×10^{4}	1.5×10^{4}	1.3×10^{4}
1973	1.1×10^{2}	1.7×10^{2}	2.8×10^{2}	1.4×10^{3}	4.5×10^{3}	6.5×10^{3}	1.3×10^{4}	1.4×10^{4}	1.3×10^{4}
1974	8.3×10	1.2×10^{2}	2.1×10^{2}	1.0×10^{3}	3.5×10^{3}	5.7×10^{3}	1.1×10^{4}	1.4×10^{4}	1.3×10^{4}
1975	5.5×10	8.2×10	1.4×10^{2}	6.8×10^{2}	2.6×10^{3}	4.9×10^{3}	9.6×10^{3}	1.3×10^{4}	1.4×10^{4}
1976	5.0×10	7.5×10	1.2×10^{2}	6.2×10^{2}	2.4×10^{3}	4.7×10^{3}	9.0×10^{3}	1.3×10^{4}	1.4×10^{4}
1977	4.5×10	6.8×10	1.1×10^{2}	5.6×10^{2}	2.2×10^{3}	4.4×10^{3}	8.5×10^{3}	1.2×10^{4}	1.4×10^{4}
1978	4.0×10	6.0×10	1.0×10^{2}	5.0×10^{2}	2.0×10^{3}	4.2×10^{3}	7.9×10^{3}	1.2×10^{4}	1.4×10^{4}
1979	3.5×10	5.3×10	8.9×10	4.4×10^{2}	1.8×10^{3}	3.9×10^{3}	7.3×10^{3}	1.1×10^{4}	1.4×10^{4}
1980	3.1×10	4.6×10	7.7×10	3.8×10^{2}	1.6×10^{3}	3.7×10^{3}	6.8×10^{3}	1.1×10^{4}	1.4×10^{4}
1981	2.7×10	4.1×10	6.8×10	3.4×10^{2}	1.4×10^{3}	3.1×10^{3}	5.7×10^{3}	1.1×10^{4}	1.4×10^{4}
1982	2.4×10	3.5×10	5.9×10	3.0×10^{2}	1.2×10^{3}	2.4×10^{3}	4.6×10^{3}	1.0×10^{4}	1.4×10^{4}
1983	2.0×10	3.0×10	5.0×10	2.5×10^{2}	9.4×10^{2}	1.8×10^{3}	3.6×10^{3}	1.0×10^{4}	1.4×10^{4}
1984	1.7×10	2.5×10	4.2×10	2.1×10^{2}	7.1×10^{2}	1.1×10^{3}	2.5×10^{3}	9.7×10^{3}	1.4×10^{4}
1985	1.3×10	2.0×10	3.3×10	1.6×10^{2}	4.8×10^{2}	4.7×10^{2}	1.4×10^{3}	9.3×10^{3}	1.4×10^{4}
1986	1.1×10	1.6×10	2.6×10	1.3×10^{2}	3.8×10^{2}	3.8×10^{2}	1.2×10^{3}	9.0×10^{3}	1.3×10^{4}

	zone 4	zone 5	zone 6	zone 7	zone 8	zone 9	zone 10	zone 11	zone 12
1987	7.9	1.2×10	2.0×10	9.8×10	2.9×10^{2}	2.8×10^{2}	9.8×10^{2}	8.8×10^{3}	1.2×10^{4}
1988	5.2	7.9	1.3×10	6.6×10	1.9×10^{2}	1.9×10^{2}	7.6×10^{2}	8.5×10^{3}	1.1×10^{4}
1989	2.6	3.9	6.6	3.3×10	9.5×10	9.5×10	5.4×10^{2}	8.2×10^{3}	1.0×10^{4}
1990	0	0	0	0	0	0	3.3×10^{2}	7.9×10^{3}	9.6×10^{3}
1991	0	0	0	0	0	0	3.1×10^{2}	7.4×10^{3}	8.9×10^{3}
1992	0	0	0	0	0	0	2.9×10^{2}	6.8×10^{3}	8.2×10^{3}
1993	0	0	0	0	0	0	2.8×10^{2}	6.3×10^{3}	7.5×10^{3}
1994	0	0	0	0	0	0	2.6×10^{2}	5.7×10^{3}	6.7×10^{3}
1995	0	0	0	0	0	0	2.4×10^{2}	5.1×10^{3}	6.0×10^{3}
1996	0	0	0	0	0	0	2.3×10^{2}	4.8×10^{3}	5.8×10^{3}
1997	0	0	0	0	0	0	2.1×10^{2}	4.5×10^{3}	5.5×10^{3}
1998	0	0	0	0	0	0	2.0×10^{2}	4.2×10^{3}	5.3×10^{3}
1999	0	0	0	0	0	0	1.8×10^{2}	3.9×10^{3}	5.0×10^{3}
2000	0	0	0	0	0	0	1.6×10^{2}	3.5×10^{3}	4.7×10^{3}
2001	0	0	0	0	0	0	1.5×10^{2}	3.1×10^{3}	4.1×10^{3}
2002	0	0	0	0	0	0	1.3×10^{2}	2.8×10^{3}	3.4×10^{3}
2003	0	0	0	0	0	0	1.1×10^{2}	2.4×10^{3}	2.7×10^{3}
2004	0	0	0	0	0	0	9.8×10	2.0×10^{3}	2.0×10^{3}
2005	0	0	0	0	0	0	8.2×10	1.6×10^{3}	1.3×10^{3}

Table 9.49 (continued): years 1941 – 2005 for zones 13 – 20

	zone 13	zone 14	zone 15	zone 16	zone 17	zone 18	zone 19	zone 20
1941	0	0	0	0	0	0	0	0
1942	0	0	0	0	0	0	0	0
1943	0	0	0	0	0	0	0	0
1944	0	0	0	0	0	0	0	0
1945	0	0	0	0	0	0	0	0
1946	3.1×10^{2}	1.4×10^{2}	1.3×10^{2}	1.6×10^{2}	5.3×10	6.6×10	6.6×10	5.3×10
1947	6.2×10^{2}	2.9×10^{2}	2.6×10^{2}	3.2×10^{2}	1.1×10^{2}	1.3×10^{2}	1.3×10^{2}	1.1×10^{2}
1948	9.3×10^{2}	4.3×10^{2}	4.0×10^{2}	4.7×10^{2}	1.6×10^{2}	2.0×10^{2}	2.0×10^{2}	1.6×10^{2}
1949	1.2×10^{3}	5.7×10^{2}	5.3×10^{2}	6.3×10^{2}	2.1×10^{2}	2.6×10^{2}	2.6×10^{2}	2.1×10^{2}
1950	1.6×10^{3}	7.2×10^{2}	6.6×10^{2}	7.9×10^{2}	2.6×10^{2}	3.3×10^{2}	3.3×10^{2}	2.6×10^{2}
1951	3.3×10^{3}	1.8×10^{3}	2.4×10^{3}	2.9×10^{3}	1.3×10^{3}	5.5×10^{2}	4.6×10^{2}	3.4×10^{2}
1952	5.0×10^{3}	2.9×10^{3}	4.0×10^{3}	5.1×10^{3}	2.3×10^{3}	7.8×10^{2}	6.0×10^{2}	4.3×10^{2}
1953	6.7×10^{3}	3.9×10^{3}	5.7×10^{3}	7.2×10^{3}	3.2×10^{3}	1.0×10^{3}	7.4×10^{2}	5.1×10^{2}
1954	8.4×10^{3}	5.0×10^{3}	7.4×10^{3}	9.3×10^{3}	4.2×10^{3}	1.2×10^{3}	8.7×10^{2}	5.9×10^{2}
1955	1.0×10^{4}	6.1×10^{3}	9.1×10^{3}	1.1×10^{4}	5.2×10^{3}	1.5×10^{3}	1.0×10^{3}	6.7×10^{2}
1956	1.1×10^{4}	6.4×10^{3}	9.6×10^{3}	1.2×10^{4}	5.6×10^{3}	1.5×10^{3}	1.0×10^{3}	6.9×10^{2}
1957	1.1×10^{4}	6.7×10^{3}	1.0×10^{4}	1.3×10^{4}	6.0×10^{3}	1.6×10^{3}	1.1×10^{3}	7.1×10^{2}
1958	1.1×10^{4}	7.0×10^{3}	1.1×10^{4}	1.4×10^{4}	6.3×10^{3}	1.7×10^{3}	1.1×10^{3}	7.3×10^{2}
1959	1.2×10^{4}	7.3×10^{3}	1.1×10^{4}	1.4×10^{4}	6.7×10^{3}	1.7×10^{3}	1.1×10^{3}	7.5×10^{2}
1960	1.2×10^{4}	7.6×10^{3}	1.2×10^{4}	1.5×10^{4}	7.1×10^{3}	1.8×10^{3}	1.2×10^{3}	7.6×10^{2}
1961	1.3×10^{4}	7.9×10^{3}	1.2×10^{4}	1.5×10^{4}	7.1×10^{3}	1.9×10^{3}	1.3×10^{3}	8.3×10^{2}
1962	1.3×10^{4}	8.1×10^{3}	1.2×10^{4}	1.5×10^{4}	7.1×10^{3}	1.9×10^{3}	1.3×10^{3}	8.9×10^{2}
1963	1.3×10^{4}	8.3×10^{3}	1.2×10^{4}	1.5×10^{4}	7.1×10^{3}	2.0×10^{3}	1.4×10^{3}	9.5×10^{2}
1964	1.4×10^{4}	8.6×10^{3}	1.2×10^{4}	1.5×10^{4}	7.1×10^{3}	2.1×10^{3}	1.5×10^{3}	1.0×10^{3}

	zone 13	zone 14	zone 15	zone 16	zone 17	zone 18	zone 19	zone 20
1965	1.4×10^{4}	8.8×10^{3}	1.2×10^{4}	1.6×10^{4}	7.1×10^{3}	2.1×10^{3}	1.6×10^{3}	1.1×10^{3}
1966	1.4×10^{4}	8.4×10^{3}	1.2×10^{4}	1.4×10^{4}	6.3×10^{3}	2.0×10^{3}	1.5×10^{3}	1.0×10^{3}
1967	1.3×10^{4}	8.1×10^{3}	1.1×10^{4}	1.3×10^{4}	5.6×10^{3}	1.8×10^{3}	1.4×10^{3}	9.6×10^{2}
1968	1.3×10^{4}	7.7×10^{3}	9.6×10^{3}	1.2×10^{4}	4.9×10^{3}	1.7×10^{3}	1.3×10^{3}	9.0×10^{2}
1969	1.2×10^{4}	7.3×10^{3}	8.7×10^{3}	1.1×10^{4}	4.2×10^{3}	1.5×10^{3}	1.2×10^{3}	8.4×10^{2}
1970	1.2×10^{4}	7.0×10^{3}	7.7×10^{3}	9.3×10^{3}	3.5×10^{3}	1.3×10^{3}	1.1×10^{3}	7.8×10^{2}
1971	1.2×10^{4}	6.8×10^{3}	7.5×10^{3}	9.1×10^{3}	3.5×10^{3}	1.4×10^{3}	1.2×10^{3}	8.5×10^{2}
1972	1.2×10^{4}	6.6×10^{3}	7.2×10^{3}	8.8×10^{3}	3.5×10^{3}	1.5×10^{3}	1.3×10^{3}	9.3×10^{2}
1973	1.2×10^{4}	6.4×10^{3}	6.9×10^{3}	8.5×10^{3}	3.5×10^{3}	1.6×10^{3}	1.3×10^{3}	1.0×10^{3}
1974	1.2×10^{4}	6.2×10^{3}	6.7×10^{3}	8.3×10^{3}	3.5×10^{3}	1.7×10^{3}	1.4×10^{3}	1.1×10^{3}
1975	1.2×10^{4}	6.0×10^{3}	6.4×10^{3}	8.0×10^{3}	3.5×10^{3}	1.8×10^{3}	1.5×10^{3}	1.1×10^{3}
1976	1.2×10^{4}	5.7×10^{3}	6.2×10^{3}	7.9×10^{3}	3.7×10^{3}	1.8×10^{3}	1.5×10^{3}	1.1×10^{3}
1977	1.1×10^{4}	5.4×10^{3}	6.1×10^{3}	7.8×10^{3}	3.8×10^{3}	1.8×10^{3}	1.5×10^{3}	1.1×10^{3}
1978	1.1×10^{4}	5.1×10^{3}	5.9×10^{3}	7.7×10^{3}	4.0×10^{3}	1.8×10^{3}	1.5×10^{3}	1.1×10^{3}
1979	1.0×10^{4}	4.7×10^{3}	5.7×10^{3}	7.6×10^{3}	4.1×10^{3}	1.8×10^{3}	1.5×10^{3}	1.1×10^{3}
1980	9.4×10^{3}	4.4×10^{3}	5.6×10^{3}	7.5×10^{3}	4.3×10^{3}	1.8×10^{3}	1.5×10^{3}	1.1×10^{3}
1981	9.2×10^{3}	4.3×10^{3}	5.4×10^{3}	7.3×10^{3}	4.2×10^{3}	1.7×10^{3}	1.4×10^{3}	1.0×10^{3}
1982	9.0×10^{3}	4.2×10^{3}	5.3×10^{3}	7.2×10^{3}	4.1×10^{3}	1.7×10^{3}	1.4×10^{3}	9.9×10^{2}
1983	8.7×10^{3}	4.1×10^{3}	5.1×10^{3}	7.0×10^{3}	4.1×10^{3}	1.6×10^{3}	1.3×10^{3}	9.4×10^{2}
1984	8.5×10^{3}	4.0×10^{3}	5.0×10^{3}	6.8×10^{3}	4.0×10^{3}	1.5×10^{3}	1.2×10^{3}	8.9×10^{2}
1985	8.3×10^{3}	3.9×10^{3}	4.8×10^{3}	6.6×10^{3}	4.0×10^{3}	1.5×10^{3}	1.2×10^{3}	8.3×10^{2}
1986	7.9×10^{3}	3.9×10^{3}	4.7×10^{3}	6.4×10^{3}	3.7×10^{3}	1.3×10^{3}	1.0×10^{3}	7.3×10^{2}
1987	7.5×10^{3}	3.8×10^{3}	4.5×10^{3}	6.1×10^{3}	3.5×10^{3}	1.2×10^{3}	8.9×10^{2}	6.3×10^{2}
1988	7.0×10^{3}	3.8×10^{3}	4.4×10^{3}	5.8×10^{3}	3.2×10^{3}	1.0×10^{3}	7.6×10^{2}	5.3×10^{2}
1989	6.6×10^{3}	3.7×10^{3}	4.2×10^{3}	5.5×10^{3}	3.0×10^{3}	8.8×10^{2}	6.3×10^{2}	4.3×10^{2}
1990	6.2×10^{3}	3.7×10^{3}	4.0×10^{3}	5.3×10^{3}	2.7×10^{3}	7.3×10^{2}	5.0×10^{2}	3.3×10^{2}
1991	5.8×10^{3}	3.5×10^{3}	3.9×10^{3}	5.1×10^{3}	2.6×10^{3}	7.2×10^{2}	4.9×10^{2}	3.2×10^{2}
1992	5.4×10^{3}	3.3×10^{3}	3.7×10^{3}	4.9×10^{3}	2.6×10^{3}	7.0×10^{2}	4.8×10^{2}	3.2×10^{2}
1993	5.0×10^{3}	3.0×10^{3}	3.6×10^{3}	4.7×10^{3}	2.5×10^{3}	6.9×10^{2}	4.8×10^{2}	3.2×10^{2}
1994	4.6×10^{3}	2.8×10^{3}	3.4×10^{3}	4.5×10^{3}	2.4×10^{3}	6.8×10^{2}	4.7×10^{2}	3.2×10^{2}
1995	4.2×10^{3}	2.6×10^{3}	3.3×10^{3}	4.3×10^{3}	2.4×10^{3}	6.7×10^{2}	4.7×10^{2}	3.1×10^{2}
1996	4.0×10^{3}	2.4×10^{3}	3.1×10^{3}	4.1×10^{3}	2.3×10^{3}	6.0×10^{2}	4.1×10^{2}	2.7×10^{2}
1997	3.7×10^{3}	2.3×10^{3}	3.0×10^{3}	3.9×10^{3}	2.2×10^{3}	5.3×10^{2}	3.5×10^{2}	2.2×10^{2}
1998	3.5×10^{3}	2.1×10^{3}	2.8×10^{3}	3.7×10^{3}	2.0×10^{3}	4.7×10^{2}	2.9×10^{2}	1.8×10^{2}
1999	3.2×10^{3}	1.9×10^{3}	2.7×10^{3}	3.5×10^{3}	1.9×10^{3}	4.0×10^{2}	2.3×10^{2}	1.3×10^{2}
2000	2.9×10^{3}	1.7×10^{3}	2.5×10^{3}	3.3×10^{3}	1.8×10^{3}	3.4×10^{2}	1.7×10^{2}	8.5×10
2001	2.6×10^{3}	1.6×10^{3}	2.2×10^{3}	2.8×10^{3}	1.5×10^{3}	2.8×10^{2}	1.4×10^{2}	7.1×10
2002	2.3×10^{3}	1.4×10^{3}	1.8×10^{3}	2.4×10^{3}	1.2×10^{3}	2.3×10^{2}	1.1×10^{2}	5.7×10
2003	1.9×10^{3}	1.2×10^{3}	1.5×10^{3}	1.9×10^{3}	9.3×10^{2}	1.7×10^{2}	8.7×10	4.3×10
2004	1.6×10^{3}	1.0×10^{3}	1.1×10^{3}	1.4×10^{3}	6.4×10^{2}	1.2×10^{2}	5.9×10	3.0×10
2005	1.3×10^{3}	8.5×10^{2}	7.6×10^{2}	9.1×10^{2}	3.4×102	6.3×10	3.2×10	1.6×10

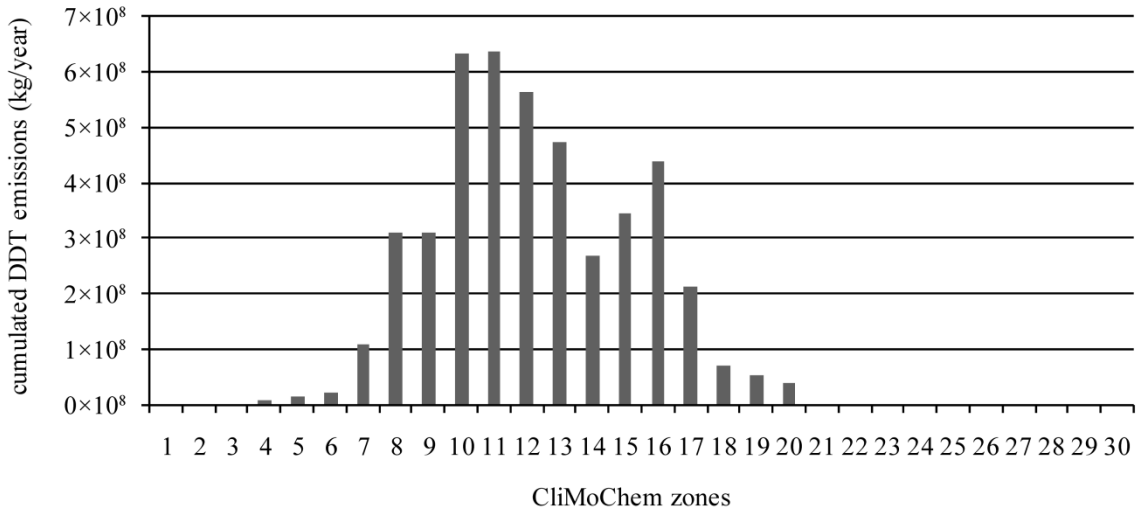

Figure 9.6: Sum of DDT emissions between 1945 and 2005, for all zones in CliMoChem. Zone 1 represents the northernmost zone, zone 30 the southernmost zone. Each zone is 6° latitude wide. Zone 15 is situated between 6° N and the equator.

9.4.3 Model Runs with Modified Parameters

To illustrate the impact of uncertainty that is associated with the model setting and the values of input parameters to the model, we present here a number of runs with modified model settings. The results from these runs are displayed in Figure 6.2 of the main text.

9.4.3.1 Decreased Temperature Dependence

Motivation: The zonal distribution in water in the model suggests a fairly uniform distribution from the tropics to the pole, whereas measurements suggest strongly decreasing concentrations. Although this information is not very reliable, because it is based on only a single study, the model results could also be biased because of the very slow degradation and important partitioning into water that result from the low temperatures in the Arctic.

Modifications: We have therefore decreased the temperature dependence of the air−water partition coefficient (energy of phase change, ΔU_{AW}) from an initial value of 72'609 J/mol to a new value of 35'000 J/mol and reduced the energy of activation (E_a) for the degradation rates in soil and water from 30'000 J/mol to 20'000 J/mol.

Results: As could be expected, concentrations in water and soil in the Arctic and temperate regions has decreased by up to a factor of 2.5, whereas the concentration in atmosphere has

increased by 40% in the Arctic (because of the higher logK_{AW}). In the tropical regions, changes remain below 15%.

Table 9.50: Ratio of the "decreased temperature dependence"-run, as compared to the standard run. The ratio is calculated based on the masses between 1985 and 2005 (corresponding to the data points in Figure 6.2 in the main text).

	Arctic	temperate	tropic
atmosphere	140%	124%	113%
water	61%	71%	102%
soil	41%	58%	103%

9.4.3.2 Increased Temperature Dependence

Motivation: A comparison of biodegradation half-lives from soils from various geographical regions suggested higher temperature dependence than the standard value of an activation energy of 30'000 J/mol: in tropical regions, DDT has been shown to degrade much faster than in cold climates.

Modifications: We have therefore increased the temperature dependence for biodegradation in soils and water. The activation energy (E_a) was increased from 30'000 J/mol to 50'000 J/mol.

Results: Whereas the changes in the tropical regions are below 10% in all compartments, the concentrations in soil and water have increased by a factor of three and two, respectively in the Arctic and temperate regions. Concentrations in atmosphere are not as strongly affected.

Table 9.51: Ratio of the "increased temperature dependence"-run, as compared to the standard run. The ratio is calculated based on the masses between 1985 and 2005 (corresponding to the data points in Figure 6.2 in the main text).

	Arctic	temperate	tropic
atmosphere	111%	110%	109%
water	199%	180%	105%
soil	294%	290%	96%

9.4.3.3 Increasing Oceanic Losses

Motivation: The zonal distribution in oceans in the model suggests uniform concentrations whereas measurements suggest decreasing concentrations toward the poles (see also model run # 1). This discrepancy might also be because of an underestimation of loss processes in

ocean, in particular in the Arctic regions. In addition, oceanic concentrations in the model are generally high. The most important processes of oceanic losses are the biodegradation and particle sedimentation into the deep ocean. In addition to this, Lohmann et al. have recently shown (Lohmann et al., 2006a) that for PCBs, the formation of deep ocean water in the North Atlantic can be an even more important loss process. This process was not included in the model by now.

Modifications: We have increased particle sedimentation rates in oceans by a factor of three, and degradation processes by a factor of two. In addition, we have included the formation of deep ocean water in the North Atlantic, as suggested by Lohmann et al. (2006a).

Results: Increasing the loss processes in oceans results in minor changes in atmosphere and soil (below 10%), but reduces concentrations in oceans by up to a factor of three. In the tropical regions, the reduction is smaller.

Table 9.52: Ratio of the "increased oceanic losses"-run, as compared to the standard run. The ratio is calculated based on the masses between 1985 and 2005 (corresponding to the data points in Figure 6.2 in the main text).

	Arctic	temperate	tropic
atmosphere	109%	109%	108%
water	36%	36%	42%
soil	104%	110%	101%

9.4.3.4 Decreasing Eddy Diffusion Velocities in Atmosphere

Motivation: The model results show an even distribution toward the north. In measurements, concentrations in the north are lower than in the model. One reason for this could be that the atmospheric transport is too efficient (transport in oceans is in the case of DDT much less important).

Modifications: Eddy diffusion coefficients that define transport efficiency in atmosphere were reduced by a factor of three.

Results: Concentrations in the Arctic atmosphere have decreased by a factor of four, whereas they increase slightly in the tropics. Concentrations in water are affected, too, whereas the impact on soils is minor. In temperate regions, the same effects can be observed, but to a smaller extent.

Table 9.53: Ratio of the "increased eddy-diffusion"-run, as compared to the standard run. The ratio is calculated based on the masses between 1985 and 2005 (corresponding to the data points in Figure 6.2 in the main text).

	Arctic	temperate	tropic
atmosphere	26%	63%	112%
water	51%	85%	109%
soil	88%	109%	101%

9.4.3.5 Higher Emissions into Atmosphere, Instead of Vegetation-Soil

Motivation: As mentioned above, model results are not very sensitive to the zone and time of emissions, but the medium in which the emissions occur is very important. In the standard scenario, we have assumed that most of the emissions are into soil, and only 10% into atmosphere. It is possible that a higher proportion of the emissions go into atmosphere, especially if DDT is sprayed from planes.

Modifications: Therefore, we have made a model run where 80% of emissions go into soils and 20% into atmosphere.

Results: In the tropical regions, concentrations in soil decrease slightly, because fewer emissions occur into this medium. Concentrations in atmosphere increase by a factor of about two, because emissions into atmosphere have increased by a factor of two. Concentrations in temperate and Arctic soils and water from all regions increase, too. Because of the higher emissions into atmosphere, the transport from the tropical regions to the temperate and Arctic zone has become more efficient, resulting in higher precipitation rates of substance in these regions.

Table 9.54: Ratio of the "modified emission compartment"-run, as compared to the standard run. The ratio is calculated based on the masses between 1985 and 2005 (corresponding to the data points in Figure 6.2 in the main text).

	Arctic	temperate	tropic
atmosphere	213%	211%	213%
water	184%	173%	164%
soil	122%	104%	86%

9.4.3.6 Reduced Particle Deposition from Atmosphere

Motivation: Particle deposition is simulated with an average particle deposition velocity in the model. This deposition was determined by Mackay et al. (1992) and based on particles with an average size of 1 μm. However, most of the chemicals are bound to much smaller particles, which have much lower particle deposition velocities (Seinfeld and Pandis, 1998). It is therefore possible, that particle deposition velocities are severely overestimated.

Modification: We have therefore reduced particle deposition velocities by a factor of 10. This results in a new particle deposition of 26 m/d, instead of 260 m/d.

Results: Atmospheric concentrations have increased in all regions, most strongly in the Arctic, where concentrations more than double. On the one hand, this is because less substance is deposited in the Arctic; on the other hand, more substance reaches the Arctic through long-range transport, because the deposition is reduced in the temperate and tropical regions. Concentrations in soil and water remain more or less constant, or decrease slightly.

Table 9.55: Ratio of the "reduced particle depostion"-run, as compared to the standard run. The ratio is calculated based on the masses between 1985 and 2005 (corresponding to the data points in Figure 6.2 in the main text).

	Arctic	temperate	tropic
atmosphere	230%	172%	122%
water	94%	79%	74%
soil	100%	107%	101%

9.4.3.7 Impact of the Various Model Setups on the Temporal Evolution

Making accurate predictions for the future requires the model to be relatively insensitive to changes in the input parameters. In the previous sections, it was seen that the absolute concentrations in the model depend strongly on the selected input parameters. Here, we would like to show that this dependence is much smaller for ratios of concentrations instead of absolute values.

If the ratio between current and future concentrations shows little sensitivity to changes in model parameters, then the model will be capable of predicting reduction ratios (that is the current level divided by the expected future concentration) with a high accuracy.

We have calculated the ratio for concentrations between 1990 and 2040 in atmosphere, water, and soil; the results are displayed in Table 9.56 below. In this table, emissions after 2005 continue at a low level.

Table 9.56: Ratios of current and future environmental concentrations (emissions continue at low levels) in atmosphere, water, and soils, using the standard (second column) and modified model settings (columns three to eight).

	std	**v1**	**v2**	**v3**	**v4**	**v5**	**v6**
air: c_{1990} / c_{2040}	2.69	2.70	2.69	2.69	2.69	2.69	2.71
ocean: c_{1990} / c_{2040}	3.55	3.42	3.90	3.30	3.52	3.34	3.83
soil: c_{1990} / c_{2040}	4.34	4.01	5.06	4.34	4.34	4.36	4.33

The table clearly shows that the model is insensitive to changes in the model settings for ratios of present to future concentrations. The differences are of less than 20%, which is much less than what could be observed for absolute values, for instance in Table 9.50.

The same kind of table can also be calculated if emissions are switched off (see Table 9.57):

Table 9.57: Ratios of current and future environmental concentrations if emissions cease in 2005 in atmosphere, water, and soils, using the standard (second column) and modified model settings (columns three to eight).

	std	**v1**	**v2**	**v3**	**v4**	**v5**	**v6**
air: c_{1990} / c_{2040}	2.8×10^{5}	8.6×10^{5}	2.1×10^{4}	7.6×10^{5}	3.5×10^{5}	4.3×10^{5}	2.3×10^{5}
ocean: c_{1990} / c_{2040}	1.3×10^{3}	9.6×10^{3}	1.0×10^{2}	1.6×10^{3}	1.5×10^{3}	1.7×10^{3}	9.9×10^{2}
soil: c_{1990} / c_{2040}	9.3×10^{2}	5.6×10^{3}	8.2×10	9.3×10^{2}	1.1×10^{3}	6.9×10^{2}	9.5×10^{2}

In this case, the picture is quite different. The ratio of the decrease between 1990 and 2040 varies widely between the different model settings. The reason for this is that if emissions are switched off completely, the system will be controlled by entirely different parameters than in the past. Therefore, even small changes in the model settings result in important changes in the resulting model concentrations.

For our present study however, these differences have little importance: The goal here is to compare the case of continuing emissions with the case where emissions cease. This means comparing a decrease of a factor of 2.69 (atmosphere, standard model settings with continuing emissions) with a decrease of a factor of 2.8×10^{5} (atmosphere, standard model

settings without emissions) or a factor of 2.1×10^4 (atmosphere, scenario 2, without emissions). In both cases, the difference between switching emissions on or off is much more important than the difference within two model settings.

9.4.4 Compilation of Measurement Data

9.4.4.1 Method of Extracting Measurement Series

When data points were taken from publications in the literature, each publication resulted in one or several measurement series (see below). From the data points included in one measurement series, the median of this particular measurement series was calculated. From the median values of all measurement series representing a certain region or period of time then again the median was derived. These median values of the medians of several measurement series are listed in Table 6.1 and displayed in Figure 6.2 in the main text. Each measurement series thus enters the calculation with the same weight. The number of measurement series that were extracted from a given publication is determined by the weight we give to this publication as compared to other publications. For instance, a publication that presents long-term air samples from several measurement stations is more informative (and therefore receives a higher weight) than a publication with a one-day measurement at one place. When data points were aggregated into measurement series, either values from one location but from different times were taken together (resulting in one measurement series per measurement site), or values from one year but from several measurement sites were taken together (resulting in one measurement series per year), or values from several sites and several years were taken together (resulting in just one measurement series for the whole publication).

In Table 9.58, all sources that were used for the compilation of measurements are given. The period in which the measurements were made, the geographic location, and environmental medium are indicated. The last column displays how each source was taken into account: either just one measurement series was generated or, if several measurement series were generated, it is stated for what these series stand.

Table 9.58: Measurements studies that were used in the current project.

Source	Measurement Period	Geographic Location, Medium	Number of Measurement Series
Aigner et al. (1998)	1995 - 1996	US corn belt, soils	one measurement series
Bailey et al. (2000)	1992 - 1995	Tagish, Yukon, Canada, atmosphere	seven series, one per source region of air masses
Bailey et al. (2005)	1999	Saskatchewan, Canada, soils	one measurement series
Bidleman and Leone (2004)	1999 - 2000	Southern US, atmosphere & soils	one measurement series
Bidleman et al. (2006)	1999 - 2000	British Columbia, Canada, atmosphere	one measurement series
Bogdal et al. (2007)	1866 - 2004	Lake Thun, Switzerland, sediment	
Dimond and Owen (1996)	1967 - 1993	Maine, US, forest soils	one measurement series
EMEP database (Hjellbrekke, 2007)	1994 - 2004	Sweden & Czech Republic, atmosphere	four series, one for each measurement station
Halsall et al. (1998)	1993 - 1994	Arctic, atmosphere	seven series, one per measurement station and year
Hargrave et al. (1988)	1986	Canadian Arctic, atmosphere	one measurement series
Harner et al. (1999)	1998 (?)	Alabama, US, soils	one measurement series
Harner et al. (2004)	2000	Ontario, Canada, atmosphere	one measurement series
Hoff et al. (1992)	1998 - 1999	Southern Ontario, Canada, atmosphere	one measurement series
Hoff et al. (1996)	1988 - 1994	Great Lakes (US & Canada), atmosphere	four series, one for each measurement station
Hung et al. (2002)	1993 - 1997	Alert, Nunavut, Canada, atmosphere	five series, one per year
Iwata et al. (1993)	1989 - 1990	Indian and Pacific Ocean from north to south, and "round-the-world" trip east-west, in atmosphere and ocean water	one series per geographical region and environmental medium
Iwata et al. (1994)	1989 - 1990	India, South-East Asia, Australia, in atmosphere and coastal (fresh-) water	one series per geographical region; measurements in freshwater were not taken into account
Iwata et al. (1995)	1992	Lake Baikal, Russia, only atmosphere & soils considered	one measurement series
Jaward et al. (2004a)	2002	Europe, atmosphere	one series per geographical region
Jonsson et al. (2000)	1932 - 1988	Baltic Sea & Gulf of Finland, sediment	
Kalantzi et al. (2001)	1998 - 1999	worldwide, butter	only used for geographical distribution
Kallenborn (2004)	1995 - 2003	Svalbard, Norway, atmosphere	one measurement series

Source	Measurement Period	Geographic Location, Medium	Number of Measurement Series
Kannan et al. (2003)	1999	Southern US, soils	one measurement series
Karlsson et al. (2000)	1997 - 1998	Lake Malawi, Mozambique, atmosphere	one measurement series
Kucklick et al. (1994)	1991	Lake Baikal, Russia, only atmosphere considered	one measurement series
Kurt-Karakus et al. (2006)	2004 - 2005	Ontario, Canada, atmosphere	one measurement series
Kurt-Karakus (2006)	1998	global, soils	one series for each geographical region
Larsson et al. (1995)	1993 - 1994	Sweden & Baltic Island, atmosphere	one measurement series
Lohmann (2007)	2004	North Atlantic, water	one measurement series
Meijer et al.(2001)	1944 - 1990	England, background soils	one measurement series
Ngabe and Bidleman (2006)	1999	Brazzaville (Congo), soils	one measurement series
Oehme et al. (1996)	1993	Svalbard, Norway, atmosphere	one measurement series
Olsson et al. (2000)	1942 - 1995	Baltic Sea, sediment	
Park et al. (2001)	1995 - 1996	Texas, US, atmosphere	one measurement series
Patton et al. (1989)	1986 - 1987	Ellesmere Island, Nunavut, Canada, atmosphere	one measurement series
Shen et al. (2005)	2000 - 2001	North America, atmosphere	one series per geographical region
Simonitch and Hites (1995)	1992 - 1995	worldwide, tree bark	only used for geographical distribution
Stern et al. (2005)	1916 - 1997	Canadian Arctic, lake sediment	
Strachan et al. (2001)	1993	Bering & Chukchi Sea, water & atmosphere	one series for atmosphere and water each
Strandberg et al. (2001)	1997 - 1999	Great Lakes (US & Canada), atmosphere	four series, one for each measurement station
Tanabe et al. (1982)	1980 - 1981	Indian and Pacific Ocean from north to south, in atmosphere and ocean water	one series, used only for degradation product fraction because previous to 1985
Thao et al. (1993a)	1991	Vietnam, soils	one measurement series
Thao et al. (1993b)	1988 - 1990	South-East Asia, soils	one measurement series
van Gaans et al. (1995)	1991	Netherlands, soils	one measurement series
van Metre and Mahler (2005)	1942 - 1998	North America, various lake sediments	
van Metre et al. (1997)	1943 - 1991	rural & urban US lakes	
Weiss (1998)	1993	Austria, soils in forests	one measurement series

Source	Measurement Period	Geographic Location, Medium	Number of Measurement Series
Wurl et al. (2006b)	2004 - 2005	Indian Ocean, atmosphere	one measurement series
Yao et al. (2006)	2003	Canada, soils	one measurement series
Zhu et al. (2005)	(?)	Beijing, China, soils	one measurement series

9.4.4.2 Quality Control Requirements

The two isomers (p,p'- and o,p'-) of DDT were not considered separately. If only one of the two isomers was measured, the concentration of the other one was estimated based on p,p'/o,p' ratios from other studies.

In the main text, three potential factors for bias in summarized measurement data are described (subsection on Measurement Data in the Methods Section). In the following, our method to minimize the influence of these biases in our study is explained.

- The first possible source of bias is differing measurement methods and protocols between different studies. With respect to spatial heterogeneity of measurement methods, we assume that there is no systematic difference between measurement protocols for different geographical regions. Under this assumption, it is possible to directly calculate mean and median values from the measured concentrations. When temporal trends are derived from measurement data, this bias could take effect, for instance if new measurement methods can detect lower concentrations than earlier ones. Therefore, within each publication, measured concentrations were normalized to one year (usually the year 1990), and only these time-normalized concentrations were compared between studies. Measurement data from different sources were not compared if each of these sources reports measured data at one point in time only (so that comparison of normalized concentrations is not possible).
- The second possible bias appears if measurement from different seasons are compared. Therefore, only yearly averages were used. If no yearly averages were available in a study (for instance because the study involved a ship cruise from North to South), this study was only compared to other studies that were conducted in approximately the same season.

- Finally, we tried to exclude all sources from our comparison that report measurements performed in areas that are not representative for background concentrations. For all sources in the present study we determined how likely it is that the reported data were influenced by non-background concentrations. In cases where it seemed likely that a non-background concentration is reported, the given study was excluded.

9.5 Supporting Information for Chapter 7: *Using Information on Uncertainty to Improve Environmental Fate Modeling: A Case Study on DDT*

9.5.1 Model Inputs and their Uncertainty Distributions

Table 9.59: Uncertainty distributions for model inputs: μ = median in normal and log-normal distributions, σ = standard deviation in normal distributions, GSD = geometric standard deviation in log-normal distributions, min – median – max = minimal, median, and maximal values in triangular distributions. For model parameters that are variable in the different zones of the CliMoChem model, scaling factors with μ = 1 are defined, and the parameter value in all zones is multiplied by that scaling factor. In the case of the different model parameter inputs, the column "Source" refers to the source of the GSD only; the source of μ is always the default parameter value in CliMoChem to avoid inconsistencies with previous calculations with CliMoChem.

Name of Model Input	Uncertainty Distribution Type	Distribution Parameters	Source
Substance property inputs – Degradation rates			
Degradation rate constant in atmosphere (k'_{air})	log-normal	$\mu=8.98\times10^{-8}$ cm^3/d/molecule, GSD=4.28	*own value*[1]
Degradation rate constant in ocean-water (k_{water})	log-normal	$\mu=1.35\times10^{-3}$ 1/d, GSD=1.73	*own value*[2]
Degradation rate constant in soil (k_{soil})	log-normal	$\mu=6.76\times10^{-4}$ 1/d, GSD=1.73	*own value*[3]
Degradation rate constant in vegetation (k_{vege})	log-normal	$\mu=6.76\times10^{-4}$ 1/d, GSD= 1.73	*own value*[4]
Substance property inputs – Partition coefficients			
logK_{OW}	normal	$\mu=-3.35$, $\sigma=0.10$	*own value*[5]
logK_{AW}	normal	$\mu=6.01$, $\sigma=0.44$	*own value*[6]

[1] Extracted from the variance of DDT degradation rates predicted by AOPWin (U.S. Environmental Protection Agency, 2004), and values presented in (Moltmann et al., 1999, Krüger et al., 2005, Liu et al., 2005, Mueller, 2005).
[2] Assumed equal to the GSD of the soil degradation rate, see below.
[3] Extracted from the variance of DDT degradation rates given by Mackay et al. (1997), Howard (1991), extrapolated using a method suggested by Arnot et al. (2005) and an own compilation presented in the Supporting Information of Schenker et al. (2008), ref. 5-23 therein.
[4] Assumed equal to the GSD of the soil degradation rate.
[5] Extracted from the variance of logK_{OW} values reported in Shen and Wania (2005).
[6] Extracted from the variance of logK_{AW} values reported in Shen and Wania (2005).

Name of Model Input	Uncertainty Distribution Type	Distribution Parameters	Source
Substance property inputs – Temperature dependencies			
Temperature dependence (activation energy) of k'_{air} (Ea_{air})	log-normal	μ=15,000 J/mol, GSD=1.50	*assumed*
Temperature dependence (activation energy) of k_{water} (Ea_{water})	log-normal	μ=30,000 J/mol, GSD=1.50	*assumed*
Temperature dependence (activation energy) of k_{soil} (Ea_{soil})	log-normal	μ=30,000 J/mol, GSD=1.50	*assumed*
Temperature dependence (activation energy) of k_{vege} (Ea_{vege})	log-normal	μ=30,000 J/mol, GSD=1.50	*assumed*
Temperature dependence (energy of phase change) of logK_{OW} (ΔU_{OW})	normal	μ=-15,262 J/mol, σ=20,000	*assumed*
Temperature dependence (energy of phase change) of logK_{AW} (ΔU_{AW})	normal	μ=72,609 J/mol, σ=20,000	*assumed*
Emissions inputs			
Scaling factor for past emissions (S_{past})	log-normal	μ=1.0, GSD=1.14	*assumed*
Scaling factor for future emissions (S_{future})	log-normal	μ=1.0, GSD=1.73	*assumed*
Ratio of emissions into soil (R_{soil})	triangular	min=0.8, median=0.9, max=1.0	*assumed*
Model parameter inputs – atmosphere			
Scaling factor for eddy diffusion in atmosphere	log-normal	μ =1, GSD=1.18	*(Hertwich et al., 1999, Maddalena et al., 2001 , MacLeod et al., 2002)*[1]
Height of atmosphere compartment	log-normal	μ =6000m, GSD=1.17	*(Maddalena et al., 2001, MacLeod et al., 2002)*
Particle load in atmosphere	log-normal	μ =8.6×10^{-5}g/m^3, GSD=1.41	*(Hertwich et al., 1999, Maddalena et al., 2001 , MacLeod et al., 2002)*
Density of air particles	log-normal	μ =2×10^{6}kg/m^3, GDS=1.12	*(Maddalena et al., 2001, MacLeod et al., 2002)*
Rain scavenging ratio	log-normal	μ =2×10^{5}, GSD=1.42	*(Maddalena et al., 2001, Meyer et al., 2005)*
Rainfall	log-normal	μ =2.3×10^{-3}m/d, GSD=1.71	*(Hertwich et al., 1999, Maddalena et al., 2001, McKone et al., 2001, MacLeod et al., 2002)*
Dry particle deposition velocity	log-normal	260m/d, GSD=2.04	*(Maddalena et al., 2001, MacLeod et al., 2002)*
Scaling factor for stability vector of atmosphere above vegetation and bare soil	log-normal	μ=1, GSD=1.2	*assumed*
Model parameter inputs – 2-film model			
Air-side diffusion velocity, air−water film	log-normal	μ=0.72m/d, GSD=1.61	*(Maddalena et al., 2001, MacLeod et al., 2002)*
Water-side diffusion velocity, air−water film	log-normal	μ=72m/d, GSD=1.74	*(Maddalena et al., 2001, MacLeod et al., 2002)*
Air-side diffusion velocity, air-soil film	log-normal	μ=24m/d, GSD=1.61	*(Maddalena et al., 2001, MacLeod et al., 2002)*
Air-filled-pores-side diffusion velocity, air-soil film	log-normal	μ=0.16m/d, GSD=1.73	*(MacLeod et al., 2002)*
Water-filled-pores-side diffusion velocity, air-soil film	log-normal	μ=6.2×10^{-5}m/d, GSD=1.73	*(MacLeod et al., 2002)*

[1] In MacLeod et al. (2002), the GSD of "regional air residence time" was used as a proxy for the GSD of the eddy diffusion in atmosphere, in Maddalena et al. (2001) the GSD of "scalar wind speed".

Name of Model Input	Uncertainty Distribution Type	Distribution Parameters	Source
Model parameter inputs – soil			
Height of soil compartment	log-normal	μ =200m, GSD=1.69	*(Hertwich et al., 1999, Maddalena et al., 2001, McKone et al., 2001, MacLeod et al., 2002)*
Fraction of air in soils	log-normal	μ =0.2, GSD=1.16	*(Hertwich et al., 1999, McKone et al., 2001, MacLeod et al., 2002)*
Fraction of water in soils	log-normal	μ =0.3, GSD=1.37	*(Hertwich et al., 1999 , Maddalena et al., 2001 , McKone et al., 2001, MacLeod et al., 2002)*
Density of solids in soil	log-normal	μ =2400kg/m^3, GSD=1.10	*(Hertwich et al., 1999, Maddalena et al., 2001 , MacLeod et al., 2002)*
Velocity of leaching (flux of water to groundwater)	log-normal	μ =9.4×10^{-4}m/d, GSD=2.04	*(McKone et al., 2001, MacLeod et al., 2002)*
Velocity of runoff (horizontal water flux above soil)	log-normal	μ =5.5×10^{-7}m/d, GSD=2.04	*(McKone et al., 2001, MacLeod et al., 2002)*
Fraction of organic carbon in bare soil	log-normal	μ =0.02, GSD=2.33	*(Hertwich et al., 1999 , Maddalena et al., 2001 , McKone et al., 2001, MacLeod et al., 2002)*
Scaling factor for fraction of organic carbon in vegetation covered soil	log-normal	μ =1, GSD=1.73	*assumed*
Model parameter inputs – water			
Scaling factor for eddy diffusion in water	log-normal	μ =1, GSD=1.21	*(Hertwich et al., 1999, Maddalena et al., 2001 , MacLeod et al., 2002)*[1]
Height of ocean-water compartment	log-normal	μ =200m, GSD=1.63	*(Hertwich et al., 1999, Maddalena et al., 2001 , MacLeod et al., 2002)*
Fraction of particles in ocean-water	log-normal	μ =5×10^{-8}, GSD=1.9	*(Hertwich et al., 1999, Maddalena et al., 2001 , MacLeod et al., 2002)*
Fraction of organic carbon in particles in ocean-water	log-normal	μ =0.3, GSD=1.28	*(Maddalena et al., 2001, MacLeod et al., 2002)*
Ocean-water particle deposition velocity (sedimentation)	log-normal	μ =1.23m/d, GSD=1.57	*(Hertwich et al., 1999, Maddalena et al., 2001 , MacLeod et al., 2002)*
Model parameter inputs – vegetation			
Scaling factor for lipid content of vegetation (f_{lipid})	log-normal	μ =1, GSD=1.60	*(Maddalena et al., 2001)*
Scaling factor for average leaf lifetime	log-normal	μ =1, GSD=1.60	*(Maddalena et al., 2001)*
Scaling factor for fraction of intercepted rainfall by vegetation	log-normal	μ =1, GSD=1.73	*assumed*
Scaling factor for volume of vegetation	log-normal	μ =1, GSD=1.34	*(Maddalena et al., 2001)*
Scaling factor for dry particle deposition velocity to vegetation	log-normal	μ =1, GSD=2.04	*assumed*
Scaling factor for gas diffusion velocity to vegetation	log-normal	μ =1, GSD=1.61	*assumed*

[1] In MacLeod et al. (2002) the parameter "regional water residence time" was used as a proxy for the GSD of the eddy diffusion in water, in Maddalena et al. (2001) the parameter "volumetric in-/outflow".

9.5.2 Temporal Evolution of DDT Concentrations with Uncertainties

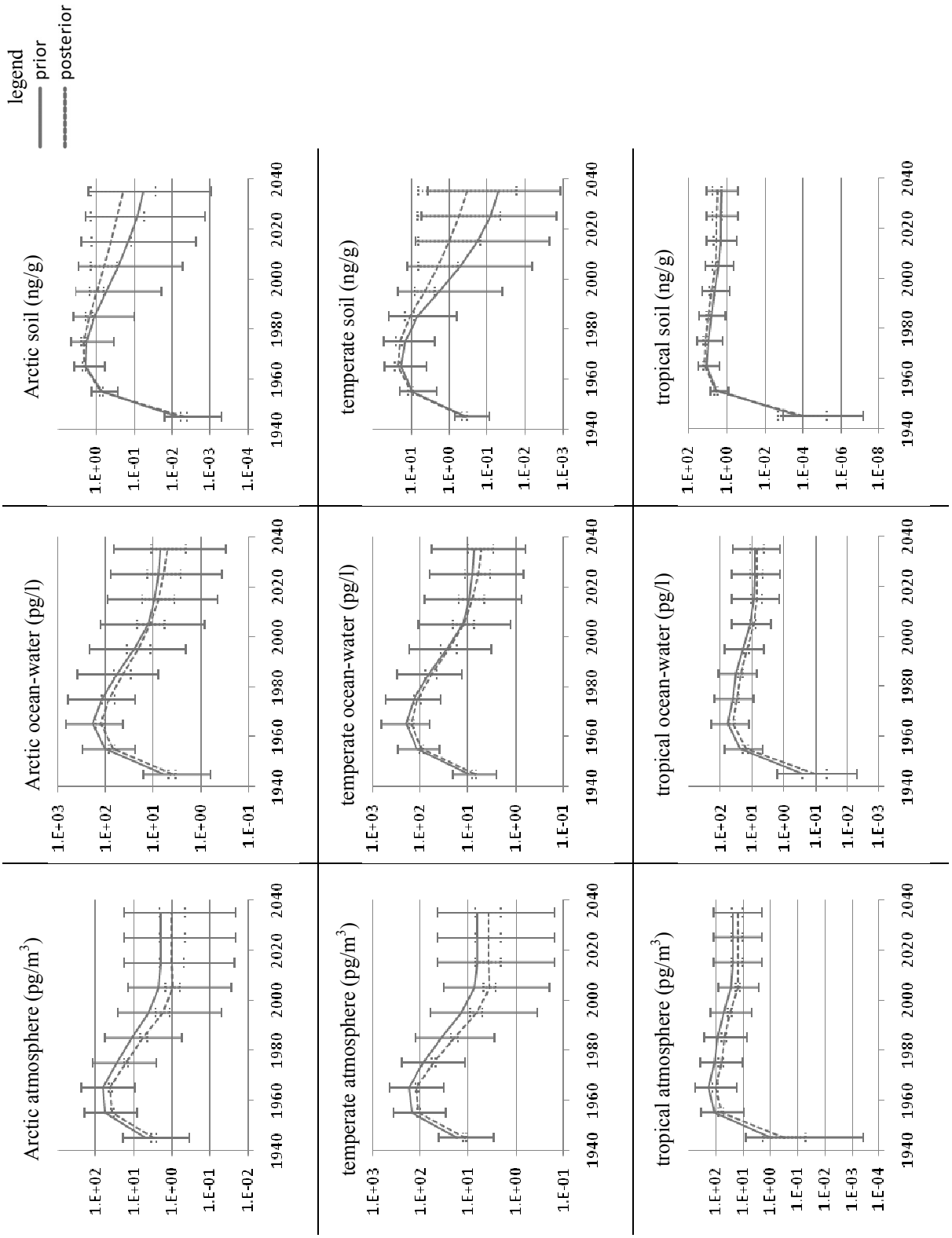

Figure 9.7: Temporal evolution of DDT concentrations in different compartments, before and after the Bayesian updating procedure. Vertical bars represent the 95% interquantile ranges.

9.5.3 Rank Correlations per Groups of Model Inputs

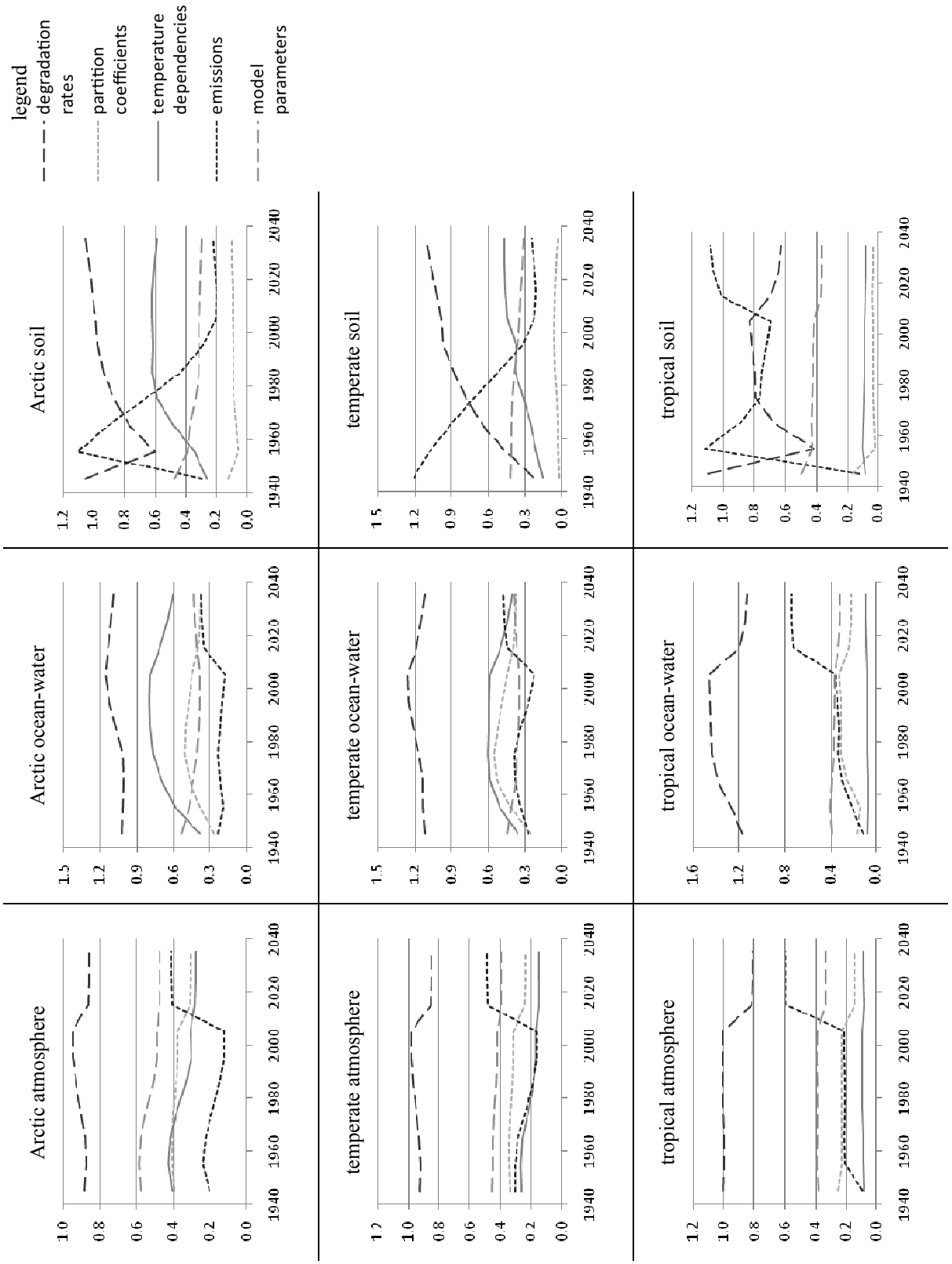

Figure 9.8: Rank correlations of group of model inputs. The sum of the absolute values of individual model inputs was taken; the groups were constructed based on the classification given in Table 9.59.

9.5.4 Highest Rank Correlations of Single Model Inputs

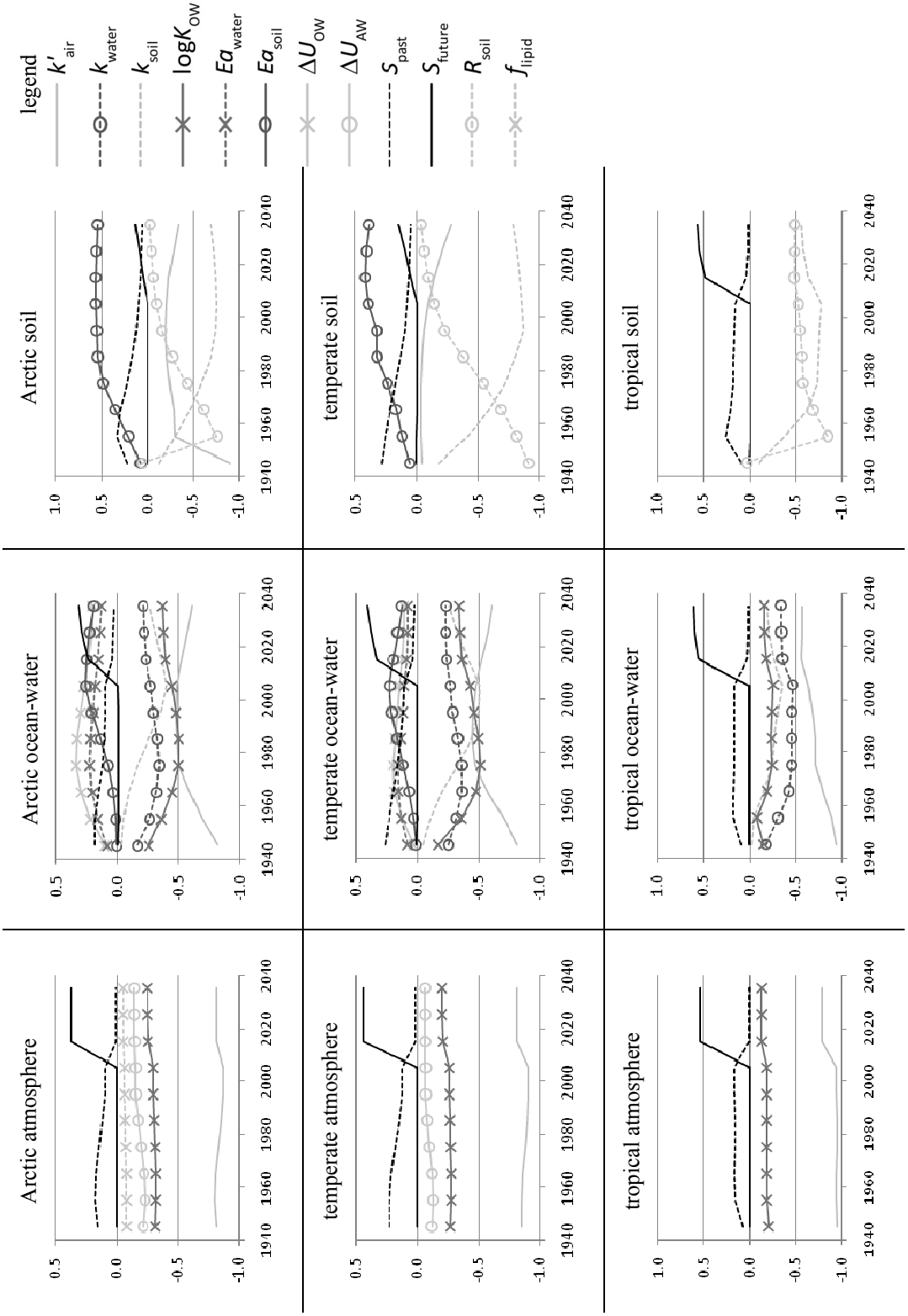

Figure 9.9: Rank correlations of the most important model inputs. Model inputs that did not markedly differ from zero over time are not shown. Abbreviations in the legend correspond to the wording used in Table 9.59

9.5.5 CDFs for Field Data, Prior, and Posterior Model Results

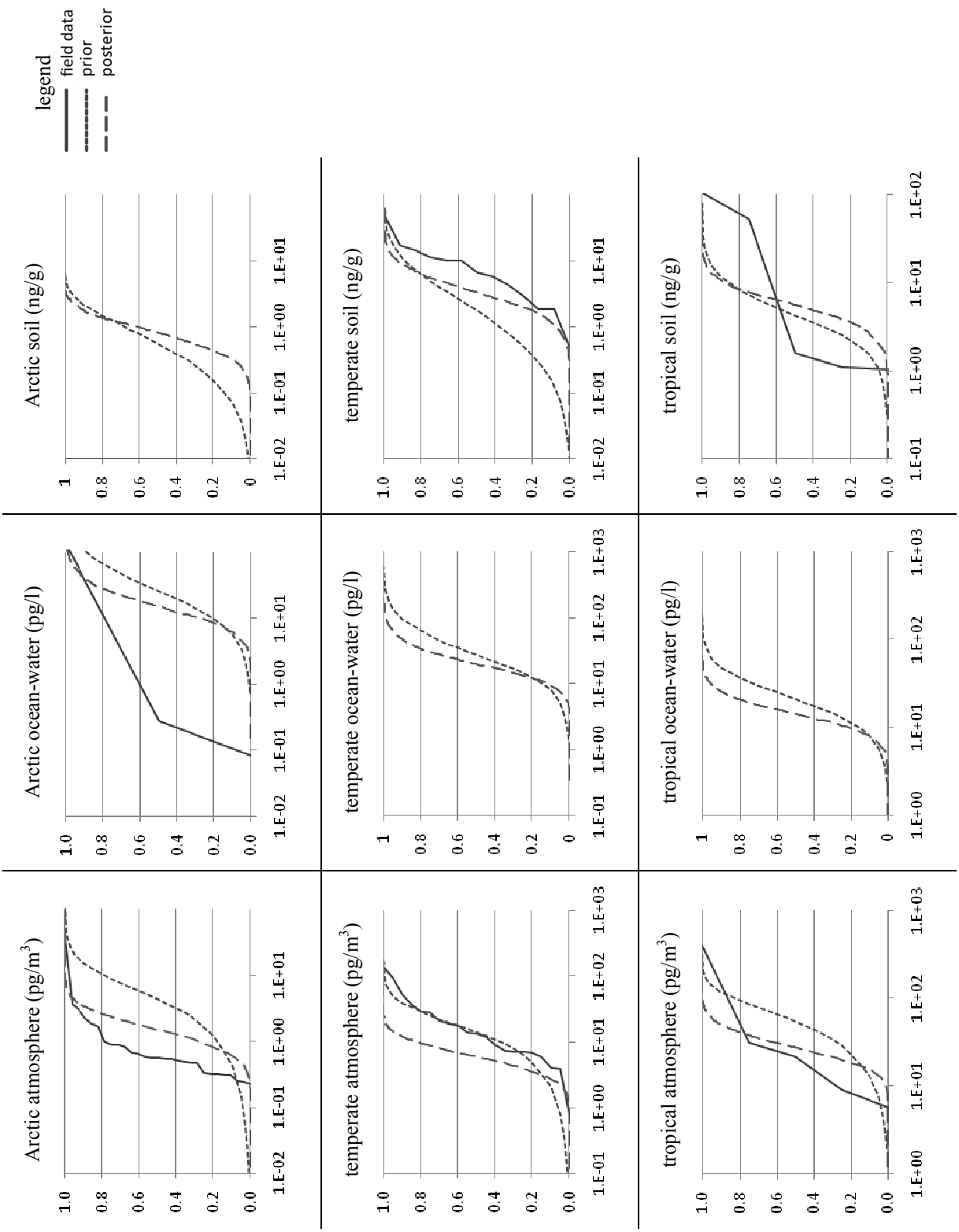

Figure 9.10: Cumulative distribution functions of model results before and after the Bayesian updating procedure, and corresponding measurements. The *y* axis gives the percentage of model runs / measurements that lie below a given concentration, the *x* axis gives the corresponding concentrations.

9.5.6 Additional Results on the Bayesian Updating Procedure

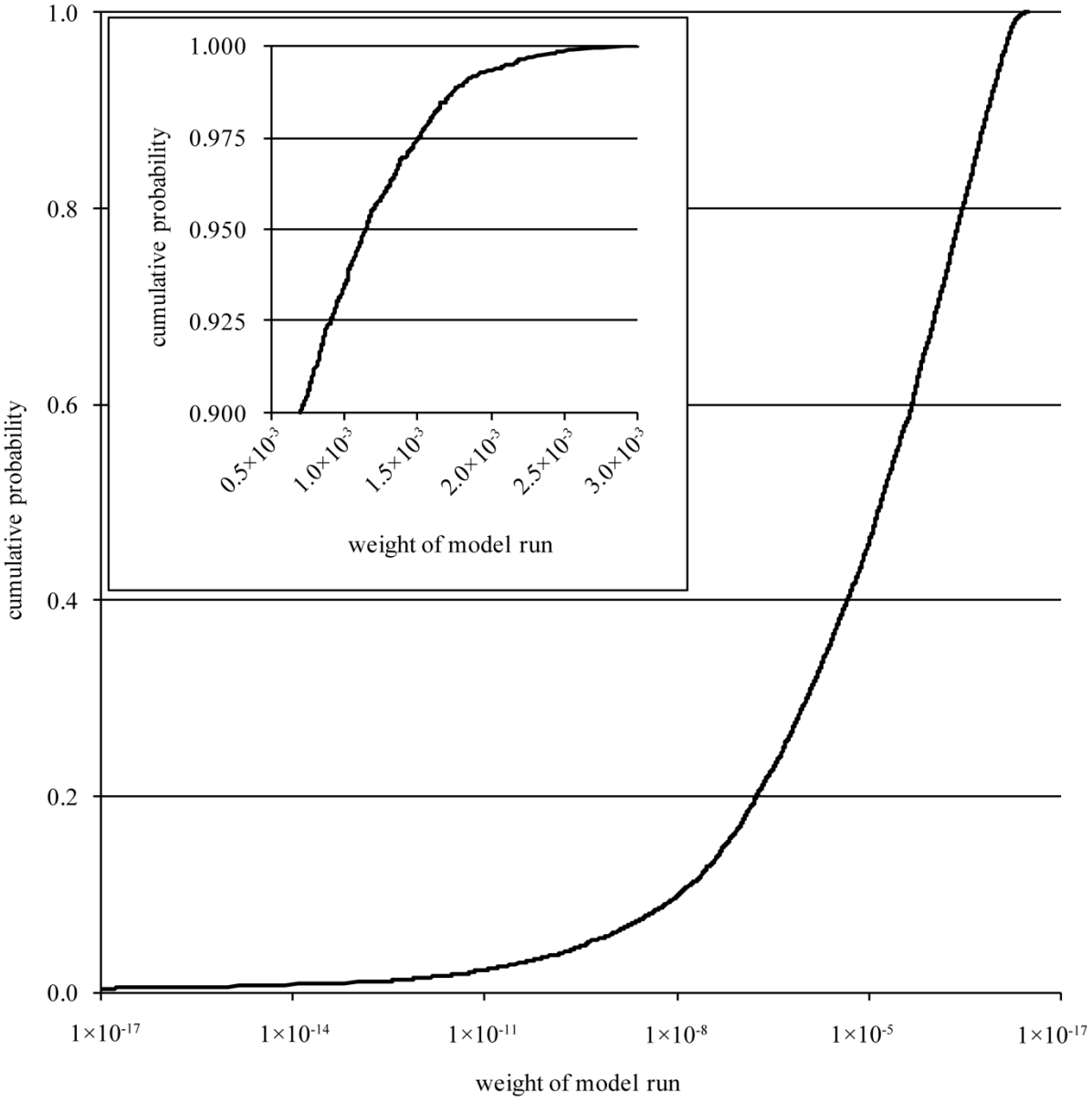

Figure 9.11: Cumulative distribution function of the weights given by the Bayesian updating procedure to the model runs. The small figure in the top-left part is a magnification of the total figure from the upper range of the cumulative probability. The *y* axis gives the percentage of model runs with a weight smaller than the corresponding value on the *x* axis. For example, 40% of all model runs have a weight below about 1×10^{-5} (big figure), 97.5% of all model runs have a weight below about 0.0015 (small figure).

References

Agarwal, H. C., Singh, D. K. and Sharma, V. B. (**1994**): Persistence, metabolism and binding of p,p'-DDT in soil in Delhi, India. *J. Environ. Sci. Health., B* 29: 73-86.

Agrell, C., ter Schure, A. F. H., Sveder, J., Bokenstrand, A., Larsson, P. and Zegers, B. N. (**2004**): Polybrominated diphenyl ethers (PBDEs) at a solid waste incineration plant I: Atmospheric concentrations. *Atmos. Environ.* 38: 5139-5148.

Ahn, M. Y., Filley, T. R., Jafvert, C. T., Nies, L., Hua, I. and Bezares-Cruz, J. (**2006**): Photodegradation of decabromodiphenyl ether adsorbed onto clay minerals, metal oxides, and sediment. *Environ. Sci. Technol.* 40: 215-220.

Aigner, E. J., Leone, A. D. and Falconer, R. L. (**1998**): Concentrations and enantiomeric ratios of organochlorine pesticides in soil from the US corn belt. *Environ. Sci. Technol.* 32: 1162-1168.

Aislabie, J. M., Richards, N. K. and Boul, H. L. (**1997**): Microbial degradation of DDT and its residues - A review. *New. Zeal. J. Agr. Res.* 40: 269-282.

Alcock, R. E., Sweetman, A. J., Prevedouros, K. and Jones, K. C. (**2003**): Understanding levels and trends of BDE-47 in the UK and North America: an assessment of principal reservoirs and source inputs. *Environ. Int.* 29: 691-698.

Andersen, M. P. S., Toft, A., Nielsen, O. J., Hurley, M. D., Wallington, T. J., Chishima, H., Tonokura, K., Mabury, S. A., Martin, J. W. and Ellis, D. A. (**2006**): Atmospheric chemistry of perfluorinated aldehyde hydrates (n-$C_xF_{2x+1}CH(OH)_2$, x=1, 3, 4): Hydration, dehydration, and kinetics and mechanism of Cl atom and OH radical initiated oxidation. *J. Phys. Chem. A* 110: 9854-9860.

Anderson, P. N. and Hites, R. A. (**1996**): OH radical reactions: The major removal pathway for polychlorinated biphenyls from the atmosphere. *Environ. Sci. Technol.* 30: 1756-1763.

Andrea, M. M., Luchini, L. C., Mello, M., Tomita, R. Y., Mesquita, T. B. and Musumeci, M. R. (**1994**): Dissipation and degradation of DDT, DDE and parathion in Brazilian soils. *J. Environ. Sci. Health., B* 29: 121-132.

Arctic Monitoring and Assessment Program (**1998**). AMAP assessment report: Arctic pollution issues. Report by: Arctic Monitoring and Assessment Program (AMAP), Oslo.

Arctic Monitoring and Assessment Program (**2004**). AMAP assessment 2002: Persistent organic pollutants in the Arctic. Report by: Arctic Monitoring and Assessment Program (AMAP), Oslo.

Arisoy, M. (**1998**): Biodegradation of chlorinated organic compounds by white-rot fungi. *Bull. Environ. Contam. Toxicol.* 60: 872-876.

Armitage, J., Cousins, I. T., Buck, R. C., Prevedouros, K., Russell, M. H., MacLeod, M. and Korzeniowski, S. H. (**2006**): Modeling global-scale fate and transport of perfluorooctanoate emitted from direct sources. *Environ. Sci. Technol.* 40: 6969-6975.

Arnot, J., Gouin, T. and Mackay, D. (**2005**). Practical methods for estimating environmental biodegradation rates. Report by: Canadian Environmental Modelling Network, Peterborough.

Arp, H. P. H., Niederer, C. and Goss, K. U. (**2006**): Predicting the partitioning behavior of various highly fluorinated compounds. *Environ. Sci. Technol.* 40: 7298-7304.

Atkinson, R. (**1987**): A structure-activity relationship for the estimation of rate constants for the gas-phase reactions of OH radicals with organic compounds. *Int. J. Chem. Kinet.* 19: 799-828.

Atkinson, R. (**2000**): Atmospheric chemistry of VOCs and NO_x. *Atmos. Environ.* 34: 2063-2101.

Atkinson, R., Baulch, D. L., Cox, R. A., Hampson, R. F., Kerr, J. A. and Troe, J. (**1989**): Evaluated kinetic and photochemical data for atmospheric chemistry. 3. Iupac subcommittee on gas kinetic data evaluation for atmospheric chemistry. *J. Phys. Chem. Ref. Data* 18: 881-1097.

Bailey, P., Waite, D., Quinnett-Abbott, L. and Ripley, B. D. (**2005**): Residues of DDT and other selected organochlorine pesticides in soils from Saskatchewan, Canada (1999). *Can. J. Soil Sci.* 85: 265-271.

Bailey, R., Barrie, L. A., Halsall, C. J., Fellin, P. and Muir, D. C. G. (**2000**): Atmospheric organochlorine pesticides in the western Canadian Arctic: Evidence of transpacific transport. *J. Geophys. Res.-Atmos.* 105: 11805-11811.

Baker, J. E., Totten, L. A., Gigliotti, C. L., Offenberg, J. H., Eisenreich, S. J., Bamford, H. A., Huie, R. E. and Poster, D. L. (**2004**): Response to comment on "Reevaluation of air-water exchange fluxes of PCBs in green bay and southern Lake Michigan". *Environ. Sci. Technol.* 38: 1629-1632.

Bamford, H. A., Poster, D. L. and Baker, J. E. (**2000**): Henry's law constants of polychlorinated biphenyl congeners and their variation with temperature. *J. Chem. Eng. Data* 45: 1069-1074.

Bandala, E. R., Gelover, S., Leal, M. T., Arancibia-Bulnes, C., Jimenez, A. and Estrada, C. A. (**2002**): Solar photocatalytic degradation of Aldrin. *Catal. Today* 76: 189.

Barber, J. L., Berger, U., Chaemfa, C., Huber, S., Jahnke, A., Temme, C. and Jones, K. C. (**2007**): Analysis of per- and polyfluorinated alkyl substances in air samples from Northwest Europe. *J. Environ. Monit.* 9: 530-541.

Baughman, G. L. and Lassiter, R. R. Prediction of environmental pollution concentration. In *Estimating the hazard of chemical substances to aquatic life*; J. Cairns, K. L. Dickson and A. W. Maki, J. Cairns, K. L. Dickson and A. W. MakiJ. Cairns, K. L. Dickson and A. W. Makis; American society for testing and materials: Philadelphia, **1978**; Vol. 657, pp 35-54.

Behymer, T. D. and Hites, R. A. (**1988**): Photolysis of polycyclic aromatic-hydrocarbons adsorbed on fly-ash. *Environ. Sci. Technol.* 22: 1311-1319.

Beyer, A., Wania, F., Gouin, T., Mackay, D. and Matthies, M. (**2002**): Selecting internally consistent physicochemical properties of organic compounds. *Environ. Toxicol. Chem.* 21: 941-953.

Bezares-Cruz, J., Jafvert, C. T. and Hua, I. (**2004**): Solar photodecomposition of decabromodiphenyl ether: Products and quantum yield. *Environ. Sci. Technol.* 38: 4149-4156.

Bidleman, T. F. and Leone, A. D. (**2004**): Soil-air exchange of organochlorine pesticides in the Southern United States. *Environ. Pollut.* 128: 49-57.

Bidleman, T. F., Leone, A. D., Wong, F., van Vliet, L., Szeto, S. and Ripley, B. D. (**2006**): Emission of legacy chlorinated pesticides from agricultural and orchard soils in British Columbia, Canada. *Environ. Toxicol. Chem.* 25: 1448-1457.

Bignert, A., Olsson, M., Persson, W., Jensen, S., Zakrisson, S., Litzen, K., Eriksson, U., Haggberg, L. and Alsberg, T. (**1998**): Temporal trends of organochlorines in Northern Europe, 1967-1995. Relation to global fractionation, leakage from sediments and international measures. *Environ. Pollut.* 99: 177-198.

Bogdal, C., Kohler, M. and Schmid, P. Personal Communication to U. Schenker, Zurich, in **2007**.

Boul, H. L. (**1995**): DDT residues in the environment - a review with a New-Zealand perspective. *New. Zeal. J. Agr. Res.* 38: 257-277.

Boul, H. L. (**1996**): Effect of soil moisture on the fate of radiolabelled DDT and DDE in vitro. *Chemosphere* 32: 855-866.

Boul, H. L., Garnham, M. L., Hucker, D., Baird, D. and Aislable, J. (**1994**): Influence of agricultural practices on the levels of DDT and its residues in soil. *Environ. Sci. Technol.* 28: 1397-1402.

Boxall, A. B. A., Sinclair, C. J., Fenner, K., Kolpin, D. and Maud, S. J. (**2004**): When synthetic chemicals degrade in the environment. *Environ. Sci. Technol.* 38: 368A-375A.

Brace, N. O. (**1962**): Long chain alkanoic and alkenoic acids with perfluoroalkyl terminal segments. *J. Org. Chem.* 27: 4491-4498.

Braekevelt, E., Tittlemier, S. A. and Tomy, G. T. (**2003**): Direct measurement of octanol-water partition coefficients of some environmentally relevant brominated diphenyl ether congeners. *Chemosphere* 51: 563-567.

Brand, K. P. and Small, M. J. (**1995**): Updating uncertainty in an integrated risk assessment: Conceptual framework and methods. *Risk Anal.* 15: 719-731.

Breivik, K., Sweetman, A., Pacyna, J. M. and Jones, K. C. (**2002**): Towards a global historical emission inventory for selected PCB congeners - a mass balance approach 2. Emissions. *Sci. Total Environ.* 290: 199-224.

Breivik, K. and Wania, F. (**2002**): Evaluating a model of the historical behavior of two hexachlorocyclohexanes in the Baltic sea environment. *Environ. Sci. Technol.* 36: 1014-1023.

Breivik, K., Wania, F., Muir, D. C. G., Alaee, M., Backus, S. and Pacepavicius, G. (**2006**): Empirical and modeling evidence of the long-range atmospheric transport of decabromodiphenyl ether. *Environ. Sci. Technol.* 40: 4612-4618.

Brown, D., (**2006**). WHO urges use of DDT in Africa, in *Washington Post* on September 16, 2006.

Burkhard, L. P., Andren, A. W. and Armstrong, D. E. (**1985a**): Estimation of vapor-pressures for polychlorinated-biphenyls - a comparison of 11 predictive methods. *Environ. Sci. Technol.* 19: 500-507.

Burkhard, L. P., Armstrong, D. E. and Andren, A. W. (**1985b**): Henry law constants for the polychlorinated-biphenyls. *Environ. Sci. Technol.* 19: 590-596.

Buser, H. R. and Müller, M. D. (**1993**): Enantioselective determination of chlordane components, metabolites, and photoconversion products in environmental-samples using chiral high-resolution gas-chromatography and mass-spectrometry. *Environ. Sci. Technol.* 27: 1211-1220.

Butt, C. M., Diamond, M. L., Truong, J., Ikonomou, M. G. and ter Schure, A. F. H. (**2004**): Spatial distribution of polybrominated diphenyl ethers in southern Ontario as measured in indoor and outdoor window organic films. *Environ. Sci. Technol.* 38: 724-731.

Butt, C. M., Muir, D. C. G., Stirling, I., Kwan, M. and Mabury, S. A. (**2007**): Rapid response of Arctic ringed seals to changes in perfluoroalkyl production. *Environ. Sci. Technol.* 41: 42-49.

Cahill, T. M., Cousins, I. and Mackay, D. (**2003**): General fugacity-based model to predict the environmental fate of multiple chemical species. *Environ. Toxicol. Chem.* 22: 483-493.

Carson, R. L. *Silent spring*; Houghton Mifflin: Boston, **1962**.

Cetin, B. and Odabasi, M. (**2005**): Measurement of Henry's law constants of seven polybrominated diphenyl ether (PBDE) congeners as a function of temperature. *Atmos. Environ.* 39: 5273-5280.

Chen, L. G., Mai, B. X., Bi, X. H., Chen, S. J., Wang, X. M., Ran, Y., Luo, X. J., Sheng, G. Y., Fu, J. M. and Zeng, E. Y. (**2006**): Concentration levels, compositional profiles, and gas-particle partitioning of polybrominated diphenyl ethers in the atmosphere of an urban city in South China. *Environ. Sci. Technol.* 40: 1190-1196.

Chiappero, M. S., Malanca, F. E., Arguello, G. A., Wooldridge, S. T., Hurley, M. D., Ball, J. C., Wallington, T. J., Waterland, R. L. and Buck, R. C. (**2006**): Atmospheric chemistry of perfluoroaldehydes ($C_xF_{2x+1}CHO$) and fluorotelomer aldehydes ($C_xF_{2x+1}CH_2CHO$): Quantification of the important role of photolysis. *J. Phys. Chem. A* 110: 11944-11953.

Ciani, A., Goss, K. U. and Schwarzenbach, R. P. (**2005**): Light penetration in soil and particulate minerals. *Eur. J. Soil Sci.* 56: 561-574.

Cohen, M. D., Draxler, R. R., Artz, R., Commoner, B., Bartlett, P., Cooney, P., Couchot, K., Dickar, A., Eisl, H., Hill, C., Quigley, J., Rosenthal, J. E., Niemi, D., Ratte, D., Deslauriers, M., Laurin, R., Mathewson-Brake, L. and McDonald, J. (**2002**): Modeling the atmospheric transport and deposition of PCDD/F to the Great Lakes. *Environ. Sci. Technol.* 36: 4831-4845.

Cole, J. G. and Mackay, D. (**2000**): Correlating environmental partitioning properties of organic compounds: The three solubility approach. *Environ. Toxicol. Chem.* 19: 265-270.

Corona-Cruz, A., Gold-Bouchot, G., Gutierrez-Rojas, M., Monroy-Hermosillo, O. and Favela, E. (**1999**): Anaerobic-aerobic biodegradation of DDT (dichlorodiphenyl trichloroethane) in soils. *Bull. Environ. Contam. Toxicol.* 63: 219-225.

Cramer, J. (**1973**): Model of Circulation of DDT on Earth. *Atmos. Environ.* 7: 241-256.

Crosby, D. G. and Moilanen, K. W. (**1977**): Vapor-phase photodecomposition of DDT. *Chemosphere* 6: 167-172.

CrystalBall. Webpage http://www.crystalball.com/crystal_ball/index.html, accessed **2008a**.

CrystalBall. Webpage http://www.decisioneering.com/support/simulation/cbl_gen_004A.html, accessed **2008b**.

D'Eon, J. C., Hurley, M. D., Wallington, T. J. and Mabury, S. A. (**2006**): Atmospheric chemistry of N-methyl perfluorobutane sulfonamidoethanol, $C_4F_9SO_2N(CH_3)CH_2CH_2OH$: Kinetics and mechanism of reaction with OH. *Environ. Sci. Technol.* 40: 1862-1868.

da Rosa, M. B., Kruger, H. U., Thomas, S. and Zetzsch, C. (**2003**): Photolytic debromination and degradation of decabromodiphenyl ether, an exploratory kinetic study in toluene. *Fresenius Environ. Bull.* 12: 940-945.

Dachs, J., Lohmann, R., Ockenden, W. A., Mejanelle, L., Eisenreich, S. J. and Jones, K. C. (**2002**): Oceanic biogeochemical controls on global dynamics of persistent organic pollutants. *Environ. Sci. Technol.* 36: 4229-4237.

Danish Environmental Protection Agency (**1999**). Brominated Flame Retardants: Substance Flow Analysis and Assessment of Alternatives. Report by: Danish Environmental Protection Agency, Copenhagen.

de Wit, C. A. (**2002**): An overview of brominated flame retardants in the environment. *Chemosphere* 46: 583-624.

Dimond, J. B. and Owen, R. B. (**1996**): Long-term residue of DDT compounds in forest soils in Maine. *Environ. Pollut.* 92: 227-230.

Ellinger, S., Hackenberg, R. and Ballschmitter, K. (**2003**): Determnination of log Kow values for polybromo diphenyl ether (PBDEs) by Capillary Gas Chromatography and by Total Surface Area (TSA) Correlation. *Organohalogen Compd.* 60-65: 341-344.

Ellis, D. A., Martin, J. W., De Silva, A. O., Mabury, S. A., Hurley, M. D., Andersen, M. P. S. and Wallington, T. J. (**2004**): Degradation of fluorotelomer alcohols: A likely atmospheric source of perfluorinated carboxylic acids. *Environ. Sci. Technol.* 38: 3316-3321.

Ellis, D. A., Martin, J. W., Mabury, S. A., Hurley, M. D., Andersen, M. P. S. and Wallington, T. J. (**2003**): Atmospheric lifetime of fluorotelomer alcohols. *Environ. Sci. Technol.* 37: 3816-3820.

Ellis, L. B. M., Hershberger, C. D. and Wackett, L. P. (**1999**): The University of Minnesota biocatalysis/biodegradation database: specialized metabolism for functional genomics. *Nucleic Acids Res.* 27: 373-376.

Ellis, L. B. M., Roe, D. and Wackett, L. P. (**2006**): The University of Minnesota biocatalysis/biodegradation database: the first decade. *Nucleic Acids Res.* 34: D517-D521.

Enderson, J. H. (**1970**): Pesticides - eggshell thinning and lowered production of young in prairie falcons. *Bioscience* 20: 355-356.

Eriksson, J., Green, N., Marsh, G. and Bergman, A. (**2004**): Photochemical decomposition of 15 polybrominated diphenyl ether congeners in methanol/water. *Environ. Sci. Technol.* 38: 3119-3125.

Espinosagonzalez, J., Garcia, V. and Ceballos, J. (**1994**): Dissipation of C-14 p,p'-DDT in 2 Panamanian soils. *J. Environ. Sci. Health., B* 29: 97-102.

European Chemicals Bureau (**2000**). European Union Risk Assessment Report: diphenyl ether; pentabromo deriv. Report by: European Chemicals Bureau, Ispra.

European Chemicals Bureau (**2002**). European Union Risk Assessment Report: bis(pentabromophenyl) ether. Report by: European Chemicals Bureau, Ispra.

European Chemicals Bureau. Webpage http://ecb.jrc.it/php-bin/reframer.php?B=/TGD, accessed **2005**.

European Chemicals Bureau (**2007**). Addendum to the May 2004 environmental risk assessment report for decabromodiphenyl ether. Report by: European Chemicals Bureau, Ispra.

European Commission, **2003**. Directive 2002/95/EC of the European Parliament and of the Council of 27 January 2003 on the restriction of the use of certain hazardous substances in electrical and electronic equipment., Rule number Directive 2002/5/EC.

European Commission. Webpage http://ec.europa.eu/environment/chemicals/reach/reach_intro.htm, accessed **2008**.

European Union, **2006**. Registration, evaluation, authorisation, and restriction of chemicals (REACH), Rule number (EC) No 1907/2006. European Union.

Falconer, R. L. and Bidleman, T. F. (**1994**): Vapor-pressures and predicted particle gas distributions of polychlorinated biphenyl congeners as functions of temperature and orthochlorine substitution. *Atmos. Environ.* 28: 547-554.

Fenner, K. (**2001**): Transformation products in environmental risk assessment: joint and secondary persistence as new indicators for the overall hazard of chemical pollutants. PhD Thesis, ETH Zurich, Zurich.

Fenner, K., Kooijman, C., Scheringer, M. and Hungerbühler, K. (**2002**): Including transformation products into the risk assessment for chemicals: The case of nonylphenol ethoxylate usage in Switzerland. *Environ. Sci. Technol.* 36: 1147-1154.

Fenner, K., Scheringer, M. and Hungerbühler, K. (**2000**): Persistence of parent compounds and transformation products in a level IV multimedia model. *Environ. Sci. Technol.* 34: 3809-3817.

Fenner, K., Scheringer, M. and Hungerbühler, K. (**2003**): Joint persistence of transformation products in chemicals assessment: case studies and uncertainty analysis. *Risk Anal.* 23: 35-53.

Finizio, A., Mackay, D., Bidleman, T. and Harner, T. (**1997**): Octanol-air partition coefficient as a predictor of partitioning of semivolatile organic chemicals to aerosols. *Atmos. Environ.* 31: 2289-2296.

Fowler, S. W. (**1990**): Critical review of selected heavy-metal and chlorinated-hydrocarbon concentrations in the marine-environment. *Mar. Environ. Res.* 29: 1-64.

Frost and Sullivan (**1997**). European flame-retardant chemical markets. Report by: Frost & Sullivan, Mountain View.

Gasser, L., Fenner, K. and Scheringer, M. (**2007**): Indicators for the exposure assessment of transformation products of organic micropollutants. *Environ. Sci. Technol.* 41: 2445-2451.

Gerecke, A. C., Hartmann, P. C., Heeb, N. V., Kohler, H. P. E., Giger, W., Schmid, P., Zennegg, M. and Kohler, M. (**2005**): Anaerobic degradation of decabromodiphenyl ether. *Environ. Sci. Technol.* 39: 1078-1083.

Goss, K. U. (**2008**): The pKa values of PFOA and other highly fluorinated carboxylic acids. *Environ. Sci. Technol.* 42: 456-458.

Goss, K. U., Wania, F., McLachlan, M. S., Mackay, D. and Schwarzenbach, R. P. (**2004**): Comment on "Reevaluation of air-water exchange fluxes of PCBs in green bay and southern Lake Michigan". *Environ. Sci. Technol.* 38: 1626-1628.

Götz, C. W., Scheringer, M., MacLeod, M., Wegmann, F., Schenker, U. and Hungerbühler, K. (**2008**): Dependence of persistence and long-range transport potential on gas-particle partitioning in multimedia models. *Environ. Sci. Technol.* in press.

Gouin, T. and Harner, T. (**2003**): Modelling the environmental fate of the polybrominated diphenyl ethers. *Environ. Int.* 29: 717-724.

Gouin, T., Thomas, G. O., Chaemfa, C., Harner, T., Mackay, D. and Jones, K. C. (**2006**): Concentrations of decabromodiphenyl ether in air from Southern Ontario: Implications for particle-bound transport. *Chemosphere* 64: 256-261.

Guillette, L. J., Gross, T. S., Masson, G. R., Matter, J. M., Percival, H. F. and Woodward, A. R. (**1994**): Developmental abnormalities of the gonad and abnormal sex-hormone concentrations in juvenile alligators from contaminated and control lakes in Florida. *Environ. Health Perspect.* 102: 680-688.

Halsall, C. J., Bailey, R., Stern, G. A., Barrie, L. A., Fellin, P., Muir, D. C. G., Rosenberg, B., Rovinsky, F. Y., Kononov, E. Y. and Pastukhov, B. (**1998**): Multi-year observations of organohalogen pesticides in the Arctic atmosphere. *Environ. Pollut.* 102: 51-62.

Hargrave, B. T., Vass, W. P., Erickson, P. E. and Fowler, B. R. (**1988**): Atmospheric transport of organochlorines to the Arctic ocean. *Tellus* 40B: 480-493.

Harner, T. and Shoeib, M. (**2002**): Measurements of octanol-air partition coefficients (K_{OA}) for polybrominated diphenyl ethers (PBDEs): Predicting partitioning in the environment. *J. Chem. Eng. Data* 47: 228-232.

Harner, T., Shoeib, M., Diamond, M., Stern, G. and Rosenberg, B. (**2004**): Using passive air samplers to assess urban - rural trends for persistent organic pollutants. 1. Polychlorinated biphenyls and organochlorine pesticides. *Environ. Sci. Technol.* 38: 4474-4483.

Harner, T., Wideman, J. L., Jantunen, L. M. M., Bidleman, T. F. and Parkhurst, M. J. (**1999**): Residues of organochlorine pesticides in Alabama soils. *Environ. Pollut.* 106: 323-332.

Hayakawa, K., Takatsuki, H., Watanabe, I. and Sakai, S. (**2004**): Polybrominated diphenyl ethers (PBDEs), polybrominated dibenzo-p-dioxins/dibenzofurans (PBDD/Fs) and monobromo-polychlorinated dibenzo-p-dioxins/dibenzofurans (MoBPXDD/Fs) in the atmosphere and bulk deposition in Kyoto, Japan. *Chemosphere* 57: 343-356.

Health Canada, **2001**. Proposed Regulatory Decision Document: Trinexapac-Ethyl, Rule number PRDD2001-05. Pest Management Regulatory Agency.

Helling, C. S., Engelke, B. F. and Doherty, M. A. (**1994**): DDT dissipation in Hawaiian in-situ soil columns. *J. Environ. Sci. Health., B* 29: 103-119.

Helmert, F. R. *Die Ausgleichungsrechnung nach der Methode der kleinsten Quadrate*; Leipzig, **1872**.

Hertwich, E. G. (**2001**): Intermittent rainfall in dynamic multimedia fate modeling. *Environ. Sci. Technol.* 35: 936-940.

Hertwich, E. G., McKone, T. E. and Pease, W. S. (**1999**): Parameter uncertainty and variability in evaluative fate and exposure models. *Risk Anal.* 19: 1193-1204.

Hjellbrekke, A. G. Online Database: http://www.nilu.no/projects/ccc/onlinedata/pops/index.html, accessed **2007**.

Hoepcke, W. *Fehlerlehre und Ausgleichsrechnung*; Gruyter: Berlin New York, **1980**.

Hoff, R. M., Muir, D. C. G. and Grift, N. P. (**1992**): Annual cycle of polychlorinated-biphenyls and organohalogen pesticides in air in Southern Ontario. 1. Air concentration data. *Environ. Sci. Technol.* 26: 266-275.

Hoff, R. M., Strachan, W. M. J., Sweet, C. W., Chan, C. H., Shackleton, M., Bidleman, T. F., Brice, K. A., Burniston, D. A., Cussion, S., Gatz, D. F., Harlin, K. and Schroeder, W. H. (**1996**): Atmospheric deposition of toxic chemicals to the Great Lakes: A review of data through 1994. *Atmos. Environ.* 30: 3505-3527.

Hoh, E. and Hites, R. A. (**2005**): Brominated flame retardants in the atmosphere of the east-central United States. *Environ. Sci. Technol.* 39: 7794-7802.

Houde, M., Martin, J. W., Letcher, R. J., Solomon, K. R. and Muir, D. C. G. (**2006**): Biological monitoring of polyfluoroalkyl substances: A review. *Environ. Sci. Technol.* 40: 3463-3473.

Howard, P. H. *Handbook of environmental fate and exposure data for organic chemicals, Vol. III. Pesticides*; Lewis: Chelsea, Michigan, **1991**.

Huang, Q. D. and Hong, C. S. (**2002**): Aqueous solubilities of non-ortho and mono-ortho PCBs at four temperatures. *Water Res.* 36: 3543-3552.

Hung, H., Blanchard, P., Halsall, C. J., Bidleman, T. F., Stern, G. A., Fellin, P., Muir, D. C. G., Barrie, L. A., Jantunen, L. M., Helm, P. A., Ma, J. and Konoplev, A. (**2005**): Temporal and spatial variabilities of atmospheric polychlorinated biphenyls (PCBs), organochlorine (OC) pesticides and polycyclic aromatic hydrocarbons (PAHs) in the Canadian Arctic: Results from a decade of monitoring. *Sci. Total Environ.* 342: 119-144.

Hung, H., Halsall, C. J., Blanchard, P., Li, H. H., Fellin, P., Stern, G. and Rosenberg, B. (**2002**): Temporal trends of organochlorine pesticides in the Canadian Arctic atmosphere. *Environ. Sci. Technol.* 36: 862-868.

Hussain, A., Maqbool, U. and Asi, M. (**1994**): Studies on dissipation and degradation of C-14 DDT and C-14 DDE in Pakistani soils under field conditions. *J. Environ. Sci. Health., B* 29: 1-15.

IAL Consultants (**1999**). The European flame retardant chemical industry 1998. Report by: IAL Consultants, London.

Ikonomou, M. G., Rayne, S. and Addison, R. F. (**2002**): Exponential increases of the brominated flame retardants, polybrominated diphenyl ethers, in the Canadian arctic from 1981 to 2000. *Environ. Sci. Technol.* 36: 1886-1892.

Iwata, H., Tanabe, S., Sakai, N., Nishimura, A. and Tatsukawa, R. (**1994**): Geographical-distribution of persistent organochlorines in air, water and sediments from Asia and Oceania, and their implications for global redistribution from lower latitudes. *Environ. Pollut.* 85: 15-33.

Iwata, H., Tanabe, S., Sakal, N. and Tatsukawa, R. (**1993**): Distribution of persistent organochlorines in the oceanic air and surface seawater and the role of ocean on their global transport and fate. *Environ. Sci. Technol.* 27: 1080-1098.

Iwata, H., Tanabe, S., Ueda, K. and Tatsukawa, R. (**1995**): Persistent organochlorine residues in air, water, sediments, and soils from the Lake Baikal region, Russia. *Environ. Sci. Technol.* 29: 792-801.

Jahnke, A., Ahrens, L., Ebinghaus, R. and Temme, C. (**2007a**): Urban versus remote air concentrations of fluorotelomer alcohols and other polyfluorinated alkyl substances in Germany. *Environ. Sci. Technol.* 41: 745-752.

Jahnke, A., Berger, U., Ebinghaus, R. and Temme, C. (**2007b**): Latitudinal gradient of airborne polyfluorinated alkyl substances in the marine atmosphere between Germany and South Africa (53 degrees N-33 degrees S). *Environ. Sci. Technol.* 41: 3055-3061.

Jaward, F. M., Farrar, N. J., Harner, T., Sweetman, A. J. and Jones, K. C. (**2004a**): Passive air sampling of PCBs, PBDEs, and organochlorine pesticides across Europe. *Environ. Sci. Technol.* 38: 34-41.

Jaward, F. M., Meijer, S. N., Steinnes, E., Thomas, G. O. and Jones, K. C. (**2004b**): Further studies on the latitudinal and temporal trends of persistent organic pollutants in Norwegian and UK background air. *Environ. Sci. Technol.* 38: 2523-2530.

Jaward, T. M., Zhang, G., Nam, J. J., Sweetman, A. J., Obbard, J. P., Kobara, Y. and Jones, K. C. (**2005**): Passive air sampling of polychlorinated biphenyls, organochlorine compounds, and polybrominated diphenyl ethers across Asia. *Environ. Sci. Technol.* 39: 8638-8645.

Jaworska, J., Dimitrov, S., Nikolova, N. and Mekenyan, O. (**2002**): Probabilistic assessment of biodegradability based on metabolic pathways: Catabol system. *SAR QSAR Environ. Res.* 13: 307-323.

Jolliet, O. and Hauschild, M. (**2005**): Modeling the influence of intermittent rain events on long-term fate and transport of organic air pollutants. *Environ. Sci. Technol.* 39: 4513-4522.

Jonsson, P., Eckhell, J. and Larsson, P. (**2000**): PCB and DDT in laminated sediments from offshore and archipelago areas of the NW Baltic Sea. *Ambio* 29: 268-276.

Jury, W. A., Spencer, W. F. and Farmer, W. J. (**1983**): Behavior assessment model for trace organics in soil. 1. Model description. *J. Environ. Qual.* 12: 558-564.

Kalantzi, O. I., Alcock, R. E., Johnston, P. A., Santillo, D., Stringer, R. L., Thomas, G. O. and Jones, K. C. (**2001**): The global distribution of PCBs and organochlorine pesticides in butter. *Environ. Sci. Technol.* 35: 1013-1018.

Kallenborn, R. Personal Communication to M. Stroebe, Zurich, in **2004**.

Kannan, K., Battula, S., Loganathan, B. G., Hong, C. S., Lam, W. H., Villeneuve, D. L., Sajwan, K., Giesy, J. P. and Aldous, K. M. (**2003**): Trace organic contaminants, including toxaphene and trifluralin, in cotton field soils from Georgia and South Carolina, USA. *Arch. Environ. Contam. Toxicol.* 45: 30-36.

Karlsson, H., Muir, D. C. G., Teixiera, C. F., Burniston, D. A., Strachan, W. M. J., Hecky, R. E., Mwita, J., Bootsma, H. A., Grift, N. P., Kidd, K. A. and Rosenberg, B. (**2000**): Persistent chlorinated pesticides in air, water, and precipitation from the Lake Malawi area, southern Africa. *Environ. Sci. Technol.* 34: 4490-4495.

Koziol, A. S. and Pudykiewicz, J. A. (**2001**): Global-scale environmental transport of persistent organic pollutants. *Chemosphere* 45: 1181-1200.

Krüger, H. U., Gavrilov, R., Liu, Q. and Zetzsch, C. (**2005**). Entwicklung eines Persistenz-Messverfahrens für den troposphärischen Abbau von mittelflüchtigen Pflanzenschutzmitteln durch OH-Radikale. Report by: Deutsches Umweltbundesamt, Berlin.

Kucklick, J. R., Bidleman, T. F., McConnell, L. L., Walla, M. D. and Ivanov, G. P. (**1994**): Organochlorines in the water and biota of Lake Baikal, Siberia. *Environ. Sci. Technol.* 28: 31-37.

Kuivikko, M., Kotiaho, T., Hartonen, K., Vähätalo, A. V. and Tanskanen, A. (**2006**): Direct photolytic decomposition of polybrominated diphenyl ethers in surface waters. *Organohalogen Compd.* 68: 1995-1998.

Kuramochi, H., Maeda, K. and Kawamoto, K. (**2007**): Physicochemical properties of selected polybrominated diphenyl ethers and extension of the UNIFAC model to brominated aromatic compounds. *Chemoshere* 67: 1858-1865.

Kurt-Karakus, P. B. (**2006**): Persistent organic pollutants and soils: Studies on their distribution, air-soil exchange and degradation. PhD Thesis, Lancaster University, Lancaster.

Kurt-Karakus, P. B., Bidleman, T. F., Staebler, R. M. and Jones, K. C. (**2006**): Measurement of DDT fluxes from a historically treated agricultural soil in Canada. *Environ. Sci. Technol.* 40: 4578-4585.

Lalah, J. O., Acholla, F. V. and Wandiga, S. O. (**1994**): Fate of C-14 p,p'-DDT in Kenyan tropical soils. *J. Environ. Sci. Health., B* 29: 57-64.

Larsson, P. (**1995**): DDT - Fate in tropical and temperate regions. *Naturwissenschaften* 82: 559 - 561.

Lau, F. K., Charles, M. J. and Cahill, T. M. (**2006**): Evaluation of gas-stripping methods for the determination of Henry's law constants for polybrominated diphenyl ethers and polychlorinated biphenyls. *J. Chem. Eng. Data* 51: 871-878.

Lau, F. K., Destaillats, H. and Charles, M. J. (**2003**): Expermimentally determined Henry's law constants for six brominated diphenyl ether congeners. *Organohalogen Compd.* 63: 333-336.

Law, R. J., Allchin, C. R., de Boer, J., Covaci, A., Herzke, D., Lepom, P., Morris, S., Tronczynski, J. and de Wit, C. A. (**2006**): Levels and trends of brominated flame retardants in the European environment. *Chemosphere* 64: 187-208.

Lee, R. G. M., Thomas, G. O. and Jones, K. C. (**2004**): PBDEs in the atmosphere of three locations in western Europe. *Environ. Sci. Technol.* 38: 699-706.

Lei, Y. D., Wania, F., Shiu, W. Y. and Boocock, D. G. B. (**2000**): HPLC-based method for estimating the temperature dependence of n-octanol-water partition coefficients. *J. Chem. Eng. Data* 45: 738-742.

Leip, A. and Lammel, G. (**2004**): Indicators for persistence and long-range transport potential as derived from multicompartment chemistry-transport modelling. *Environ. Pollut.* 128: 205-221.

Leung, A. O. W., Luksemburg, W. J., Wong, A. S. and Wong, M. H. (**2007**): Spatial distribution of polybrominated diphenyl ethers and polychlorinated dibenzo-p-dioxins and dibenzofurans in soil and combusted residue at Guiyu, an electronic waste recycling site in southeast China. *Environ. Sci. Technol.* 41: 2730-2737.

Li, N. Q., Wania, F., Lei, Y. D. and Daly, G. L. (**2003**): A comprehensive and critical compilation, evaluation, and selection of physical-chemical property data for selected polychlorinated biphenyls. *J. Phys. Chem. Ref. Data* 32: 1545-1590.

Li, Y. F. and Bidleman, T. F. (**2003**). Usage and emissions of organochlorine pesticides, Canadian Arctic contaminants assessment report II, Physical environment, part II, chapter A.2. Report by: Minister of Indian Affairs and Northern Development, Ottawa.

Li, Y. F. and Macdonald, R. W. (**2005**): Sources and pathways of selected organochlorine pesticides to the Arctic and the effect of pathway divergence on HCH trends in biota: a review. *Sci. Total Environ.* 342: 87-106.

Li, Y. F., Venkatesh, S. and Li, D. (**2004**): Modeling global emissions and residues of pesticides. *Environ. Model. Assess.* 9: 237-243.

Li, Y. F., Zhulidov, A. V., Robarts, R. D., Korotova, L. G., Zhulidov, D. A., Yurtovaya, T. Y. and Ge, L. P. (**2006**): Dichlorodiphenyltrichloroethane usage in the former Soviet Union. *Sci. Total Environ.* 357: 138-145.

Liu, Q., Krueger, H. U. and Zetzsch, C., *Degradation study of the aerosol-borne insecticides dicofol and DDT in an aerosol smog chamber facility by OH radicals in relation to the POPs convention*. Conference proceeding to European Geosciences Union, **2005**, Vienna.

Lohmann, R. Personal Communication to U. Schenker, Zurich, in **2007**.

Lohmann, R., Jurado, E., Pilson, M. E. Q. and Dachs, J. (**2006a**): Oceanic deep water formation as a sink of persistent organic pollutants. *Geophys. Res. Lett.* 33: L12607.

Lohmann, S. C., Schilling, B., Mayer, B. and Meyer, R. (**2006b**): Long-term variability of solar direct and global irradiance derived from ISCCP data and comparison with re-analysis data. *Solar Energy* 80: 1390-1401.

Luo, Y. Z. and Yang, X. S. (**2007**): A multimedia environmental model of chemical distribution: Fate, transport, and uncertainty analysis. *Chemosphere* 66: 1396-1407.

Mackay, D. (**1979**): Finding fugacity feasible. *Environ. Sci. Technol.* 13: 1218-1223.

Mackay, D., di Guardo, A., Paterson, S. and Cowan, C. E. (**1996**): Evaluating the environmental fate of a variety of types of chemicals using the EQC model. *Environ. Toxicol. Chem.* 15: 1627-1637.

Mackay, D. and Paterson, S. (**1991**): Evaluating the multimedia fate of organic-chemicals - a level-III fugacity model. *Environ. Sci. Technol.* 25: 427-436.

Mackay, D., Paterson, S. and Shiu, W. Y. (**1992**): Generic models for evaluating the regional fate of chemicals. *Chemosphere* 24: 695-717.

Mackay, D., Shiu, W. Y. and Ma, K. C. *Illustrated handbook of physical-chemical properties and environmental fate for organic chemicals*; Lewis: Boca-Raton, **1997**.

MacLeod, M., Fraser, A. J. and Mackay, D. (**2002**): Evaluating and expressing the propagation of uncertainty in chemical fate and bioaccumulation models. *Environ. Toxicol. Chem.* 21: 700-709.

MacLeod, M., McKone, T. E., Foster, K. L., Maddalena, R. L., Parkerton, T. F. and Mackay, D. (**2004**): Applications of contaminant fate and bioaccumulation models in assessing ecological risks of chemicals: A case study for gasoline hydrocarbons. *Environ. Sci. Technol.* 38: 6225-6233.

MacLeod, M., Scheringer, M. and Hungerbühler, K. (**2007**): Estimating enthalpy of vaporization from vapor pressure using Trouton's rule. *Environ. Sci. Technol.* 41: 2827-2832.

MacLeod, M., Woodfine, D. G., Mackay, D., McKone, T., Bennett, D. and Maddalena, R. (**2001**): BETR North America: A regionally segmented multimedia contaminant fate model for North America. *Environ. Sci. Pollut. R.* 8: 156-163.

Maddalena, R. L., McKone, T. E., Hsieh, D. P. H. and Geng, S. (**2001**): Influential input classification in probabilistic multimedia models. *Stoch. Env. Res. Risk A.* 15: 1-17.

Martin, J. W., Ellis, D. A., Mabury, S. A., Hurley, M. D. and Wallington, T. J. (**2006**): Atmospheric chemistry of perfluoroalkanesulfonamides: Kinetic and product studies of the OH radical and Cl atom initiated oxidation of N-ethyl perfluorobutanesulfonamide. *Environ. Sci. Technol.* 40: 864-872.

Martin, J. W., Muir, D. C. G., Moody, C. A., Ellis, D. A., Kwan, W. C., Solomon, K. R. and Mabury, S. A. (**2002**): Collection of airborne fluorinated organics and analysis by gas chromatography/chemical ionization mass spectrometry. *Anal. Chem.* 74: 584-590.

McKone, T. E. (**1994**): Uncertainty and variability in human exposures to soil contaminants through home-grown food - a Monte Carlo assessment. *Risk Anal.* 14: 449-463.

McKone, T. E., Bodnar, A. B. and Hertwich, E. G. (**2001**). Development and evaluation of state-specific landscape data sets for multimedia source-to-dose models. Report by: Ernest Orlando Lawrence Berkeley National Laboratory, Berkeley.

Meijer, S. N., Halsall, C. J., Harner, T., Peters, A. J., Ockenden, W. A., Johnston, A. E. and Jones, K. C. (**2001**): Organochlorine pesticide residues in archived UK soil. *Environ. Sci. Technol.* 35: 1989-1995.

Meironyte, D., Noren, K. and Bergman, A. (**1999**): Analysis of polybrominated diphenyl ethers in Swedish human milk. A time-related trend study, 1972-1997. *J. Toxicol. Environ. Health-Part A* 58: 329-341.

Meyer, T. and Wania, F. (**2007**): What environmental fate processes have the strongest influence on a completely persistent organic chemical's accumulation in the Arctic? *Atmos. Environ.* 41: 2757-2767.

Meyer, T., Wania, F. and Breivik, K. (**2005**): Illustrating sensitivity and uncertainty in environmental fate models using partitioning maps. *Environ. Sci. Technol.* 39: 3186-3196.

Mikhail, E. M. and Ackermann, F. *Observations and least squares*; IEP-Dun-Donnelley: New York, **1976**.

Miramichi Salmon Conservation Center. Webpage http://www.salmoncentre.ca/ddt.html, accessed **2008**.

Moltmann, J. F., Küppers, K., Knacker, T., Klöpffer, W., Schmidt, E. and Renner, I. (**1999**). Verteilung persistenter Chemikalien in marinen Ökosystem. Report by: ECT Oekotoxikologie GmbH, Floersheim am Main.

Morf, L., Buser, A. and Taverna, R. (**2007**). Dynamic substance flow analysis model for selected brominated flame retardants as a base for decision making on risk reduction measures (FABRO). Report by: Geo Partner AG Resource Management, Zürich.

Morgan, M. G., Henrion, M. and Small, M. *Uncertainty a guide to dealing with uncertainty in quantitative risk and policy analysis*; Cambridge University Press: Cambridge etc., **1990**.

Mueller, M. (**2005**). Gutachten zur Validierung von QSAR-Modellen zur Abschätzung des atmosphärischen Abbaus mit einem Datensatz von ca. 760 Stoffen. Report by: Frauenhofer-Institut für Molekularbiologie und Angewandte Oekologie, Schmallenberg.

Nair, A., Samuel, T. and Pillai, M. K. K. (**1992**): Behavior of DDT in 3 soils exposed to solar radiations under different conditions. *Pestic. Sci.* 34: 333-340.

Ngabe, B. and Bidleman, T. F. (**2006**): DDT concentrations in soils of Brazzaville, Congo. *Bull. Environ. Contam. Toxicol.* 76: 697-704.

Niemeier, W. *Ausgleichungsrechnung: eine Einführung für Studierende und Praktiker des Vermessungs- und Geoinformationswesens*; de Gruyter: Berlin, **2001**.

Norris, J. M., Ehrmantraut, J. W., Gibbons, C. L., Kociba, R. J., Schwetz, B. A., Rose, J. Q., Humiston, C. G., Jewett, G. L., Crummett, W. B., Gehring, P. J., Tirsell, J. B. and Brosier, J. S. (**1973**): Toxicological and environmental factors involved in the selection of decabromodiphenyl oxide as a fire retardant chemical. *Appl. Polym. Symp.* 22: 195-219.

Oehme, M., Schlabach, M., Kallenborn, R. and Haugen, J. E. (**1996**): Sources and pathways of persistent polychlorinated pollutants to remote areas of the North Atlantic and levels in the marine food chain: A research update. *Sci. Total Environ.* 186: 13-24.

Olsman, H., Hagberg, J., Kalbin, G., Julander, A., van Bavell, B., Strid, A., Tysklind, M. and Engwall, M. (**2006**): Ah receptor agonists in UV-exposed toluene solutions of decabromodiphenyl ether (decaBDE) and in soils contaminated with polybrominated diphenyl ethers (PBDEs). *Environ. Sci. Pollut. R.* 13: 161-169.

Olsson, M., Bignert, A., Eckhell, J. and Jonsson, P. (**2000**): Comparison of temporal trends (1940s-1990s) of DDT and PCB in Baltic sediment and biota in relation to eutrophication. *Ambio* 29: 195-201.

Organization for Economic Co-ordination and Development (**2006**): Results of the 2006 survey on the production and use of PFOS, PFAS, PFOA, PFCA, their related substances and products/mixtures containing these substances.

Paasivirta, J. and Asplund, L. *New types of persistent halogenated compounds*; Springer: Berlin, **2000**.

Paasivirta, J., Palm, H., Paukku, R., Akhabuhaya, J. and Lodenius, M. (**1988**): Chlorinated insecticide residues in Tanzanian environment - tanzadrin. *Chemosphere* 17: 2055-2062.

Palm, A., Cousins, I. T., Mackay, D., Tysklind, M., Metcalfe, C. and Alaee, M. (**2002**): Assessing the environmental fate of chemicals of emerging concern: a case study of the polybrominated diphenyl ethers. *Environ. Pollut.* 117: 195-213.

Palm, W. U., Kopetzky, R., Sossinka, W., Ruck, W. and Zetzsch, C. (**2004**): Photochemical reactions of brominated diphenylethers in organic solvents and adsorbed on silicon dioxide in aqueous suspension. *Organohalogen Compd.* 66: 4105-4110.

Park, J. S., Wade, T. L. and Sweet, S. (**2001**): Atmospheric deposition of organochlorine contaminants to Galveston Bay, Texas. *Atmos. Environ.* 35: 3315-3324.

Patton, G. W., Hinckley, D. A., Walla, M. D. and Bidleman, T. F. (**1989**): Airborne organochlorines in the Canadian High Arctic. *Tellus* 41B: 243-255.

Peterman, P. H., Orazio, C. E. and Feltz, K. P. (**2003**): Sunlight photolysis of 39 mono-hepta PBDE congeners in lipid. *Organohalogen Compd.* 63: 357-360.

Piekarz, A. M., Primbs, T., Field, J. A., Barofsky, D. F. and Simonich, S. (**2007**): Semivolatile fluorinated organic compounds in Asian and western U.S. air masses. *Environ. Sci. Technol.* 41: 8248-8255.

Pinsuwan, S., Li, A. and Yalkowsky, S. H. (**1995**): Correlation of octanol water solubility ratios and partition-coefficients. *J. Chem. Eng. Data* 40: 623-626.

Pontolillo, J. and Eganhouse, R. P. (**2001**). The search for reliable aqueous solubility (Sw) and octanol-water partition coefficient (Kow) data for hydrophobic organic compounds: DDT and DDE as a case study. Report by: U. S. Geological Survey, Reston, Virginia.

Prevedouros, K., Cousins, I. T., Buck, R. C. and Korzeniowski, S. H. (**2006**): Sources, fate and transport of perfluorocarboxylates. *Environ. Sci. Technol.* 40: 32-44.

Prevedouros, K., Jones, K. C. and Sweetman, A. J. (**2004**): Estimation of the production, consumption, and atmospheric emissions of pentabrominated diphenyl ether in Europe between 1970 and 2000. *Environ. Sci. Technol.* 38: 3224-3231.

Quartier, R. and Müller-Herold, U. (**2000**): On secondary spatial ranges of transformation products in the environment. *Ecol. Model.* 135: 187-198.

Raff, J. D. and Hites, R. A. (**2006**): Gas-phase reactions of brominated diphenyl ethers with OH radicals. *J. Phys. Chem. A* 110: 10783-10792.

Raff, J. D. and Hites, R. A. (**2007**): Deposition versus Photochemical Removal of PBDEs from Lake Superior Air. *Environ. Sci. Technol.* 41: 6725-6731.

Rahman, F., Langford, K. H., Scrimshaw, M. D. and Lester, J. N. (**2001**): Polybrominated diphenyl ether (PBDE) flame retardants. *Sci. Total Environ.* 275: 1-17.

Rayne, S. and Ikonomou, M. G. (**2005**): Polybrominated diphenyl ethers in an advanced wastewater treatment plant. Part 1: Concentrations, patterns, and influence of treatment processes. *J. Environ. Eng. Sci.* 4: 353-367.

Rayne, S., Wan, P. and Ikonomou, M. (**2006**): Photochemistry of a major commercial polybrominated diphenyl ether flame retardant congener: 2,2 ',4,4 ',5,5 '-Hexabromodiphenyl ether (BDE153). *Environ. Int.* 32: 575-585.

Risk and Policy Analysts LTD (**2004**). Perfluorooctane sulphonate. Risk reduction strategy and analysis of advantages and drawbacks. Report by: Risk and Policy Analysts LTD in association with BRE Environment, Norfolk.

Roberts, T. R. and Hutson, D. H. *Metabolic pathways of agrochemicals*; The Royal Society of Chemistry: Cambridge, **1998**.

Rothenbacher, K. (**2007**): Does decabromodiphenylether (deca-BDE) contribute to the lower brominated diphenylethers found in the environment? *Organohalogen Compd.* 69: 461-464.

Sakai, S., Hirai, Y., Aizawa, H., Ota, S. and Muroishi, Y. (**2006a**): Emission inventory of deca-brominated diphenyl ether (DBDE) in Japan. *J. Mater. Cycles Waste Manage.* 56-62.

Sakai, S., Hirai, Y., Ninomiya, T., Aizawa, H., Nakano, T. and Muroishi, Y. (**2006b**): Emissions inventory of polybrominated diphenyl ehers (PBDEs) on a homologue basis. *Organohalogen Compd.* 68: 1828-1831.

Sakai, S. I., Hirai, Y., Ota, S. and Makiya, K., *Emission factors of PBDD/DFs and PBDEs from textile processing and BFR production, and the tentative PBDE emission inventory*. Conference proceeding to Dioxin Meeting, **2005**, Toronto.

Samuel, T., Agarwal, H. C. and Pillai, M. K. K. (**1988**): Persistence and binding of DDT and gamma-HCH in a sandy loam soil under field conditions in Delhi, India. *Pestic. Sci.* 22: 1-15.

Sanchez-Prado, L., Llompart, M., Lores, M., Garcia-Jares, C. and Cela, R. (**2005**): Investigation of photodegradation products generated after UV-irradiation of five polybrominated diphenyl ethers using photo solid-phase microextraction. *J. Chromatogr. A* 1071: 85-92.

Schenker, U., MacLeod, M., Scheringer, M. and Hungerbühler, K. (**2005a**): Improving accuracy and quality of data for environmental fate models: A least-squares adjustment procedure for harmonizing physicochemical properties of organic compounds. *Environ. Sci. Technol.* 39: 8434-8441.

Schenker, U., MacLeod, M., Scheringer, M. and Hungerbühler, K. Online Database: http://www.sust-chem.ethz.ch/research/product/least_squares_adjustment.xls, accessed **2005b**.

Schenker, U., Scheringer, M. and Hungerbühler, K. (**2007**): Including degradation products of persistent organic pollutants in a global multi-media box model. *Environ. Sci. Pollut. R.* 14: 145-152.

Schenker, U., Scheringer, M. and Hungerbühler, K. (**2008**): Investigating the global fate of DDT: model evaluation and estimation of future trends. *Environ. Sci. Technol.* 42: 1178-1184.

Schenker, U., Wegmann, F., Scheringer, M. and Hungerbühler, K., (**2006**). *Emission scenario comparison*. ETH Zurich. Unpublished Work.

Scheringer, M. (**1996**): Persistence and spatial range as endpoints of an exposure-based assessment of organic chemicals. *Environ. Sci. Technol.* 30: 1652-1659.

Scheringer, M. (**1997**): Characterization of the environmental distribution behavior of organic chemicals by means of persistence and spatial range. *Environ. Sci. Technol.* 31: 2891-2897.

Scheringer, M., Salzmann, M., Stroebe, M., Wegmann, F., Fenner, K. and Hungerbühler, K. (**2004**): Long-range transport and global fractionation of POPs: insights from multimedia modeling studies. *Environ. Pollut.* 128: 177-188.

Scheringer, M., Stroebe, M., Wegmann, F., Salzmann, M. and Hungerbühler, K. (**2002**): Investigating the long-range transport of semivolatile organic chemicals with the two multimedia fate models "ChemRange" and "CliMoChem". *Epidemiology* 13: S116-S116.

Scheringer, M., Wegmann, F., Fenner, K. and Hungerbühler, K. (**2000**): Investigation of the cold condensation of persistent organic pollutants with a global multimedia fate model. *Environ. Sci. Technol.* 34: 1842-1850.

Schmidt, M. (**1996**): University of Minnesota biocatalysis biodegradation database. *Asm News* 62: 102-102.

Schwarzenbach, R. P., Gschwend, P. M. and Imboden, D. M. *Environmental organic chemistry*; Wiley-Interscience: Hoboken, New Jersey, **2003**.

Scott, B. F., Spencer, C., Mabury, S. A. and Muir, D. C. G. (**2006**): Poly and perfluorinated carboxylates in North American precipitation. *Environ. Sci. Technol.* 40: 7167-7174.

Seinfeld, J. H. and Pandis, S. N. *Atmospheric chemistry and physics*; Wiley-Interscience: New York, **1998**.

Semeena, S. and Lammel, G. (**2003**): Effects of various scenarios of entry of DDT and gamma-HCH on the global environmental fate as predicted by a multicompartment chemistry-transport model. *Fresenius Environ. Bull.* 12: 925-939.

Semenza, J. C., Tolbert, P. E., Rubin, C. H., Guillette, L. J. and Jackson, R. J. (**1997**): Reproductive toxins and alligator abnormalities at Lake Apopka, Florida. *Environ. Health Perspect.* 105: 1030-1032.

Shen, L. and Wania, F. (**2005**): Compilation, evaluation, and selection of physical-chemical property data for organochlorine pesticides. *J. Chem. Eng. Data* 50: 742-768.

Shen, L., Wania, F., Lei, Y. D., Teixeira, C., Muir, D. C. G. and Bidleman, T. F. (**2005**): Atmospheric distribution and long-range transport behavior of organochlorine pesticides in North America. *Environ. Sci. Technol.* 39: 409-420.

Shoeib, M., Harner, T., Wilford, B. H., Jones, K. C. and Zhu, J. P. (**2005**): Perfluorinated sulfonamides in indoor and outdoor air and indoor dust: Occurrence, partitioning, and human exposure. *Environ. Sci. Technol.* 39: 6599-6606.

Simonich, S. L. and Hites, R. A. (**1995**): Global distribution of persistent organochlorine compounds. *Science* 269: 1851-1854.

Sjoeib, F., Anwar, E. and Tungguldihardjo, M. S. (**1994**): Behavior of DDT and DDE in Indonesian tropical environments. *J. Environ. Sci. Health., B* 29: 17-24.

Slob, W. (**1994**): Uncertainty Analysis in Multiplicative Models. *Risk Anal.* 14: 571-576.

Soderstrom, G., Sellstrom, U., De Wit, C. A. and Tysklind, M. (**2004**): Photolytic debromination of decabromodiphenyl ether (BDE 209). *Environ. Sci. Technol.* 38: 127-132.

Sohn, M. D., Small, M. J. and Pantazidou, M. (**2000**): Reducing uncertainty in site characterization using Bayes Monte Carlo methods. *J. Environ. Eng.-ASCE* 126: 893-902.

Soltermann, F. (**2007**): Modelling the global fate of polybrominated diphenyl ethers (PBDEs): Does debromination of higher brominated PBDEs significantly contribute to the presence of lowly brominated PBDEs in the environment? Diploma-Thesis, ETH Zurich, Zurich.

Stenzel, J. I. and Markley, B. J. (**1997**). Pentabromodiphenyl oxide: determination of the water solubility. Report by: Wildlife International LTD, Arlington.

Stephens, J., Maeda, D. N., Ngowi, A. V., Moshi, A. O., Mushy, P. and Mausa, E. (**1994**): Dissipation and degradation of C-14 p,p'-DDT and C-14 p,p'-DDE in Tanzanian soils under field conditions. *J. Environ. Sci. Health., B* 29: 65-71.

Stern, G. A., Braekevelt, E., Helm, P. A., Bidleman, T. F., Outridge, P. M., Lockhart, W. L., McNeeley, R., Rosenberg, B., Ikonomou, M. G., Hamilton, P., Tomy, G. T. and Wilkinson, P. (**2005**): Modem and historical fluxes of halogenated organic contaminants to a lake in the Canadian arctic, as determined from annually laminated sediment cores. *Sci. Total Environ.* 342: 223-243.

Stevens, G. C., Ghanem, R., Thomas, J. L., Horrocks, A. R. and Kandola, B., *Understanding flame retardant release to the environment*. Conference proceedings to Flame Retardants Conference, **2004**, London.

Stock, N. L., Furdui, V. I., Muir, D. C. G. and Mabury, S. A. (**2007**): Perfluoroalkyl contaminants in the canadian Arctic: Evidence of atmospheric transport and local contamination. *Environ. Sci. Technol.* 41: 3529-3536.

Stock, N. L., Lau, F. K., Ellis, D. A., Martin, J. W., Muir, D. C. G. and Mabury, S. A. (**2004**): Polyfluorinated telomer alcohols and sulfonamides in the North American troposphere. *Environ. Sci. Technol.* 38: 991-996.

Strachan, W. M. J., Burniston, D. A., Williamson, M. and Bohdanowicz, H. (**2001**): Spatial differences in persistent organochlorine pollutant concentrations between the Bering and Chukchi Seas (1993). *Mar. Pollut. Bull.* 43: 132-142.

Strand, A. and Hov, O. (**1993**): A 2-dimensional zonally averaged transport model including convective motions and a new strategy for the numerical-solution. *J. Geophys. Res.-Atmos.* 98: 9023-9037.

Strand, A. and Hov, O. (**1996**): A model strategy for the simulation of chlorinated hydrocarbon distributions in the global environment. *Water Air Soil Poll.* 86: 283-316.

Strandberg, B., Dodder, N. G., Basu, I. and Hites, R. A. (**2001**): Concentrations and spatial variations of polybrominated diphenyl ethers and other organohalogen compounds in Great Lakes air. *Environ. Sci. Technol.* 35: 1078-1083.

Su, Y., Hung, H., Sverko, E., Fellin, P. and Li, H. (**2007**): Multi-year measurements of polybrominated diphenyl ethers (PBDEs) in the Arctic atmosphere. *Atmos. Environ.* 41: 8725-8735.

Switzer, B. C., Wolfe, F. H. and Lewin, V. (**1972**): Eggshell thinning and DDE. *Nature* 240: 162-163.

Tanabe, S., Tatsukawa, R., Kawano, M. and Hidaka, H. (**1982**): Global distribution and atmospheric transport of chlorinated hydrocarbons: HCH (BHC) isomers and DDT compounds in the Western Pacific, Eastern Indian and Antarctic Oceans. *J. Oceanogr. Soc. Japan* 38: 137 - 148.

ten Hulscher, T. E. M., Vandervelde, L. E. and Bruggeman, W. A. (**1992**): Temperature-dependence of henry law constants for selected chlorobenzenes, polychlorinated-biphenyls and polycyclic aromatic-hydrocarbons. *Environ. Toxicol. Chem.* 11: 1595-1603.

ter Schure, A. F. H., Larsson, P., Agrell, C. and Boon, J. P. (**2004**): Atmospheric transport of polybrominated diphenyl ethers and polychlorinated biphenyls to the Baltic sea. *Environ. Sci. Technol.* 38: 1282-1287.

Thao, V. D., Kawano, M., Matsuda, M., Wakimoto, T., Tatsukawa, R., Cau, H. D. and Quynh, H. T. (**1993a**): Chlorinated-hydrocarbon insecticide and polychlorinated biphenyl residues in soils from southern provinces of Vietnam. *Int. J. Environ. An. Ch.* 50: 147-159.

Thao, V. D., Kawano, M. and Tatsukawa, R. (**1993b**): Persistent organochlorine residues in soils from tropical and subtropical Asian countries. *Environ. Pollut.* 81: 61-71.

Tittlemier, S. A., Halldorson, T., Stern, G. A. and Tomy, G. T. (**2002**): Vapor pressures, aqueous solubilities, and Henry's law constants of some brominated flame retardants. *Environ. Toxicol. Chem.* 21: 1804-1810.

Tomy, G. T., Palace, V. P., Halldorson, T., Braekevelt, E., Danell, R., Wautier, K., Evans, B., Brinkworth, L. and Fisk, A. T. (**2004**): Bioaccumulation, biotransformation, and biochemical effects of brominated diphenyl ethers in juvenile lake trout (Salvelinus namaycush). *Environ. Sci. Technol.* 38: 1496-1504.

Toose, L., Woodfine, D. G., MacLeod, M., Mackay, D. and Gouin, J. (**2004**): BETR-World: a geographically explicit model of chemical fate: application to transport of alpha-HCH to the Arctic. *Environ. Pollut.* 128: 223-240.

U.S. Environmental Protection Agency. Webpage http://www.epa.gov/opptintr/exposure/pubs/episuitedl.htm, accessed **2004**.

Ueno, D., Darling, C., Alaee, M., Pacepavicius, G., Teixeira, C., Campbell, L., Letcher, R. J., Bergman, A., Marsh, G. and Muir, D. C. G. (**2008**): Hydroxylated polybrominated diphenyl ethers (OH-PBDEs) in the abiotic environment: surface water and precipitation from Ontario, Canada. *Environ. Sci. Technol.* 42: 1657-1664.

United Nations (**2006**). Human Development Index report. Report by: United Nations, New York.

United Nations Environmental Program. Webpage http://www.pops.int/documents/convtext/convtext_en.pdf, accessed **2004**.

United Nations Environmental Program. Webpage http://www.pops.int/, accessed **2008**.

United Nations Statistics Division. Online Database: http://unstats.un.org/unsd/cdb/cdb_advanced_data_extract_cr.asp?HSrID=1070&srID=1070&srID=1070&continue=Continue+%3E%3E, accessed **1995**.

van Gaans, P. F. M., Vriend, S. P., Bleyerveld, S., Schrage, G. and Vos, A. (**1995**): Assessing environmental soil quality in rural-areas - a base-line study in the province of Zeeland, the Netherlands and reflections on soil monitoring network designs. *Environ. Monit. Assess.* 34: 73.

van Metre, P. C., Callender, E. and Fuller, C. C. (**1997**): Historical trends in organochlorine compounds in river basins identified using sediment cores from reservoirs. *Environ. Sci. Technol.* 31: 2339.

van Metre, P. C. and Mahler, B. J. (**2005**): Trends in hydrophobic organic contaminants in urban and reference lake sediments across the United States, 1970-2001. *Environ. Sci. Technol.* 39: 5567-5574.

van Noort, P. C. M. (**2004**): Fugacity ratio estimations for high-melting rigid aromatic compounds. *Chemosphere* 56: 7-12.

Varca, L. M. and Magallona, E. D. (**1994**): Dissipation and degradation of DDT and DDE in Philippine soil under field conditions. *J. Environ. Sci. Health., B* 29: 25-35.

Voorspoels, S., Covaci, A. and Schepens, P. (**2003**): Polybrominated diphenyl ethers in marine species from the Belgian North Sea and the Western Scheldt Estuary: Levels, profiles and distribution. *Environ. Sci. Technol.* 37: 4348-4357.

Walker, K. (**2000**): Cost-comparison of DDT and alternative insecticides for malaria control. *Med. Vet. Entomol.* 14: 345-354.

Wallington, T. J., Hurley, M. D., Xia, J., Wuebbles, D. J., Sillman, S., Ito, A., Penner, J. E., Ellis, D. A., Martin, J., Mabury, S. A., Nielsen, O. J. and Andersen, M. P. S. (**2006**): Formation of $C_7F_{15}COOH$ (PFOA) and other perfluorocarboxylic acids during the atmospheric oxidation of 8 : 2 fluorotelomer alcohol. *Environ. Sci. Technol.* 40: 924-930.

Wang, X. M., Ding, X., Mai, B. X., Xie, Z. Q., Xiang, C. H., Sun, L. G., Sheng, G. Y., Fu, J. M. and Zeng, E. Y. (**2005**): Polybrominated diphenyl ethers in airborne particulates collected during a research expedition from the Bohai Sea to the Arctic. *Environ. Sci. Technol.* 39: 7803-7809.

Wang, Y., Jiang, G., Lam, P. K. S. and Li, A. (**2007**): Polybrominated diphenyl ether in the East Asian environment: A critical review. *Environ. Int.* 33: 963-973.

Wania, F. (**2003**): Assessing the potential of persistent organic chemicals for long-range transport and accumulation in polar regions. *Environ. Sci. Technol.* 37: 1344-1351.

Wania, F. (**2004**): Schadstoffe ohne Grenzen - Ferntransport persistenter organischer Umweltchemikalien in die Kälteregionen der Erde. *GAIA* 13: 176-185.

Wania, F. (**2007**): A global mass balance analysis of the source of perfluorocarboxylic acids in the Arctic ocean. *Environ. Sci. Technol.* 41: 4529-4535.

Wania, F. and Dugani, C. B. (**2003**): Assessing the long-range transport potential of polybrominated diphenyl ethers: A comparison of four multimedia models. *Environ. Toxicol. Chem.* 22: 1252-1261.

Wania, F. and Mackay, D. (**1995**): A global distribution model for persistent organic-chemicals. *Sci. Total Environ.* 161: 211-232.

Wania, F., Mackay, D., Li, Y. F., Bidleman, T. F. and Strand, A. (**1999**): Global chemical fate of alpha-hexachlorocyclohexane. 1. Evaluation of a global distribution model. *Environ. Toxicol. Chem.* 18: 1390-1399.

Watanabe, I. and Tatsukawa, R. (**1987**): Formation of brominated dibenzofurans from the photolysis of flame-retardant decabromobiphenyl ether in hexane solution by UV and sun light. *Bull. Environ. Contam. Toxicol.* 39: 953-959.

Watanabe, I., Tatsukawa, R., *Anthropogenic brominated aromatics in the Japanese environment.* Conference proceeding to Workshop on brominated aromatic flame retardants, **1989**, Skokloster, Sweden.

Waterland, R. L. and Dobbs, K. D. (**2007**): Atmospheric chemistry of linear perfluorinated aldehydes: Dissociation kinetics of $C_nF_{2n+1}CO$ radicals. *J. Phys. Chem. A* 111: 2555-2562.

Wegmann, F. (**2004**): The global dynamic multicompartment model CliMoChem for persistent organic pollutants: Investigations of the vegetation influence, the cold condensation and the global fractionation. PhD Thesis, ETH Zurich, Zurich.

Wegmann, F., Scheringer, M. and Hungerbühler, K. (**2006**): First investigations of mountainous cold condensation effects with the CliMoChem model. *Ecotox. Environ. Safe.* 63: 42-51.

Wegmann, F., Scheringer, M., Moller, M. and Hungerbühler, K. (**2004**): Influence of vegetation on the environmental partitioning of DDT in two global multimedia models. *Environ. Sci. Technol.* 38: 1505-1512.

Weiss, P. (**1998**). Persistente Organische Schadstoffe in Hintergrund-Waldgebieten Oesterreichs. Report by: Österreichisches Bundesministerium fuer Umwelt, Jugend und Familie, Wien.

Widmer, R., Oswald-Krapf, H., Sinha-Khetriwal, D., Schnellmann, M. and Boni, H. (**2005**): Global perspectives on e-waste. *Environ. Impact Assess.* 25: 436-458.

Wiemeyer, S. N. and Porter, R. D. (**1972**): Eggshell thinning and DDE. *Nature* 240: 163-163.

Wong, A., Lei, Y. D., Alaee, M. and Wania, F. (**2001**): Vapor pressures of the polybrominated diphenyl ethers. *J. Chem. Eng. Data* 46: 239-242.

Woodwell, G. M., Craig, P. P. and Johnson, H. A. (**1971**): DDT in biosphere - Where does it go. *Science* 174: 1101-1107.

World Health Organization (**1994**). Brominated diphenyl ethers, IPCS, Environmental Health Criteria 162. Report by: World Health Organization, Geneva.

World Health Organization. Webpage http://www.who.int/mediacentre/news/releases/2006/pr50/en/, accessed **2006**.

Wurl, O., Lam, P. K. S. and Obbard, J. P. (**2006a**): Occurrence and distribution of polybrominated diphenyl ethers (PBDEs) in the dissolved and suspended phases of the sea-surface microlayer and seawater in Hong Kong, China. *Chemosphere* 65: 1660-1666.

Wurl, O., Potter, J. R., Obbard, J. P. and Durville, C. (**2006b**): Persistent organic pollutants in the equatorial atmosphere over the open Indian Ocean. *Environ. Sci. Technol.* 40: 1454-1461.

WWF (**1998**). Resolving the DDT Dilemma. Report by: WWF Canada and WWF US, Toronto.

Xiao, H., Li, N. Q. and Wania, F. (**2004**): Compilation, evaluation, and selection of physical-chemical property data for alpha-, beta-, and gamma-hexachlorocyclohexane. *J. Chem. Eng. Data* 49: 173-185.

Yamashita, N., Kannan, K., Taniyasu, S., Horii, Y., Petrick, G. and Gamo, T. (**2005**): A global survey of perfluorinated acids in oceans. *Mar. Pollut. Bull.* 51: 658-668.

Yao, Y., Tuduri, L., Harner, T., Blanchard, P., Waite, D., Poissant, L., Murphy, C., Belzer, W., Aulagnier, F., Li, Y. F. and Sverko, E. (**2006**): Spatial and temporal distribution of pesticide air concentrations in Canadian agricultural regions. *Atmos. Environ.* 40: 4339-4351.

Yarwood, G., Kemball-Cook, S., Keinath, M., Waterland, R. L., Korzeniowski, S. H., Buck, R. C., Russell, M. H. and Washburn, S. T. (**2007**): High-resolution atmospheric modeling of fluorotelomer alcohols and perfluorocarboxylic acids in the North American troposphere. *Environ. Sci. Technol.* 41: 5756 - 5762.

Young, C. J., Furdui, V. I., Franklin, J., Koerner, R. M., Muir, D. C. G. and Mabury, S. A. (**2007**): Perfluorinated acids in Arctic snow: New evidence for atmospheric formation. *Environ. Sci. Technol.* 41: 3455-3461.

Zayed, S., Mostafa, I. Y. and Elarab, A. E. (**1994**): Degradation and fate of C-14 DDT and C-14 DDE in Egyptian soil. *J. Environ. Sci. Health., B* 29: 47-56.

Zepp, R. G., Wolfe, N. L., Azarraga, L. V., Cox, R. H. and Pape, C. W. (**1977**): Photochemical transformation of DDT and methoxychlor degradation products, DDE and DMDE, by sunlight. *Arch. Environ. Contam. Toxicol.* 6: 305-314.

Zetzsch, C., Palm, W. U. and Krueger, H. U. (**2004**): Photochemistry of 2,2',4,4',5,5'-HexaBDE (BDE-153) in THF and adsorbed on SiO_2: First observation of OH reactivity of BDEs an aerosol. *Organohalogen Compd.* 66: 2256 - 2261.

Zhu, Y. F., Liu, H., Xi, Z. Q., Cheng, H. X. and Xu, X. B. (**2005**): Organochlorine pesticides (DDTs and HCHs) in soils from the outskirts of Beijing, China. *Chemosphere* 60: 770-778.

CURRICULUM VITAE

PERSONAL DATA

Name:	Urs Schenker
Address:	Konradstrasse 33, 8005 Zürich
E-mail:	urs.schenker@switzerland.org
Born on:	7 December 1977 in Bern
Citizen of:	Schönenwerd (SO), Däniken (SO), Olten (SO)

EDUCATION & STUDIES

1991 – 1998	Mathematisch-Naturwissenschaftliches Gymnasium in Bern
June 1998	Kantonale Matur Typ C
1998 – 2003	Studies in Environmental Sciences and Engineering at EPFL, Lausanne, with exchange projects at Laval University, Canada (one year) and Massachusetts Institute of Technology (MIT), USA (three months)
March 2003	Graduation as ing. gén. rur. dipl. EPF Lausanne
2004 – 2006	Post Graduate Studies in Management of Technology and Economics, ETH Zurich
2004 – 2008	PhD Studies at ETH Zurich, with exchange project at University of California at Berkeley, USA (three months)

PROFESSIONAL EXPERIENCE

2002 – 2004	Assistant to Environmental Manager, Coca-Cola Beverages (Switzerland), Bussigny
2006	Master Thesis for Post Graduate Studies at SBB (Swiss Federal Railways) on “Implementation of a Risk Management System at the Passenger Transportation Division”